Numerical Methods for Nonlinear Singularly Perturbed Differential Equations

Jason Quinn B.Sc.

Supervisor: Professor Eugene O'Riordan

School of Mathematical Sciences
Dublin City University

A dissertation submitted for the Degree of
Doctor of Philosophy

September 2012

Declaration

I hereby certify that this material, which I now submit for assessment on the programme of study leading to the award of Doctor of Philosophy in Mathematics is entirely my own work, that I have exercised reasonable care to ensure the work is original, and does not to the best of my knowledge breach any law of copyright, and has not been taken from the work of others save and to the extent that such work has been cited and acknowledged within the text of my work.

Signed: 

I.D. Number: 54011716

Date: 19th September 2012

Acknowledgements

Eugene, thanks a million! Thanks for the powerful help; for trying to guide me through a problem but standing back and letting me get on with it to work it out myself.

I hope to God you won't miss being head of the maths school too much!

For any favours, don't even think twice about asking.

To Joe and my Mother Christy

You'll always be my sisters

CONTENTS

ABSTRACT

In this thesis, parameter-uniform numerical methods are constructed and analysed for nonlinear singularly perturbed ordinary differential equations. In the case of first order problems, several classes of nonlinear problems are examined and various types of initial layers are identified. In the case of second order boundary value problems, singularly perturbed quasilinear problems of convection-diffusion type are studied. Problems with boundary turning points and problems with internal layers are examined. For all problems, the numerical methods consist of monotone nonlinear finite difference operators and appropriate piecewise-uniform Shishkin meshes. The transition points in the Shishkin meshes are constructed based on sharp parameter-explicit bounds on the singular components of the continuous solution. Existence and uniqueness of both the continuous and discrete solutions are established using the method of upper and lower solutions. Numerical results are presented to both illustrate the theoretical error bounds and to display the performance of the numerical methods in practice.

List of Figures

List of Tables

List of Notations

The following is a table of symbols used throughout the thesis. In general, continuous functions are denoted by lower case letters, sometimes with the subscript ε, and discrete mesh functions are denoted by capital letters with the superscript N (the discretisation parameter) and sometimes with the subscript ε.

Item	Continuous Problem	Discrete Problem
Problem Classes:	$(\mathscr{A}_\varepsilon)$, $(\mathscr{A}_L)$, $(\mathscr{A}_R)$, $(\mathscr{B}_\varepsilon)$, $(\mathscr{C}_\varepsilon)$.	$(\mathscr{A}_\varepsilon^N)$, $(\mathscr{A}_L^N)$, $(\mathscr{A}_L^N)$, $(\mathscr{B}_\varepsilon^N)$, $(\mathscr{C}_\varepsilon^N)$.
Solutions:	u_ε, y_ε, z_ε, z_1, z_2, z_3	$U_\varepsilon^N, Y_\varepsilon^N, Z_\varepsilon^N, Z_1^N, Z_2^N, Z_3^N$
Domain:	Ω	Ω^N, Ω_ε^N
Regular Component:	v_ε, v_L, v_R, v_L, v_R	V_ε^N, V_L^N, V_R^N
Layer Component:	w_ε, w_L, w_R, ω_L, ω_R	W_ε^N, W_L^N, W_R^N
Linear Differential/Finite Difference Operator:	$\mathcal{L}_\varepsilon$, $\mathcal{L}_*$, $\mathcal{L}^\pm$	${\mathcal{L}_\varepsilon}^N$, ${\mathcal{L}_*}^N$, $\mathcal{L}^{\pm,N}$
Problem Data:	a, b, f, g, q, F	
Boundary Conditions:	A, B, y_0, y_1	
Upper and Lower Solutions	$\underline{u}$, $\overline{u}$, $\underline{y}$, $\overline{y}$, $\underline{z}$, $\overline{w}$.	$\underline{U}^N$, $\overline{U}^N$, $\overline{\overline{U}}^N$, $\underline{Y}^N$, $\overline{Y}^N$.

If Z^N is any mesh function then $Z^N(x_i)$ is the value of Z^N at the meshpoint x_i. We sometimes use the shorter notation Z_i^N for $Z^N(x_i)$. The following are the finite difference operators we use throughout the thesis.

$$D^+Z^N(x_i)=\frac{1}{x_{i+1}-x_i}(Z^N(x_{i+1})-Z^N(x_i)),\quad D^-Z^N(x_i)=D^+Z^N(x_{i-1}),$$
$$\delta^2Z^N(x_i)=\frac{2}{x_{i+1}-x_{i-1}}(D^+-D^-)Z^N(x_i).$$

If f is a sufficiently smooth function then we use the following notation for the k-th derivative and the maximum norm:

$$f^{(k)}=\frac{d^kf}{dx^k},\quad \|f\|_\Omega=\max_{x\in\Omega}|f(x)|.$$

Sometimes we write $\|f\|$ when the domain Ω is obvious.

Generic or arbitrary positive constants independent of ε or N will be denoted by

$$C, \quad C', \quad C_1, \quad C_2.$$

Throughout the thesis, we frequently assume that ε is sufficiently small and N is sufficiently large. When we say this, we mean that if C_1 and C_2 are two positive constants, independent of ε and N, then we are assuming that

$$C_1 - C_2(\varepsilon + N^{-1}) > 0.$$

We preserve the symbol x^* as notation indicating Howes' point as defined in (4.2.5) which is an approximation to the location of an interior layer for convection diffusion problems.

CHAPTER: 1

INTRODUCTION

1.1: BACKGROUND

Singularly perturbed differential equations are typically characterised by the presence of a small parameter, denoted throughout the thesis by ε, multiplying the highest derivative term in the differential equation. This small parameter is referred to as the singular perturbation parameter. The solution of any differential equation, if it exists, depends on the problem data. Specifically, the magnitude of the derivatives of the solution of a singularly perturbed problem, are inversely proportional to the singular perturbation parameter. As the perturbation parameter ε becomes arbitrary small, the derivatives of the solution become arbitrary large. For this reason, singularly perturbed differential equations are problematic to solve numerically. Singularly perturbed problems arise in numerous areas of engineering and science. For example, they appear in such diverse areas as Mathematical Biology ([14]), Financial Mathematics ([3] and references therein), Combustion Modelling and Control Theory ([13]) and Fluid Dynamics ([21]).

1.2: KEY ISSUE IN NUMERICALLY SOLVING SINGULARLY PERTURBED PROBLEMS

Let us consider a very simple linear singularly perturbed initial value problem. Find a function y_ε satisfying

$$(\varepsilon y_\varepsilon' + \alpha y_\varepsilon)(x) = 0, \quad x \in (0,1], \quad y_\varepsilon(0) = 1, \quad \alpha > 0, \quad 0 < \varepsilon \ll 1, \tag{1.2.1}$$

where α is a constant. This problem is easily solved and it is unnecessary to approximate the solution numerically. However it is a convenient problem for us to demonstrate the issues raised by the presence of the singular perturbation parameter. The solution has the following properties

$$y_\varepsilon(x) = e^{-\alpha x/\varepsilon}, \qquad y_\varepsilon^{(k)}(x) = (-1)^k \frac{\alpha^k}{\varepsilon^k} e^{-\alpha x/\varepsilon}, \quad k = 1,2,\ldots. \tag{1.2.2}$$

Observe the fact that

$$y_\varepsilon(0)=1 \qquad \text{and} \qquad y_\varepsilon(x)\leqslant \varepsilon \quad \text{if} \quad x\geqslant \frac{\varepsilon}{\alpha}\ln\left(\frac{1}{\varepsilon}\right). \tag{1.2.3}$$

From (1.2.3), we see that near the initial point, the solution is $O(1)$ and outside a neighbourhood of $x=0$, the solution is $O(\varepsilon)$. Also, the derivatives are bounded outside a neighbourhood of $x=0$. That is

$$|y_\varepsilon^{(k)}(x)|\leqslant C \quad \text{if} \quad x\geqslant k\frac{\varepsilon}{\alpha}\ln\frac{1}{\varepsilon}.$$

Finally, we observe that

$$|y_\varepsilon(x)|\leqslant CN^{-1} \quad \text{if} \quad x\geqslant \frac{\varepsilon}{\alpha}\ln(N), \tag{1.2.4}$$

where N is a discretisation parameter. We say that there is an initial layer of width $O(\varepsilon)$ in the solution $y_\varepsilon(x)$.

To numerically approximate the solution of (1.2.1), we use the following backward Eular finite difference operator on a uniform mesh Ω^N:

$$(\varepsilon D^- Y_\varepsilon^N+\alpha Y_\varepsilon^N)(x_i)=0, \quad x_i\in\overline{\Omega}^N\setminus\{0\}, \quad Y_\varepsilon^N(x_0)=1, \tag{1.2.5a}$$

$$\overline{\Omega}^N:=\left\{ ih,\ h=\frac{1}{N}\,\middle|\, 0\leqslant i\leqslant N\right\}, \tag{1.2.5b}$$

$$D^- Y_\varepsilon^N(x_i):=(Y_\varepsilon^N(x_i)-Y_\varepsilon^N(x_{i-1}))/h_i, \qquad h_i=x_i-x_{i-1}=h. \tag{1.2.5c}$$

To find the difference between the numerical solution Y_ε^N and the solution y_ε at each mesh point $x_i\in\Omega^N$, (i.e. the pointwise error), we use the fact that at each mesh point $x_i>0$ we have

$$\varepsilon D^- Y_\varepsilon^N(x_i)+\alpha Y_\varepsilon^N(x_i)=\varepsilon y_\varepsilon'(x_i)+\alpha y_\varepsilon(x_i), \quad x_i\in\overline{\Omega}^N\setminus\{0\}.$$

Hence, the error $E_\varepsilon^N:=Y_\varepsilon^N-y_\varepsilon$ satisfies the discrete initial value problem:

$$\varepsilon D^- E_\varepsilon^N(x_i)+\alpha E_\varepsilon^N(x_i)=\varepsilon(y_\varepsilon'-D^- y_\varepsilon)(x_i), \quad x_i\in\overline{\Omega}^N\setminus\{0\}, \quad E_\varepsilon^N(0)=0. \tag{1.2.6}$$

We refer to $\tau^N:=\varepsilon(y_\varepsilon'-D^- y_\varepsilon)$ as the truncation error which is given by the explicit expression

$$\tau^N(x_i)=\varepsilon(y_\varepsilon'-D^- y_\varepsilon)(x_i)=\frac{1}{h_i}\int_{x_{i-1}}^{x_i}\int_t^{x_i} y_\varepsilon''(s)\,ds\,dt.$$

Using (1.2.2), we can bound the truncation error as follows

$$\frac{\alpha^2}{2}e^{-\alpha x_i/\varepsilon}\frac{h_i}{\varepsilon}\leqslant\tau^N(x_i)\leqslant\frac{\alpha^2}{2}e^{-\alpha x_{i-1}/\varepsilon}\frac{h_i}{\varepsilon}. \tag{1.2.7}$$

To bound the error E_ε^N, we can solve the discrete problem (1.2.6) exactly to find

$$E_\varepsilon^N(x_i)=\sum_{j=1}^{i}\frac{h_i}{\varepsilon}\tau^N(x_i)\prod_{k=j}^{i}\left(1+\alpha\frac{h_k}{\varepsilon}\right)^{-1}. \tag{1.2.8}$$

Using the bounds in (1.2.7) and the inequality $1+t \leqslant e^t$, $t>0$ with the expression (1.2.8) we have

$$\frac{\alpha^2}{2}\sum_{j=1}^{i} e^{-(2\alpha x_i/\varepsilon)}\left(\frac{h_j}{\varepsilon}\right)^2 \leqslant E_\varepsilon^N(x_i) \leqslant \frac{\alpha^2}{2} i \max_{j\leqslant i}\left(\frac{h_j}{\varepsilon}\right)^2. \tag{1.2.9}$$

In fact, it suffices to examine the error at the first internal mesh point x_1 to demonstrate a key issue in numerically solving singularly perturbed problems. The error at the first mesh point x_1 is bounded above and below by

$$\frac{\alpha^2}{2} e^{-(2\alpha h/\varepsilon)}\frac{h}{\varepsilon} \leqslant E_\varepsilon^N(x_1) \leqslant \frac{\alpha^2}{2}\frac{h}{\varepsilon}. \tag{1.2.10}$$

Ideally, we would like these upper and lower bounds to tend to zero for increasing N (decreasing h). In particular, a necessary condition for convergence is that the lower bound in (1.2.10) tends to zero as $h \to 0$. At this stage, we have reached a key issue that manifests itself throughout the error analysis associated with singularly perturbed problems - controlling the magnitude of the quantity $\frac{h}{\varepsilon}$ i.e. the mesh spacing divided by the singular perturbation parameter. The only way the bounds in (1.2.10) will shrink for increasing N (decreasing h) is if $h/\varepsilon = \varepsilon^{-1}N^{-1}$ tends to zero. Hence, for the pointwise error to decrease (with increasing N) at the first mesh point, we would need the magnitude of N^{-1} to be smaller than ε^{-1}. For example, suppose $\varepsilon = 10^{-6}$ and we required an error of magnitude 10^{-2}. To guarantee this, we would require N to have a magnitude of at least 10^8. That is, split $[0,1]$ into 10^8 subintervals. This would be a highly impractical numerical method. Ideally the only factor in choosing the value of the mesh parameter N should be the desired bound on the error and not the value of the perturbation parameter.

There are two potential remedies to this issue:

1. Select a different finite difference operator; or

2. Select an alternative mesh to the uniform mesh.

1.3: Linear versus Nonlinear Problems

The simple problem (1.2.1) considered in §1.2 was of course linear. There is an extensive body of literature existing for linear singularly perturbed problems [7],[29]. In general, nonlinear problems are considerably more difficult to analyse than linear problems. We outline some differences involved in analysing linear and nonlinear problems below.

To bound the solution of a linear problem, we typically use a maximum principle, which is relatively easy to establish (e.g. see Th $\stackrel{\text{m}}{=}$ 3.2.1, pg. 62). The technique of using a maximum principle

is highly convenient, since finding a barrier function that satisfies the maximum principle generates an upper and lower bound on the solution (e.g. see (3.2.4), pg. 63). This is in stark contrast to bounding the solution of a nonlinear problem. To establish a maximum principle for a nonlinear problem, we would require a bound on the solution to the problem itself. Hence the technique of a maximum principle is not directly applicable to nonlinear problems. Instead, we use the technique of upper and lower solutions ([16]), as demonstrated in Chapters 2 and 3. We bound the solution of a nonlinear problem from above and below separately by constructing an upper and lower solution respectively. Immediately, we have an extra step in bounding solutions of nonlinear problems. Moreover, for a nonlinear problem, due to the nature of the nonlinearity, it may be easy to construct an upper solution. However, this has no bearing on the difficulty in constructing a lower solution or *vice versa*.

Establishing upper and lower bounds on a solution implies that a solution to the problem exists but does not imply that the solution is unique. In the case of linear problems, as soon as a solution is shown to exist, a relatively simple argument can be applied to prove uniqueness. That is, suppose a solution to the differential equation $\mathcal{L}_\varepsilon y = q$, $y = g(x)$ on a boundary Ω, exists, where $\mathcal{L}_\varepsilon$ is any linear differential operator of any order. If v_1 and v_2 are two particular solutions then $\Delta v := v_1 - v_2$ satisfies $\mathcal{L}_\varepsilon(\Delta v) = 0$, $\Delta v = 0$ on Ω. Hence $\Delta v \equiv 0$ and thus the solution is unique. This simple argument cannot be directly applied in the case of nonlinear problems. In general, proving uniqueness of a solution to a nonlinear problem is not a straightforward task.

Another difference in the numerical analysis between linear and nonlinear problems is the effect of the initial\boundary conditions. In general, the boundary conditions of a linear problem have no effect or influence on the existence of a solution. This can be demonstrated easily using a maximum principle. However, that is not the case with nonlinear problems. The nature of the nonlinearity may mean we can only establish existence of a solution for a restricted set of boundary conditions. Additional restrictions can also arise in the analysis, due to the need for sharp upper and lower solutions, as we will see in Chapter 3.

In general, once a maximum principle and a sufficiently sharp barrier function has been established to bound the solution of a linear problem, they can be ultimately used to bound the error between the numerical solution and the continuous solution. In a sense, a sharp barrier function can be recycled throughout the analysis. Later in §1.5, we discuss boundary and interior layers. However, to obtain information about the character of the solution within the layers, we split the solution into the sum of two components - a regular component and a layer component. Thus for a linear problem, the two components satisfy an analogous linear problem,

for which a suitably sharp barrier function established to bound the solution of the problem, can be re-used to bound the regular and layer components. This is not the case with nonlinear problems where novel upper and lower solutions must be constructed to bound the regular and layer components. Each of these components may satisfy a nonlinear equation not encountered previously in the analysis of their sum.

A further difference between using a maximum principle for a linear problem and using upper and lower solutions for a nonlinear problem is that a barrier function is explicitly constructed to bound the solution of the linear problem. This is in contrast to a nonlinear problem where an upper or lower solution may be difficult or impossible to construct. Instead a solution to an alternative problem is proven to be an upper or lower solution. The solution to this alternative problem is then bounded using upper and lower solutions. This then provides an upper or lower bound for the solution of the main problem under consideration. An example of this will be seen in Chapter 3.

These examples are differences that arise in the analysis of the continuous problem. When we begin to analyse the discrete problem, all these differences manifest themselves again in a discrete manner, i.e., discrete maximum principle versus discrete upper and lower solutions, uniqueness of a solution to a discrete linear scheme versus a discrete nonlinear scheme etc.

In conclusion, wide classes of linear problems can be studied using the same analytical techniques. However, for nonlinear problems, due to the particular nonlinearity and due to the boundary conditions and\or problem data, a generalised approach is not available and classes of nonlinear problems are studied on a case-by-case basis.

Note that we are mainly concerned with nonlinear problems in this thesis.

Further note that when we present and analyse a finite difference scheme for a nonlinear problem, the finite difference scheme itself is nonlinear and thus cannot be explicitly solved. This is in contrast to a linear finite difference scheme. To solve a nonlinear finite difference scheme, we may use a variety of methods. In this thesis we use Newton's Method, solving the scheme exactly where possible (e.g. a quadratic nonlinearity) and the Continuation Method. We will describe these methods in more detail as they appear in the thesis.

1.4: Parameter Uniform Convergence and Fitted Methods

To formalise the idea in §1.2 of choosing the mesh parameter N solely for the desired error bound and not based on the singular perturbation parameter, we cite the following definition.

Definition 1.4.1. *([20, pg. 12]) Consider a family of mathematical problems family parametrised by a singular perturbation parameter ε, where ε lies in the semi-open interval $0 < \varepsilon \leqslant 1$. Assume that each problem in the family has a unique solution denoted by u_ε, defined on the interval $\overline{\Omega}$, and that each u_ε is approximated by a sequence of numerical solutions $\{(U_\varepsilon^N, \overline{\Omega}^N)\}_{N=1}^{\infty}$ where U_ε^N is defined on the mesh $\overline{\Omega}^N$ and N is a discretisation parameter. Let $\overline{U}_\varepsilon$ denote the piecewise linear interpolant over $\overline{\Omega}^N$ of the discrete solution U_ε^N. Then, the numerical solutions U_ε^N are said to converge ε-uniformly to the exact solution u_ε, if there exist a positive integer N_0, and positive numbers C and p, where N_0, C and p are all independent of N and ε, such that for all $N \geqslant N_0$*

$$\sup_{0<\varepsilon\leqslant 1} \|\overline{U}_\varepsilon^N - u_\varepsilon\|_{\overline{\Omega}} \leqslant CN^{-p} \tag{1.4.1}$$

Here p is called ε-uniform rate of convergence and C is called the ε-uniform error constant.

Note that Def $\overset{n}{=}$ 1.4.1 is a slightly modified version of the orginal ([20, pg. 12]) whereby we require a bound on the globally defined quantity $\|\overline{U}_\varepsilon^N - u_\varepsilon\|_{\overline{\Omega}}$ of the form (1.4.1) as opposed to on the pointwise defined quantity $\|U_\varepsilon^N - u_\varepsilon\|_{\overline{\Omega}^N}$ of the same form required in the original definition.

Remark: The ε-uniform error constant referred to in Def $\overset{n}{=}$ 1.4.1, in general, depends on the problem data in the problem class. Through careful analysis, this constant could be determined explicitly for any of the problems looked at in this thesis. However, we do not examine this issue in this thesis.

We always aim to establish parameter-uniform convergence for any proposed numerical method. However, this may not be possible for certain classes of singularly perturbed problems, as we will see in Chapter 2.

Returning to the 'remedies' mentioned in §1.2, we mentioned altering the finite difference operator. Fitted operator methods (where a mesh function, referred to as a 'fitting factor', is included into the finite difference operator) have been used with success for some linear problems [29]. However, this method is not appropriate for nonlinear problems. In [9], the authors show that it is impossible to find a frozen (constant) fitting factor to generate a parameter-uniform numerical method for the following class of nonlinear problems:

$$\varepsilon u''(x) - b(u(x))u(x) = 0, \quad x \in (0,1), \quad u(0) = 1, \quad u(0) = 0, \tag{1.4.2a}$$

$$b(u(x)) \geqslant \beta > 0, \quad x \in [0,1], \tag{1.4.2b}$$

if one uses a uniform mesh. For these reasons, we choose the other remedy mentioned earlier - altering the mesh. We refer to such methods as fitted mesh or layer-adapted mesh methods. A popular option is the relatively recent Shishkin mesh method [30]. A Shishkin mesh consists of fine and coarse uniform meshes. The fine meshes are located in the layer regions and the coarse meshes outside. The fine and coarse meshes are joined at appropriately chosen transition points. These transition points are chosen analytically before the mesh is explicitly defined.

We quickly illustrate how a Shishkin mesh is a convenient remedy to the issue raised in §1.2. We choose the transition point $\sigma = \frac{\varepsilon}{\alpha}\ln(N)$ based on the inequality (1.2.4). In essence, this means the boundary layer function is negligible beyond the transition point σ for sufficiently large N. The Shishkin mesh is then defined as

$$\overline{\Omega}^N = \left\{ x_i | x_i = \frac{2\sigma}{N},\ 0 \leqslant i \leqslant \tfrac{N}{2},\ x_i = \frac{2(1-\sigma)}{N},\ \tfrac{N}{2} < i \leqslant N \right\}, \quad \sigma = \min\left\{ \frac{1}{2}, \frac{\varepsilon}{\alpha}\ln(N) \right\},$$

whereby we place half of the N mesh intervals within the boundary layer at $x = 0$ and the transition point σ (the fine mesh). The remaining mesh intervals are located outside the layer in the interval $[\sigma, 1]$ (the coarse mesh). The error (1.2.9) is then bounded on the fine mesh $x_i \in [0,\sigma] \cap \Omega_\varepsilon^N$, for sufficiently small ε, as

$$|E_\varepsilon^N(x_i)| \leqslant \frac{\alpha^2}{2}\frac{N}{2}\left(\frac{1}{\alpha}\frac{2}{N}\ln(N)\right)^2 = N^{-1}(\ln(N))^2, \quad x_i \in [x_0, x_{\frac{N}{2}}].$$

To bound the error on the coarse mesh $x_i \in [\sigma, 1] \cap \Omega_\varepsilon^N$, we can solve and bound the discrete solution of (1.2.5) on the fine mesh exactly as

$$0 \leqslant Y_\varepsilon^N(x_i) \leqslant 1, \quad 0 \leqslant i \leqslant N, \qquad Y_\varepsilon^N(x_i) = \left(1 + \frac{\alpha h_i}{\varepsilon}\right)^{-i} \leqslant 2e^{-\alpha x_i/\varepsilon}, \quad 0 \leqslant i \leqslant \frac{N}{2},$$

and hence from (1.2.5) we have $Y_\varepsilon^N(x_{i+1}) \leqslant Y_\varepsilon^N(x_i)$. Thus for all x_i on the coarse mesh area $(\sigma, 1]$, we have

$$|(Y_\varepsilon^N - y_\varepsilon)(x_i)| \leqslant |Y_\varepsilon^N(\sigma)| + |y_\varepsilon(\sigma)| \leqslant 3N^{-1}, \quad x_i \in [x_{\frac{N}{2}}, 1].$$

We can continue the argument to finally establish the corresponding parameter-uniform global error bound

$$\|\overline{Y}_\varepsilon^N - y_\varepsilon\|_{[0,1]} \leqslant CN^{-1}(\ln(N))^2,$$

where $\overline{Y}_\varepsilon^N$ is the linear interpolant of Y_ε^N.

Again, this was a very basic linear example just to illustrate difficulties appearing due to the presence of the singular perturbation parameter. An alternative fitted mesh method was originally proposed by Bakhvalov in [2]. Like Shishkin's mesh, it is comprised of fine and coarse

parts. The suitable transition point is not as easily determined though as it may be described as the solution of a nonlinear equation (see [7, §3.1], [29, §2.4.1] for more details). In general, the construction and the discrete analysis pertaining to a Shishkin mesh is simpler than that for a Bakhvalov-type mesh.

Our *modus operandi* when analysing the various classes of problems considered in this thesis will be establishing parameter-uniform convergence of numerical methods using Shishkin meshes as a layer-adaptive mesh method.

1.5: Boundary and Interior Layers

For a singularly perturbed problem, if a layer appears at an end-point of the domain, then it is called a boundary layer. As mentioned in §1.3, to perform the numerical analysis, we split the solution of a problem into two components - a regular component and a layer component - for which their sum satisfies the problem under consideration. The location of the layer and the layer width is determined from tight bounds on the layer component of the solution. This information can suggest a suitable choice for the transition point(s) for the Shishkin mesh. For a boundary layer problem, since the layer location is known, there is no ambiguity as to where to locate the fine mesh. However, for an interior layer problem, the solution exhibits a layer not at the boundary, but somewhere in the interior of the problem interval, at a location that may be unknown. In the linear case e.g. a linear turning point problem, it is a known co-efficient in the problem that generates the interior layer and thus the location can be deduced from this co-efficient. However, in the nonlinear case, estimating the location of the interior layer is a difficult task. The interior layer location is crucial as this is where we would centre a fine mesh in the numerical method.

1.6: Nonlinear Singularly Perturbed Convection-Diffusion Interior Layer Problem

A particular problem class of interest in this thesis is a class of nonlinear singularly perturbed interior layer problems of convection-diffusion type (second order problem with a first derivative term present). Namely, problems with the fundamental form of a Burgers' type equation with an interior layer;

$$\varepsilon y'' - y y' - b y = q, \quad b(x) \geqslant 0, \quad x \in (0,1), \quad y(0) > 0 > y(1). \tag{1.6.1}$$

In general, the exact location of the interior layer is unknown. In [12], Howes establishes an explicit point in the domain $[0,1]$ where an interior layer of width $O(\varepsilon)$ occurs. We aim in this

thesis to examine parameter uniform convergence of numerical approximations generated on a Shishkin mesh centred at this Howes point. A further issue in the numerical approximation of (1.6.1) is the choice of finite difference operator. In [27], Osher presents a finite difference operator to numerically solve (1.6.1) and establishes the stability of the scheme but no error estimate is given. In [19], Lorenz shows that the Osher scheme for $\varepsilon = 0$ generates first order approximations to the discontinuous limiting solution consisting of the left and right reduced solutions joined at the Howes point. Note the first order approximations hold true except for at most two mesh points around the Howes point. Collectively, this is ample motivation to approximate the solution of (1.6.1) using an Osher's type finite difference operator on a Shishkin mesh centred at the Howes point. An obstacle is that it has not been established if the Howes point is a root of the solution y of (1.6.1). We believe that this unknown root is the optimal location to centre a Shishkin mesh.

In [31], Shishkin considers (1.6.1) and presents an approximation to the interior layer location that equates to Howes' point. He presents a numerical method based on approximating the solution to (1.6.1) with boundary turning point problems defined to the left and right of his approximation. Furthermore, in [32], Shishkin presents a technical algorithm to numerically solve a class of time dependent interior layer problems that includes a time dependent version of problem (1.6.1). The algorithm outlined in [32] is cumbersome to implement. We describe in detail and implement this algorithm in Chapter 6. Both algorithms ([31] and [32]) are not immediately parameter uniform in areas around the approximations of the interior layer. We will describe this in more detail in Chapter 6.

We note in passing that Kopteva has examined nonlinear singularly perturbed problems with interior layers (e.g. [15]). However, the interior layer problems in [15] are of reaction-diffusion type. This thesis will not examine nonlinear reaction-diffusion problems.

1.7: Outline of Thesis

This thesis examines a set of problem classes related to the problem class (1.6.1). For all problem classes analysed, we conduct numerical experiments to demonstrate the convergence rates established theoretically.

Chapter 2

We examine a set of nonlinear initial value problems which include;

$$\varepsilon y' + y^n = f(x), \quad y(0) = A, \quad x \in (0,1]. \tag{1.7.1}$$

We show that the layer widths depend on the value of n, widening for larger n. This influences the choice of transition point for the Shishkin mesh. We then examine the following class of nonlinear initial value problems

$$\varepsilon y' = k(x,y) := a(x)(y-g_1)(y-g_2)^2, \quad y(0) = A, \quad x \in (0,1],$$
$$a(x) \leqslant -\alpha < 0, \quad g_1 \neq g_2.$$

We consider either g_1 or g_2 as stable reduced solutions. Their respective multiplicities of 1 and 2 correspond to the values $n = 1$, $n = 2$ in (1.7.1). We consider $\frac{\partial^n k}{\partial y^n} > 0$ in regions around the stable reduced solution. We see that in this case, the layer widths again widen with increasing n. To bound the solution in this case, sharp upper and lower solutions are required and restrictions are placed on the behaviour of the surrounding unstable reduced solutions.

Moreover we examine the case where the initial condition is within ε of an unstable reduced solution. In this case, the solution exhibits a 'delayed layer'. In [13, pg. 69], O'Malley examines a similar problem with the same type of initial condition. However, due to the nonlinearity, the 'delayed layer' effect is exacerbated in [13] and the solution exhibits an interior layer.

Finally, we examine the classical Dahlquist knee problem [13, pg. 46]. This is a classical problem that highlights some of the failings of standard mathematical software packages in solving singularly perturbed problems. There are intersecting reduced solutions which cause a switch in stability between these reduced solutions. We will show there exists a weak layer in the solution at the point of intersection of the reduced solutions that requires the use of a fine mesh.

The main results in this chapter appear in [25].

Chapter 3

We examine a linear boundary turning-point problem of the form

$$(\varepsilon y'' + a_\varepsilon y' - by)(x) = q(x), \quad x \in (0,1), \quad y(0) = 0,\ y(1) > 0, \tag{1.7.2a}$$

$$b(x) \geqslant 0, \quad a_\varepsilon(x) \approx C(1 - e^{-\alpha x/\varepsilon}). \tag{1.7.2b}$$

Note that the convection co-efficient exponentially approaches zero at the boundary $x = 0$. This problem acts as a model for the corresponding nonlinear boundary turning-point problem:

$$(\varepsilon u'' + u u' - bu)(x) = q(x), \quad b(x) > 0, \quad x \in (0,1), \quad u(0) = 0, \quad u(1) > 0.$$

The convection co-efficient is the solution u itself, which is zero at the boundary point $x = 0$. The solution u is shown to have the same character as the co-efficient a_ε in (1.7.2).

Note, the main contents of this chapter have appeared in [24].

Chapter 4

We utilise the results from Chapter 3 to investigate if nonlinear interior layer problems, having the fundamental structure (1.6.1) and with certain restrictions placed on the boundary conditions, can be suitably approximated with a left and right boundary turning point problem 'joined' together at some point. It transpires that this interface point is required to be within a fine mesh point of the unknown root of the solution. Since our only approximation to the layer location, as far as this author knows, is the Howes point [12], this numerical method may not be valuable. The results from this chapter indicate that an interior layer problem is not akin to solving two boundary turning point problems.

Note, the main contents of this chapter have been published in [23].

Chapter 5

As in Chapter 3, we consider a linear interior layer problem to act as a model for the corresponding nonlinear interior layer problem. The problem we consider is;

$$(\varepsilon u'' + a u' - bu)(x) = q(x), \quad x \in (0,1), \quad u(0) > 0 > u(1),$$

$$b(x) \geq 0, \quad |a(x)| \geq C \tanh\left(\frac{\alpha}{\varepsilon}|x - d|\right), \quad d \in (0,1).$$

The convection co-efficient has an interior turning point of exponential form and the solution exhibits an interior layer at $x = d$. A similar problem, in which the convection co-efficient is discontinuous and changing sign in the interior was examined in [8]. However, we study the above problem as it is a more suitable model for the corresponding nonlinear problem in which the convection co-efficient is continuous. Furthermore, the 'optimal' point to centre a fine Shishkin mesh is the point where the linear convection co-efficient vanishes. We investigate how far away from this point we can centre the fine mesh and maintain parameter uniform convergence. The results are encouraging. It transpires that a practical and reasonable distance of $O(\varepsilon)$ suffices. This does not mean that that the same result will apply to the corresponding nonlinear problem. However it is further motivation in centring a fine mesh at the Howes point when seeking an approximation to (1.6.1).

Note, the main contents of this chapter have appeared in [26].

Chapter 6

We experiment with the Shishkin algorithm outlined in [32]. The algorithm, as written, is somewhat vague and ambiguous in places. The user is left to decide on how to implement the required theoretical steps. We propose certain choices in these cases and slight alternatives purely so that the algorithm is implementable.

This chapter is purely computational. However, as far as the author knows, there is no equivalent Howes' point type approximation for a time-dependent interior layer problem. This chapter demonstrates that such an approximation is computable. Furthermore, analysis in [32] may assist in any of our future analysis of Burgers'-type problems.

The contents of this chapter have been submitted to the proceedings of the Fifth Conference on Numerical Analysis and Applications, June 15-20, 2012, Lozenetz, Bulgaria, (to appear in Lecture Notes in Computer Science, Springer).

CHAPTER: 2

NONLINEAR INITIAL VALUE PROBLEMS

2.1: INTRODUCTION

In this chapter we study several classes of singularly perturbed nonlinear initial value problems. We start in §2.2, by considering the singularly perturbed initial value problem

$$\varepsilon y' = f(x,y), \quad y(0) \text{ given},$$

with a restriction placed on the y-derivatives of f and on the initial condition. We will see that under this restriction on the nonlinearity, the character of the problem is close in nature to the singularly perturbed nonlinear problem $\varepsilon y' + y^n = 0$, $n \in \mathbb{N}$, $y(0) > 0$. We perform a careful analysis of the truncation error to establish an error bound on numerical approximations of the form (1.4.1) with $p = 1/n$.

In §2.3, we consider an extension of the problem class studied in [22], the Riccati problem:

$$\varepsilon u' + a(u^2 - g^2) = 0, \quad x > 0, \quad u(0) + \gamma > 0,$$
$$a, g \in C^1(0,1], \quad a(x) \geq \alpha > 0, \quad g(x) \geq \gamma > 0, \quad x \geq 0.$$

In this chapter, the constraint $u(0)+\gamma > 0$ from [22], which limits how close the initial condition can be to the unstable root $-g(x)$, is relaxed to $u(0)+g(0) > 0$. This allows initial conditions $u(0)$ to be close to $-g(0)$ and allows $-g'(x) > 0$. Furthermore, we study the cases where the stable root has multiplicity two and the initial condition is arbitrary close to an unstable reduced solution. The following problem class is examined:

$$\varepsilon u'(x) + a(x)\prod_{j=1}^{p}(u(x) - g_j(x)) = 0, \quad g_i(x) < g_j(x) \quad \text{if} \quad i < j,$$
$$\varepsilon u'(x) + a(x)\prod_{j=1}^{p}(u(x) - g_j(x))^2 = 0, \quad g_i(x) < g_j(x) \quad \text{if} \quad i < j.$$

The conditions on the initial condition $u(0)$ for a stable initial layer to form are identified. We construct upper and lower solutions which indicate that the character of a stable initial layer

function in the vicinity of a double root of the reduced problem is different to the standard layer structures appearing in the neighbourhood of a single root. Note that our main aim in this chapter is to establish parameter uniform convergence for any stated initial value problem class; however, such a bound is not established in the case where the initial condition is arbitrary close (within ε) to an unstable reduced solution. In this case, we present a *parameter explicit* error bound and present results of numerical experiments which confirm the parameter explicit bound.

In §2.4, we present results for the problem

$$\varepsilon z'(x)+a(x)(z(x)-\beta)(z(x)-g(x))=0, \quad \beta \text{ constant},$$
$$g'(x)\leqslant 0, \quad x\in[0,1], \quad g(d)=\beta, \quad d\in(0,1),$$

where a layer arises in the vicinity of the point where the two reduced solutions β, $g(x)$ intersect.

In §2.5, we present results of numerical experiments to test the adequacy of the parameter uniform bounds established in earlier sections. We also present results from using some inbuilt MATLAB functions to solve initial value problems when applied to our sample problems. These results display the inadequacy of employing standard packages to solve singularly perturbed problems.

In §2.6, we casually discuss two nonlinear problems that are similar to, but not contained within the classes of problems studied in the previous sections of this chapter.

2.2: A General Nonlinear Initial Value Problem

2.2.1 The Continuous Problem

Consider the nonlinear singularly perturbed initial value problem: find $y_\varepsilon \in C^1(\Omega)$ such that

$$\varepsilon y_\varepsilon'(x)=f(x,y_\varepsilon(x)), \qquad x\in\Omega:=(0,1], \qquad y_\varepsilon(0)=A, \tag{$\mathscr{A}_\varepsilon$}$$

where the data f and A satisfy Assumption 2.2.1 set out below.

2.2.1.1 Reduced Solutions

For the problem ($\mathscr{A}_\varepsilon$), a *reduced solution* is a solution $\tilde{r}$ of the zero order equation

$$f(x,\tilde{r}(x))=0, \quad x\in\Omega.$$

A reduced solution $\tilde{r}_1$ is *stable* on the interval $(a_1, b_1) \subset \Omega$ if it satisfies $f_y(x, \tilde{r}_1(x)) < 0$, $\forall\ x \in (a_1, b_1)$. If on the interval $(b_1, c_1) \subset \Omega$, another reduced solution $\tilde{r}_2$ is stable where $\tilde{r}_1(b_1) = \tilde{r}_2(b_1)$, then we may refer to the changeover of $\tilde{r}_1$ to $\tilde{r}_2$ satisfying $f_y < 0$ as a *switch in stability* from $\tilde{r}_1$ to $\tilde{r}_2$ at $x = b$. Moreover a reduced solution $\tilde{r}_3$ is *stable from above* if $f_y(x, \tilde{r}_3(x)) = 0$, $f_{yy}(x, \tilde{r}_3(x)) \leqslant 0$ and $\tilde{r}_3'(x) \leqslant 0$, $x \in \Omega$. Furthermore a reduced solution $\tilde{r}_4$ is *stable from below* if $f_y(x, \tilde{r}_4(x)) = 0$, $f_{yy}(x, \tilde{r}_4(x)) \geqslant 0$ and $\tilde{r}_4'(x) \geqslant 0$, $x \in \Omega$. A similar definition of stability can be constructed for a reduced solution $\tilde{r}_5$ satisfying $\partial^j f / \partial y^j(x, \tilde{r}_5(x)) = 0$, $\forall\ j < n$ for $n \geqslant 2$.

Assumption 2.2.1. *Assume $f \in C^n[S_\delta(r), \mathbb{R}]$ for $n \geqslant 1$ and that there exists $r \in C^1[\Omega, \mathbb{R}]$ such that*

$$\frac{\partial^j f}{\partial y^j}(x, r(x)) = 0 \quad \forall \quad 0 \leqslant j < n, \quad x \in \Omega, \tag{2.2.1a}$$

$$\frac{\partial^n f}{\partial y^n}(x, y) \leqslant -m < 0, \quad m > 0, \quad (x, y) \in S_\delta(r), \tag{2.2.1b}$$

$$\text{for } n \geqslant 2: \quad A \geqslant r(0) \quad \text{and} \quad r'(x) \leqslant 0, \tag{2.2.1c}$$

where

$$S_\delta(r) := \{(x, y) \,|\, x \in \Omega, \quad (r - \delta_1)(x) \leqslant y \leqslant (r + \delta_2)(x)\};$$

if $n = 1$, $\delta_1(x) > \min\{0, (A - r(0))e^{-mx/\varepsilon}\}$ and $\delta_2(x) > \max\{0, (A - r(0))e^{-mx/\varepsilon}\}$;
if $n \geqslant 2$, $\delta_1(x) > 0$ and $\delta_2(x) > (A - r(0))(1 + \theta_m x/\varepsilon)^{-1/(n-1)}$, $\theta_m < (A - r(0))^{n-1} m(n-1)/n!$
for all $x \in \Omega$.

We will see below that (2.2.1c) is merely convenient when n is odd and is necessary when n is even so that r acts as a lower solution. Furthermore, for $n \geqslant 2$, if $A \leqslant r(0)$ and $r' \geqslant 0$ then analogous results hold throughout when the inequalities in (2.2.1b) are reversed.

2.2.1.2 Existence and Uniqueness

For the problem $(\mathscr{A}_\varepsilon)$, a function $\underline{y} \in C^1[\Omega, \mathbb{R}]$ is a *lower solution* of $(\mathscr{A}_\varepsilon)$ if

$$\varepsilon \underline{y}' \leqslant f(x, \underline{y}) \quad \text{for} \quad x \in \Omega \quad \text{and} \quad \underline{y}(0) \leqslant A.$$

An *upper solution* is defined analogously. We use the concept of lower and upper solutions to prove existence of a solution to $(\mathscr{A}_\varepsilon)$ in the closed set $S = \{(x, t) \,|\, x \in \overline{\Omega},\ \underline{y}(x) \leqslant t \leqslant \overline{y}(x)\}$.

Theorem 2.2.1. *([16]) Let $\underline{y}, \overline{y} \in C^1[S_\delta(r)]$ be lower and upper solutions of $(\mathscr{A}_\varepsilon)$ such that $\underline{y} \leqslant \overline{y}$ on Ω and $f \in C^0[S, \mathbb{R}]$. Then there exists a solution y_ε of $(\mathscr{A}_\varepsilon)$ such that $\underline{y}(x) \leqslant y_\varepsilon(x) \leqslant \overline{y}(x)$ on $\overline{\Omega}$.*

Theorem 2.2.2. *Under Assumption 2.2.1 and for ε sufficiently small, there exists a unique solution y_ε to $(\mathscr{A}_\varepsilon)$ satisfying*

$$|(y_\varepsilon - r)(x)| \leqslant |A - r(0)| + C\varepsilon^{1/n}, \qquad x \in \overline{\Omega}.$$

Proof. Using

$$f(x,\alpha)-f(x,\beta)=(\alpha-\beta)\int_{t=0}^{1} f_y(x,\beta+t(\alpha-\beta))\,dt, \tag{2.2.2}$$

we can show inductively $\forall\ n\in\mathbb{N}$ that

$$f(x,\alpha)-f(x,\beta)-\sum_{i=1}^{n-1}\frac{1}{i!}(\alpha-\beta)^i\frac{\partial^i f}{\partial y^i}(x,\beta)=(\alpha-\beta)^n\mathcal{T}(f;\alpha,\beta,n), \quad \text{where} \tag{2.2.3a}$$

$$\mathcal{T}(f;\alpha,\beta,n):=\int_{t_1=0}^{1} t_1^{n-1}\int_{t_2=0}^{1} t_2^{n-2}\ldots\int_{t_n=0}^{1}\frac{\partial^n f}{\partial y^n}(x,\beta+(\alpha-\beta)\prod_{j_1=1}^{n}t_{j_1})\prod_{j_2=1}^{n}dt_{n+1-j_2}. \tag{2.2.3b}$$

If we define $\ell:=y_\varepsilon-r$ then using ($\mathscr{A}_\varepsilon$), Assumption 2.2.1 and (2.2.3) we can show that ℓ satisfies the problem

$$\varepsilon\ell'(x)-\mathcal{T}(f;(\ell+r)(x),r(x),n)(\ell(x))^n=-\varepsilon r'(x), \quad x\in\Omega, \quad \ell(0)=A-r(0). \tag{2.2.4}$$

Consider the solution to the problem

$$\varepsilon\bar{\ell}'(x)+\frac{m}{n!}(\bar{\ell}(x))^n=\varepsilon\|r'\|, \quad x\in\Omega, \quad \bar{\ell}(0)=A-r(0). \tag{2.2.5}$$

Using an expansion of $((\alpha-\beta)+\beta)^n$ and with $R_\varepsilon:=(\frac{n!}{m}\|r'\|\varepsilon)^{\frac{1}{n}}$, we can express the equation in (2.2.5) as

$$\varepsilon\bar{\ell}'(x)+\frac{m}{n!}(\bar{\ell}-R_\varepsilon)^n+\frac{m}{n!}\sum_{i=1}^{n-1}\frac{1}{i!}({}^nP_i){R_\varepsilon}^{n-i}(\bar{\ell}-R_\varepsilon)^i=0. \tag{2.2.6}$$

Consider the solution to the problem $\varepsilon\psi'+(m/n!)(\psi-R_\varepsilon)^n=0$, $\psi(0)=A-r(0)$ which is

$$\psi(x)=(A-r(0)-R_\varepsilon)e^{-mx/\varepsilon}+R_\varepsilon, \quad \text{if} \quad n=1,$$

$$\psi(x)=(A-r(0)-R_\varepsilon)\left(1+(A-r(0)-R_\varepsilon)^{n-1}\frac{(n-1)m}{n!}\frac{x}{\varepsilon}\right)^{-1/(n-1)}+R_\varepsilon, \quad \text{if} \quad n\geqslant 2.$$

Since $A-r(0)>0$ for $n\geqslant 2$ and supposing $A-r(0)>0$ if $n=1$ (the case of $n=1$ and $A-r(0)<0$ is proved analogously) then using (2.2.6) we can show, assuming ε is sufficiently small, that ψ is an upper solution of (2.2.5). Then using Assumption 2.2.1 and (2.2.5) we can show that $\bar{\ell}$ is an upper solution of (2.2.4). Also note that 0 (when $n\geqslant 2$) or $-R_\varepsilon$ (when $n=1$) is a lower solution for (2.2.4). Hence the existence of ℓ is established, which in turn establishes the existence of $y_\varepsilon=\ell+r$.

Now suppose y_1 and y_2 are two solutions to ($\mathscr{A}_\varepsilon$). Noting that $f\in C^1[S_\delta(r),\mathbb{R}]$, then $\Delta y:=y_1-y_2$ is the solution of the problem

$$\varepsilon(\Delta y)'=(\Delta y)\int_{t=0}^{1} f_y(x,y_2+t(\Delta y))dt, \quad x\in\Omega, \quad (\Delta y)(0)=0.$$

Hence

$$(\Delta y)(x)=(\Delta y)(0)\exp\left(\int_{s=0}^{x}\int_{t=0}^{1} f_y(s,u_2+t(\Delta y))dt\,ds\right)\equiv 0.$$

□

Remark: Note that for all odd n, if we did not assume that $r' \leqslant 0$ then $-R_\varepsilon$ would be a lower solution for (2.2.4).

2.2.1.3 Regular and Layer Components

Express the solution y_ε as the sum of two components v_ε and w_ε, where the regular component v_ε is defined as the solution to the problem

$$\varepsilon v_\varepsilon' = f(x, v_\varepsilon), \qquad x \in \Omega, \qquad v_\varepsilon(0) = r(0). \tag{2.2.7}$$

From Theorem 2.2.2, this problem has a unique solution v_ε satisfying

$$\min\{r(x)\} \leqslant v_\varepsilon(x) \leqslant \max\{r(x)\}, \qquad x \in \overline{\Omega}.$$

The unique layer component $w_\varepsilon = y_\varepsilon - v_\varepsilon$ satisfies the problem

$$\varepsilon w_\varepsilon' = \left(\frac{f(x, y_\varepsilon) - f(x, v_\varepsilon)}{y_\varepsilon - v_\varepsilon}\right) w_\varepsilon, \qquad x \in \Omega, \qquad w_\varepsilon(0) = (y_\varepsilon - v_\varepsilon)(0). \tag{2.2.8}$$

Theorem 2.2.3. *Under Assumption 2.2.1, if v_ε is the solution of (2.2.7) and w_ε is the solution of (2.2.8) then for sufficiently small ε we have*

$$\|v_\varepsilon - r\| \leqslant \left(\frac{n!}{m}\|r'\|\varepsilon\right)^{1/n} \qquad \text{and} \qquad \|v_\varepsilon'\| \leqslant \frac{C}{m}\|r'\|; \tag{2.2.9a}$$

$$|w_\varepsilon(x)| \leqslant |w_\varepsilon(0)| e^{-mx/\varepsilon}, \qquad n = 1; \tag{2.2.9b}$$

$$|w_\varepsilon(x)| \leqslant |w_\varepsilon(0)| \left(1 + |w_\varepsilon(0)|^{n-1} \frac{m(n-1)}{n!} \frac{x}{\varepsilon}\right)^{-1/(n-1)}, \qquad n \geqslant 2, \qquad x \in \overline{\Omega}. \tag{2.2.9c}$$

Proof. If we define $\chi := v_\varepsilon - r$, then from the proof in Theorem 2.2.2 we have

$$|(v_\varepsilon - r)(x)| \leqslant R_\varepsilon := \left(\frac{n!}{m}\|r'\|\varepsilon\right)^{1/n}, \quad n = 1, \quad 0 \leqslant (v_\varepsilon - r)(x) \leqslant R_\varepsilon, \quad n \geqslant 2, \quad x \in \overline{\Omega}. \tag{2.2.10}$$

Furthermore, using Assumption 2.2.1 and (2.2.3) we can show that

$$|v_\varepsilon'(x)| = \frac{1}{\varepsilon}|f(x, (r+\chi)(x))| \leqslant \frac{1}{\varepsilon}\|v_\varepsilon - r\|^n \frac{1}{n!}\left\|\frac{\partial^n f}{\partial y^n}\right\| \leqslant \frac{C}{m}\|r'\|.$$

Using (2.2.3) we can expand the equation (2.2.8) for the layer component in the following way

$$\varepsilon w_\varepsilon' = f(x, y_\varepsilon) - f(x, v_\varepsilon) = \mathcal{T}(f; y_\varepsilon, v_\varepsilon, n) w_\varepsilon^n + \sum_{i=1}^{n-1} \frac{1}{i!} \frac{\partial^i f}{\partial y^i}(x, v_\varepsilon) w_\varepsilon^i. \tag{2.2.11}$$

Note that when $n = 1$ the summation term in (2.2.11) is zero. For $n \geqslant 2$ and $i < n$ we can use Assumption 2.2.1, (2.2.3) and (2.2.10) to show that

$$\frac{\partial^i f}{\partial y^i}(x, v_\varepsilon) = \frac{\partial^i f}{\partial y^i}(x, v_\varepsilon) - \frac{\partial^i f}{\partial y^i}(x, r) - \sum_{j=i+1}^{n-1} \frac{1}{(j-i)!}(v_\varepsilon - r)^{(j-i)} \frac{\partial^j f}{\partial y^j}(x, r)$$

$$= (v_\varepsilon - r)^{(n-i)} \int_{t_1=0}^{1} t_1^{n-i-1} \dots \int_{t_{n-i}=0}^{1} \frac{\partial^n f}{\partial y^n}(x, r + (v_\varepsilon - r)\prod_{j_1=1}^{n-i} t_{j_1}) \prod_{j_2=1}^{n-i} d\, t_{n-i+1-j_2} \leqslant 0. \tag{2.2.12}$$

Hence if $A - r(0) > 0$ in the case of $n = 1$, then for all $n \in \mathbb{N}$ we can show that the solution $\overline{w}$ to

$$\varepsilon \overline{w}' + \frac{m}{n!}\overline{w}^n = 0, \qquad \overline{w}(0) = w_\varepsilon(0), \qquad x \in \Omega,$$

is an upper solution and that $\underline{w} = 0$ is a lower solution of (2.2.11). If $n = 1$ with $A - r(0) < 0$ then the layer component is bounded in the same manner. By explicitly solving for $\overline{w}$, the bounds in (2.2.9) follow. □

2.2.2 The Discrete Problem

Consider the discrete nonlinear problem: find a mesh function Y_ε^N such that

$$\varepsilon D^- Y_\varepsilon^N(x_i) = f(x_i, Y_\varepsilon^N(x_i)), \qquad x_i \in \Omega_n^N, \qquad Y_\varepsilon^N(0) = A, \tag{$\mathscr{A}_\varepsilon^N$}$$

where $D^- Y_\varepsilon^N(x_i) := \frac{1}{h_i}(Y_\varepsilon^N(x_i) - Y_\varepsilon^N(x_{i-1}))$, $h_i = x_i - x_{i-1}$. As illustrated in [7], when the layer component is bounded by an ε-dependent decaying exponential of the form $e^{-\theta x/\varepsilon}$ then we have $e^{-\theta x/\varepsilon} \leqslant \frac{1}{N}$ if $x \geqslant \frac{\varepsilon}{\theta}\ln N$. This motivates the choice of $\frac{\varepsilon}{\theta}\ln N$ as a transition point between a fine initial mesh and a coarse outer mesh. For $n \geqslant 2$, similarly we solve for $w_\varepsilon(x) \leqslant 1/\Phi(N)$, for some positive function Φ decreasing in N which we choose momentarily, and take a transition point of the form $\frac{n!\varepsilon}{m(n-1)}\Phi(N)^{n-1}$. Define the mesh Ω_n^N as follows

$$\Omega_n^N := \left\{ x_i \,\middle|\, x_i = \frac{2\sigma}{N} i, \quad 0 \leqslant i \leqslant \frac{N}{2}, \;\; x_i = \sigma + \frac{2(1-\sigma)}{N}\left(i - \frac{N}{2}\right), \;\; \frac{N}{2} < i \leqslant N \right\}, \tag{2.2.13a}$$

$$\sigma := \min\left\{\frac{1}{2}, \frac{\mu_n n!\varepsilon}{m} L_n(N)\right\}, \quad \mu_1 = 1, \quad \mu_n > \frac{1}{n-1} \;\; \forall \;\; n \geqslant 2, \tag{2.2.13b}$$

$$\text{where} \quad L_1(N) := \ln N \quad \text{and} \quad L_n(N) = \Phi(N)^{n-1} := N^{\frac{n-1}{n}} \;\; \forall \;\; n \geqslant 2. \tag{2.2.13c}$$

We explain the motivation for this choice of $\Phi(N)$ in the following. Suppose $\sigma < \frac{1}{2}$, when $i \leqslant \frac{N}{2}$ we require $h_i \varepsilon^{-1} = O(N^{-1}\Phi(N)^{n-1}) \to 0$ as $N \to \infty$ and when $i > \frac{N}{2}$ we require $1/\Phi(N) \to 0$ as $N \to \infty$. If $\Phi(N)$ is of the form $\Phi(N) = N^p$, $p > 0$, then $p(n-1) - 1 < 0 \iff p < \frac{1}{n-1}$. Thus a choice of $p = \frac{1}{n}$ suffices to guarantee convergence as N increases when $\Phi(N) = N^p$.

The next theorem provides for the existence of a discrete solution via the existence of discrete lower and upper solutions. The proof of this theorem is an obvious extension of the proof in [22, pg. 377] to the problem ($\mathscr{A}_\varepsilon^N$).

Theorem 2.2.4. *Suppose there exists two mesh functions $\overline{Y}^N$ and $\underline{Y}^N$ such that $\overline{Y}^N(0) \geqslant y_\varepsilon(0) \geqslant \underline{Y}^N(0)$, $\overline{Y}^N \geqslant \underline{Y}^N$ and $\varepsilon D^- \overline{Y}^N - f(x_i, \overline{Y}^N) \geqslant 0 \geqslant \varepsilon D^- \underline{Y}^N - f(x_i, \underline{Y}^N)$ on Ω_n^N then there is a solution Y_ε^N to ($\mathscr{A}_\varepsilon^N$) satisfying $\underline{Y}^N \leqslant Y_\varepsilon^N \leqslant \overline{Y}^N$, $x_i \in \Omega_n^N$.*

For ($\mathscr{A}_\varepsilon^N$), we establish the existence of a solution by bounding the discrete regular and layer components in the decomposition $Y_\varepsilon^N = V_\varepsilon^N + W_\varepsilon^N$. The discrete regular component V_ε^N is

defined as the solution of

$$\varepsilon D^- V_\varepsilon^N(x_i) = f(x_i, V_\varepsilon^N(x_i)), \qquad x_i \in \Omega_n^N, \qquad V_\varepsilon^N(0) = v_\varepsilon(0). \tag{2.2.14}$$

The discrete layer component W_ε^N is defined as the solution of

$$\varepsilon D^- W_\varepsilon^N(x_i) = \left(\frac{f(x_i, Y_\varepsilon^N(x_i)) - f(x_i, V_\varepsilon^N(x_i))}{Y_\varepsilon^N(x_i) - V_\varepsilon^N(x_i)} \right) W_\varepsilon^N(x_i), \quad x_i \in \Omega_n^N, \quad W_\varepsilon^N(0) = w_\varepsilon(0). \tag{2.2.15}$$

We show the existence of a solution to $(\mathscr{A}_\varepsilon^N)$ in the following theorem.

Theorem 2.2.5. *If V_ε^N and W_ε^N are the discrete solutions of (2.2.14) and (2.2.15) respectively then the solution to $(\mathscr{A}_\varepsilon^N)$ is unique and satisfies $Y_\varepsilon^N = V_\varepsilon^N + W_\varepsilon^N$. For sufficiently small ε and sufficiently large N and $\mu > 1$ we have the following bounds*

$$|(V_\varepsilon^N - r)(x_i)| \leqslant \frac{\|r'\|}{m}\varepsilon, \quad n = 1, \quad 0 \leqslant (V_\varepsilon^N - r)(x_i) \leqslant \left(\frac{n!\|r'\|}{m}\varepsilon \right)^{1/n}, \quad n \geqslant 2, \quad x \in \Omega_n^N. \tag{2.2.16a}$$

$$|W_\varepsilon^N(x_i)| \leqslant \mu |w_\varepsilon(0)| e^{-m x_i/\varepsilon} + CN^{-1}, \quad x_i \in \Omega_n^N, \quad n = 1, \tag{2.2.16b}$$

$$|W_\varepsilon^N(x_i)| \leqslant |w_\varepsilon(0)| \left(1 + \frac{|w_\varepsilon(0)|^{n-1} m(n-1)}{\mu n!} \frac{x_i}{\varepsilon} \right)^{-1/(n-1)} + CN^{-1/n}, \quad x_i \in \Omega_n^N, \quad n \geqslant 2. \tag{2.2.16c}$$

Proof. Define $\Gamma^N := V_\varepsilon^N - r$. As in the proof of Theorem 2.2.2 we can use discrete upper and lower solutions to show that Γ^N exists and satisfies $0 \leqslant \Gamma^N(x_i) \leqslant R_\varepsilon$ for $n \geqslant 2$ and $|\Gamma^N(x_i)| \leqslant R_\varepsilon$ for $n = 1$ for all $x_i \in \Omega_n^N$, where $R_\varepsilon := (n!\|r'\|\varepsilon/m)^{1/n}$.

As in the proof of Theorem 2.2.3, we expand the equation for the discrete layer component as follows

$$\varepsilon D^- W_\varepsilon^N(x_i) = \mathcal{T}(f; (V_\varepsilon^N + W_\varepsilon^N)(x_i), V_\varepsilon^N(x_i), n) W_\varepsilon^N(x_i)^n + \sum_{j=1}^{n-1} \frac{1}{j!} \frac{\partial^j f}{\partial y^j}(x_i, V_\varepsilon^N(x_i)) W_\varepsilon^N(x_i)^j. \tag{2.2.17}$$

Note that when $n = 1$ the summation term in (2.2.17) is zero. For $n \geqslant 2$ and $i < n$ we can use Assumption 2.2.1, (2.2.3) and (2.2.16a) to show that $\frac{\partial^i f}{\partial y^i}(x_i, V_\varepsilon^N) \leqslant 0$.

We first consider $\sigma < 1/2$. If $n = 1$, suppose that $A - r(0) > 0$ and consider the discrete function

$$\overline{W}^N(x_i) := w_\varepsilon(0) \prod_{j=1}^{i} \left(1 + m\frac{h_j}{\varepsilon} \right)^{-1} \quad 0 < i \leqslant \frac{N}{2}, \qquad \overline{W}^N(x_0) := w_\varepsilon(0). \tag{2.2.18}$$

We state a few useful inequalities that we use occasionally throughout the thesis:

$$\underbrace{e^{(1-t/2)t} \leqslant 1 + t \leqslant \overbrace{e^t}^{t\in[0,0.5]} \leqslant 1 + 2t}_{t>0} \tag{2.2.19a}$$

$$e^{-(1+t)t} \leqslant 1 - t \leqslant e^{-t} \leqslant 1 - t/2, \quad t \in [0, 0.5], \tag{2.2.19b}$$

Using (2.2.19) for sufficiently small ε and sufficiently large N, we can show that $\overline{W}^N(x_i) \leqslant \mu w_\varepsilon(0)e^{-mx_i/\varepsilon}$ for $i \leqslant N/2$ for some $\mu > 1$. Then using Assumption 2.2.1 and (2.2.16a) we can show, using upper and lower solutions, that $0 \leqslant W_\varepsilon^N(x_i) \leqslant \overline{W}^N(x_i)$ for $i \leqslant N/2$. At $i = N/2$, using (2.2.13) with (2.2.18), we have $\overline{W}^N(\sigma) \leqslant CN^{-1}$. Thus we can show through upper and lower solutions that $0 \leqslant W_\varepsilon^N(x_i) \leqslant CN^{-1}$ for $i > N/2$. The proof of the case $n = 1$ and $A - r(0) < 0$ follows the same argument.

For $n \geqslant 2$, where we have $w_\varepsilon(0) > 0$, consider the function ω such that

$$\omega(x)^{n-1} = w_\varepsilon(0)^{n-1}\left(1+\theta\frac{x}{\varepsilon}\right)^{-1}, \quad \theta = \frac{1}{\mu n!}w_\varepsilon(0)^{n-1}(n-1)m, \quad \mu > 1, \quad x \in \overline{\Omega}. \tag{2.2.20}$$

Note that

$$0 \geqslant \omega(x_i)^{n-1} - \omega(x_{i-1})^{n-1} \geqslant -Ch_i\varepsilon^{-1}\omega(x_{i-1})^{n-1}, \quad x_i \in \Omega_n^N \setminus \{x_0\}.$$

Using (2.2.13) we have $\mu\omega(x_i)^{n-1} - \omega(x_{i-1})^{n-1} \geqslant 0$ for $i \leqslant N/2$ for $\mu > 1$ and for sufficiently large N. Clearly, we also have $\omega(x_{i-1}) > \omega(x_i)$. Under Assumption 2.2.1, we have $-\mathcal{T}(f;(V_\varepsilon^N + \omega)(x_i), V_\varepsilon^N(x_i), n) \geqslant m/n!$. Using a factorisation of $\alpha^n - \beta^n$ and using the notation $\omega_i^n := \omega(x_i)^n$ we can show that

$$\varepsilon D^-\omega_i + \theta\, w_\varepsilon(0)^{1-n}\frac{\omega_i^{n-1}\omega_{i-1}^{n-1}}{\sum_{k=0}^{n-2}\omega_i^{n-2-k}\omega_{i-1}^k} = 0.$$

Using (2.2.17) with the notation $\mathcal{T}^+ = -\mathcal{T}(f;(V_\varepsilon^N+\omega)(x_i), V_\varepsilon^N(x_i), n)$ and using the inequalities in the previous paragraph, we can show that

$$\varepsilon D^-\omega_i + \mathcal{T}^+{\omega_i}^n - \sum_{j=1}^{n-1}\frac{1}{j!}\frac{\partial^j f}{\partial y^j}(x_i, V_\varepsilon^N(x_i)){\omega_i}^j \geqslant \mathcal{T}^+{\omega_i}^n - \theta\, w_\varepsilon(0)^{1-n}\frac{\omega_i^{n-1}\omega_{i-1}^{n-1}}{\sum_{k=0}^{n-2}\omega_i^{n-2-k}\omega_{i-1}^k}$$

$$\geqslant \omega_i\left(\mathcal{T}^+\omega_i^{n-1} - \frac{\theta\, w_\varepsilon(0)^{1-n}}{n-1}\omega_{i-1}^{n-1}\right) \geqslant \frac{m}{\mu n!}\omega_i\left(\mu{\omega_i}^{n-1} - {\omega_{i-1}}^{n-1}\right) \geqslant 0.$$

Thus ω is an upper solution and since 0 is a lower solution we have $0 \leqslant W_\varepsilon^N(x_i) \leqslant \omega(x_i)$ for $i \leqslant N/2$. At $i = N/2$, using (2.2.13) with (2.2.20), we have $\omega(\sigma) \leqslant CN^{-\frac{1}{n}}$. Thus we can show through upper and lower solutions that $0 \leqslant W_\varepsilon^N(x_i) \leqslant CN^{-\frac{1}{n}}$ for $i > N/2$.

The proof of the case $\sigma = 1/2$ is analogous to the case $\sigma < 1/2$ and $i \leqslant N/2$, where we use (2.2.13) to show that $h_i\varepsilon^{-1} \leqslant CN^{-1}L_n(N)$, $\forall\, 0 \leqslant i \leqslant N$ for all $n \geqslant 1$.

Therefore $Y_\varepsilon^N = V_\varepsilon^N + W_\varepsilon^N$ exists and satisfies $\varepsilon D^- Y_\varepsilon^N(x_i) = f(x_i, Y_\varepsilon^N(x_i))$, $x_i \in \Omega_n^N$, $Y_\varepsilon^N(0) = A$. To prove uniqueness, suppose Y_1^N and Y_2^N are two solutions of $(\mathscr{A}_\varepsilon^N)$ then $(\Delta Y)^N := Y_1^N - Y_2^N$ satisfies $\varepsilon D^-(\Delta Y)^N(x_i) = f(x_i, Y_1^N(x_i)) - f(x_i, Y_2^N(x_i))$, $(\Delta Y)^N(x_0) = 0$. Hence using Assumption 2.2.1 we have

$$(\Delta Y)^N(x_i) = (\Delta Y)^N(x_{i-1})\left(1 - \frac{h_i}{\varepsilon}\int_{t=0}^1 f_y(x_i, (Y_2^N + t(\Delta Y)^N)(x_i)\right)^{-1} \equiv 0.$$

□

We establish a bound on the error $(Y_\varepsilon^N - y_\varepsilon)(x_i)$ in the following theorem.

Theorem 2.2.6. *Under Assumption 2.2.1, if y_ε is the solution to $(\mathscr{A}_\varepsilon)$ and $\overline{Y}_\varepsilon$ is the piecewise linear interpolation of Y_ε^N, the solution to $(\mathscr{A}_\varepsilon^N)$, then for sufficiently small ε and sufficiently large N we have*

$$\|\overline{Y}_\varepsilon^N - y_\varepsilon\|_{[0,1]} \leqslant \begin{cases} CN^{-1}\ln N, & n=1, \\ CN^{-1/n}, & n \geqslant 2. \end{cases}$$

Proof. Consider $\sigma < 1/2$. We first bound the truncation error for $i \leqslant N/2$. That is,

$$\tau^N(x_i) := \varepsilon(D^- y_\varepsilon - y_\varepsilon')(x_i) = h^{-1}\int_{x_{i-1}}^{x_i} \varepsilon y_\varepsilon'(t) - \varepsilon y_\varepsilon'(x_i)\,dt, \quad h := x_i - x_{i-1}, \quad i \leqslant N/2.$$

Using (2.2.3), for any $0 \leqslant t \leqslant x$ we have

$$f(x, y_\varepsilon(t)) - f(x, y_\varepsilon(x)) \tag{2.2.21a}$$

$$= \sum_{j=1}^{n-1} \frac{1}{j!}\frac{\partial^j f}{\partial y^j}(x, y_\varepsilon(x))(y_\varepsilon(t) - y_\varepsilon(x))^j + \mathcal{T}(f; y_\varepsilon(t), y_\varepsilon(x), n)(y_\varepsilon(t) - y_\varepsilon(x))^n. \tag{2.2.21b}$$

Note that when $n = 1$ the summation term in (2.2.21) is zero. For $n \geqslant 2$, we can show in the same manner as (2.2.12) that $\frac{\partial^j f}{\partial y^j}(x, y_\varepsilon(x)) \leqslant 0$, $j < n$. Using Assumption 2.2.1, (2.2.3) and Theorem 2.2.3 we have

$$\varepsilon y_\varepsilon'(x) = f(x, y(x)) = (y(x) - r(x))^n \mathcal{T}(f; y_\varepsilon, r, n) \leqslant 0.$$

That is $y_\varepsilon' \leqslant 0$ and $\|y_\varepsilon'\| \leqslant C\varepsilon^{-1}$. Using Assumption 2.2.1 we have $\mathcal{T}(f; y_\varepsilon(t), y_\varepsilon(x), n) \leqslant -m/n!$. Using these inequalities we can bound the truncation error for all $n \in \mathbb{N}$ as follows

$$-C\left(h + \sum_{j=1}^{n-1}\frac{1}{j!}\left|\frac{\partial^j f}{\partial y^j}(x_i, y_\varepsilon(x_i))\right| h^j \varepsilon^{-j} + h^n \varepsilon^{-n}\right) \leqslant \tau^N(x_i) \leqslant Ch. \tag{2.2.22}$$

For all $n \in \mathbb{N}$, $x_i \in \Omega_n^N$ and for any $\sigma \leqslant 1/2$ we can bound the truncation error for the regular component using $\varepsilon|(D^- v_\varepsilon - v_\varepsilon')(x_i)| \leqslant C \max h_i \leqslant CN^{-1}$.

Now we bound the error $E^N := Y_\varepsilon^N - y_\varepsilon$ for $i \leqslant N/2$. At all mesh points $x_i \in \Omega_n^N$, from $(\mathscr{A}_\varepsilon)$ and $(\mathscr{A}_\varepsilon^N)$, we have

$$\varepsilon D^- Y_\varepsilon^N(x_i) - \varepsilon y_\varepsilon'(x_i) = f(x_i, Y_\varepsilon^N(x_i)) - f(x_i, y_\varepsilon(x_i)).$$

Using expansions as before, we see that the error E^N satisfies

$$(\varepsilon D^- E^N + \tau^N)(x_i) = \mathcal{T}(f; Y_\varepsilon^N(x_i), y_\varepsilon(x_i), n)E^N(x_i)^n + \sum_{j=1}^{n-1}\frac{1}{j!}\frac{\partial^j f}{\partial y^j}(x_i, y_\varepsilon(x_i))E^N(x_i)^j, \; E^N(0) = 0. \tag{2.2.23}$$

For $n=2$, recalling that $\frac{\partial^j f}{\partial y^j}(x_i, y_\varepsilon(x_i)) \leqslant 0$ and using (2.2.22) we can show that $\overline{E}^N(x_i) := Ch\varepsilon^{-1}(1+x_i)$ is an upper solution of (2.2.23).

Writing

$$\varepsilon D^- Y_\varepsilon^N(x_i) - \varepsilon y_\varepsilon'(x_i) = -(f(x_i, y_\varepsilon(x_i)) - f(x_i, Y_\varepsilon^N(x_i))),$$

expanding $(f(x_i, y_\varepsilon(x_i)) - f(x_i, Y_\varepsilon^N(x_i)))$ and using Theorem 2.2.5 to show that $\frac{\partial^j f}{\partial y^j}(x_i, Y_\varepsilon^N(x_i)) \leqslant 0$, $j < n$, we can rewrite (2.2.23) and show that $-\overline{E}^N$ is a lower solution. For $n=1$ we can similarly show that $|E^N(x_i)| \leqslant Ch\varepsilon^{-1}$ for $i \leqslant N/2$. Therefore, $\forall\ n \in \mathbb{N}$ and $i \leqslant N/2$, we have $|(Y_\varepsilon^N - y_\varepsilon)(x_i)| \leqslant Ch\varepsilon^{-1} \leqslant CN^{-1}L_n(N)$.

We now bound the error E^N for $i \geqslant N/2$. First we bound the error $E_v^N := V_\varepsilon^N - v_\varepsilon$ for all $x_i \in \Omega_n^N$ and for all $\sigma \leqslant 1/2$. As with the error E^N, and using the notation $\tau_v^N(x_i) := \varepsilon(D^- v_\varepsilon - v_\varepsilon')(x_i)$, we can show that E_v^N satisfies

$$(\varepsilon D^- E_v^N + \tau_v^N)(x_i) = \mathcal{T}(f; V_\varepsilon^N(x_i), v_\varepsilon(x_i), n)E_v^N(x_i)^n + \sum_{j=1}^{n-1} \frac{1}{j!}\frac{\partial^j f}{\partial y^j}(x_i, v_\varepsilon(x_i))E_v^N(x_i)^j,\ E_v^N(0) = 0. \tag{2.2.24}$$

As before, for all $n \geqslant 2$ we can show that $\frac{\partial^j f}{\partial y^j}(x, v_\varepsilon(x_i)) \leqslant 0$ and $\frac{\partial^j f}{\partial y^j}(x, V_\varepsilon^N(x_i)) \leqslant 0$, $j < n$. Hence, for all $n \in \mathbb{N}$ we can establish that $E^{N\pm}_v = \pm(n!/m\|\tau_v\|)^{1/n}$ are upper and lower solutions respectfully. Thus $\forall\ n \in \mathbb{N}$ we have $|(V_\varepsilon^N - v_\varepsilon)(x_i)| \leqslant CN^{-\frac{1}{n}}$, $x_i \in \Omega_n^N$, $\sigma \leqslant 1/2$. Thus using (2.2.13) and Theorems 2.2.3 and 2.2.5, for $i \geqslant N/2$ we have that

$$|(Y_\varepsilon^N - y_\varepsilon)(x_i)| \leqslant |(V_\varepsilon^N - v_\varepsilon)(x_i)| + |(W_\varepsilon^N - w_\varepsilon)(x_i)| \leqslant CN^{-1/n} + |W_\varepsilon^N(x_i)| + |w_\varepsilon(x_i)| \leqslant CN^{-1/n}.$$

The proof of the case $\sigma = 1/2$ is analogous to the case $\sigma < 1/2$ and $i \leqslant N/2$, where we note that $h\varepsilon^{-1} \leqslant CN^{-1}L_n(N)$, for all $n \geqslant 1$. The global error bound can be established in the same manner as in [22, pg. 381]. □

2.3: A Particular Class of Nonlinear Problems

2.3.1 The Continuous Problem

Consider the following nonlinear singularly perturbed initial value problem: find $u_\varepsilon \in C^1(\Omega)$ such that

$$\varepsilon u_\varepsilon' = k(x, u_\varepsilon(x)) := -a(x)\prod_{j=1}^{p}(u_\varepsilon(x) - g_j(x))^{n_j}, \quad x \in \Omega := (0,1], \quad u_\varepsilon(0) = A,$$

$$n_j \in \mathbb{N}, \quad a \in C^0[\Omega, \mathbb{R}], \quad g_i \in C^1[\Omega, \mathbb{R}], \quad \underline{\gamma}_i := \min_{x\in\Omega} g_i(x),\ \overline{\gamma}_i := \max_{x\in\Omega} g_i(x),\ 1 \leqslant i \leqslant p, \qquad (\mathscr{B}_\varepsilon)$$

$$g_i(x) < g_j(x), \quad 1 \leqslant i < j \leqslant p, \quad a(x) \geqslant \alpha > 0, \quad x \in \Omega.$$

Note that the inequality $g_i(x) < g_j(x)$ above is strict, implying that the reduced solutions are all distinct.

2.3.1.1 Stability of the Reduced Solutions

From §2.2.1.1, each function g_i in $(\mathscr{B}_\varepsilon)$ is a reduced solution. Suppose the given initial condition satisfies $g_q(0) < u_\varepsilon(0) < g_{q+1}(0)$ for some $q \in \{1, 2, \ldots, p-1\}$, then note the following:

(1) If $\sum_{j=q+1}^{p} n_j$ is even then we only examine the cases of either (a) $n_q = 1$ or (b) $n_q = 2$ and $g_q' \leqslant 0$ on $[0,1]$.

(2) If $\sum_{j=q+1}^{p} n_j$ is odd then we only examine the cases of either (a) $n_{q+1} = 1$ or (b) $n_{q+1} = 2$ and $g_{q+1}' \geqslant 0$ on $[0,1]$.

(3) Furthermore, if $u_\varepsilon(0) < g_1(0)$ then we only consider $\sum_{j=1}^{p} n_j$ odd and the cases (a) $n_1 = 1$ or (b) $n_1 = 2$ and $g_1' \geqslant 0$. On the other hand, if $u_\varepsilon(0) > g_n(0)$ then we only consider the cases (a) $n_p = 1$ or (b) $n_p = 2$ and $g_p' \leqslant 0$.

These restrictions are used to show that g_q in case (1), g_{q+1} in case (2) or g_1 or g_p in case (3) are stable, all according to the discussion in §2.2.1.1. Hence, for any $u_\varepsilon(0)$, there is a reduced solution g_s, $1 \leqslant s \leqslant p$, that satisfies one of the stability definitions. To ease notation, we refer to this g_s as the *stable reduced solution of* $(\mathscr{B}_\varepsilon)$ *associated with* $u_\varepsilon(0)$ but we explicitly state the value of n_s and the sign of g_s' when required. It follows that:

$$\text{If } n_s = 1 \text{ then } \sum_{j=s+1}^{p} n_j \text{ is even.} \tag{2.3.1a}$$

$$\text{If } n_s = 2 \text{ and } g_s \text{ is stable from above then } \sum_{j=s+1}^{p} n_j \text{ is even.} \tag{2.3.1b}$$

$$\text{If } n_s = 2 \text{ and } g_s \text{ is stable from below then } \sum_{j=s+1}^{p} n_j \text{ is odd.} \tag{2.3.1c}$$

In the case of $n_s = 1$, we consider both the initial condition bounded away from an unstable reduced solution and the initial condition arbitrary close to an unstable reduced solution i.e. (a) $u_\varepsilon(0) = g_{s-1}(0) + \lambda\varepsilon$ or (b) $u_\varepsilon(0) = g_{s+1}(0) - \lambda\varepsilon$, $\lambda > 0$. In such cases, we pose the following restrictions

$$\text{If } u_\varepsilon(0) = g_{s-1}(0) + \lambda\varepsilon \text{ then } g_s \text{ is a constant function, } g_{s-1}(0) = \overline{\gamma}_{s-1} \text{ and } n_{s-1} = 1. \tag{2.3.2a}$$

$$\text{If } u_\varepsilon(0) = g_{s+1}(0) - \lambda\varepsilon \text{ then } g_s \text{ is a constant function, } g_{s+1}(0) = \underline{\gamma}_{s+1} \text{ and } n_{s+1} = 1. \tag{2.3.2b}$$

2.3.1.2 Existence and Uniqueness

Since $k \in C^1(\Omega)$, uniqueness is established by Theorem 2.2.2. Referring to §2.2.1.2, we establish the existence of a solution to $(\mathscr{B}_\varepsilon)$ by the construction of lower and upper solutions. In Theorem 2.3.1, we establish the existence of a solution when the initial condition is sufficiently close to the stable reduced solution. In Theorem 2.3.2, existence is established for initial conditions which are not sufficiently close to the stable reduced solution.

We introduce two parameters $\underline{\mu}$ and $\overline{\mu}$, independent of ε, with $0 < \underline{\mu}, \overline{\mu} < 1$. Define the constants

$$\underline{A}_s := \overline{\gamma}_{s-1} + \underline{\mu}(\underline{\gamma}_s - \overline{\gamma}_{s-1}), \quad s > 1, \qquad \overline{A}_s := \underline{\gamma}_{s+1} - \overline{\mu}(\underline{\gamma}_{s+1} - \overline{\gamma}_s), \quad s < p, \tag{2.3.3}$$

where particular choices for $\underline{\mu}$ and $\overline{\mu}$ are taken in the proof of Theorem 2.3.4 below. Since $g_i < g_j$, $1 \leqslant i < j \leqslant p$ in $(\mathscr{B}_\varepsilon)$ and from the bounds on $\underline{\mu}$ and $\overline{\mu}$, the strict inequality for $1 < s < p$ follows

$$g_{s-1}(x) < \underline{A}_s < g_s(x) < \overline{A}_s < g_{s+1}(x), \quad x \in [0,1]. \tag{2.3.4}$$

The following theorem considers $\underline{A}_s \leqslant u_\varepsilon(0) \leqslant \overline{A}_s$, $1 < s < p$ or the equivalent for $s = 1, p$.

Theorem 2.3.1. *Let g_s be the stable reduced solution of $(\mathscr{B}_\varepsilon)$ associated with $u_\varepsilon(0)$. Let $\underline{A}_s$ and $\overline{A}_s$ be any constants satisfying (2.3.4) for $1 < s < p$ or the equivalent for $s = 1, p$. If $\underline{A}_s \leqslant u_\varepsilon(0) \leqslant \overline{A}_s$, $1 < s < p$ (or $-\infty < u_\varepsilon(0) \leqslant \overline{A}_s$ if $s = 1$ or $\underline{A}_s \leqslant u_\varepsilon(0) < \infty$ if $s = p$) then there exists a unique solution u_ε to $(\mathscr{B}_\varepsilon)$ satisfying $\min\{u_\varepsilon(0), \underline{\gamma}_s\} \leqslant u_\varepsilon(x) \leqslant \max\{u_\varepsilon(0), \overline{\gamma}_s\}$, $x \in \overline{\Omega}$.*

Proof. Using (2.3.1) and the restrictions on the sign of g_s' in the respective cases, we can easily show that the stated bounds on u_ε are lower and upper solutions of $(\mathscr{B}_\varepsilon)$. □

The above constant lower and upper solutions suffice for our analysis when the initial condition is sufficiently close to the stable reduced solution associated with $u_\varepsilon(0)$. In the next theorem, we present more informative lower and upper solutions in the case where $g_{s-1}(0) < u_\varepsilon(0) < \underline{A}_s$ for $s > 1$ or $\overline{A}_s < u_\varepsilon(0) < g_{s+1}(0)$ for $s < p$. Note that for $n_s = 1$, the sub cases $g_{s-1}(0) < u_\varepsilon(0) \leqslant \overline{\gamma}_{s-1}$ and $g_{s+1}(0) > u_\varepsilon(0) \geqslant \underline{\gamma}_{s+1}$ of the latter two cases respectively, were not considered in [22]. The theorem presents a restriction, ((2.3.6) below), on g_{s-1}' which can be interpreted as a condition to prevent $u_\varepsilon(t) = g_{s-1}(t)$ at some $t > 0$.

Theorem 2.3.2. *Let g_s be the stable reduced solution associated with $u_\varepsilon(0)$, where $g_{s-1}(0) < u_\varepsilon(0) < \underline{A}_s$, $\underline{A}_s$ as in (2.3.3).*

(a) If $n_s = 1$ or if $n_s = 2$ and g_s is stable from below with $g_s' \geqslant 0$ then $\overline{u} = \overline{\gamma}_s$ or $\overline{u} = g_s$ are upper solutions of $(\mathscr{B}_\varepsilon)$ respectively. Moreover, assuming (2.3.2), if $n_s = 1$ and $u_\varepsilon(0) = g_{s-1}(0) + \lambda\varepsilon$ then $\underline{u} = g_{s-1}(0)$ is a lower solution of $(\mathscr{B}_\varepsilon)$.

(b) If $n_s = 1$ or if $n_s = 2$ and g_s is stable from below and $u_\varepsilon(0) - g_{s-1}(0) \geqslant C > 0$, then let $\underline{u}(x) := \underline{A}_s - (\underline{A}_s - u_\varepsilon(0))e^{-\theta x/\varepsilon}$ and assume that the parameter θ satisfies

$$0 < \theta \leqslant \left(\alpha \prod_{j=1}^{s-2} (u_\varepsilon(0) - \overline{\gamma}_j)^{n_j} (u_\varepsilon(0) - g_{s-1}(0))^{n_s} \prod_{j=s}^{p} (\underline{\gamma}_j - \underline{A}_s)^{n_j} \right) / \left(\underline{A}_s - u_\varepsilon(0) \right). \tag{2.3.5}$$

If

$$\underline{u}'(x) > g'_{s-1}(x) \quad \text{on} \quad \left[0, \frac{\varepsilon}{\theta} \ln \left(\frac{\underline{A}_s - u_\varepsilon(0)}{\varepsilon} \right) \right], \tag{2.3.6}$$

then for sufficiently small ε, $\underline{u}$ is a lower solution of $(\mathscr{B}_\varepsilon)$.

(c) Furthermore, the solution u_ε to $(\mathscr{B}_\varepsilon)$ is unique and for sufficiently small ε

$$\min_{x \in \overline{\Omega}} \{(u_\varepsilon - g_{s-1})(x)\} \geqslant \min \{u_\varepsilon(0) - g_{s-1}(0), \underline{\varsigma}\} \tag{2.3.7}$$

for any $\underline{\varsigma} < \underline{A}_s - \overline{\gamma}_{s-1}$.

Proof. a) Noting (2.3.1)-(2.3.2), the proof is analogous to the proof of Theorem 2.3.1.

b)Note that $\underline{u} = \underline{A}_s - \varepsilon$ when $x = \zeta := \frac{\varepsilon}{\theta} \ln \left((\underline{A}_s - u_\varepsilon(0))/\varepsilon \right)$. Consider $x \in [0, \zeta]$, where from (2.3.6) we have $(\underline{u} - g_{s-1})(x) \geqslant (u_\varepsilon - g_{s-1})(0)$. From (2.3.1) it can be checked that $k(x, \underline{u}) > 0$ for $x \in \Omega$ and we bound $k(x, \underline{u})$ from below on $[0, \zeta]$ as follows.

$$k(x, \underline{u}) \geqslant \alpha \prod_{j=1}^{s-2} (u_\varepsilon(0) - \overline{\gamma}_j)^{n_j} (u_\varepsilon(0) - g_{s-1}(0))^{n_{s-1}} (\underline{\gamma}_s - \underline{A}_s)^{n_s} \prod_{j=s+1}^{p} (\underline{\gamma}_j - \underline{A}_s)^{n_j}.$$

Using (2.3.1) it can be checked that this lower bound is positive. Similarly bounding $\varepsilon \underline{u}'$ from above by $\theta(\underline{A}_s - u_\varepsilon(0))$ shows that the inequality $\varepsilon \underline{u}' \leqslant k(x, \underline{u})$ follows from (2.3.5).

Consider $x \in [\zeta, 1]$. On this interval $\varepsilon \underline{u}' \leqslant \varepsilon\theta$ and $\underline{u} - \underline{A}_s = O(\varepsilon)$. Thus by (2.3.1) and (2.3.3) we have $\varepsilon \underline{u}' - k(x, \underline{u}) \equiv O(\varepsilon) - k(x, \underline{A}_s) < 0$ for sufficiently small ε. Hence $\underline{u}$ is a lower solution for $(\mathscr{B}_\varepsilon)$.

c)The proof of uniqueness is analogous to Theorem 2.3.1. Consider the solution u_ε on $[0, \zeta]$. We have $u_\varepsilon - g_{s-1} \geqslant \underline{u} - g_{s-1} \geqslant (u_\varepsilon - g_{s-1})(0)$. Next consider u_ε on $(\zeta, 1]$. We have

$$u_\varepsilon - g_{s-1} \geqslant \underline{A}_s - \varepsilon - \overline{\gamma}_{s-1} = \underline{\mu}(\underline{\gamma}_s - \overline{\gamma}_{s-1}) - \varepsilon > \underline{\varsigma},$$

for sufficiently small ε and for any $\underline{\varsigma} < \underline{\mu}(\underline{\gamma}_s - \overline{\gamma}_{s-1})$. □

A corresponding Theorem and proof to the above can be presented for the case where $\overline{A}_s < u_\varepsilon(0) < g_{s+1}(0)$ for $s < p$, for $\overline{A}_s$ as in (2.3.3).

Remark: The inequality in (2.3.6) is satisfied when $g'_{s-1}(x) < \theta$ on $0 \leqslant x \leqslant \frac{\varepsilon}{\theta} \ln \left((\underline{A}_s - u_\varepsilon(0))/\varepsilon \right)$.

2.3.1.3 Regular and Layer Components

Express the solution u_ε as the sum of two components v_ε and w_ε, where the regular component v_ε is defined as the solution of the initial value problem

$$\varepsilon v_\varepsilon'(x) = k(x, v_\varepsilon(x)), \qquad x \in \Omega, \qquad v_\varepsilon(0) = g_s(0). \tag{2.3.8}$$

Since this problem corresponds to the general problem in §2.2, the next theorem is implied.

Theorem 2.3.3. *Let g_s be the stable reduced solution of $(\mathscr{B}_\varepsilon)$ associated with $u_\varepsilon(0)$. There exists a unique solution v_ε to (2.3.8) satisfying*

$$\underline{\gamma}_s \leqslant v_\varepsilon(x) \leqslant \overline{\gamma}_s, \qquad \|v_\varepsilon - g_s\| \leqslant C(\varepsilon \|g_s'\|)^{1/n_s}, \qquad \|v_\varepsilon'\| \leqslant C\|g_s'\|, \qquad x \in \Omega.$$

The unique layer component w_ε is defined as the solution of

$$\varepsilon w_\varepsilon' = \left(\frac{k(x, u_\varepsilon) - k(x, v_\varepsilon)}{u_\varepsilon - v_\varepsilon} \right) w_\varepsilon, \quad x \in \Omega, \quad w_\varepsilon(0) = u_\varepsilon(0) - g_s(0). \tag{2.3.9}$$

In the next theorem, we establish bounds on the layer component and its first derivative.

Theorem 2.3.4. *Let g_s be the stable reduced solution of $(\mathscr{B}_\varepsilon)$ associated with $u_\varepsilon(0)$ and w_ε be the layer component satisfying (2.3.9). Let $i = 0, 1$ then $\forall\ 1 \leqslant j \leqslant p$, $j \neq s$ we have;*

(a) If $n_s = 1$ and $\min\{|u_\varepsilon(0) - g_j(0)|\} \geqslant C > 0$ then

$$|w_\varepsilon^{(i)}(x)| \leqslant C\varepsilon^{-i} |u_\varepsilon(0) - g_s(0)| e^{-Cx/\varepsilon}, \quad x \in \Omega.$$

(b) If $n_s = 1$ and $\min\{|u_\varepsilon(0) - g_j(0)|\} = \lambda\varepsilon$, then, assuming (2.3.2),

$$|w_\varepsilon^{(i)}(x)| \leqslant C\varepsilon^{-i} \left(1 + C\varepsilon e^{Cx/\varepsilon}\right)^{-1}, \quad x \in \Omega.$$

(c) If $n_s = 2$ and $\min\{|u_\varepsilon(0) - g_j(0)|\} \geqslant C > 0$, then

$$|w_\varepsilon^{(i)}(x)| \leqslant C|u_\varepsilon(0) - g_s(0)|\varepsilon^{-i} \left(1 + C|u_\varepsilon(0) - g_s(0)|\frac{x}{\varepsilon}\right)^{-1}, \quad x \in \Omega.$$

Proof. Define the function K as follows

$$K(y; s, j) := (y - g_s)^{n_s - j} \prod_{\substack{i=1 \\ i \neq s}}^{p} (y - g_i)^{n_i}, \qquad n_s \geqslant j \geqslant 0. \tag{2.3.10}$$

Note that

$$\begin{aligned}
&\frac{\prod_{i=1}^p (u_\varepsilon - g_i)^{n_i} - \prod_{i=1}^p (v_\varepsilon - g_i)^{n_i}}{u_\varepsilon - v_\varepsilon} \\
&= K(u_\varepsilon; s, 1) + (v_\varepsilon - g_s)\left(\frac{K(u_\varepsilon; s, 1) - K(v_\varepsilon; s, 1)}{u_\varepsilon - v_\varepsilon} \right) && \text{(2.3.11a)} \\
&= K(u_\varepsilon; s, 1) + (v_\varepsilon - g_s)\left(K(u_\varepsilon; s, 2) + (v_\varepsilon - g_s)\left(\frac{K(u_\varepsilon; s, 2) - K(v_\varepsilon; s, 2)}{u_\varepsilon - v_\varepsilon} \right) \right), && \text{(2.3.11b)}
\end{aligned}$$

where (2.3.11a) is valid when $n_s \geqslant 1$ and (2.3.11b) is valid when $n_s \geqslant 2$.

(a) Consider $n_s = 1$. By using (2.3.1) and Theorems 2.3.1 and 2.3.2, a positive lower bound b for $aK(u_\varepsilon; s, 1)$ is as presented in (2.3.20) below. Note that lower bounds in the three cases are used as mesh constants and thus we avoid repetition by stating these in (2.3.19)-(2.3.20) below. Using (2.3.11a), (2.3.20) and Theorem 2.3.3 we have

$$-\left(\frac{k(x,u_\varepsilon)-k(x,v_\varepsilon)}{u_\varepsilon - v_\varepsilon}\right) \geqslant b - C\varepsilon > \kappa, \tag{2.3.12}$$

for sufficiently small ε. Consider $\overline{w} := |u_\varepsilon(0) - g_s(0)|e^{-\kappa x/\varepsilon}$. Using (2.3.12) it can be easily shown that $\overline{w}$ is an upper solution and similarly that $\underline{w} = -\overline{w}$ is a lower solution for (2.3.9). It follows from (2.3.9) that

$$|w_\varepsilon^{(p)}(x)| \leqslant |w_\varepsilon(0)|(Cp+1)\varepsilon^{-p}e^{-\kappa x/\varepsilon}, \quad p = 0, 1. \tag{2.3.13}$$

(b) Next suppose $u_\varepsilon(0) = g_{s+1}(0) - \lambda\varepsilon$, $\lambda > 0$ and assume (2.3.2) (which means $n_s = n_{s+1} = 1$ and $v_\varepsilon \equiv g_s$). Express (2.3.11a) as

$$K(u_\varepsilon; s, 1) + 0 = \prod_{\substack{j=1 \\ j\neq s}}^{p} (u_\varepsilon - g_j)^{n_j} = (w_\varepsilon + v_\varepsilon - g_{s+1}) \prod_{\substack{j=1 \\ j\neq s,\ s+1}}^{p} (y - g_j)^{n_j}.$$

Using this expression we can write (2.3.9) as

$$\varepsilon w_\varepsilon' - B_1(x, u_\varepsilon)(w_\varepsilon - B_2(x, v_\varepsilon))w_\varepsilon = 0, \qquad w_\varepsilon(0) = g_{s+1}(0) - \lambda\varepsilon - g_s(0), \tag{2.3.14}$$

$$\text{where} \qquad B_1(x, u_\varepsilon) := -a \prod_{\substack{j=1 \\ j\neq s,s+1}}^{p} (u_\varepsilon - g_j)^{n_j}(x) \qquad \text{and} \qquad B_2(x, v_\varepsilon) := (g_{s+1} - v_\varepsilon)(x).$$

Using Theorems 2.3.2 and 2.3.3 we can establish that $B_1 \geqslant \kappa_1$ and $B_2 \geqslant \kappa_2$ where κ_1 and κ_2 are presented in (2.3.19). Using these bounds and (2.3.2), it can easily be checked that the solution to the problem $\varepsilon\overline{w}' - \kappa_1(\overline{w} - \kappa_2)\overline{w} = 0, \overline{w}(0) = w_\varepsilon(0)$, is an upper solution to (2.3.9). We can then bound w_ε' as required. The proof of the case where $u_\varepsilon(0) = g_{s-1}(0) + \lambda\varepsilon$ with $n_{s-1} = 1$ is analogous to the above. Hence, in both cases, we have the bounds

$$|w_\varepsilon^{(p)}(x)| \leqslant (Cp+1)\varepsilon^{-p}\kappa_2 \left(1 + \frac{\lambda\varepsilon}{\kappa_2 - \lambda\varepsilon}e^{\kappa_1\kappa_2 x/\varepsilon}\right)^{-1}, \quad p = 0, 1. \tag{2.3.15}$$

(c) Finally, consider $n_s = 2$ and g_s stable from above. From (2.3.11b) it follows that

$$\begin{aligned} &\frac{\prod_{i=1}^{p}(u_\varepsilon - g_i)^{n_i} - \prod_{i=1}^{p}(v_\varepsilon - g_i)^{n_i}}{u_\varepsilon - v_\varepsilon} \\ &= w_\varepsilon \prod_{\substack{j=1 \\ j\neq s}}^{n} (u_\varepsilon - g_j)^{n_j} + (v_\varepsilon - g_s)\Big(2K(u_\varepsilon; s, 2) + (v_\varepsilon - g_s)K_y(\xi; s, 2)\Big), \end{aligned} \tag{2.3.16}$$

for some well defined $\min\{u_\varepsilon, v_\varepsilon\} \leqslant \xi \leqslant \max\{u_\varepsilon, v_\varepsilon\}$. It can easily be established that the bounds b as defined in (2.3.20), applicable to the value of $u_\varepsilon(0)$, are a lower bound for $aK(u_\varepsilon; s, 2)$. Using (2.3.9) and (2.3.16) we write an equation for w_ε as follows

$$\varepsilon w_\varepsilon' + aK(u_\varepsilon; s, 2)(w_\varepsilon + (v_\varepsilon - g_s)(2 + (v_\varepsilon - g_s)\frac{K_y(\xi; s, 2)}{K(u_\varepsilon; s, 2)}))w_\varepsilon = 0,\ w_\varepsilon(0) = (u_\varepsilon - g_s)(0). \quad (2.3.17)$$

Consider the problem $\varepsilon\overline{w}' + b\overline{w}^2 = 0$, $\overline{w}(0) = w_\varepsilon(0)$. Using Theorem 2.3.3 it can easily be checked that for sufficiently small ε, $\overline{w}$ is an upper solution to (2.3.17) and $\underline{w} = 0$ is a lower solution. We can solve for $\overline{w}$ explicitly and it follows from (2.3.9) that

$$|w_\varepsilon^{(p)}(x)| \leqslant (Cp+1)\varepsilon^{-p}\left(\frac{bx}{\varepsilon} + \frac{1}{|u_\varepsilon(0) - g_s(0)|}\right)^{-1}, \quad p = 0, 1. \quad (2.3.18)$$

The proof of the case where $n_s = 2$ and g_s is stable from below is analogous to the above. □

Remark: Depending on whether $n_s = 1$ or $n_s = 2$, or whether the distance between the initial condition and an unstable reduced solution is ε-dependent or not, the layer component has a different character, which influences our choice of mesh in the following section. A graph is shown in Figure 2.4 displaying the difference in the layer structure for the two cases considered when $n_s = 1$. Note that a graph for the case $n = 2$ of the general problem ($\mathscr{A}_\varepsilon$) is shown in Figure 2.1. We also note from the proof of Theorem 2.3.4 that for case (b) above, we have

$$|w_\varepsilon'(0)| \quad \leqslant \quad \varepsilon^{-1}B_1(0, u_\varepsilon)|w_\varepsilon(0) - B_2(0, u_\varepsilon)|w_\varepsilon(0) \quad \leqslant \quad C\lambda(g_{s+1}(0) - g_s).$$

Hence $|w_\varepsilon'(0)|$ is bounded independently of ε, implying the layer may be somewhat delayed away from $x = 0$. An example of this delay is seen in Figure 2.4.

2.3.2 The Discrete Problem

The Discrete Problem is described as follows: find a mesh function U_ε^N such that

$$\varepsilon D^- U_\varepsilon^N(x_i) = k(x_i, U_\varepsilon^N(x_i)), \qquad x_i \in \Omega^N, \qquad U_\varepsilon^N(0) = u_\varepsilon(0). \qquad (\mathscr{B}_\varepsilon^N)$$

The piecewise uniform mesh Ω^N is as described in (2.2.13), but with a different choice for the transition point σ. As in subsection 2.2.2, we choose our transition point motivated by Theorem 2.3.4 as follows;

$$\sigma := \min\left\{\frac{1}{2}, \frac{\varepsilon}{\kappa_1\kappa_2}\ln\left(\frac{N}{\varepsilon}\right)\right\} \quad \text{in case B,} \quad (2.3.19a)$$

where κ_1 and κ_2 are defined as

$$\kappa_1 := \begin{cases} \alpha \prod_{j=1}^{s-1} (g_s - \overline{\gamma}_j)^{n_j} \prod_{j=s+2}^{p} (\underline{\gamma}_j - g_{s+1}(0))^{n_j} & \text{if} \quad u_\varepsilon(0) = g_{s+1}(0) - \lambda\varepsilon, \\ \alpha \prod_{j=1}^{s-2} (g_{s-1}(0) - \overline{\gamma}_j)^{n_j} \prod_{j=s+1}^{p} (\underline{\gamma}_j - g_s)^{n_j} & \text{if} \quad u_\varepsilon(0) = g_{s-1}(0) + \lambda\varepsilon, \end{cases} \tag{2.3.19b}$$

$$\kappa_2 := \begin{cases} g_{s+1}(0) - g_s & \text{if} \quad u_\varepsilon(0) = g_{s+1}(0) - \lambda\varepsilon, \\ g_s - g_{s-1}(0) & \text{if} \quad u_\varepsilon(0) = g_{s-1}(0) + \lambda\varepsilon. \end{cases} \tag{2.3.19c}$$

In the other cases,

$$\sigma := \min\left\{\frac{1}{2}, \frac{\varepsilon}{\kappa} L(N)\right\},\ \kappa < b, \quad L(N) := \ln(N) \text{ in case A or } L(N) := N^{\frac{1}{2}} \text{ in case C} \tag{2.3.20a}$$

where in both cases the parameter b is defined as

$$b := \begin{cases} b_1 & \text{if} \quad \overline{A}_s < u_\varepsilon(0) < g_{s+1}(0), \quad 1 \leqslant s < p, \\ b_2 & \text{if} \quad g_s(0) < u_\varepsilon(0) \leqslant \overline{A}_s, \quad 1 \leqslant s < p, \quad \text{or if} \quad g_n(0) < u_\varepsilon(0),\ s = n, \\ b_3 & \text{if} \quad \underline{A}_s \leqslant u_\varepsilon(0) < g_s(0), \quad 1 < s \leqslant p, \quad \text{or if} \quad u_\varepsilon(0) < g_1(0),\ s = 1, \\ b_4 & \text{if} \quad g_{s-1}(0) < u_\varepsilon(0) < \underline{A}_s, \quad 1 \leqslant s < p, \end{cases} \tag{2.3.20b}$$

$$b_1 := \alpha \prod_{j=1}^{s-1} (\underline{\gamma}_s - \overline{\gamma}_j)^{n_j} \min\{g_{s+1}(0) - u_\varepsilon(0), \overline{\varsigma}\}^{n_{s+1}} \prod_{j=s+2}^{p} (\underline{\gamma}_j - u_\varepsilon(0))^{n_j}; \tag{2.3.20c}$$

$$b_2 := \alpha \prod_{j=1}^{s-1} (\underline{\gamma}_s - \overline{\gamma}_j)^{n_j} \prod_{j=s+1}^{p} (\underline{\gamma}_j - \max\{u_\varepsilon(0), \overline{\gamma}_s\})^{n_j}; \tag{2.3.20d}$$

$$b_3 := \alpha \prod_{j=1}^{s-1} (\min\{u_\varepsilon(0), \underline{\gamma}_s\} - \overline{\gamma}_j)^{n_j} \prod_{j=s+1}^{p} (\underline{\gamma}_j - \overline{\gamma}_s)^{n_j}; \tag{2.3.20e}$$

$$b_4 := \alpha \prod_{j=1}^{s-2} (u_\varepsilon(0) - \overline{\gamma}_j)^{n_j} \min\{u_\varepsilon(0) - g_{s-1}(0), \underline{\varsigma}\}^{n_{s-1}} \prod_{j=s+1}^{p} (\underline{\gamma}_j - \overline{\gamma}_s)^{n_j}; \tag{2.3.20f}$$

where $\overline{A}_s, \underline{A}_s$ as in (2.3.3) where we choose $\underline{A}_s = \overline{\gamma}_{s-1} + \frac{1}{2}(\underline{\gamma}_s - \overline{\gamma}_{s-1})$ and $\overline{A}_s = \underline{\gamma}_{s+1} - \frac{1}{2}(\underline{\gamma}_{s+1} - \overline{\gamma}_s)$ and for any $\underline{\varsigma} < \frac{1}{2}(\underline{\gamma}_s - \overline{\gamma}_{s-1})$ and $\overline{\varsigma} < \frac{1}{2}(\underline{\gamma}_{s+1} - \overline{\gamma}_s)$. Note that we can choose specific values of $\underline{\varsigma}$, $\overline{\varsigma}$ and κ in section 5.

The discrete equivalent of the lower and upper solutions constructed in Theorems 2.3.1 and 2.3.2 can be shown to hold for $(\mathscr{B}_\varepsilon^N)$. As before, since $k \in C^1$, uniqueness can also be established.

2.3.2.1 Error Analysis

Throughout this section, we refer to the case where $n_s = 1$ and $u_\varepsilon(0)$ is not within $O(\varepsilon)$ of an unstable reduced solution as case A otherwise as case B and the case where $n_s = 2$ as case C. In

all the cases, the transition point σ of the mesh Ω^N is of the form

$$\sigma = \min\left\{\frac{1}{2}, M\varepsilon L(N)\right\}, \quad \text{where} \tag{2.3.21a}$$

$$M = \frac{1}{\kappa} \quad \text{and} \quad L(N) = \ln N \quad \text{in case A;} \tag{2.3.21b}$$

$$M = \frac{1}{\kappa_1\kappa_2} \quad \text{and} \quad L(N) = \ln\frac{N}{\varepsilon} \quad \text{in case B;} \tag{2.3.21c}$$

$$M = \frac{1}{\kappa} \quad \text{and} \quad L(N) = \sqrt{N} \quad \text{in case C.} \tag{2.3.21d}$$

We express the discrete solution U_ε^N as the sum of V_ε^N and W_ε^N, where V_ε^N is a solution of the problem

$$\varepsilon D^- V_\varepsilon^N(x_i) = k(x_i, V_\varepsilon^N(x_i)), \qquad x_i \in \Omega^N, \qquad V_\varepsilon^N(0) = g_s(0). \tag{2.3.22}$$

From §2.2, the following can be established.

Theorem 2.3.5. *If V_ε^N is the solution of (2.3.22) then*

$$\underline{\gamma}_s \leqslant V_\varepsilon^N(x_i) \leqslant \overline{\gamma}_s, \quad |(V_\varepsilon^N - g_s)(x_i)| \leqslant C(\varepsilon\|g_s'\|)^{1/n_s} \quad \textit{and} \quad |(V_\varepsilon^N - v_\varepsilon)(x_i)| \leqslant CN^{-1/n_s}, \quad x_i \in \Omega^N.$$

The discrete layer component satisfies

$$\varepsilon D^- W_\varepsilon^N(x_i) = \left(\frac{k(x_i, U_\varepsilon^N(x_i)) - k(x_i, V_\varepsilon^N(x_i))}{U_\varepsilon^N(x_i) - V_\varepsilon^N(x_i)}\right) W_\varepsilon^N(x_i), \quad x_i \in \Omega^N, \quad W_\varepsilon^N(0) = w_\varepsilon(0). \tag{2.3.23}$$

We bound the discrete layer component in the following.

Theorem 2.3.6. *Let g_s be the stable reduced solution of $(\mathscr{B}_\varepsilon)$ associated with $u_\varepsilon(0)$ and W_ε^N be the discrete layer component satisfying (2.3.23). Then on the meshes (2.3.19)-(2.3.20) and $\forall$ $1 \leqslant j \leqslant p$, $j \neq s$ we have;*

(a) If $n_s = 1$ and $\min\{|u_\varepsilon(0) - g_j(0)|\} \geqslant C > 0$ then

$$|W_\varepsilon^N(x_i)| \leqslant 2|w_\varepsilon(0)|e^{-\kappa x_i/\varepsilon}, \qquad i \leqslant \tfrac{N}{2} \ (\textit{if } \sigma < \tfrac{1}{2}), \quad i \leqslant N \ (\textit{if } \sigma = \tfrac{1}{2}), \tag{2.3.24a}$$

$$|W_\varepsilon^N(x_i)| \leqslant CN^{-1}, \qquad \tfrac{N}{2} \leqslant i \leqslant N \ (\textit{if } \sigma < \tfrac{1}{2}). \tag{2.3.24b}$$

(b) If $n_s = 1$ and $\min\{|u_\varepsilon(0) - g_j(0)|\} = \lambda\varepsilon$, then, assuming (2.3.2),

$$|W_\varepsilon^N(x_i)| \leqslant 2\kappa_2\left(1 + \frac{\lambda\varepsilon}{\kappa_2 - \lambda\varepsilon}e^{\kappa_1\kappa_2 x_i/\varepsilon}\right)^{-1}, \quad i \leqslant \tfrac{N}{2} \ (\textit{if } \sigma < \tfrac{1}{2}), \quad i \leqslant N \ (\textit{if } \sigma = \tfrac{1}{2}), \tag{2.3.25a}$$

$$|W_\varepsilon^N(x_i)| \leqslant CN^{-1}, \qquad \tfrac{N}{2} \leqslant i \leqslant N \ (\textit{if } \sigma < \tfrac{1}{2}). \tag{2.3.25b}$$

(c) If $n_s = 2$ and $\min\{|u_\varepsilon(0) - g_j(0)|\} \geqslant C > 0$, then

$$|W_\varepsilon^N(x_i)| \leqslant 2\left(\frac{1}{|w_\varepsilon(0)|} + \frac{bx_i}{\varepsilon}\right)^{-1}, \qquad i \leqslant \tfrac{N}{2} \ (\textit{if } \sigma < \tfrac{1}{2}), \quad i \leqslant N \ (\textit{if } \sigma = \tfrac{1}{2}), \tag{2.3.26a}$$

$$|W_\varepsilon^N(x_i)| \leqslant CN^{-1/2}, \qquad \tfrac{N}{2} \leqslant i \leqslant N \ (\textit{if } \sigma < \tfrac{1}{2}). \tag{2.3.26b}$$

Proof. Considering case A, analogously to case (a) in Theorem 2.3.4 we can establish through discrete upper and lower solutions that

$$|W_\varepsilon^N(x_i)| \leqslant |w_\varepsilon(0)| \left(1+\kappa\frac{h}{\varepsilon}\right)^{-i}, \quad \text{for} \quad i \leqslant \frac{N}{2}, \tag{2.3.27a}$$

$$|W_\varepsilon^N(x_i)| \leqslant |w_\varepsilon(0)| \left(1+\kappa\frac{h}{\varepsilon}\right)^{-\frac{N}{2}} \left(1+\kappa\frac{H}{\varepsilon}\right)^{-(i-\frac{N}{2})}, \quad \text{for} \quad i > \frac{N}{2}. \tag{2.3.27b}$$

For $i \leqslant K$ where $K = N/2$ if $\sigma < 1/2$ and $K = N$ if $\sigma = 1/2$ we have $h_i = h$ and $h/\varepsilon \leqslant CN^{-1}\ln(N)$. Thus using (2.2.19) with (2.3.27) for sufficiently large N, we have

$$\begin{aligned}
|W_\varepsilon^N(x_i)| &\leqslant |w_\varepsilon(0)| \left(1+\kappa\frac{h}{\varepsilon}\right)^{-i} \leqslant |w_\varepsilon(0)| \exp\left(-\left(1-\frac{\kappa}{2}\frac{h}{\varepsilon}\right)\kappa\frac{hi}{\varepsilon}\right) \\
&\leqslant |w_\varepsilon(0)| \exp(C(h/\varepsilon)^2 i)) \exp(-\kappa x_i/\varepsilon) \\
&\leqslant |w_\varepsilon(0)| \exp(CN^{-1}\ln^2(N)) \exp(-\kappa x_i/\varepsilon) \leqslant 2|w_\varepsilon(0)| e^{-\kappa x_i/\varepsilon}.
\end{aligned}$$

If $\sigma < 1/2$, then for $i \geqslant N/2$, using (2.3.20) and (2.3.27b), we have $|W_\varepsilon^N(x_i)| \leqslant CN^{-1}$.

Considering case B, analogously to case (b) in Theorem 2.3.4, we can establish through upper and lower solutions that

$$0 \leqslant W_\varepsilon^N(x_i) \leqslant \kappa_2 \left(1+\frac{\lambda\varepsilon}{\kappa_2-\lambda\varepsilon}\left(1+\kappa_1\kappa_2\frac{h}{\varepsilon}\right)^i\right)^{-1}, \quad \text{for} \quad i < \frac{N}{2}, \tag{2.3.28a}$$

$$0 \leqslant W_\varepsilon^N(x_i) \leqslant \kappa_2 \left(1+\frac{\lambda\varepsilon}{\kappa_2-\lambda\varepsilon}\left(1+\kappa_1\kappa_2\frac{h}{\varepsilon}\right)^{\frac{N}{2}}\left(1+\kappa_1\kappa_2\frac{H}{\varepsilon}\right)^{i-\frac{N}{2}}\right)^{-1}, \quad \text{for} \quad i \geqslant \frac{N}{2}, \tag{2.3.28b}$$

where $h := 2N^{-1}\sigma$, $H := 2N^{-1}(1-\sigma)$. Again, for $i \leqslant K$ where $K = N/2$ if $\sigma < 1/2$ and $K = N$ if $\sigma = 1/2$ we have $h_i = h$ and $h/\varepsilon \leqslant CN^{-1}\ln(N/\varepsilon)$. Thus using (2.2.19) with (2.3.28) for sufficiently large N, we have

$$\begin{aligned}
&1+\frac{\lambda\varepsilon}{\kappa_2-\lambda\varepsilon}\left(1+\kappa_1\kappa_2\frac{h}{\varepsilon}\right)^i \\
&\geqslant 1+\frac{\lambda\varepsilon}{\kappa_2-\lambda\varepsilon}\exp(-0.5(\kappa_1\kappa_2)^2(h/\varepsilon)^2 i)\exp(\kappa_1\kappa_2 x_i/\varepsilon) \geqslant \frac{1}{2}\left(1+\frac{\lambda\varepsilon}{\kappa_2-\lambda\varepsilon}e^{\kappa_1\kappa_2 x_i/\varepsilon}\right).
\end{aligned}$$

The bound in (2.3.25) follows after using (2.3.19) with (2.3.28b).

Considering case C, analogously to case (c) in Theorem 2.3.4 we can rewrite problem (2.3.23) in the form

$$\varepsilon D^- W_\varepsilon^N + aK(U_\varepsilon^N;s,2)\left(W_\varepsilon^N + (V_\varepsilon^N - g_s)\left(2+(V_\varepsilon^N-g_s)\frac{K_y(\xi;s,2)}{K(U_\varepsilon^N;s,2)}\right)\right)W_\varepsilon^N = 0. \tag{2.3.29}$$

Since $w_\varepsilon(0) > 0$, a lower solution to the problem is $\underline{W}^N \equiv 0$. For $i \leqslant K$ where $K = N/2$ if $\sigma < 1/2$ and $K = N$ if $\sigma = 1/2$, consider the problem

$$\varepsilon D^- \overline{W}^N(x_i) + \mu b \overline{W}^N(x_i)\overline{W}^N(x_{i-1}) = 0, \quad 0 < \mu < 1, \quad 0 < i \leqslant K, \quad \overline{W}^N(0) = w_\varepsilon(0),$$

for which the solution can be solved exactly as $\overline{W}^N(x_i) = w_\varepsilon(0)(1+w_\varepsilon(0)\mu b x_i/\varepsilon)^{-1}$. For sufficiently large N, we can easily show that $\mu\overline{W}^N(x_i) \leqslant \overline{W}^N(x_{i-1})$ and we can use this to show that $\overline{W}^N$ is an upper solution of (2.3.29) for $i \leqslant K$. If $\sigma < 1/2$, then at $i = N/2$, using (2.3.20), we have $\overline{W}^N(x_{N/2}) \leqslant CN^{-\frac{1}{2}}$ and this is easily shown to be a constant upper solution of (2.3.29) for $N/2 \leqslant i \leqslant N$. Take $\mu = 1/2$, to obtain the bound in (2.3.26) □

The following theorem establishes global uniform convergence.

Theorem 2.3.7. *Assuming (2.3.2), if u_ε is the solution to $(\mathscr{B}_\varepsilon)$ and $\overline{U}_\varepsilon^N$ is the piecewise linear interpolation of U_ε^N, a solution to $((\mathscr{B}_\varepsilon^N)$, (2.3.19)-(2.3.20)), then for $1 \leqslant j \leqslant p$, $j \neq s$ and for sufficiently small ε we have*

$$\|\overline{U}_\varepsilon^N - u_\varepsilon\|_{[0,1]} \leqslant CN^{-1}\ln N, \quad \text{if } n_s = 1 \text{ and } \min\{|(u_\varepsilon - g_j)(0)|\} \geqslant C > 0,$$

$$\|\overline{U}_\varepsilon^N - u_\varepsilon\| \leqslant C\min\left\{1, \frac{N^{-1}}{\varepsilon^p}\ln\left(\frac{N}{\varepsilon}\right)\right\},\ p > 1, \text{ if } n_s = 1,\ \min\{|(u_\varepsilon - g_j)(0)|\} = \lambda\varepsilon,\ \sigma < \tfrac{1}{2},$$

$$\|\overline{U}_\varepsilon^N - u_\varepsilon\| \leqslant CN^{-0.9}, \text{ if } n_s = 1,\ \min\{|(u_\varepsilon - g_j)(0)|\} = \lambda\varepsilon,\ \sigma = \tfrac{1}{2},$$

$$\|\overline{U}_\varepsilon^N - u_\varepsilon\| \leqslant CN^{-\frac{1}{2}}, \quad \text{if } n_s = 2, \text{ and } \min\{|(u_\varepsilon - g_j)(0)|\} \geqslant C > 0.$$

Proof.

We first identify a range of values around $g_s(0)$ where, if the initial value $u_\varepsilon(0)$ lies within, the results of Theorem 2.2.6 apply. Considering $n_s = 1$, from §2.3.1.1, for $1 < s \leqslant p$, $k_y(x, g_{s-1}(x)) \geqslant 0$ and $k_y(x, g_s(x)) < 0$. Thus $\exists\ \underline{\xi}_1(x)$ satisfying $g_{s-1} < \underline{\xi}_1 < g_s$ and $k_y(x, \underline{\xi}_1(x)) = 0$ on $[0,1]$. Similarly for $1 \leqslant s < p$ $\exists\ \overline{\xi}_1(x)$ satisfying $g_s < \overline{\xi}_1 < g_{s+1}$ and $k_y(x, \overline{\xi}_1(x)) = 0$ on $[0,1]$. In an analogy with Assumption 2.2.1, we can choose $\delta^+, \delta^- > 0$ such that $k_y(x,\tilde{y}) \leqslant -\tilde{m}_1 < 0$, $\forall\ \tilde{y}$ s.t. $\max\underline{\xi}_1 + \delta^+ \leqslant \tilde{y} \leqslant \min\overline{\xi}_1 - \delta^-$, where $\tilde{m}_1 > 0$ is independent of ε. Similarly, if $n_s = 2$, $s < p$ and g_s is stable from above then $\exists\ \xi_2(x)$, $g_{s+1} > \xi_2(x) > g_s$ such that $k_{yy}(x,\tilde{y}) \leqslant -\tilde{m}_2 < 0\ \forall\ \tilde{y} \leqslant \min\xi_2 - \delta^-$. Hence if $\max\underline{\xi}_1 + \delta^+ \leqslant u_\varepsilon(0) \leqslant \min\overline{\xi}_1 - \delta^-$ for $n_s = 1$ or $g_s(0) \leqslant u_\varepsilon(0) \leqslant \min\xi_2 - \delta^-$ for $n_s = 2$ then the conditions required to apply Theorem 2.2.6 hold. By constructing a similar statement when $s = 1$ or $s = p$ for $n_s = 1,2$ or $n_s = 2$ and g_s is stable from below, we have $\|U_\varepsilon^N - u_\varepsilon\| \leqslant CN^{-1}L(N)$. Note this argument applies only to the subcases of case A and case C.

We now examine the situation where the argument in the previous paragraph cannot be directly applied; that is where $n_s = 1$ and $u_\varepsilon(0) \notin [\max\underline{\xi}_1 + \delta^+, \min\overline{\xi}_1 - \delta^-]$ (applicable to case B and to a sub case of case A) or $n_s = 2$ and g_s is stable from above with $u_\varepsilon(0) > \min\xi_2 - \delta^-$ or g_s is stable from below with $u_\varepsilon(0)$ satisfying an analgous inequality (a subcase of case C). We first consider $n_s = 1$ and $u_\varepsilon(0) > \min\overline{\xi}_1 - \delta^-$ or $n_s = 2$, g_s is stable from above and $u_\varepsilon(0) > \min\xi_2 - \delta^-$.

First, suppose $\sigma < 1/2$. Considering outside the layer region ($\sigma \leqslant x_i \leqslant 1$) and using (2.3.19)-(2.3.20) with (2.3.13), (2.3.15) and (2.3.18) and Theorems 2.3.5 and 2.3.6, we have in all three cases

$$|(U_\varepsilon^N - u_\varepsilon)(x_i)| \leqslant |W_\varepsilon^N(x_{N/2})| + |w_\varepsilon(\sigma)| + CN^{-1/n_s} \leqslant CN^{-1/n_s}.$$

Now considering inside the layer region ($0 \leqslant x_i \leqslant \sigma$) for which in all three cases we have $h_i/\varepsilon \leqslant CN^{-1}L(N)$. To bound the error $E^N := U_\varepsilon^N - u_\varepsilon$ on $0 \leqslant i \leqslant N/2$ we follow the method of proof used in [22, pg. 379]. By using ($\mathscr{B}_\varepsilon$) and ($\mathscr{B}_\varepsilon^N$), the error E^N satisfies

$$\varepsilon D^- E_\varepsilon^N(x_i) = \left(\frac{k(x_i, U_\varepsilon^N(x_i)) - k(x_i, u_\varepsilon(x_i))}{U_\varepsilon^N(x_i) - u_\varepsilon(x_i)} \right) E_\varepsilon^N(x_i) + \tau^N(x_i), \quad E_\varepsilon^N(x_0) = 0, \tag{2.3.30}$$

where τ^N is the truncation error $\tau^N := \varepsilon(u'_\varepsilon - D^- u_\varepsilon)$. We can show that this expressions equates to

$$E_\varepsilon^N(x_i) = \sum_{j=1}^{i} \frac{h}{\varepsilon} \tau^N(x_i) \prod_{s=j}^{i} \left(1 - k_y(x_i, \zeta(x_i)) \frac{h}{\varepsilon} \right)^{-1}. \tag{2.3.31}$$

for some well defined ζ s.t. $\min\{U_\varepsilon^N(x_i), u_\varepsilon(x_i)\} \leqslant \zeta(x_i) \leqslant \max\{U_\varepsilon^N(x_i), u_\varepsilon(x_i)\}$. In all three cases, as in Theorem 2.2.6, we can show that the truncation error satisfies $|\tau^N(x_i)| \leqslant Ch/\varepsilon \leqslant CN^{-1}L(N)$. Below, we will show that their exists an integer $J < N/2$ such that $k_y(x_i, \zeta(x_i)) < -\tilde{m} < 0$ for $i \geqslant J$. Hence, once established, the problem (2.3.30) with the new initial condition $E_\varepsilon^N(x_J)$, can be examined in the same manner as in Theorem 2.2.6, to find that

$$|E_\varepsilon^N(x_i)| \leqslant CN^{-1}L(N) + |E_\varepsilon^N(x_J)|, \quad \forall \ J < i < N/2. \tag{2.3.32}$$

We now establish the existence of such an integer $J < N/2$. In all three cases, from Theorems 2.3.3-2.3.4 and Theorems 2.3.5-2.3.6 and (2.3.21), we can solve

$$\max\{U_\varepsilon^N(x_i), u_\varepsilon(x_i)\} \leqslant \min \overline{\xi}_1 - \delta^- \quad \Leftrightarrow \quad x_i \geqslant M\varepsilon q := M\varepsilon q_{A\setminus B\setminus C}, \quad \text{where} \tag{2.3.33a}$$

$$q_A = \ln\left(\frac{2w_\varepsilon(0)}{\min \overline{\xi}_1 - \delta_1^- - \overline{\gamma}_s} \right), \quad \text{in case A;} \tag{2.3.33b}$$

$$q_B = \ln\left(\frac{\kappa_2 - \lambda\varepsilon}{\lambda\varepsilon} \left(\frac{2\kappa_2}{\min \overline{\xi}_1 - \delta_1^- - \overline{\gamma}_s} - 1 \right) \right), \quad \text{in case B;} \tag{2.3.33c}$$

$$q_C = \left(\frac{2}{\min \xi_2 - \delta^- - \overline{\gamma}_s} - \frac{1}{w_\varepsilon(0)} \right), \quad \text{in case C.} \tag{2.3.33d}$$

This means, we have $q_A = \ln(C)$, $q_B = \ln(C/\varepsilon)$ and $q_C = C$. For sufficiently large N, we have $q = q_{A\setminus B\setminus C} < L(N)$ (recall $L(N) = \ln(N/\varepsilon)$ in case B). Hence $\max\{U_\varepsilon^N(x_i), u_\varepsilon(x_i)\} \leqslant \min \overline{\xi}_1 - \delta^-$ for $x_i \geqslant x_J$ for some mesh point x_J within the fine mesh satisfying

$$M\varepsilon q \leqslant x_J = Jh \leqslant M\varepsilon q + h < x_{\frac{N}{2}}. \tag{2.3.34}$$

This means we have

$$M\varepsilon q/h \leqslant J \leqslant M\varepsilon q/h + 1. \tag{2.3.35}$$

Hence, using (2.3.31) for all $i \leqslant J$ we have

$$|E_\varepsilon^N(x_i)| \leqslant C(h/\varepsilon)^2(J)\left(1 - \|k_y\|\frac{h}{\varepsilon}\right)^{-J}. \tag{2.3.36}$$

Note the following inequalities, which can be established using (2.2.19); for any $t \leqslant 1/2$ and $q > 0$ we have

$$(1+t)^{-q/t} \leqslant e^{-q}e^{qt/2}, \qquad (1-t)^{-q/t} \leqslant e^{q}e^{qt}. \tag{2.3.37}$$

Thus using (2.3.21), (2.3.33), (2.3.35), (2.3.36) and (2.3.37), for each case A, B, C, we have

$$\begin{aligned}
|E_\varepsilon^N(x_i)| \leqslant & Cq_{A\setminus B\setminus C}N^{-1}L(N)\left(1 - \|k_y\|\frac{h}{\varepsilon}\right)^{-q_{A\setminus B\setminus C}\varepsilon M/h} \\
= & Cq_{A\setminus B\setminus C}N^{-1}L(N)\left(1 - \|k_y\|\frac{h}{\varepsilon}\right)^{-P}, \quad P = \frac{q_{A\setminus B\setminus C}\|k_y\|M}{\|k_y\|h/\varepsilon} \\
\leqslant & Cq_{A\setminus B\setminus C}N^{-1}L(N)\exp(q_{A\setminus B\setminus C}\|k_y\|M)\exp(q_{A\setminus B\setminus C}\|k_y\|^2 Mh/\varepsilon) \\
\leqslant & Cq_{A\setminus B\setminus C}N^{-1}L(N)\exp(q_{A\setminus B\setminus C}\|k_y\|M)\exp(Cq_{A\setminus B\setminus C}N^{-1}L(N)).
\end{aligned}$$

Hence, in cases A and C, since $q_{A\setminus C} \leqslant C$, for sufficiently large N, we have $|(U_\varepsilon^N - u_\varepsilon)(x_i)| \leqslant CN^{-1}\ln(N)$ in case A and $|(U_\varepsilon^N - u_\varepsilon)(x_i)| \leqslant CN^{-\frac{1}{2}}$ in case C for all $0 \leqslant i \leqslant J$. However, in case B, where $q_B = \ln(C/\varepsilon)$, we have

$$|E_\varepsilon^N(x_i)| \leqslant C\ln(1/\varepsilon)N^{-1}\ln(N/\varepsilon)e^{\ln(1/\varepsilon)\|k_y\|\theta} \leqslant C\varepsilon^{-\|k_y\|/(\kappa_1\kappa_2)}\ln(1/\varepsilon)N^{-1}\ln(N/\varepsilon). \tag{2.3.38}$$

We then obtain the required bounds over $[x_J, x_{\frac{N}{2}}]$ in all cases by using (2.3.32).

The case where $\sigma = 1/2$ is dealt in the same way as $i \leqslant N/2$ when $\sigma < 1/2$ and we obtain identical error bounds. Note that when $\sigma = 1/2$, we have $1/\varepsilon \leqslant CL(N)$. Furthermore, we can easily establish the inequality

$$\ln(x) \leqslant \frac{x^p}{p}, \quad x \geqslant 1, \quad p > 0. \tag{2.3.39}$$

Applying (2.3.39) to (2.3.38) when $\sigma = 1/2$ (whereby we choose suitably small p's that are independent of ε in (2.3.39)), we can obtain the ε-uniform bound

$$|E_\varepsilon^N(x_i)| \leqslant CN^{-0.9}, \quad i \in [0, N].$$

in case C.

The proof of the case where $u_\varepsilon(0) < \max\underline{\xi}_1 + \delta^+$ in case A, $u_\varepsilon(0) = g_{s-1}(0) + \lambda\varepsilon$ in case B or where g_s is stable from below in case C is analogous to the above. The global bound follows as in [22, pg. 381]. □

2.4: Stability Switch in a Class of Nonlinear Problems

In problem ($\mathscr{B}_\varepsilon$), the reduced solutions are bounded away from each other. In this section we consider a problem where the reduced solutions intersect at one point.

Consider the following problem: find $z_\varepsilon \in C^1(\Omega)$ satisfying

$$\begin{gathered}\varepsilon z_\varepsilon'(x) = q(x,z_\varepsilon) := -a(x)(z_\varepsilon-\beta)(z_\varepsilon-g)(x), \qquad x\in\Omega := (0,1], \qquad z_\varepsilon(0)=A,\\ \beta \text{ constant}, \;\; g\in C^1(\Omega), \;\; a\in C^0(\Omega), \;\; a(x)\geqslant\alpha, \;\; g'(x)\leqslant 0 \;\; x\in[0,1], \qquad (\mathscr{C}_\varepsilon)\\ g(x)=\beta \text{ at only one point } x=d\in\Omega, \text{ where } d \text{ is independent of } \varepsilon.\end{gathered}$$

For convenience we consider $z_\varepsilon(0)\geqslant g(0)$ and through lower and upper solutions it follows that $\max\{g(x),\beta\}\leqslant z_\varepsilon(x)\leqslant z_\varepsilon(0)$ for $x\in\overline{\Omega}$. Uniqueness of a solution is established as in the previous sections. Referring to §2.2.1.1, g is stable on $[0,d)$ and β is stable on $(d,1]$ and there is a switch in stability from g to β at $x=d$.

We consider the problem ($\mathscr{C}_\varepsilon$) on three separate subintervals as follows:

$$\varepsilon z_j'(x) = q(x,z_j), \qquad x\in X_j, \qquad z_j(\inf\{X_j\})=A_j, \quad j=1,2,3, \tag{2.4.1a}$$

$$X_1 := (0,d^*], \quad X_2 := (d^*,d], \quad X_3 := (d,1], \tag{2.4.1b}$$

$$A_1 = z_\varepsilon(0), \quad A_2 = z_1(d^*), \quad A_3 = z_2(d), \tag{2.4.1c}$$

where $d^*<d$ but neither d^* nor $d-d^*$ is of order $O(\varepsilon)$. As before, we decompose each z_j into the sum $z_j=v_j+w_j$ where v_j is the solution to

$$\varepsilon v_j'(x) = q(x,v_j), \qquad x\in X_j, \qquad v_j(\inf\{X_j\})=g(\inf\{X_j\}), \quad j=1,2,3, \tag{2.4.2}$$

and w_j, $j=1,2,3$, is the solution to

$$\varepsilon w_j'(x) = \left(\frac{q(x,z_j)-q(x,v_j)}{z_j-v_j}\right) w_j(x), \quad x\in X_j, \quad w_j(\inf\{X_j\})=A_j-g(\inf\{X_j\}). \tag{2.4.3}$$

The discrete solutions Z_j^N and the discrete regular and layer components V_j^N and W_j^N are defined in the same manner.

For ((2.4.1), $j=1$), through lower and upper solutions we have $g(x)\leqslant z_1(x)\leqslant z_\varepsilon(0)$ for $x\in[0,d^*]$ which can be used to show that $q_y(x,z_1(x))\leqslant -m_1 := -\alpha(g(d^*)-\beta)<0$ and thus the results of section 1 hold, giving $g(d^*)\leqslant z_1(d^*)\leqslant g(d^*)+C\varepsilon$ and $\|Z_1^N-z_1\|\leqslant CN^{-1}\ln N$.

For ((2.4.1), $j=2$), through lower and upper solutions we have $g(x)\leqslant z_2(x)\leqslant z_1(d^*)$. Since

$0 \leqslant w_2(d^*) \leqslant C\varepsilon$ it can easily be shown that $0 \leqslant w_2(x) \leqslant w_2(d^*)$ and $\|w_2'\| \leqslant C$. Thus in effect there is no layer in this region. However we show below that the regular component, v_2, displays an ε-dependent layer for which we should adopt a mesh.

Theorem 2.4.1. *If v_2 is the solution to ((2.4.2), $j=2$) then for $x \in [d^*, d]$ we have*

$$0 \leqslant (v_2 - g)(x) \leqslant \frac{1}{2}\left(-(g(x)-\beta) + \sqrt{(g(x)-\beta)^2 + 4\|g'\|\varepsilon/\alpha}\right), \quad |v_2'(x)| \leqslant \frac{C}{\sqrt{\varepsilon}}, \quad x \in [d^*, d].$$

Proof. If $\chi = v_2 - g$ then using ((2.4.1), $j=2$), χ satisfies

$$\varepsilon\chi' + a\chi^2 + a(g-\beta)\chi + \varepsilon g' = 0, \quad x \in (d^*, d], \quad \chi(d^*) = 0.$$

Clearly 0 is a lower solution and it can be easily checked the solution $\overline{\chi}$ of the following differential equation is an upper solution:

$$\varepsilon\overline{\chi}' + \alpha\overline{\chi}^2 + \alpha(g-\beta)\overline{\chi} - \|g'\|\varepsilon = 0, \quad x \in (d^*, d], \quad \overline{\chi}(d^*) = 0.$$

By factoring the last three terms we have the equation

$$\varepsilon\overline{\chi}' + \alpha(\overline{\chi} - R^-)(\overline{\chi} - R^+) = 0, \quad x \in (d^*, d], \quad \overline{\chi}(d^*) = 0, \tag{2.4.4a}$$

$$R^{\mp} := \tfrac{1}{2}\left(-(g-\beta) \mp \sqrt{(g-\beta)^2 + 4\|g'\|\varepsilon/\alpha}\right). \tag{2.4.4b}$$

Since $R^{\mp\prime} \geqslant 0$ we have

$$R^-(d^*) \leqslant R^-(x) \leqslant -\sqrt{\|g'\|\varepsilon/\alpha} \quad \text{and} \quad 0 < R^+(d^*) \leqslant R^+(x) \leqslant \sqrt{\|g'\|\varepsilon/\alpha}.$$

Thus we have $R^- < R^+$ implying the problem (2.4.4) is in a subclass of the problem ($\mathscr{B}_\varepsilon$) with $s = p = 2$ and since $R^{+\prime} \geqslant 0$, R^+ is an upper solution and 0 is a lower solution. From ((2.4.1), $j=2$) we have $|v_2'(x)| \leqslant CR^+(x)\varepsilon^{-1} \leqslant C\varepsilon^{-1/2}$, $x \in [d^*, d]$. □

Remark: The quantity R^+ can be written as

$$R^+ = \frac{2\|g'\|\varepsilon/\alpha}{(g-\beta) + \sqrt{(g-\beta)^2 + 4\|g'\|\varepsilon/\alpha}}.$$

We can see that if $g - \beta \geqslant C > 0$ then R^+ is of order $O(\varepsilon)$, but when $g-\beta$ is of order $O(\sqrt{\varepsilon})$, R^+ is of order $O(\sqrt{\varepsilon})$. Thus for small ε, R^+ switches in magnitude from $O(\varepsilon)$ to $O(\sqrt{\varepsilon})$ in an ε-dependent neighbourhood of $x = d$. Hence R^+, in a sense, displays a 'weak-layer'.

Choosing $\Phi_2(N)$ later, we note that

$$R^+ \geqslant \frac{\sqrt{\varepsilon}}{\Phi_2(N)} \quad \Longleftrightarrow \quad x \geqslant d - \frac{\sqrt{\varepsilon}}{\alpha}\Phi_2(N).$$

Thus choosing a transition point of the form $\sigma_2 = \min\{\frac{d-d^*}{2}, \frac{\sqrt{\varepsilon}}{\alpha}\Phi_2(N)\}$ we construct a mesh, consisting of a fine mesh and coarse mesh, in the usual manner which we specify later. Since

$\|w_2'\| \leqslant C$, we have $\|D^- w_2 - w_2'\| \leqslant CN^{-1}$ and from Theorem 2.4.1 we have $\|z_2'\| \leqslant C\varepsilon^{-1/2}$. From ((2.4.1), $j=2$), since $z_1(d^*) \geqslant z_2(x) \geqslant g(x)$, we have $z_2' \leqslant 0$. Note that $q_y(x,z_2) = -a(2z_2 - g - \beta)(x) \leqslant 0$ on $x \in [d^*, d]$. Similarly, we can show that $q_y(x,Z_2) \leqslant 0$. Expanding $q(x,z)$ in the same way as Theorem 2.2.6, we can show that at any mesh point x_i, with $h_i := x_i - x_{i-1}$, we have

$$-C(N^{-1} + {h_i}^2\varepsilon^{-1} + h_i\varepsilon^{-1/2}) \leqslant \varepsilon(D^- z_2 - z_2')(x_i) \leqslant CN^{-1}.$$

We choose $\Phi_2(N)$ such that $h_i\varepsilon^{-1/2} = O(N^{-1}\Phi_2(N)) \to 0$ in the fine mesh and $\Phi_2(N)^{-1} \to 0$ in the coarse mesh as $N \to \infty$. As in §2.2.2, we choose $\Phi_2(N) = N^{-1/2}$. Using the same methods as in Theorem 2.2.6, we can show that $\|Z_2^N - z_2\| \leqslant CN^{-\frac{1}{2}}$.

For ((2.4.1), $j=3$), through lower and upper solutions we have $\beta \leqslant z_3 \leqslant z_2(d)$ where $z_2(d) \leqslant \beta + C\sqrt{\varepsilon}$. We can then easily show that $\overline{z} = \beta + (\alpha(x-d)/\varepsilon + 1/(z_3(d) - \beta))^{-1}$ is a tighter upper solution. Using the same analysis as with ((2.4.1), $j=2$), we can derive that $\|Z_3^N - z_3\| \leqslant CN^{-\frac{1}{2}}$.

In conclusion we describe the discrete problem corresponding to ($\mathscr{C}_\varepsilon$) as: find Z_ε^N satisfying

$$\varepsilon D^- Z_\varepsilon^N(x_i) = q(x_i, Z_\varepsilon^N(x_i)), \qquad x_i \in \Omega_d^N, \qquad Z_\varepsilon^N(0) = z_\varepsilon(0), \tag{$\mathscr{C}_\varepsilon^N$}$$

where the mesh Ω_d^N is defined as

$$\Omega_d^N = \left\{ x_i \;\middle|\; \begin{array}{cc} x_i = \frac{4\sigma_1}{N} i, & i \leqslant \frac{N}{4}, \\ x_i = \sigma_1 + \frac{4(d-\sigma_2-\sigma_1)}{N}(i - \frac{N}{4}), & \frac{N}{4} < i \leqslant \frac{N}{2}, \\ x_i = d - \sigma_2 + \frac{8\sigma_2}{N}(i - \frac{N}{2}), & \frac{N}{2} < i \leqslant \frac{5N}{8}, \\ x_i = d + \frac{8\sigma_3}{N}(i - \frac{5N}{8}), & \frac{5N}{8} < i \leqslant \frac{3N}{4}, \\ x_i = d + \sigma_3 + \frac{4(1-d-\sigma_3)}{N}(i - \frac{3N}{4}), & \frac{3N}{4} < i \leqslant N, \end{array} \right\} \quad \begin{array}{c} \sigma_1 = \min\{\frac{d^*}{2}, \frac{\varepsilon}{\alpha(g(d^*)-\beta)} \ln N\}, \\ \sigma_2 = \min\{\frac{d-d^*}{2}, \frac{\sqrt{\varepsilon}}{\alpha} N^{\frac{1}{2}}\}, \\ \sigma_3 = \min\{\frac{1-d}{2}, \frac{\sqrt{\varepsilon}}{\alpha} N^{\frac{1}{2}}\}, \\ d^* = \rho d \text{ for any } 0 < \rho < 1. \end{array} \tag{2.4.5}$$

Note, in the next section, we choose $d^* = d/2$. We summarise the bound on $\|Z_\varepsilon^N - z_\varepsilon\|$ established above in the following.

Theorem 2.4.2. *If z_ε is the solution of ($\mathscr{C}_\varepsilon$) and $\overline{Z}_\varepsilon^N$ is the linear interpolation of Z_ε^N, the solution of ($\mathscr{C}_\varepsilon^N$), then for sufficiently small ε and for sufficiently large N we have*

$$|(Z_\varepsilon^N - z_\varepsilon)(x_i)| \leqslant \left\{ \begin{array}{ll} CN^{-1}\ln N & i \leqslant \frac{N}{3}, \\ CN^{-\frac{1}{2}} & i > \frac{N}{3}, \end{array} \right. \qquad x_i \in \Omega_d^N, \tag{2.4.6a}$$

$$\|\overline{Z}_\varepsilon^N - z_\varepsilon\|_{[0,1]} \leqslant CN^{-\frac{1}{2}}. \tag{2.4.6b}$$

2.5: NUMERICAL EXAMPLES

In the following examples we solve the problems from each of the classes $(\mathscr{A}_\varepsilon)$, $(\mathscr{B}_\varepsilon)$ and $(\mathscr{C}_\varepsilon)$. Unless otherwise stated, we use Newton's method to solve the nonlinear finite difference schemes $(\mathscr{A}_\varepsilon^N)$, $(\mathscr{B}_\varepsilon^N)$ and $(\mathscr{C}_\varepsilon^N)$ as outlined in the following:

Newton's Method:

For each t, solve for $U^N(t)$ where $D^-U^N(t) = g(t, U^N(t))$, $U^N(0) = u_0$ by linearising as follows: evaluate the sequence $\{U^{N,k}(t)\}$ where

$$D^-U^{N,k}(t) = g(t, U^{N,k-1}(t)) + g_u(t, U^{N,k-1}(t))(U^{N,k} - U^{N,k-1})(t), \quad U^{N,k}(0) = u_0$$

using an initial condition $U^{N,1}(t)$ until $\max_t |(U^{N,j} - U^{N,j-1})(t)|$ is less than a prescribed tolerance for some $j > 1$. Take $U^{N,j}(t)$ as the approximation for $U^N(t)$.

We use a tolerance of 10^{-9} and we use the appropriate stable reduced solution of the problem as the initial guess unless otherwise stated. In the following examples we present the differences and rates defined by

$$D_\varepsilon^N := \max_{0 \leqslant i \leqslant N} |U^N_{\varepsilon,\sigma^N}(x_i) - U^{2N}_{\varepsilon,\sigma^N}(x_{2i})|, \quad D^N := \max_\varepsilon D_\varepsilon^N, \tag{2.5.1a}$$

$$R_\varepsilon^N := \log_2 \frac{D_\varepsilon^N}{D_\varepsilon^{2N}} \quad \text{and} \quad R^N := \log_2 \frac{D^N}{D^{2N}}. \tag{2.5.1b}$$

Here, $U^N_{\varepsilon,\sigma^N}$ is the numerical solution obtained using N mesh points and $U^{2N}_{\varepsilon,\sigma^N}$ is the numerical solution obtained using $2N$ mesh intervals, but both using the transition point, σ^N, defined for N mesh points.

Also in the following examples, we present the results from using the built-in MATLAB o.d.e. functions. We will observe an exacerbation of 'technical problems' relating to the built-in functions as the singular perturbation becomes smaller. Admittedly, we are using the MATLAB functions employing all the default options or settings. The MATLAB documentation details a number of extra options or settings. However, it is felt that these details are advanced for the non-expert. It could be argued that one needs to manually change and customize the default settings for smaller values of the perturbation parameter. However, in our opinion, that is an unsatisfactory argument in itself since we would prefer numerical methods that work for a range of small values of the perturbation parameter.

Example 2.1

In this example from the class ($\mathscr{A}_\varepsilon$), examined in §2.2, we consider $1 \leqslant n \leqslant 4$ in the problem

$$\varepsilon y'_\varepsilon(x) = f(x, y_\varepsilon(x)) := -(y_\varepsilon - (\tfrac{1}{10}\cos(10x) - 1))(y_\varepsilon - (1 - \tfrac{x^2}{2}))^n, \quad y_\varepsilon(0) = A. \tag{2.5.2}$$

If $A = 2 > r(x) = 1 - x^2/2$, then r is stable for all $n \in \mathbb{N}$. We can show that $\frac{\partial^n f}{\partial y^n}(x, y_\varepsilon) \leqslant -m := -1.4n!$. In (2.2.13), we choose the practical value of $\mu_n = 1/(n-1)$ for $n \geqslant 2$. Figure 2.1 shows the numerical solutions for this example for $1 \leqslant n \leqslant 4$ in the layer region.

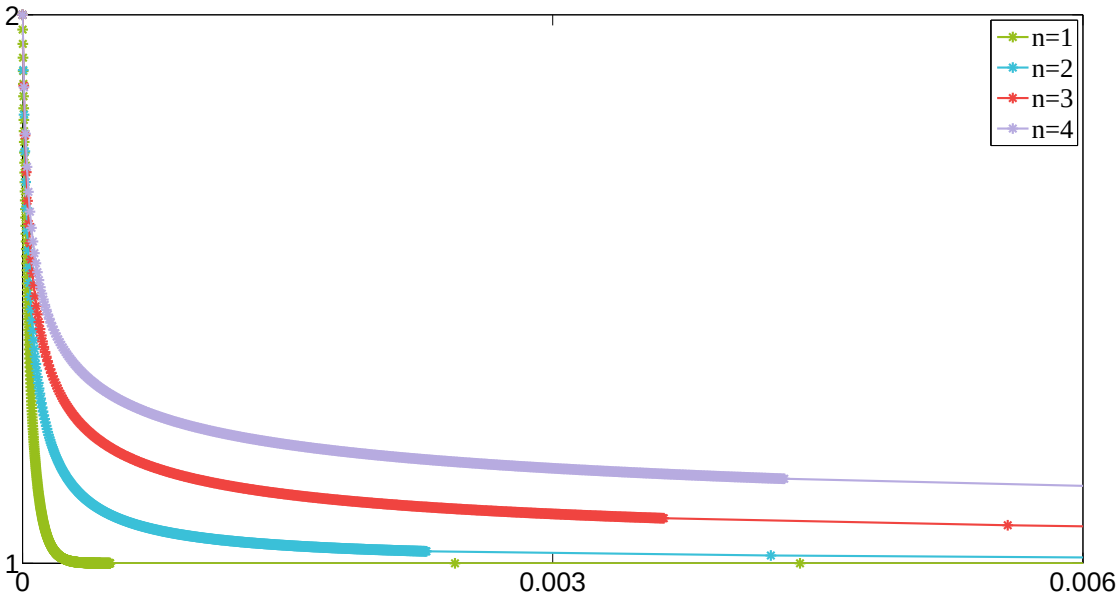

Figure 2.1: Plot of the layer structures in the numerical solutions of (2.5.2), computed using Newton's Method (pg. 38) on the mesh (2.2.13), over $x_i \in [0, 0.006]$ for $1 \leqslant n \leqslant 4$ where $\varepsilon = 10^{-4}$ and $N = 1024$.

Tables 2.1 and 2.2 show the computed rates R_ε^N for some sample values of $\varepsilon \geqslant 2^{-20}$. The rates are in line with the theoretical rates of $N^{-1}\ln N$ for $n = 1$ (see [7, Table 8.4] which illustrates the $\ln N$ effect on the rates as N increases) and $1/n$ for $n \geqslant 2$ established in Theorem 2.2.6.

	$\mathbf{R}_\varepsilon^N$											
ε \ N	2^5	2^6	2^7	2^8	2^9	2^{10}	2^{11}	2^{12}	2^{13}	$\cdots$	2^{17}	2^{18}
	n = 1											
2^0	0.95	0.98	0.99	0.99	1	1	1	1	1	$\cdots$	1	1
2^{-1}	0.91	0.95	0.98	0.99	0.99	1	1	1	1	$\cdots$	1	1
2^{-2}	0.84	0.91	0.95	0.98	0.99	0.99	1	1	1	$\cdots$	1	1
2^{-3}	0.57	0.68	0.74	0.94	0.98	0.99	0.99	1	1	$\cdots$	1	1
2^{-4}	0.57	0.68	0.74	0.79	0.82	0.85	0.87	0.88	0.89	$\cdots$	1	1
2^{-5}	0.58	0.68	0.74	0.79	0.82	0.85	0.87	0.88	0.89	$\cdots$	0.92	0.92
2^{-6}	0.58	0.68	0.74	0.79	0.82	0.85	0.87	0.88	0.89	$\cdots$	0.92	0.92
$\vdots$	$\vdots$	$\vdots$	$\vdots$	$\vdots$	$\vdots$	$\vdots$	$\vdots$	$\vdots$	$\vdots$	$\cdots$	$\vdots$	$\vdots$
2^{-20}	0.58	0.68	0.74	0.79	0.82	0.85	0.87	0.88	0.89	$\cdots$	0.92	0.92
$\mathbf{R}^N$	0.58	0.68	0.74	0.79	0.82	0.85	0.87	0.88	0.89	$\cdots$	0.92	0.92
	n = 2											
2^0	0.92	0.96	0.98	0.99	0.99	1	1	1	1	$\cdots$	1	1
2^{-1}	0.87	0.93	0.96	0.98	0.99	0.99	1	1	1	$\cdots$	1	1
2^{-2}	0.78	0.87	0.93	0.96	0.98	0.99	1	1	1	$\cdots$	1	1
2^{-3}	0.64	0.79	0.88	0.93	0.96	0.98	0.99	1	1	$\cdots$	1	1
2^{-4}	0.28	0.37	0.79	0.88	0.93	0.96	0.98	0.99	1	$\cdots$	1	1
2^{-5}	0.28	0.35	0.38	0.42	0.88	0.93	0.96	0.98	0.99	$\cdots$	1	1
2^{-6}	0.28	0.36	0.38	0.41	0.43	0.46	0.93	0.96	0.98	$\cdots$	1	1
2^{-7}	0.28	0.36	0.38	0.41	0.43	0.45	0.46	0.48	0.96	$\cdots$	1	1
2^{-8}	0.28	0.36	0.38	0.41	0.43	0.45	0.46	0.47	0.48	$\cdots$	1	1
2^{-9}	0.28	0.36	0.38	0.41	0.43	0.45	0.46	0.47	0.48	$\cdots$	0.99	1
2^{-10}	0.28	0.36	0.38	0.41	0.43	0.45	0.46	0.47	0.48	$\cdots$	0.49	0.51
2^{-11}	0.28	0.36	0.38	0.41	0.43	0.45	0.46	0.47	0.48	$\cdots$	0.49	0.50
$\vdots$	$\vdots$	$\vdots$	$\vdots$	$\vdots$	$\vdots$	$\vdots$	$\vdots$	$\vdots$	$\vdots$	$\cdots$	$\vdots$	$\vdots$
2^{-20}	0.28	0.36	0.38	0.41	0.43	0.45	0.46	0.47	0.48	$\cdots$	0.49	0.50
$\mathbf{R}^N$	0.28	0.36	0.38	0.41	0.43	0.45	0.46	0.47	0.48	$\cdots$	0.49	0.50

Table 2.1: Computed rates of convergence R_ε^N and R^N (as defined in (2.5.1)), measured from the numerical solutions of (2.5.2), calculated using Newton's Method (pg. 38) on the mesh (2.2.13), for $n = 1$ and $n = 2$.

	$\mathbf{R}_\varepsilon^{\mathbf{N}}$											
ε \ **N**	2^5	2^6	2^7	2^8	2^9	2^{10}	2^{11}	2^{12}	2^{13}	…	2^{17}	2^{18}
	n = 3											
2^0	0.9	0.94	0.97	0.99	0.99	1	1	1	1	⋯	1	1
2^{-1}	0.84	0.9	0.95	0.97	0.99	0.99	1	1	1	⋯	1	1
2^{-2}	0.74	0.84	0.91	0.95	0.97	0.99	0.99	1	1	⋯	1	1
2^{-3}	0.52	0.75	0.84	0.91	0.95	0.97	0.99	0.99	1	⋯	1	1
2^{-4}	0.2	0.31	0.75	0.84	0.91	0.95	0.97	0.99	0.99	⋯	1	1
2^{-5}	0.2	0.19	0.23	0.64	0.84	0.91	0.95	0.97	0.99	⋯	1	1
2^{-6}	0.2	0.19	0.23	0.26	0.39	0.84	0.91	0.95	0.97	⋯	1	1
2^{-7}	0.2	0.19	0.23	0.26	0.24	0.27	0.71	0.91	0.95	⋯	1	1
2^{-8}	0.2	0.19	0.23	0.26	0.24	0.27	0.27	0.45	0.91	⋯	0.99	1
2^{-9}	0.2	0.19	0.23	0.26	0.24	0.27	0.27	0.28	0.29	⋯	0.99	0.99
2^{-10}	0.2	0.19	0.23	0.26	0.24	0.27	0.27	0.28	0.29	⋯	0.97	0.99
2^{-11}	0.2	0.19	0.23	0.26	0.24	0.27	0.27	0.28	0.29	⋯	0.81	0.97
2^{-12}	0.2	0.19	0.23	0.26	0.24	0.27	0.27	0.28	0.29	⋯	0.31	0.49
2^{-13}	0.2	0.19	0.23	0.26	0.24	0.27	0.27	0.28	0.29	⋯	0.31	0.32
⋮	⋮	⋮	⋮	⋮	⋮	⋮	⋮	⋮	⋮	⋯	⋮	⋮
2^{-20}	0.2	0.19	0.23	0.26	0.24	0.27	0.27	0.28	0.29	⋯	0.31	0.32
$\mathbf{R}^{\mathbf{N}}$	0.2	0.19	0.23	0.26	0.24	0.27	0.27	0.28	0.29	⋯	0.31	0.32
	n = 4											
2^0	0.88	0.93	0.96	0.98	0.99	1	1	1	1	⋯	1	1
2^{-1}	0.8	0.88	0.94	0.97	0.98	0.99	1	1	1	⋯	1	1
2^{-2}	0.7	0.81	0.89	0.94	0.97	0.98	0.99	1	1	⋯	1	1
2^{-3}	0.41	0.71	0.81	0.89	0.94	0.97	0.98	0.99	1	⋯	1	1
2^{-4}	0.17	0.24	0.71	0.81	0.89	0.94	0.97	0.98	0.99	⋯	1	1
2^{-5}	0.17	0.13	0.15	0.67	0.81	0.89	0.94	0.97	0.98	⋯	1	1
2^{-6}	0.17	0.13	0.15	0.16	0.5	0.81	0.89	0.94	0.97	⋯	1	1
2^{-7}	0.17	0.13	0.15	0.16	0.18	0.32	0.81	0.89	0.94	⋯	1	1
2^{-8}	0.17	0.13	0.15	0.16	0.18	0.19	0.18	0.76	0.89	⋯	0.99	1
2^{-9}	0.17	0.13	0.15	0.16	0.18	0.19	0.18	0.2	0.56	⋯	0.98	0.99
2^{-10}	0.17	0.13	0.15	0.16	0.18	0.19	0.18	0.2	0.2	⋯	0.97	0.98
2^{-11}	0.17	0.13	0.15	0.16	0.18	0.19	0.18	0.2	0.2	⋯	0.94	0.97
2^{-12}	0.17	0.13	0.15	0.16	0.18	0.19	0.18	0.2	0.2	⋯	0.61	0.94
2^{-13}	0.17	0.13	0.15	0.16	0.18	0.19	0.18	0.2	0.2	⋯	0.22	0.39
2^{-14}	0.17	0.13	0.15	0.16	0.18	0.19	0.18	0.2	0.2	⋯	0.22	0.22
⋮	⋮	⋮	⋮	⋮	⋮	⋮	⋮	⋮	⋮	⋯	⋮	⋮
2^{-20}	0.17	0.13	0.15	0.16	0.18	0.19	0.18	0.2	0.2	⋯	0.22	0.22
$\mathbf{R}^{\mathbf{N}}$	0.17	0.13	0.15	0.16	0.18	0.19	0.18	0.2	0.2	⋯	0.22	0.22

Table 2.2: Computed rates of convergence R_ε^N and R^N (as defined in (2.5.1)), measured from the numerical solutions of (2.5.2), calculated using Newton's Method (pg. 38) on the mesh (2.2.13), for $n = 3$ and $n = 4$.

We present some results from using the built-in o.d.e. solvers in MATLAB. In the MATLAB documentation, the following solvers are prescribed for non-stiff systems of first order equations: *ode45*, *ode23* and *ode113*. In Table 2.3, we present the number of mesh intervals on $[0,1]$ each solver uses to numerically solve (2.5.2). We see that the number of mesh intervals used, increases proportionally to the inverse power of the perturbation parameter.

	ode45		*ode23*		*ode113*	
ε	**n=1**	**n=2**	**n=1**	**n=2**	**n=1**	**n=2**
$\mathbf{10^{-1}}$	56	52	19	18	30	30
$\mathbf{10^{-2}}$	236	72	82	25	158	44
$\mathbf{10^{-3}}$	2236	132	741	41	1176	69
$\mathbf{10^{-4}}$	22156	324	7327	87	11451	15841
$\mathbf{10^{-5}}$	221344	780	73187	133860	114229	188881

Table 2.3: Number of mesh intervals on $[0,1]$ used by MATLAB solvers to approximate the solution to (2.5.2).

In the MATLAB documentation, the following solvers are prescribed for stiff systems of first order equations: *ode15s*, *ode23s*, *ode23t* and *ode23tb*. In Figures 2.2 and 2.3, graphs of numerical approximations of the solution of (2.5.2) are displayed. Note that in (2.5.2), the stable reduced solution is $1-\frac{x^2}{2}$ and the unstable reduced solution is $\frac{1}{10}\cos(10x)-1$. Furthermore, from §2.2, the solution to (2.5.2) is bounded below by $1-\frac{x^2}{2}$. We see in Figure 2.2, the solution breaks this bound 'mildly'. We say 'mildly' here as it could be argued that we know from the theory that the solution is within $O(\varepsilon)$ of the reduced solution outside the layer region. Thus we are mainly concerned with approximating the solution in the layer region. However, as shown in Figure 2.2, the *ode23s* algorithm breaks a theoretical bound on the solution, albeit close to the end of the layer region, but nevertheless, within the layer region. In Figure 2.3 we see the graphs of nonsensical numerical solutions, returned by the *ode15s*, *ode23t* and *ode23tb* solvers, which approach the unstable reduced solution.

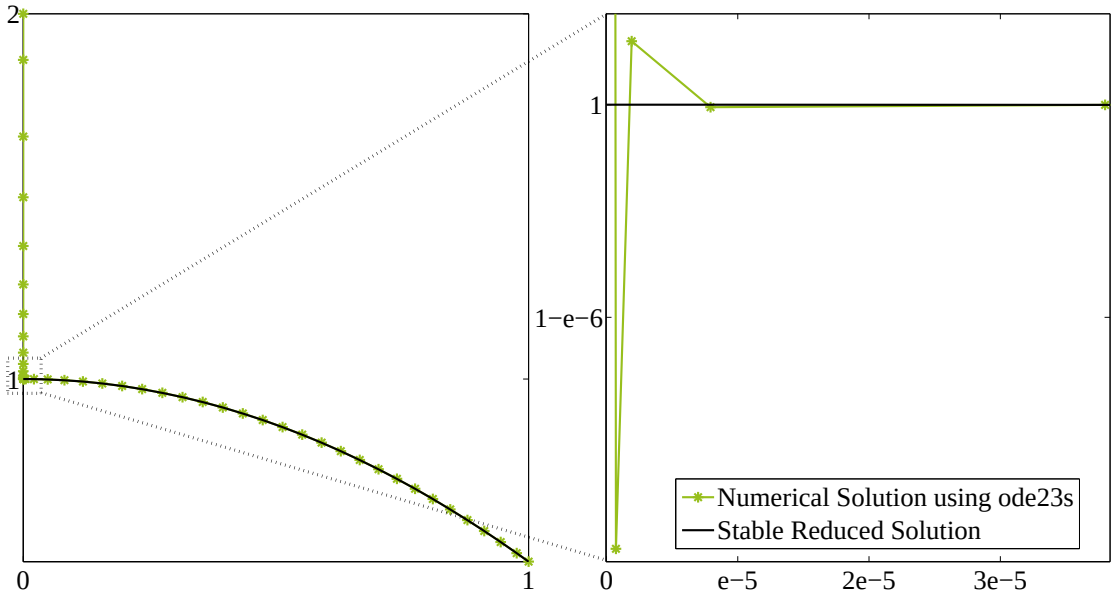

Figure 2.2: Plot of the numerical solution of (2.5.2), computed using the MATLAB solver *ode23s*, with $n = 1$ and $\varepsilon = 10^{-7}$.

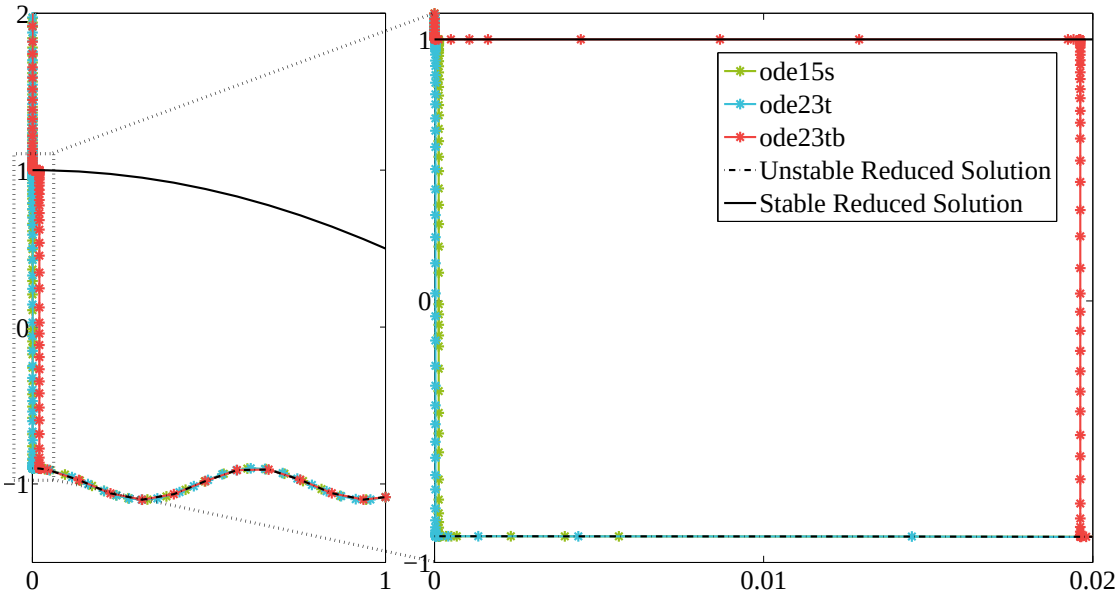

Figure 2.3: Plots of the numerical solution of (2.5.2), computed using the MATLAB solvers *ode15s*, *ode23t* and *ode23tb*, with $n = 2$ and $\varepsilon = 10^{-8}$.

Example 2.2

From the problem class ($\mathscr{B}_\varepsilon$), we consider $n_s = 1$ and $g_{s+1} - u_\varepsilon(0) \geqslant C > 0$ in the problem

$$\varepsilon u'_\varepsilon + 2e^x(u_\varepsilon - (\tfrac{1}{10}\cos 10x))(u_\varepsilon - (2 + 2(x - \tfrac{1}{2})^2))(u_\varepsilon - (4 + \tfrac{1}{10}\sin x)) = 0,\ u_\varepsilon(0) = A. \qquad (2.5.3)$$

If $A = 2.05$ then $g_1 = \frac{1}{10}\cos 10x$ is the stable reduced solution. Furthermore $k_u(0, u_\varepsilon(0)) > 0$ and $g_{s+1}(0) > u_\varepsilon(0) > \underline{\gamma}_{s+1}$, which is a case not examined in [22]. For the mesh (2.2.13, 2.3.20), we choose the practical values of $\kappa = b = 1.52$, $\underline{\varsigma} = \frac{1}{2}(\underline{\gamma}_s - \overline{\gamma}_{s-1})$ and $\overline{\varsigma} = \frac{1}{2}(\underline{\gamma}_{s+1} - \overline{\gamma}_s)$. Table 2.4 shows the computed rates R_ε^N which are in agreement with the rate associated with the bound $N^{-1}\ln N$ established in Theorem 2.3.7.

	$\mathbf{R_\varepsilon^N}$								
ε \ **N**	**32**	**64**	**128**	**256**	**512**	**1024**	**2048**	**4096**	**8192**
$\mathbf{2^0}$	0.96	1	0.99	1	1	1	1	1	1
$\mathbf{2^{-1}}$	0.74	0.8	0.96	1	1	1	1	1	1
$\mathbf{2^{-2}}$	0.7	0.83	0.84	0.86	0.87	0.88	0.89	0.9	0.91
$\mathbf{2^{-3}}$	0.33	0.62	0.78	0.82	0.84	0.98	1	1	1
$\mathbf{2^{-4}}$	0.32	0.6	0.78	0.82	0.84	0.86	0.87	0.88	0.89
$\mathbf{2^{-5}}$	0.31	0.59	0.78	0.82	0.84	0.86	0.87	0.88	0.89
⋮	⋮	⋮	⋮	⋮	⋮	⋮	⋮	⋮	⋮
$\mathbf{2^{-20}}$	0.31	0.58	0.78	0.82	0.84	0.86	0.87	0.88	0.89
$\mathbf{R^N}$	0.33	0.62	0.78	0.82	0.84	0.86	0.87	0.88	0.89

Table 2.4: Computed rates of convergence R_ε^N and R^N (as defined in (2.5.1)), measured from the numerical solutions of (2.5.3), calculated using Newton's Method (pg. 38) on the mesh (2.3.20), for $u_\varepsilon(0) = 2.05$.

Example 2.3 (**Arbitrarily close to an unstable root**)

In this example from the class ($\mathscr{B}_\varepsilon$) we consider $n_s = 1$ and $u_\varepsilon(0) - g_{s-1}(0) = \varepsilon$ in the problem

$$\varepsilon u'_\varepsilon + (5 + 1/(x + 0.5))(u_\varepsilon - \cos 10x)(u_\varepsilon - 2) = 0, \quad u_\varepsilon(0) = A. \qquad (2.5.4)$$

If $A = 1 + \varepsilon$ then $g_2 = 2$ is the stable reduced solution. We can solve the difference scheme exactly, and for the mesh (2.2.13, 2.3.19), we calculate $\kappa_1 = \alpha = 17/3$ and $\kappa_2 = 1$. Table 2.5 shows the differences D_ε^N and rates R_ε^N for sample values of $\varepsilon \geqslant 2^{-40}$. We can see that although the rates behave well, as $\varepsilon \to 0$, the computed differences, D_ε^N , steadily increase. This is in agreement with the ε-dependent rate associated with the bound of $\max\{C, \varepsilon^{-p}N^{-1}\ln(N/\varepsilon)\}$, $p > 1$, established in Theorem 2.3.7. Note that as $\varepsilon \to 0$ the initial condition tends to an unstable value.

	$\mathbf{D}_{\varepsilon}^{\mathbf{N}}$								
ε \ **N**	**64**	**128**	**256**	**512**	**1024**	**2048**	**4096**	**8192**	**16384**
$\mathbf{2^{-4}}$	0.024	0.013	0.007	0.004	0.002	0.001	0.001	0	0
$\mathbf{2^{-8}}$	0.104	0.054	0.028	0.015	0.008	0.004	0.002	0.001	0.001
$\mathbf{2^{-12}}$	0.230	0.116	0.059	0.031	0.016	0.008	0.004	0.002	0.001
$\mathbf{2^{-16}}$	0.392	0.198	0.101	0.052	0.027	0.014	0.007	0.004	0.002
$\mathbf{2^{-20}}$	0.579	0.299	0.151	0.077	0.040	0.020	0.010	0.005	0.003
$\mathbf{2^{-24}}$	0.770	0.413	0.211	0.107	0.055	0.028	0.014	0.007	0.004
$\mathbf{2^{-28}}$	0.908	0.535	0.280	0.142	0.073	0.037	0.019	0.010	0.005
$\mathbf{2^{-32}}$	0.995	0.654	0.354	0.182	0.093	0.047	0.024	0.012	0.006
$\mathbf{2^{-36}}$	0.998	0.757	0.435	0.226	0.115	0.058	0.030	0.015	0.008
$\mathbf{2^{-40}}$	0.999	0.847	0.516	0.273	0.140	0.071	0.036	0.018	0.010

	$\mathbf{R}_{\varepsilon}^{\mathbf{N}}$							
ε \ **N**	**64**	**128**	**256**	**512**	**1024**	**2048**	**4096**	**8192**
$\mathbf{2^{-4}}$	0.86	0.88	0.88	0.89	0.9	0.91	0.91	0.92
$\mathbf{2^{-8}}$	0.95	0.93	0.92	0.92	0.93	0.93	0.93	0.93
$\mathbf{2^{-12}}$	0.99	0.96	0.95	0.94	0.94	0.94	0.94	0.94
$\mathbf{2^{-16}}$	0.98	0.98	0.96	0.95	0.95	0.95	0.95	0.95
$\mathbf{2^{-20}}$	0.95	0.98	0.97	0.96	0.96	0.96	0.96	0.96
$\mathbf{2^{-24}}$	0.90	0.97	0.97	0.97	0.97	0.96	0.96	0.96
$\mathbf{2^{-28}}$	0.76	0.94	0.97	0.97	0.97	0.97	0.97	0.97
$\mathbf{2^{-32}}$	0.61	0.89	0.96	0.98	0.97	0.97	0.97	0.97
$\mathbf{2^{-36}}$	0.40	0.80	0.95	0.97	0.98	0.97	0.98	0.97
$\mathbf{2^{-40}}$	0.24	0.71	0.92	0.97	0.98	0.97	1.01	0.83

Table 2.5: Computed differences D_{ε}^{N} and computed rates of convergence R_{ε}^{N} (as defined in (2.5.1)), measured from the numerical solutions of (2.5.4), solved exactly using the numerical method (($\mathscr{B}_{\varepsilon}^{N}$), (2.3.19)), for $u_{\varepsilon}(0)=1+\varepsilon$.

The delayed structure of the layer is shown in Figure 2.4 which shows the numerical solution of the problem in this example compared with the numerical solution of the same problem except with the initial condition sufficiently close to the stable reduced solution.

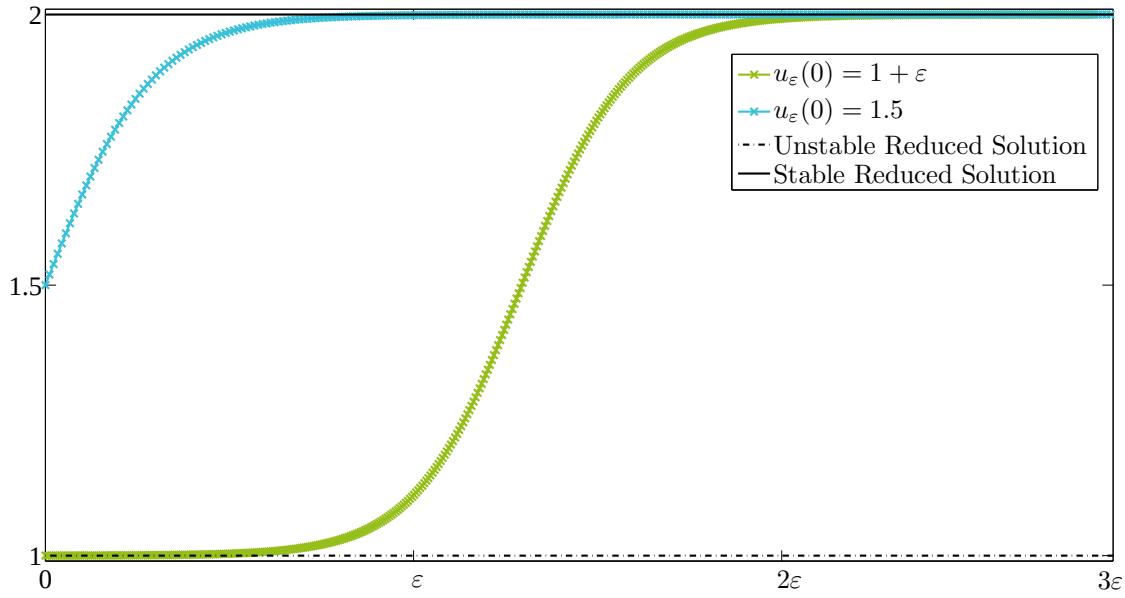

Figure 2.4: Plot of the layer structures in the numerical solution of (2.5.4), solved exactly using the numerical method ($(\mathscr{B}_\varepsilon^N)$, (2.3.19)), over $x_i \in [0, 3\varepsilon]$ for $u_\varepsilon(0) = 1.5$ and $u_\varepsilon(0) = 1+\varepsilon$ where $\varepsilon = 10^{-4}$ and $N = 1024$.

Even though the difference scheme can be solved exactly, we still present some results when the built-in MATLAB ode functions are used to approximate the solution of (2.5.4). In Table 2.6, we present the number of mesh intervals on $[0,1]$ the solvers *ode45*, *ode23* and *ode113* use to numerically solve (2.5.4). As in Example 2.1, we observe that the solvers use a number of mesh intervals that is inversely proportional to the perturbation parameter.

ε	*ode45*	*ode23*	*ode113*
$\mathbf{10^{-1}}$	168	53	76
$\mathbf{10^{-2}}$	1516	504	777
$\mathbf{10^{-3}}$	15032	4969	7827
$\mathbf{10^{-4}}$	150192	49622	77136

Table 2.6: Number of mesh intervals on $[0,1]$ used by MATLAB solvers to approximate the solution to (2.5.4).

In Figure 2.5, graphs of numerical approximations of the solution of (2.5.4) are displayed. Note that in (2.5.4), the stable reduced solution is 2 and the unstable reduced solution is $\cos(10x) - 1$. Furthermore, from §2.2, the solution to (2.5.4) is bounded below by $A = 1+\varepsilon$. In Figure 2.5, we see nonsensical numerical solutions that break this bound and approach the unstable reduced solution.

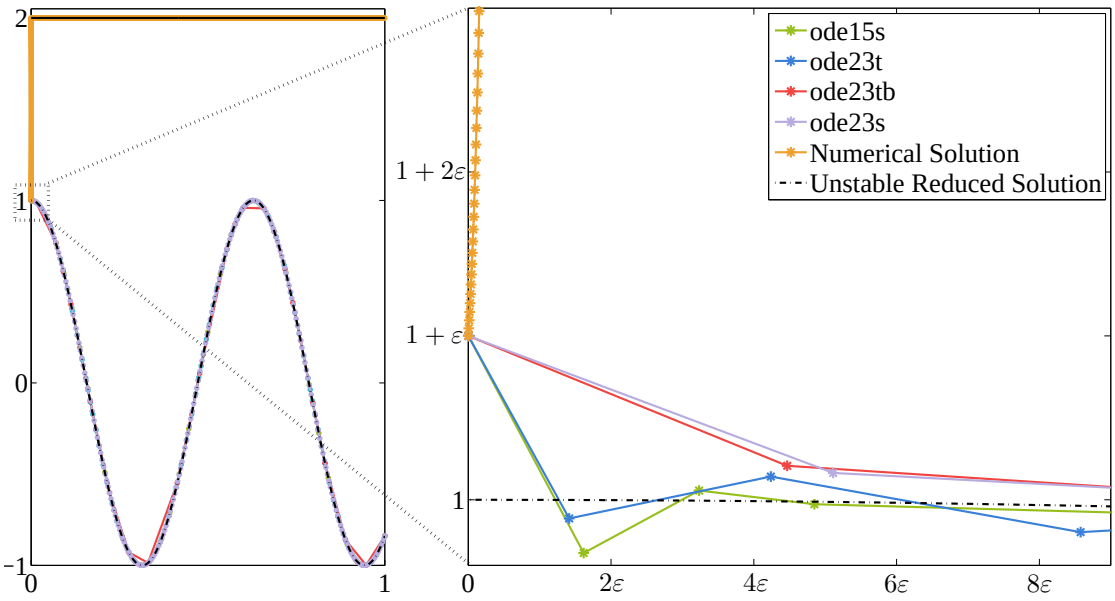

Figure 2.5: Plot of the numerical solution of (2.5.4), solved exactly using the numerical method (($\mathscr{B}_\varepsilon^N$), (2.3.19)) with $N = 1024$, and also computed using various MATLAB inbuilt functions, all with $\varepsilon = 10^{-5}$.

Example 2.4 (**Double root example**)

In this example from the class ($\mathscr{B}_\varepsilon$) we consider $n_s = 2$ in the problem

$$\varepsilon u_\varepsilon' + a(x)(u_\varepsilon - (\tfrac{1}{10}\cos 8x)(u_\varepsilon - (2-\ln(x+1)))^2(u_\varepsilon - (4+\tfrac{1}{10}\cos 12x))^2 = 0,\ u_\varepsilon(0) = A, \quad (2.5.5)$$

where $a(x) = 1.5 + \tanh(x-0.5)$. If $A = 3.1$ then $g_2(x) = 2 - \ln(x+1)$ is the stable reduced solution and $k_{uu}(0, u_\varepsilon(0)) > 0$. For (2.2.13, 2.3.20), we choose the practical values of $\kappa = b$, $\underline{\varsigma} = \frac{1}{2}(\underline{\gamma}_s - \overline{\gamma}_{s-1})$ and $\overline{\varsigma} = \frac{1}{2}(\underline{\gamma}_{s+1} - \overline{\gamma}_s)$ and b is calculated as $b = 1.13$. We use $g_2(x) + (A - g_2(0))(1 + (A - g_2(0))px/\varepsilon)^{-1}$ for the initial condition. Table 2.7 shows the computed rates R_ε^N which are in agreement with the asymptotic rate of $\frac{1}{2}$ established in Theorem 2.3.7.

	$\mathbf{R}_\varepsilon^{\mathbf{N}}$								
ε \ **N**	**32**	**64**	**128**	**256**	**512**	**1024**	**2048**	**4096**	**8192**
$\mathbf{2^0}$	0.96	0.98	0.99	1	1	1	1	1	1
$\mathbf{2^{-1}}$	0.94	0.96	0.98	0.99	1	1	1	1	1
$\mathbf{2^{-2}}$	0.87	0.93	0.96	0.98	0.99	0.99	1	1	1
$\mathbf{2^{-3}}$	0.74	0.86	0.93	0.96	0.98	0.99	0.99	1	1
$\mathbf{2^{-4}}$	0.37	0.58	0.86	0.93	0.96	0.98	0.99	0.99	1
$\mathbf{2^{-5}}$	0.37	0.34	0.42	0.69	0.93	0.96	0.98	0.99	0.99
$\mathbf{2^{-6}}$	0.37	0.34	0.42	0.41	0.45	0.76	0.96	0.98	0.99
$\mathbf{2^{-7}}$	0.37	0.34	0.42	0.41	0.45	0.46	0.47	0.79	0.98
$\mathbf{2^{-8}}$	0.37	0.33	0.42	0.41	0.45	0.46	0.47	0.48	0.49
$\vdots$	$\vdots$	$\vdots$	$\vdots$	$\vdots$	$\vdots$	$\vdots$	$\vdots$	$\vdots$	$\vdots$
$\mathbf{2^{-20}}$	0.37	0.33	0.42	0.41	0.45	0.46	0.47	0.48	0.49
$\mathbf{R^N}$	0.37	0.33	0.42	0.41	0.45	0.46	0.47	0.48	0.49

Table 2.7: Computed rates of convergence R_ε^N and R^N (as defined in (2.5.1)), measured from the numerical solutions of (2.5.5), calculated using Newton's Method (pg. 38) on the mesh (2.3.20), for $u_\varepsilon(0)=3.1$.

Example 2.5

In this example from the class ($\mathscr{C}_\varepsilon$) examined in section 4, we consider the problem

$$\varepsilon z'(x)+(3+\ln(x+1))(z-\beta)(z-g)(x)=0, \quad z(0)=A, \tag{2.5.6}$$

where $g(x)=5+\tanh(5(0.5-x))$, $\beta=5$ and $g(d)=\beta$ at $d=0.5$. For the mesh (2.4.5), we choose $d^*=\frac{d}{2}=0.25$. We can solve the difference scheme exactly. Table 2.8 shows the computed rates R_ε^N and R^N for some sample values of $\varepsilon \geqslant 2^{-20}$. We consider $A=6.25>g(0)$ for which the error in the initial layer is dominant and $A=g(0)$ for which there is no initial layer and the error in the layer near the point d dominates. Note that the calculation of D_ε^N in (2.5.1) is done as in the previous examples where for each N we solve the problem numerically using N mesh points and the layer widths (σ_1^N, σ_2^N, σ_3^N) defined in (2.4.5). We compare the resulting numerical solution to that obtained using $2N$ mesh intervals, but using the same layer widths defined for using N mesh points i.e. the σ_i^N's. The computed rates are in agreement with the asymptotic rates established in Theorem 2.4.6.

	$\mathbf{R}_\varepsilon^{\mathbf{N}}$								
ε \ **N**	**32**	**64**	**128**	**256**	**512**	**1024**	**2048**	**4096**	**8192**
	$\mathbf{z(0)=6.25>g(0)}$								
$\mathbf{2^0}$	0.94	0.96	0.98	0.99	1.00	1.00	1.00	1.00	1.00
$\mathbf{2^{-1}}$	0.88	0.94	0.97	0.98	0.99	1.00	1.00	1.00	1.00
$\mathbf{2^{-2}}$	0.85	0.92	0.96	0.98	0.99	0.99	1.00	1.00	1.00
$\mathbf{2^{-3}}$	0.81	0.89	0.94	0.97	0.99	0.99	1.00	1.00	1.00
$\mathbf{2^{-4}}$	0.56	0.65	0.84	0.94	0.97	0.99	0.99	1.00	1.00
$\mathbf{2^{-5}}$	0.56	0.65	0.72	0.78	0.82	0.85	0.86	0.88	0.89
$\mathbf{2^{-6}}$	0.56	0.65	0.72	0.78	0.82	0.85	0.86	0.88	0.89
$\mathbf{R^N}$	**0.56**	**0.65**	**0.72**	**0.78**	**0.82**	**0.85**	**0.86**	**0.88**	**0.89**
	$\mathbf{z(0)=g(0)}$								
$\mathbf{2^0}$	0.94	0.96	0.98	0.99	0.99	1.00	1.00	1.00	1.00
$\mathbf{2^{-3}}$	0.81	0.89	0.94	0.97	0.99	0.99	1.00	1.00	1.00
$\mathbf{2^{-6}}$	0.70	0.68	0.88	0.92	0.97	0.98	0.99	1.00	1.00
$\mathbf{2^{-9}}$	0.23	0.53	0.36	0.78	0.91	0.95	0.98	0.99	0.99
$\mathbf{2^{-12}}$	0.23	0.44	0.35	0.44	0.48	0.49	0.86	0.97	0.98
$\mathbf{2^{-15}}$	0.23	0.44	0.35	0.44	0.44	0.46	0.47	0.51	0.51
$\mathbf{2^{-18}}$	0.23	0.44	0.35	0.44	0.44	0.46	0.47	0.48	0.49
$\mathbf{R^N}$	**0.81**	**0.89**	**0.92**	**0.95**	**0.97**	**0.98**	**0.99**	**0.99**	**1.00**

Table 2.8: Computed rates of convergence R_ε^N and R^N (as defined in (2.5.1)), measured from the numerical solutions of (2.5.6), solved exactly using the numerical method ($(\mathscr{C}_\varepsilon^N)$, (2.4.5)), for $z(0)>g(0)$ and $z(0)=g(0)$.

Figure 2.6 displays a numerical solution to this problem for $\varepsilon = 10^{-5}$. Figure 2.6 also includes a plot of the numerical solution around the point at which there is a switch in stability, which evidences the change in magnitude of the bound established in Theorem 2.4.1.

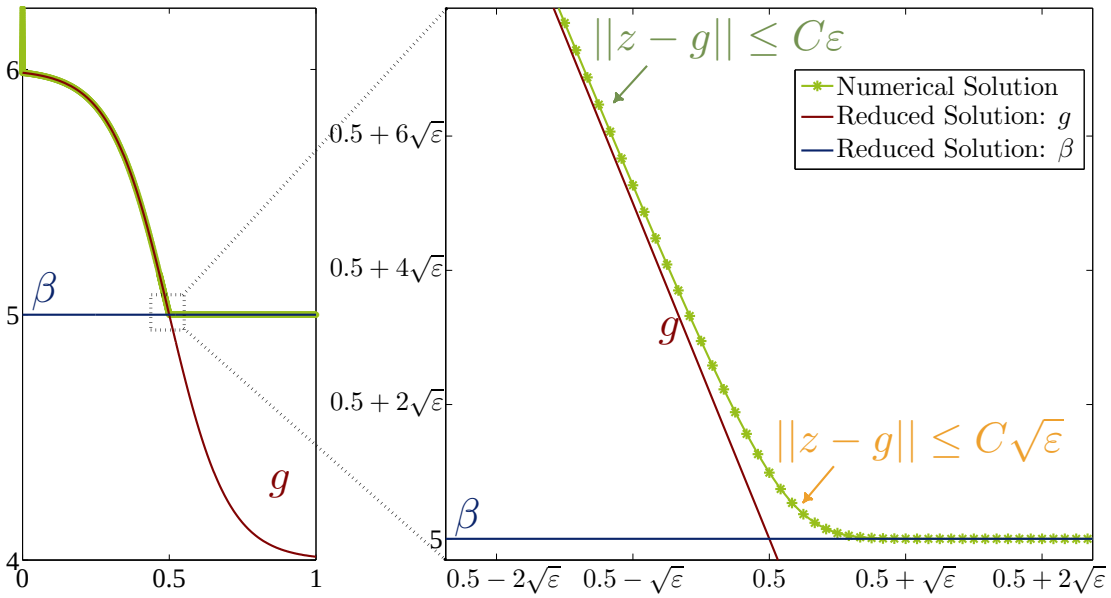

Figure 2.6: Plots of the numerical solution of (2.5.6), solved exactly using the numerical method (($\mathscr{C}_\varepsilon^N$), (2.4.5)), over $x_i \in [0,1]$ and over $x_i \in [0.49, 0.51]$, around $d = 0.5$ (switch in stability), for $u_\varepsilon(0) = 6.25$ where $\varepsilon = 10^{-5}$ and $N = 1024$.

Again, even though the difference scheme can be solved exactly, we present some results when the built-in MATLAB ode functions are used to approximate the solution of (2.5.4). The built-in solvers *ode45*, *ode23* and *ode113* display the same behaviour as in Examples 2.1 and 2.3 whereby the number of mesh intervals used to approximate the solution is inversely proportional to the perturbation parameter. In Figure 2.7, graphs of numerical approximations of the solution of (2.5.6) are displayed. We see that the solvers return oscillatory approximations and in the case of *ode23tb*, do not capture the switch in stability between the two reduced solutions. We also see that in the case of *ode23s*, the approximation to the solution captures the switch in stability but only 'switches' at a considerable distance past the point of intersection of the reduced solutions.

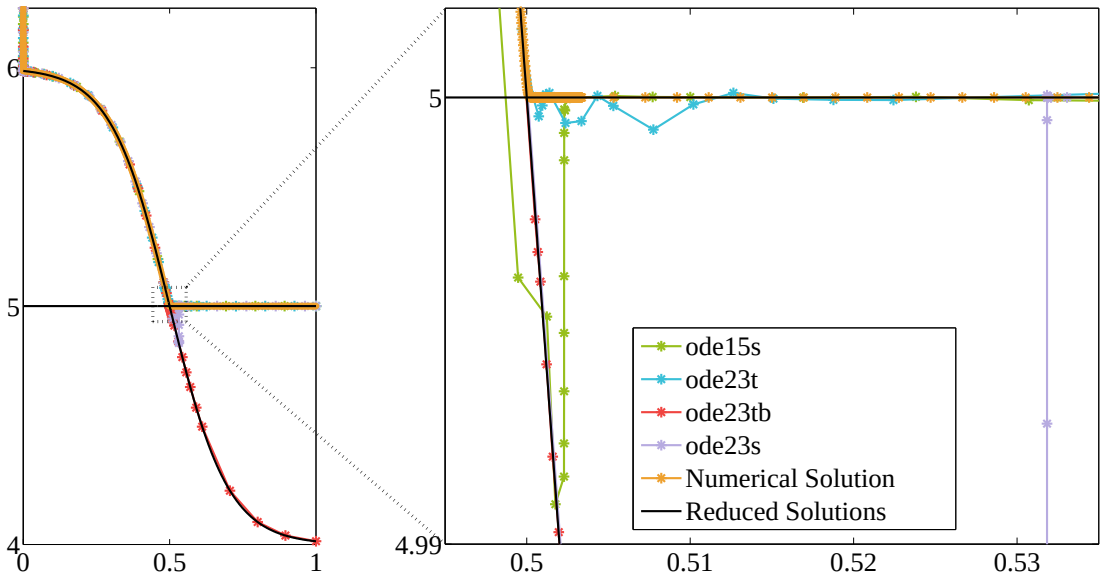

Figure 2.7: Plots of the numerical solution of (2.5.6), solved exactly using the numerical method (($\mathscr{C}_\varepsilon^N$), (2.4.5)) for $N = 1024$, and also computed using various MATLAB inbuilt functions, all with $\varepsilon = 10^{-7}$.

2.6: Further Problems and Future Work

In this section, we casually discuss two problems that may be worthy of consideration in the future. Note that this discussion did not appear in [25].

2.6.1 A Combustion Problem

In [13, pg. 69], O'Malley analyses the following problem, originally presented in [28], as a model of a class of trimolecular reactions: find $\tilde{z}$ such that

$$\tilde{z}'(t) = \tilde{z}^2(1-\tilde{z})(t), \quad t > 0, \quad \tilde{z}(0) = \tilde{\varepsilon}, \tag{2.6.1}$$

where $\tilde{\varepsilon}$ is a small parameter representing a disturbance of the pre-ignition state. The reduced solutions are 0 (unstable) and 1 (stable). If we consider the transform $\tilde{x} = \tilde{\varepsilon} t$, then we obtain the singularly perturbed problem

$$\tilde{\varepsilon} z'(\tilde{x}) = z^2(1-z)(\tilde{x}), \quad \tilde{x} > 0, \quad z(0) = \tilde{\varepsilon}. \tag{2.6.2}$$

This is a problem from the class ($\mathscr{B}_\varepsilon$), however we only considered the unstable root to have multiplicity 1 as in (2.3.2a), in such a case. For (2.6.1), O'Malley establishes that a layer occurs at a $O(1/\tilde{\varepsilon})$ location in the problem domain. This motivates us to consider the transform $x = \tilde{\varepsilon}^2 t$, $\varepsilon = \tilde{\varepsilon}^2$ on (2.6.1) to obtain

$$\varepsilon y' = y^2(1-y), \quad x > 0, \quad y(0) = \sqrt{\varepsilon}, \tag{2.6.3}$$

where we expect a layer in a $O(\sqrt{\varepsilon})$ neighbourhood of $x = 0$. Using upper and lower solutions, we can establish that a solution to (2.6.3), y, exists satisfying

$$0 \leqslant 1 - y(x) \leqslant \left(1 + \frac{\sqrt{\varepsilon}}{1-\sqrt{\varepsilon}} e^{x/\sqrt{\varepsilon}}\right)^{-1}, \quad x \geqslant 0. \tag{2.6.4}$$

Hence from (2.6.3), we have

$$0 \leqslant y'(0) \leqslant 1 - \sqrt{\varepsilon} \leqslant 1, \quad \text{and} \quad |y'(x)| \leqslant \frac{1}{\varepsilon}\left(1 + \frac{\sqrt{\varepsilon}}{1-\sqrt{\varepsilon}} e^{x/\sqrt{\varepsilon}}\right)^{-1} \leqslant \frac{1}{\varepsilon}. \tag{2.6.5}$$

Thus the solution exhibits a 'delayed-layer' effect at $x = 0$. We choose an appropriate transition point for a numerical scheme by solving the inequality

$$1 - y(x) \leqslant N^{-1} \qquad \Leftrightarrow \qquad x \geqslant \sqrt{\varepsilon} \ln\left(\frac{N}{\sqrt{\varepsilon}}\right).$$

In an attempt to solve the problem numerically on $[0,1]$, we consider the scheme

$$\varepsilon D^- Y^N(x_i) = Y^N(x_i)^2(1 - Y^N(x_i)), \quad x_i \in \Omega^N \setminus \{0\}, \quad Y^N(0) = \sqrt{\varepsilon}, \tag{2.6.6a}$$

$$\Omega^N := \left\{ x_i | x_i = \frac{2\sigma}{N} i,\ i \leqslant \tfrac{N}{2}, \quad x_i = \frac{2(1-\sigma)}{N} i,\ i > \tfrac{N}{2} \right\}, \quad \sigma := \min\left\{ \frac{1}{2},\ \sqrt{\varepsilon} \ln\left(\frac{N}{\sqrt{\varepsilon}}\right) \right\}. \tag{2.6.6b}$$

Using upper and lower solutions, and (2.2.19) for sufficiently large N, we can establish that

$$0 \leqslant 1 - Y^N(x_i) \leqslant \begin{cases} \left(1 + \frac{\sqrt{\varepsilon}}{1-\sqrt{\varepsilon}}(1+\frac{h}{\sqrt{\varepsilon}})^i\right)^{-1}, & i \leqslant N/2 \\ \left(1 + \frac{\sqrt{\varepsilon}}{1-\sqrt{\varepsilon}}(1+\frac{h}{\sqrt{\varepsilon}})^{\frac{N}{2}}(1+\frac{H}{\sqrt{\varepsilon}})^{i-\frac{N}{2}}\right)^{-1}, & i > N/2 \end{cases}$$

$$\leqslant \begin{cases} \left(1 + \frac{\sqrt{\varepsilon}}{1-\sqrt{\varepsilon}}\mu e^{x/\sqrt{\varepsilon}}\right)^{-1}, & i \leqslant N/2\,(\sigma < \frac{N}{2}),\ i \leqslant N,\ (\sigma = \frac{1}{2}) \\ 2N^{-1}, & i \geqslant N/2\,(\sigma < \frac{1}{2}), \end{cases}$$

where $h = 2\sigma/N$ and $H = 2(1-\sigma)/N$ and $\mu \in (0.5, 1)$ is arbitrary. In an attempt to bound the error, we have for $\sigma < 1/2$

$$|(Y^N - y)(x_i)| = |1 - y(x_i) + Y^N(x_i) - 1| \leqslant 3N^{-1}. \tag{2.6.7}$$

We can use (2.6.3)-(2.6.5) to bound the truncation error

$$\varepsilon|(\tfrac{d}{dx} - D^+)y(x_i)| = \frac{1}{x_i - x_{i-1}}\left|\int_{x_{i-1}}^{x_i} \varepsilon(y'(x_i) - y'(t))\,dt\right| \leqslant 5h_i\varepsilon^{-1}.$$

However, note that, in the fine mesn, $h_i/\varepsilon = h/\varepsilon \leqslant (C/\sqrt{\varepsilon})N^{-1}\ln(N/\sqrt{\varepsilon})$ and thus, we cannot attempt to repeat the same error analysis as in Theorem 2.3.7. Thus we are left to ask - is our analysis tight enough or is it possible to establish uniform convergence for the cases when the initial condition is arbitrary close an unstable reduced solution?

We will solve (2.6.6) using Newtons' Method (pg. 38) to generate numerical approximations U^N. We will use the constant 1 at all the mesh points for an initial condition, except at the first mesh point, where we use the value $y(0) = \sqrt{\varepsilon}$. Table 2.9 presents the computed differences D_ε^N and D^N and Table 2.10 presents the computed rates of convergence R_ε^N and R^N defined by

$$D_\varepsilon^N := \max_{x_i \in \overline{\Omega}_\varepsilon^N} |(U_\varepsilon^N - \overline{U}_\varepsilon^{2N})(x_i)|, \quad D^N := \max_\varepsilon D_\varepsilon^N, \tag{2.6.8a}$$

$$R_\varepsilon^N := \log_2 \frac{D_\varepsilon^N}{D_\varepsilon^{2N}} \quad \text{and} \quad R^N := \log_2 \frac{D^N}{D^{2N}}, \tag{2.6.8b}$$

where $\overline{U}_\varepsilon^{2N}$ is the interpolation of U_ε^{2N}, the numerical solution using $2N$ mesh intervals.

	D_ε^N										
ε \ N	2^5	2^6	2^7	2^8	2^9	2^{10}	2^{11}	2^{12}	2^{13}	2^{14}	2^{15}
2^{-2}	0.001	0.001	0.000	0.000	0.000	0.000	0.000	0.000	0.000	0.000	0.000
2^{-3}	0.006	0.003	0.001	0.001	0.000	0.000	0.000	0.000	0.000	0.000	0.000
2^{-4}	0.021	0.011	0.005	0.003	0.001	0.001	0.000	0.000	0.000	0.000	0.000
2^{-5}	0.066	0.033	0.016	0.008	0.004	0.002	0.001	0.001	0.000	0.000	0.000
2^{-6}	0.192	0.093	0.045	0.022	0.011	0.006	0.003	0.001	0.001	0.000	0.000
2^{-7}	0.534	0.250	0.116	0.058	0.028	0.014	0.007	0.004	0.002	0.001	0.000
2^{-8}	0.346	0.650	0.246	0.143	0.070	0.035	0.017	0.009	0.004	0.002	0.001
2^{-9}	0.035	0.864	0.423	0.241	0.128	0.068	0.037	0.020	0.010	0.005	0.003
2^{-10}	0.034	0.024	0.931	0.405	0.215	0.116	0.061	0.033	0.017	0.009	0.005
2^{-11}	0.027	0.039	0.956	0.698	0.328	0.192	0.102	0.054	0.029	0.015	0.008
2^{-12}	0.020	0.033	0.040	0.976	0.543	0.299	0.164	0.089	0.047	0.025	0.013
2^{-13}	0.014	0.025	0.040	0.983	0.946	0.448	0.261	0.142	0.075	0.040	0.021
2^{-14}	0.010	0.018	0.032	0.044	0.990	0.664	0.397	0.224	0.119	0.063	0.033
2^{-15}	0.007	0.013	0.023	0.039	0.033	0.993	0.575	0.329	0.185	0.099	0.052
2^{-16}	0.005	0.009	0.017	0.030	0.045	0.995	0.741	0.472	0.282	0.154	0.081
2^{-17}	0.003	0.006	0.012	0.022	0.037	0.045	0.997	0.665	0.406	0.234	0.126
D^N	**0.534**	**0.864**	**0.956**	**0.983**	**0.990**	**0.995**	**0.997**	**0.665**	**0.406**	**0.234**	**0.126**

Table 2.9: Computed differences D_ε^N and D^N (as defined in (2.6.8)), measured from the numerical solutions of the combustion problem (2.6.3), calculated using Newton's method (pg. 38) on the mesh (2.6.6b).

	$\mathbf{R}_\varepsilon^{\mathbf{N}}$									
ε \ **N**	$\mathbf{2^5}$	$\mathbf{2^6}$	$\mathbf{2^7}$	$\mathbf{2^8}$	$\mathbf{2^9}$	$\mathbf{2^{10}}$	$\mathbf{2^{11}}$	$\mathbf{2^{12}}$	$\mathbf{2^{13}}$	$\mathbf{2^{14}}$
$\mathbf{2^{-2}}$	0.98	0.99	1.00	1.00	1.00	1.00	1.00	1.00	1.00	1.00
$\mathbf{2^{-3}}$	0.99	0.99	1.00	1.00	1.00	1.00	1.00	1.00	1.00	1.00
$\mathbf{2^{-4}}$	1.01	1.00	1.00	1.00	1.00	1.00	1.00	1.00	1.00	1.00
$\mathbf{2^{-5}}$	1.00	1.02	1.00	1.00	1.00	1.00	1.00	1.00	1.00	1.00
$\mathbf{2^{-6}}$	1.05	1.04	1.02	1.01	1.00	1.00	1.00	1.00	1.00	1.00
$\mathbf{2^{-7}}$	1.09	1.10	1.02	1.02	1.01	1.00	1.00	1.00	1.00	1.00
$\mathbf{2^{-8}}$	-0.91	1.40	0.78	1.03	1.02	1.01	1.00	1.00	1.00	1.00
$\mathbf{2^{-9}}$	-4.61	1.03	0.81	0.91	0.91	0.89	0.85	1.00	1.00	1.00
$\mathbf{2^{-10}}$	0.49	-5.27	1.20	0.91	0.89	0.92	0.91	0.92	0.92	0.92
$\mathbf{2^{-11}}$	-0.56	-4.60	0.45	1.09	0.77	0.90	0.92	0.92	0.92	0.93
$\mathbf{2^{-12}}$	-0.74	-0.26	-4.62	0.85	0.86	0.87	0.89	0.92	0.92	0.93
$\mathbf{2^{-13}}$	-0.81	-0.67	-4.62	0.06	1.08	0.78	0.88	0.92	0.93	0.93
$\mathbf{2^{-14}}$	-0.85	-0.78	-0.50	-4.48	0.58	0.74	0.83	0.91	0.92	0.93
$\mathbf{2^{-15}}$	-0.88	-0.84	-0.73	0.24	-4.92	0.79	0.81	0.83	0.91	0.93
$\mathbf{2^{-16}}$	-0.90	-0.87	-0.81	-0.61	-4.46	0.43	0.65	0.74	0.87	0.92
$\mathbf{2^{-17}}$	-0.91	-0.89	-0.86	-0.77	-0.28	-4.48	0.59	0.71	0.80	0.89
$\mathbf{R^N}$	**-0.70**	**-0.15**	**-0.04**	**-0.01**	**-0.01**	**-0.00**	**0.59**	**0.71**	**0.80**	**0.89**

Table 2.10: Computed rates R_ε^N and R^N (as defined in (2.6.8)), measured from the numerical solutions of the combustion problem (2.6.3), calculated using Newton's method (pg. 38) on the mesh (2.6.6b).

We see from the table that it appears, for any small ε, we must have sufficiently large N to observe convergence. The pattern of increasing computed differences in Table 2.9 and negative rates in Table 2.10 is easily explained with a graph. Figure 2.8 displays the numerical approximations for $\varepsilon = 2^{-12}$ and $N = 32, 64, \ldots$ as used to compute the Tables.

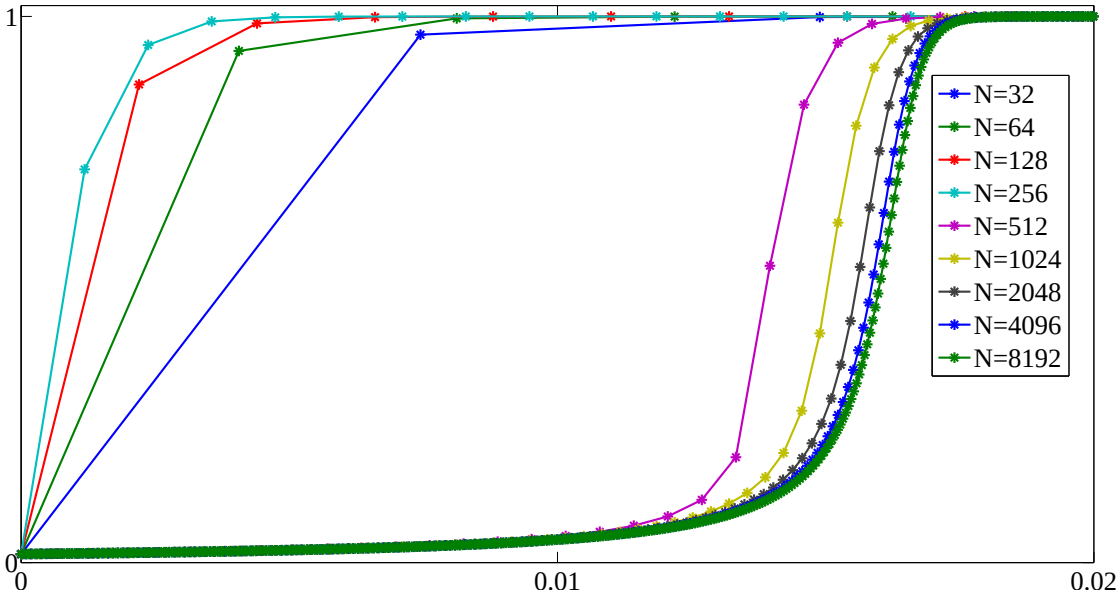

Figure 2.8: Plots of the numerical solutions of (2.6.3), computed using Newton's Method (pg. 38) on the mesh (2.6.6b), over $x_i \in [0, 0.02]$ for $N = 32, 64, \ldots$ and $\varepsilon = 2^{-12}$.

We can see from the graph, that for this given value of ε, the numerical approximations are sequentially poor for lower values of N and improve for increasing N. Note the diagram may appear to suggest that the initial condition we use is unsuitable. In experiments, when we used the lower bound for y in (2.6.4) as the initial condition, we found that the approximations for lower values of N where equally as poor.

2.6.2 Switch in stability between distinct reduced solutions.

Recall that the problem in ($\mathscr{C}_\varepsilon$) involved two intersecting reduced solutions where, one lost, and the other gained, stability at the point of intersection. We did not examine the case where the reduced solutions are distinct. For ($\mathscr{B}_\varepsilon$), when the multiplicity n_s of the stable reduced solution g_s is 2 and the initial condition A is such that $A < g_s$, we restrict our analysis to the case of $g_s' \geqslant 0$. We set this restriction because if $g_s'(x) \geqslant 0$ on $[0,1]$, then g_s is globally stable from below. However, if $g_s'(x) \geqslant 0$ on $0 \leqslant x \leqslant d < 1$ but $g_s' < 0$ for $x > d$, then g_s is not a stable reduced solution beyond d and there is a possibility that the actual solution exhibits an interior layer as it 'tends to the next stable reduced solution above g_s'. As an example, let us consider

the problem

$$\varepsilon y' = (y - r(x))^2(1-y), \quad x \in (0,1], \quad r(x) = 0.5 - (x-0.5)^2, \quad y(0) = A < r(0) = 0.5. \tag{2.6.9}$$

For (2.6.9), we have that r is stable from below on $[0, 0.5]$ and the constant reduced solution 1 is globally stable. Using upper and lower solutions, we can show $A \leqslant y \leqslant 1$ and so $y' \geqslant 0$. In Figure 2.9, graphs of numerical approximations of (2.6.9) using Newton's method on a fine uniform mesh with $N = 16384$ and with the initial condition r, for sample values of ε are displayed along with the reduced solutions.

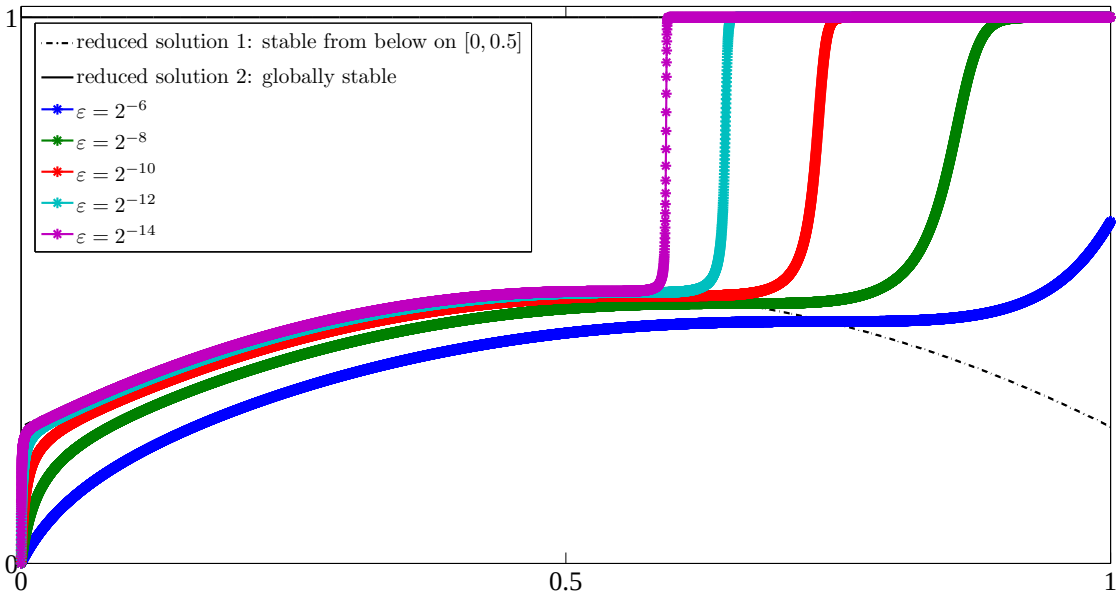

Figure 2.9: Plots of the numerical solutions of (2.6.9), computed using Newton's Method (pg. 38) on a fine uniform mesh with $N = 16384$ for $\varepsilon = 2^{-6}, 2^{-8}, 2^{-10}, 2^{-12}$ and 2^{-14}.

Using (2.6.9), we can loosely detail the magnitudes of y' as follows:

If	Then
$r - y \geqslant C > 0$	$y' = O(\frac{1}{\varepsilon})$
$r - y = O(\sqrt{\varepsilon})$	$y' = O(1)$
$r - y = O(\varepsilon)$	$y' = O(\varepsilon)$
$y = r$	$y' = 0$
$y - r = O(\varepsilon)$	$y' = O(\varepsilon)$ $(\sharp)$
$y - r = O(\sqrt{\varepsilon})$	$y' = O(1)$ $(\flat)$
$y - r \geqslant C > 0$	$y' = O(\frac{1}{\varepsilon})$

Notice the similarities between the cases $(\sharp)$ and $(\flat)$ and the problems (2.6.1) and (2.6.2) where the initial condition is ε and $\sqrt{\varepsilon}$ above a reduced solution with multiplicity 2, all respectively. This would motivate us to analyse (2.6.9) under the transform $\tilde{x} = \varepsilon x$ in anticipation that the

actual solution of the transformed problem is negligibly close to the reduced solution 1 outside an $O(\varepsilon)$ neighbourhood of $\tilde{x}=0$ (i.e. that there is/are $O(\varepsilon)$ layer(s) of some character in an $O(\varepsilon)$ neighbourhood of $x=0$). In such a case we would aim to establish a numerical method using a Shishkin mesh at $\tilde{x}=0$ only. Using such a transform, we obtain

$$\varepsilon^* y' = (y - r\left(x/\sqrt{\varepsilon^*}\right))^2(1-y), \quad x \in (0,1], \qquad y(0)=A, \tag{2.6.10}$$

where $\varepsilon^* = \varepsilon^2$. We will solve (2.6.10) using Newtons' Method (pg. 38) on the mesh (2.6.6b), but using the transition point $\sqrt{\varepsilon^*}\ln(N)$, to generate numerical approximations U^N. We will use the constant 1 at all the mesh points for an initial condition, except at the first mesh point, where we use the value $y(0)=A$. Table 2.11 presents the computed rates of convergence defined in (2.6.8).

	$\mathbf{R}^{\mathbf{N}}_{\varepsilon^*}$								
ε^* \ **N**	$\mathbf{2^5}$	$\mathbf{2^6}$	$\mathbf{2^7}$	$\mathbf{2^8}$	$\mathbf{2^9}$	$\mathbf{2^{10}}$	$\mathbf{2^{11}}$	$\mathbf{2^{12}}$	$\mathbf{2^{13}}$
$\mathbf{2^{-0}}$	0.96	0.98	0.99	1.00	1.00	1.00	1.00	1.00	1.00
$\mathbf{2^{-1}}$	1.13	1.07	1.03	1.02	1.01	1.00	1.00	1.00	1.00
$\mathbf{2^{-2}}$	0.93	0.97	0.99	0.99	1.00	1.00	1.00	1.00	1.00
$\mathbf{2^{-3}}$	0.90	0.97	0.98	0.99	1.00	1.00	1.00	1.00	1.00
$\mathbf{2^{-4}}$	0.86	0.97	0.97	0.99	0.99	1.00	1.00	1.00	1.00
$\mathbf{2^{-5}}$	0.74	0.98	0.95	0.98	0.99	1.00	1.00	1.00	1.00
$\mathbf{2^{-6}}$	0.75	0.69	0.90	0.97	0.99	0.99	1.00	1.00	1.00
$\mathbf{2^{-7}}$	-0.31	0.45	0.54	0.90	0.98	0.99	1.00	1.00	1.00
$\mathbf{2^{-8}}$	0.77	0.65	0.81	0.73	0.81	0.77	0.85	1.00	1.00
$\mathbf{2^{-9}}$	1.32	0.29	0.72	0.82	0.79	0.83	0.85	0.87	0.88
$\mathbf{2^{-10}}$	-0.64	0.96	0.71	0.68	0.81	0.84	0.85	0.87	0.88
$\mathbf{2^{-11}}$	-0.82	0.08	0.49	0.77	0.80	0.84	0.85	0.87	0.88
$\mathbf{2^{-12}}$	-0.39	1.47	0.54	0.88	0.76	0.83	0.86	0.87	0.88
$\mathbf{2^{-13}}$	-3.59	0.90	0.98	0.84	0.76	0.84	0.86	0.87	0.88
$\mathbf{2^{-14}}$	0.78	0.32	1.27	0.83	0.71	0.82	0.87	0.87	0.88
$\mathbf{2^{-15}}$	-4.16	0.81	1.05	0.97	0.75	0.87	0.86	0.88	0.89
$\mathbf{2^{-16}}$	-0.24	-4.41	1.24	1.08	0.90	0.86	0.88	0.88	0.89
$\mathbf{2^{-17}}$	-0.42	-0.14	-4.63	1.93	0.91	0.81	0.88	0.89	0.89
$\mathbf{2^{-18}}$	-0.48	-0.49	-3.12	-1.58	2.26	0.94	0.79	0.90	0.89
$\mathbf{2^{-19}}$	-0.50	-0.57	-0.50	-4.66	1.84	0.83	0.87	0.88	0.89
$\mathbf{2^{-20}}$	-0.52	-0.60	-0.63	-0.29	-4.70	2.21	0.84	0.83	0.90
$\mathbf{R^N}$	**-0.15**	**-0.13**	**-0.08**	**-0.06**	**-0.02**	**2.21**	**0.84**	**0.83**	**0.9**

Table 2.11: Computed rates $R^N_{\varepsilon^*}$ and R^N (as defined in (2.6.8)), measured from the numerical solutions of the (2.6.10), calculated using Newton's method (pg. 38) on the mesh (2.6.6b) with the transition point $\sigma = \sqrt{\varepsilon^*}\ln(N)$.

Again, the pattern in the Table can be explained by poor numerical approximations for lower values of N.

CHAPTER: 3

LINEAR AND NONLINEAR BOUNDARY TURNING POINT PROBLEMS

3.1: INTRODUCTION

In this chapter, we consider linear and nonlinear boundary turning point problems. We are mainly concerned with nonlinear convection-diffusion problems of the form

$$(\varepsilon u'' + u u' - b u)(x) = q(x), \quad b(x) > 0, \quad x \in (0,1), \quad u(0) = 0, \quad u(1) > 0, \tag{3.1.1}$$

where the coefficient of the first derivative, the solution u, is zero at the boundary. We will see that the solution has a boundary layer in the vicinity of $x = 0$. Problems of the above form have been analysed by Vulanović in [34] and more recently in [35]. In [34] the numerical approximations U^N, of the proposed numerical method, satisfy an ε-dependent error bound on the constructed mesh Ω^N, of the form

$$\|u - U^N\| \leqslant C(\varepsilon + N^{-1} \ln N).$$

Thus this method is suitable for sufficiently small values of ε such that $\varepsilon \leqslant N^{-1}$. Analysis in [34] involves integrating the above equation, and establishing that the solution of the resulting first order problem is within $O(\varepsilon)$ of the singularly perturbed Riccati problem studied in [22].

In this chapter, we present a direct numerical method (3.1.1), whose numerical approximations satisfy the parameter-uniform error bound

$$\|U^N - u\| \leqslant C N^{-1} \ln N.$$

In Vulanović's more recent paper [35], a generalised form of the homogeneous problem corresponding to (3.1.1) is examined and a parameter-uniform error bound of the form

$$\|U^N - u\| \leqslant C N^{-1} (\ln N)^3$$

is established. The analysis and numerical method presented in [35] are different to what is given in this chapter. In passing, we note that the same problem class as in [35] was examined in earlier papers ([33],[36]), where parameter-uniform convergence in the L_1 norm was established for schemes involving a uniform mesh.

Nonlinear boundary value problems of the above form, with the boundary conditions $u(0), u(1) > 0$, have been studied in [10] and [18] using monotone finite difference operators on piecewise-uniform Shishkin meshes. If the boundary conditions $u(0)$ and $u(1)$ are strictly positive, the nature of the solution of (3.1.1) is strongly related to the linear problem

$$(\varepsilon u'' + a u' - b u)(x) = q(x), \quad x \in (0,1), \quad a(x) \geq \alpha > 0, \quad x \in [0,1].$$

The reciprocal of α, which is the strictly positive lower bound on the coefficient of the first derivative, appears throughout the analysis of these numerical methods. Thus if $\alpha \equiv 0$, as is in the problems examined in this chapter, then the analysis in [10] and [18] is not directly applicable. Linear boundary turning point problems of the form

$$\varepsilon u''(x) + x^p (b u' - c u)(x) = x^p q(x), \quad x \in (0,1), \quad u(0) = 0,\ u(1) > 0, \tag{3.1.2a}$$

$$b(x),\ c(x) > 0, \quad p \geq 0. \tag{3.1.2b}$$

have been studied in [17]. The coefficient of the first derivative is zero valued at the boundary point $x = 0$. In [17], it is shown that the width of the boundary layer depends on p. The nature of the layers in the nonlinear problem (3.1.1) is different to the layers in the linear boundary turning-point problem (3.1.2). In the first part of this chapter, we examine a linear boundary turning-point problem of the form

$$(\varepsilon u'' + a u' - b u)(x) = q(x), \quad x \in (0,1), \quad u(0) = 0,\ u(1) > 0, \tag{3.1.3a}$$

$$b(x) \geqslant 0, \quad a(x) \geqslant C(1 - e^{-\alpha x/\varepsilon}). \tag{3.1.3b}$$

It transpires that the width of the layer in the linear problem (3.1.3) is the same as the nonlinear problem (3.1.1). The analysis of the linear problem is useful when we come to construct and analyse a parameter-uniform numerical method for the nonlinear problem (3.1.1). The second part of this chapter, presents a numerical method and the associated numerical analysis for a nonlinear class of problems containing (3.1.1).

3.2: Linear Problem

3.2.1 Continuous Problem

Consider the following problem class on the unit interval $\Omega := (0,1)$. Find y_ε such that

$$\mathcal{L}_\varepsilon y_\varepsilon(x) := \left(\varepsilon \tfrac{d^2}{dx^2} + a_\varepsilon \tfrac{d}{dx} - b\right) y_\varepsilon(x) = q(x), \quad x \in \Omega, \quad y_\varepsilon(0) = A, \ y_\varepsilon(1) = B,$$
$$a_\varepsilon(0) = 0, \quad a_\varepsilon(x) > 0, \quad x \in (0,1], \tag{$\mathscr{D}_\varepsilon$}$$
$$a_\varepsilon \in C^2(0,1) \cap C^0[0,1], \quad b, q \in C^2[0,1], \quad b(x) \geqslant 0, \quad x \in \overline{\Omega}.$$

Our primary interest is in the nonlinear problem (3.1.1). To this end, we place some restrictions on the function a_ε so that this linear problem, ($\mathscr{D}_\varepsilon$), has some features of the nonlinear problem (3.1.1).

Assumptions on the coefficient a_ε in ($\mathscr{D}_\varepsilon$)

For all $x \in \overline{\Omega}$, define the limiting function a_0 as

$$a_0(x) := \lim_{\varepsilon \to 0} a_\varepsilon(x), \ \ x > 0 \quad \text{and} \quad a_0(0) := \lim_{x \to 0} a_0(x). \tag{3.2.1a}$$

Assume the following conditions on a_ε for $x \in [0,1]$;

$$a_\varepsilon(x) \geqslant \alpha_\varepsilon(x) := \theta(1 - e^{-rx/\varepsilon}), \quad r \geqslant 2\theta > 0, \tag{3.2.1b}$$
$$\int_{t=0}^{x} \left|a_\varepsilon'(t)\right| dt \leqslant C, \tag{3.2.1c}$$
$$\varphi_\varepsilon(x) := (a_0 - a_\varepsilon)(x) \quad \text{satisfies} \quad |\varphi_\varepsilon(x)| \leqslant |\varphi_\varepsilon(0)| e^{-\theta x/\varepsilon}, \tag{3.2.1d}$$
$$a_0 \in C^2[0,1]. \tag{3.2.1e}$$

Note that (3.2.1b) implies $a_0(x) \geqslant \theta$, $\forall\ x \in \overline{\Omega}$. The differential operator $\mathcal{L}_\varepsilon$ defined in problem ($\mathscr{D}_\varepsilon$) satisfies the following minimum principle.

Theorem 3.2.1. *Let $\mathcal{L}_\varepsilon$ be the differential operator defined in ($\mathscr{D}_\varepsilon$) and $z \in C^2(\Omega) \cap C^0(\overline{\Omega})$. If $\min\{z(0), z(1)\} \geqslant 0$ and $\mathcal{L}_\varepsilon z(x) \leqslant 0$ for $x \in \Omega$, then $z(x) \geqslant 0$ for all $x \in \overline{\Omega}$.*

Proof. The proof is by contradiction. Assume that there exists a point $p \in \overline{\Omega}$ such that $z(p) < 0$. It follows from the hypotheses that $p \notin \{0,1\}$. Define the auxiliary function $u = z \exp(\frac{1}{2\varepsilon}\int_{t=0}^{x} \alpha_\varepsilon(t)dt)$ and note that $u(p) < 0$. Choose $s \in \Omega$ such that $u(s) = \min u(x) < 0$. Therefore, from the definition of s, we have $u'(s) = 0$ and $u''(s) \geqslant 0$. But then

$$\mathcal{L}_\varepsilon z(s) = \left[\varepsilon u'' + \left(\frac{\alpha_\varepsilon}{2\varepsilon}(a_\varepsilon - \alpha_\varepsilon/2) + \frac{\alpha_\varepsilon'}{2} + b\right)(-u)\right](s) \exp\left(-\frac{1}{2\varepsilon}\int_{t=0}^{s} \alpha_\varepsilon(t)dt\right) > 0$$

which is a contradiction. □

We decompose the solution y_ε into the sum of a regular component, v_ε, and a layer component, w_ε. If a_ε satisfied the bound $a_\varepsilon \geqslant C > 0$ for all $x \in [0,1]$, then we would simply define the regular component as the solution of $\mathcal{L}_\varepsilon v_\varepsilon = q$ with suitable boundary conditions and the layer component as the solution of $\mathcal{L}_\varepsilon w_\varepsilon = 0$, $w_\varepsilon(0) = (y_\varepsilon - v_\varepsilon)(0)$, $w_\varepsilon(1) = 0$. Since a_ε does not satisfy such a bound, we study the problem

$$\mathcal{L}_* v_\varepsilon(x) := \left(\varepsilon \tfrac{d^2}{dx^2} + a_0 \tfrac{d}{dx} - b\right) v_\varepsilon(x) = q(x), \quad x \in \Omega, \quad v_\varepsilon(0) = (v_0 + \varepsilon v_1)(0), \quad v_\varepsilon(1) = B, \tag{3.2.2a}$$

where $v_\varepsilon = v_0 + \varepsilon v_1 + \varepsilon^2 v_2$ and v_0, v_1, v_2 satisfy

$$(a_0 v_0' - b v_0)(x) = q(x), \quad x \in [0,1), \quad v_0(1) = B, \tag{3.2.2b}$$

$$(a_0 v_1' - b v_1)(x) = -v_0''(x), \quad x \in (0,1), \quad v_1(1) = 0; \quad v_1(0) := \lim_{t \downarrow 0} v_1(t), \tag{3.2.2c}$$

$$\mathcal{L}_* v_2(x) = -v_1''(x), \quad x \in \Omega, \quad v_2(0) = v_2(1) = 0. \tag{3.2.2d}$$

Note that in problem (3.2.2), the coefficient a_ε, of the first derivative term, has been replaced by a_0 (defined in (3.2.1a)). We incorporate the error $(\mathcal{L}_\varepsilon - \mathcal{L}_*)v_\varepsilon$ into the layer component w_ε, which is, noting (3.2.1d), defined as the solution of

$$\mathcal{L}_\varepsilon w_\varepsilon(x) = (\varphi_\varepsilon v_\varepsilon')(x), \quad x \in \Omega, \quad w_\varepsilon(0) = (y_\varepsilon - v_\varepsilon)(0), \quad w_\varepsilon(1) = 0. \tag{3.2.3}$$

Lemma 3.2.1. *If v_ε is the solution of (3.2.2) and w_ε is the solution of (3.2.3) then for $k = 0,1,2$, we have the following bounds on the derivatives of v_ε and w_ε:*

$$|v_\varepsilon^{(k)}(x)| \leqslant C(1 + \varepsilon^{2-k}) \quad \textit{and} \quad |w_\varepsilon^{(k)}(x)| \leqslant C\varepsilon^{-k} e^{-(\theta/2)x/\varepsilon}, \quad x \in \Omega.$$

Proof. The solution of (3.2.2b) can be solved exactly. Also (3.2.2b) is independent of ε and since a_0, b, $q \in C^2[0,1]$ we can easily show that $\|v_0^{(k)}\| \leqslant C$ for $k = 0,1,2,3$. For (3.2.2c), under the same argument, we can show $\|v_1^{(k)}\| \leqslant C$ for $k = 0,1,2$. For (3.2.2d), consider the functions

$$\psi^\pm(x) = \frac{\|v_1''\|}{\theta}(1-x) \pm v_2(x), \quad x \in \overline{\Omega}, \tag{3.2.4}$$

where θ is defined in (3.2.1b). From (3.2.2d), we have $\min\{\psi^\pm(0), \psi^\pm(1)\} = 0$ and

$$\mathcal{L}_* \psi^\pm(x) = -\frac{a_0(x)\|v_1''\|}{\theta} - b\frac{\|v_1''\|}{\theta}(1-x) \mp v_1''(x) \leqslant -\|v_1''\| \mp v_1''(x) \leqslant 0, \quad x \in \Omega.$$

Hence, using Theorem 3.2.1, we have $\|v_2\| \leqslant \frac{\|v_1''\|}{\theta}$. Note that Theorem 3.2.1 holds for the operator $\mathcal{L}_*$, the proof of this can be easily repeated by replacing α_ε in the proof by θ. Integrating (3.2.2d) over $[0,\eta]$ for any $\eta \in \overline{\Omega}$, we have

$$\varepsilon v_2'(\eta) - \varepsilon v_2'(0) = \int_0^x (b v_2)(t)\, dt - \left(a_0 v_2|_0^x - \int_0^x (a_0' v_2)(t)\, dt\right) - \int_0^x v_1''(t)\, dt.$$

Thus we can bound the left hand side as

$$\varepsilon |v_2'(\eta) - v_2'(0)| \leqslant (\|b\| + \|a_0\| + \|a_0'\|)\|v_2\| + \|v_1''\| =: C_1\|v_2\| + \|v_1''\|. \tag{3.2.5}$$

From the mean value theorem, $\exists\, \xi \in (0,\varepsilon)$ s.t. $v_2(\varepsilon)-v_2(0)=\varepsilon v_2'(\xi)$ hence $\varepsilon|v_2'(\xi)| \leqslant \|v_2(\varepsilon)\| \leqslant C_2$. Thus letting $\eta=\xi$ in (3.2.5), we have $\varepsilon|v_2'(0)| \leqslant C_1\|v_2\|+\|v_1''\|+C_2$ and hence for any $x\in\Omega$, we have $\varepsilon|v_2'(x)| \leqslant 2(C_1\|v_2\|+\|v_1''\|)+C_2$. From (3.2.2d), we have $\|v_2''\| \leqslant C\varepsilon^{-2}$. Hence using $v_\varepsilon = v_0+\varepsilon v_1+\varepsilon^2 v_2$, we can retrieve the required bounds on $v_\varepsilon^{(k)}$ for $k=0,1,2$. To bound w_ε, consider the functions

$$\psi^{\pm}(x)=|w_\varepsilon(0)|\exp\left(-\frac{1}{2\varepsilon}\int_{t=0}^{x}\alpha_\varepsilon(t)dt\right)\pm w_\varepsilon(x), \quad x\in\Omega,$$

which are nonnegative at $x=0,1$. Using (3.2.1), we can easily check that

$$\frac{1}{2}\alpha_\varepsilon(x)^2+\varepsilon\alpha_\varepsilon'(x)\geqslant\frac{\theta^2}{2}.$$

Thus for ε sufficiently small, we have

$$\mathcal{L}_\varepsilon\psi^{\pm}(x)\leqslant-\frac{1}{2\varepsilon}\left(\left(\frac{1}{2}{\alpha_\varepsilon}^2+\varepsilon\alpha_\varepsilon'\right)(x)-2\varepsilon|\varphi_\varepsilon(0)|\|v_\varepsilon'\|\right)e^{-(\theta/2)x/\varepsilon}\leqslant 0.$$

Use (3.2.1) and the minimum principle in Theorem 3.2.1 to obtain

$$|w_\varepsilon(x)|\leqslant|w_\varepsilon(0)|\exp\left(-\frac{1}{2\varepsilon}\int_{t=0}^{x}\alpha_\varepsilon(t)dt\right)\leqslant Ce^{-(\theta/2)x/\varepsilon}. \tag{3.2.6}$$

We now bound the derivatives of w_ε. Integrating (3.2.3) over $[\eta,1]$ for any $\eta>0$ and recalling $w_\varepsilon(1)=0$, from (3.2.1) we have

$$\varepsilon|(w_\varepsilon'(\eta)-w_\varepsilon'(1))|\leqslant(\|a_\varepsilon\|+\|b\|)|w_\varepsilon(\eta)|+\frac{C}{\theta}|\varphi_\varepsilon(0)|\varepsilon e^{-(\theta/2)\eta/\varepsilon}+Ce^{-(\theta/2)\eta/\varepsilon}. \tag{3.2.7}$$

Using the mean value theorem and (3.2.6), there exists a point $z\in(1-\varepsilon,1)$ such that $\varepsilon|w_\varepsilon'(z)|\leqslant|w_\varepsilon(1-\varepsilon)|\leqslant Ce^{-(\theta/2)/\varepsilon}$. Letting $\eta=z$ we have $\varepsilon|w_\varepsilon'(1)|\leqslant Ce^{-(\theta/2)\eta/\varepsilon}$. Letting $\eta=x\in\Omega$ then similarly we have $\varepsilon|w_\varepsilon'(x)|\leqslant Ce^{-(\theta/2)x/\varepsilon}$. Complete the proof by using (3.2.3) to bound w_ε''. □

Remark: We will see below that a bound on the third derivative of v_ε and w_ε is not required in the truncation error analysis in Lemmas 3.2.2 and 3.2.4.

3.2.2 The Discrete Problem and Error Analysis

Consider the following finite difference method. Find Y_ε^N such that

$${\mathcal{L}_\varepsilon}^N Y_\varepsilon^N(x_i):=(\varepsilon\delta^2+a_\varepsilon D^+-b)Y_\varepsilon^N(x_i)=q(x_i),\quad x_i\in\Omega_\varepsilon^N,\quad Y_\varepsilon^N(0)=A,\quad Y_\varepsilon^N(1)=B,\qquad (\mathscr{D}_\varepsilon^N)$$

where

$$D^+Z(x_i):=\frac{Z(x_{i+1})-Z(x_i)}{h_{i+1}},\quad \delta^2Z(x_i):=\frac{D^+(Z(x_i)-Z(x_{i-1}))}{(h_{i+1}+h_i)/2},\quad h_i:=x_i-x_{i+1},$$

and Ω_ε^N is the piecewise-uniform fitted mesh described by

$$\overline{\Omega}_\varepsilon^N:=\left\{x_i\,\middle|\,x_i=\frac{2\sigma i}{N},\ 0\leqslant i\leqslant\tfrac{N}{2},\quad x_i=\sigma+\frac{2(1-\sigma)(i-\frac{N}{2})}{N},\ \tfrac{N}{2}<i\leqslant N\right\}, \tag{3.2.8a}$$

$$\sigma:=\min\left\{\frac{1}{2},\frac{2\varepsilon}{\theta}\ln(N)\right\},\quad \Omega_\varepsilon^N=\overline{\Omega}_\varepsilon^N\setminus\{x_0,x_N\}. \tag{3.2.8b}$$

The finite difference operator ${\mathcal{L}_\varepsilon}^N$ satisfies the following discrete minimum principle.

Theorem 3.2.2. *Let ${\mathcal{L}_\varepsilon}^N$ be the difference operator defined in $(\mathscr{D}_\varepsilon^N)$ and Z^N be a mesh function on $\overline{\Omega}_\varepsilon^N$. If $\min\{Z^N(x_0), Z^N(x_N)\} \geqslant 0$ and ${\mathcal{L}_\varepsilon}^N Z^N(x_i) \leqslant 0$ for $x_i \in \Omega_\varepsilon^N$, then $Z^N(x_i) \geqslant 0$ for all $x_i \in \overline{\Omega}_\varepsilon^N$.*

Proof. Suppose that $Z^N(x_k) = \min_i Z^N(x_i)$. If follows from the hypotheses that $k \notin \{0, N\}$ and $x_k \in \Omega_\varepsilon^N$. Since $Z^N(x_k)$ is the minimum value we have $D^+Z^N(x_k) \geqslant 0$ and $\delta^2 Z^N(x_k) \geqslant 0$. To avoid a contradiction we must have ${\mathcal{L}_\varepsilon}^N Z^N(x_k) \leqslant 0$ but if $b(x_k) > 0$ then ${\mathcal{L}_\varepsilon}^N Z^N(x_k) > 0$ or if $b(x_k) = 0$ then $Z^N(x_{k-1}) = Z^N(x_k) = Z^N(x_{k+1}) < 0$. Repeating this argument will eventually lead us to conclude that either ${\mathcal{L}_\varepsilon}^N Z^N(x_k) > 0$ or $Z^N(x_N) < 0$ which is a contradiction. □

As in the continuous case, we decompose the solution Y_ε^N into the sum of a discrete regular component, V_ε^N, and a discrete layer component, W_ε^N. We define the regular component as the solution of the following problem

$$ {\mathcal{L}_*}^N V_\varepsilon^N(x_i) := (\varepsilon\delta^2 + a_0 D^+ - b) V_\varepsilon^N(x_i) = q(x_i), \;\; x_i \in \Omega_\varepsilon^N, \;\; V_\varepsilon^N(0) = (V_0^N + \varepsilon V_1^N)(0), \;\; V_\varepsilon^N(1) = B, \tag{3.2.9a} $$

where $V_\varepsilon^N = V_0^N + \varepsilon V_1^N + \varepsilon^2 V_2^N$ and V_0^N, V_1^N, V_2^N satisfy

$$ (a_0 D^+ - b) V_0^N(x_i) = q(x_i), \quad x_i \in \overline{\Omega}_\varepsilon^N \setminus x_N, \quad V_0^N(x_N) = B, \tag{3.2.9b} $$

$$ (a_0 D^+ - b) V_1^N(x_i) = -\delta^2 V_0^N(x_i), \quad x_i \in \Omega_\varepsilon^N, \quad V_1^N(x_N) = 0; \quad V_1^N(x_0) := V_1^N(x_1) \tag{3.2.9c} $$

$$ {\mathcal{L}_*}^N V_2^N(x_i) = -\delta^2 V_1^N(x_i), \quad x_i \in \Omega_\varepsilon^N, \quad V_2^N(x_j) = 0, \; j = 0, N. \tag{3.2.9d} $$

We present bounds on V_ε^N, $D^+ V_\varepsilon^N$ and on the error $V_\varepsilon^N - v_\varepsilon$ in the following lemma.

Lemma 3.2.2. *If v_ε is the solution of (3.2.2) and V_ε^N is the solution of (3.2.9) then we have the following bounds*

$$ |V_\varepsilon^N(x_i)| \leqslant C, \quad |(V_\varepsilon^N - v_\varepsilon)(x_i)| \leqslant CN^{-1}, \;\; x_i \in \overline{\Omega}_\varepsilon^N, \qquad |D^+ V_\varepsilon^N(x_i)| \leqslant C, \;\; x_i \in \overline{\Omega}_\varepsilon^N \setminus x_N. $$

Proof. If Z^N is a mesh function on $\overline{\Omega}_\varepsilon^N$ then we can easily prove the following by contradiction in the same manner as Theorem 3.2.2:

$$ \text{if} \quad Z^N\big|_{x_N} \geqslant 0 \quad \text{and} \quad (a_0 D^+ - b) Z^N\big|_{\overline{\Omega}_\varepsilon^N \setminus x_N} \leqslant 0 \quad \text{then} \quad Z^N\big|_{\overline{\Omega}_\varepsilon^N} \geqslant 0. \tag{3.2.10} $$

Using the mesh functions $\Psi^{N\pm}(x_i) = B + \frac{\|q\|}{\theta}(1 - x_i) \pm V_0^N(x_i)$ with (3.2.9b) and (3.2.10) we can show $|V_0^N(x_i)| \leqslant C$, $x_i \in \overline{\Omega}_\varepsilon^N$. Thus, clearly from (3.2.9b), we have $|D^+ V_0^N(x_i)| \leqslant C$, $x_i \in \overline{\Omega}_\varepsilon^N \setminus x_N$. Using (3.2.9b), we have

$$ \begin{aligned} &D^+ V_0^N(x_i) - D^+ V_0^N(x_{i-1}) \\ &= \left(\frac{1}{a_0(x_i)} - \frac{1}{a_0(x_{i-1})} \right) (b V_0^N + q)(x_i) + \frac{1}{a_0(x_{i-1})} \left((b V_0^N + q)(x_i) - (b V_0^N + q)(x_{i-1}) \right) \\ &= h_i \left[-(D^- a_0(x_i)) \frac{(b V_0^N + q)(x_i)}{a_0(x_i) a_0(x_{i-1})} + \frac{1}{a_0(x_{i-1})} \left((b D^- V_0^N)(x_i) + V_0^N(x_{i-1}) D^- b(x_i) + D^- q(x_i) \right) \right]. \end{aligned} $$

Note that for any $z \in C^1[0,1]$ we have

$$|D^- z(x_i)| = \frac{1}{h_i}\left|\int_{x_{i-1}}^{x_i} z'(t)\,dt\right| \leqslant \max_{t\in(x_{i-1},x_i)} |z'(t)|.$$

Hence, for $x_i \in \Omega_\varepsilon^N$, we have

$$|\delta^2 V_0^N(x_i)| = \left|\tfrac{2(D^+-D^-)V_0^N(x_i)}{h_i+h_{i+1}}\right| \leqslant \frac{2h_i}{h_i+h_{i+1}} C \max\{\|a_0'\|, \|b'\|, \|q'\|, \max_i |D^- V_0^N(x_i)|\} \leqslant C. \quad (3.2.11)$$

Note, we can bound V_1^N in the same manner as V_0^N.

For (3.2.9d), using the functions

$$\Psi^{N\pm}(x_i) = \frac{1}{\theta}\max_{x_i\in\Omega_\varepsilon^N}\{|\delta^2 V_1^N(x_i)|\}(1-x_i) \pm V_2^N(x_i), \quad (3.2.12)$$

which are nonnegative at $x_i = 0, 1$, with Theorem 3.2.2, we can show $|V_2^N(x_i)| \leqslant C$ for $x_i \in \overline{\Omega}_\varepsilon^N$. We can repeat [7, §3.5, Lemma 3.14] and obtain $\varepsilon|D^+ V_2^N| \leqslant C$ and thus it follows that

$$|V_\varepsilon^N(x_i)| \leqslant C \quad \text{on} \quad x_i \in \overline{\Omega}_\varepsilon^N \quad \text{and} \quad |D^+ V_\varepsilon^N(x_i)| \leqslant C \quad \text{for} \quad x_i \in \overline{\Omega}_\varepsilon^N \setminus x_N. \quad (3.2.13)$$

We now bound the error $E^N := V_\varepsilon^N - v_\varepsilon$. The errors $E_0^N := V_0^N - v_0$, $E_1^N := V_1^N - v_1$, where the v_i's satisfy (3.2.2), are defined as the solutions of

$$(a_0 D^+ - b)E_0^N(x_i) = a_0(v_0' - D^+ v_0)(x_i), \quad x_i \in \overline{\Omega}_\varepsilon^N \setminus x_N, \quad E_0^N(x_N) = 0, \quad (3.2.14a)$$

$$\begin{gathered}(a_0 D^+ - b)E_1^N(x_i) = (a_0(v_1' - D^+ v_1) + \tau_0^N)(x_i), \quad x_i \in \Omega_\varepsilon^N, \quad E_1^N(x_N) = 0, \\ \tau_0^N(x_i) := (v_0'' - \delta^2 V_0^N)(x_i); \quad E_1^N(0) := V_1^N(x_0) - v_1(0),\end{gathered} \quad (3.2.14b)$$

$$\mathcal{L}_*{}^N E^N(x_i) = (\mathcal{L}_* - \mathcal{L}_*{}^N)v_\varepsilon(x_i), \quad x_i \in \Omega_\varepsilon^N, \quad E^N(0) = (E_0^N + \varepsilon E_1^N)(0), \quad E^N(x_N) = 0. \quad (3.2.14c)$$

Note the following truncation error bound

$$|\varepsilon(\delta^2 v_\varepsilon - v_\varepsilon'')(x_i)| \leqslant \frac{2\varepsilon}{h_{i+1}+h_i}\sum_{j=i}^{i+1}\frac{1}{h_j}\left|\int_{t=x_{j-1}}^{x_j}\int_{s=x_i}^{t} v_\varepsilon''(s) - v_\varepsilon''(x_i)\,ds\,dt\right|. \quad (3.2.15)$$

Using standard local truncation error estimates and using (3.2.2), (3.2.9), (3.2.11), (3.2.13), (3.2.15) and Lemma 3.2.1 and recalling that $a_0, b, q \in C^2[0,1]$, we can show that

$$\max\left\{|(v_0' - D^+ v_0)(x_i)|,\ |(v_1' - D^+ v_1)(x_i)|,\ |(\mathcal{L}_* - \mathcal{L}_*{}^N)v_\varepsilon(x_i)|\right\} \leqslant CN^{-1}, \quad x_i \in \Omega_\varepsilon^N, \quad (3.2.16a)$$

$$|\tau_0^N(x_i)| \leqslant \begin{cases} CN^{-1}, & i \neq \frac{N}{2}, \\ C, & i = \frac{N}{2}. \end{cases} \quad (3.2.16b)$$

Thus for (3.2.14a), it is easily shown using (3.2.10) that $|E_0^N(x_i)| \leqslant CN^{-1}(1-x_i)$, $x_i \in \overline{\Omega}_\varepsilon^N$. Rewrite (3.2.14b) as

$$E_1^N(x_i) = \left[E_1^N(x_{i+1}) - \left((v_1' - D^+ v_1) + \frac{1}{a_0}\tau_0^N\right)(x_i)h_{i+1}\right]\left(1 + \tfrac{b}{a_0}(x_i)h_{i+1}\right)^{-1}.$$

Since $(1+\frac{b}{a_0}(x_i)h_{i+1})>1$ and using (3.2.16a) it can be shown that

$$|E_1^N(x_{N-j})| \leqslant CN^{-1} + C\sum_{k=1}^{j}|\tau_0^N(x_{N-k})|h_{N-k+1}.$$

Thus using (3.2.16b) we can show that if $j \leqslant N/2-1$ then $|E_1^N(x_{N-j})| \leqslant CN^{-1}$ and if $N/2 \leqslant j < N$ then

$$|E_1^N(x_{N-j})| \leqslant CN^{-1} + |\tau_0^N(x_{N/2})|h_{N/2+1} + CN^{-1} \leqslant CN^{-1}.$$

At the meshpoint x_0, we have

$$|E_1^N(x_0)| = |V_1^N(x_1) - v_1(x_1) + v_1(x_1) - v_1(0)| \leqslant CN^{-1} + (|x_1|)\|v_1'\| \leqslant CN^{-1}.$$

Complete the proof by using Theorem 3.2.2 with (3.2.14c) and (3.2.16a) and the barrier functions

$$\Psi^{N\pm}(x_i) = \frac{1}{\theta}CN^{-1}(1-x_i) \pm E^N(x_i).$$

□

We incorporate the error $(\mathcal{L}_\varepsilon{}^N - \mathcal{L}_*{}^N)V_\varepsilon^N$ into the discrete layer component, W_ε^N, defined as the solution of the following finite difference method

$$\mathcal{L}_\varepsilon{}^N W_\varepsilon^N(x_i) = (\mathcal{L}_*{}^N - \mathcal{L}_\varepsilon{}^N)V_\varepsilon^N(x_i) = (\varphi_\varepsilon D^+ V_\varepsilon^N)(x_i), \quad x_i \in \Omega_\varepsilon^N, \quad W_\varepsilon^N(k) = w_\varepsilon(k), \quad k = 0,1. \tag{3.2.17}$$

A bound on W_ε^N is now given in the following lemma.

Lemma 3.2.3. *If W_ε^N is the solution of (3.2.17) then W_ε^N satisfies*

$$|W_\varepsilon^N(x_i)| \leqslant \begin{cases} Ce^{-(\theta/2)x_i/\varepsilon} + CN^{-1}, & 0 \leqslant i \leqslant N \ (\text{if } \sigma = \frac{1}{2}), \quad 0 \leqslant i \leqslant \frac{N}{2}, \ (\text{if } \sigma < \frac{1}{2}) \\ CN^{-1}, & \frac{N}{2} \leqslant i \leqslant N, \ (\text{if } \sigma < \frac{1}{2}). \end{cases}$$

Proof. Using (3.2.1), we first establish a few inequalities. Using ((2.2.19), pg. 19), define and bound the mesh function $\hat{W}^N$ as follows

$$\hat{W}^N(x_0) := 1, \quad \hat{W}^N(x_i) := \prod_{j=1}^{i}\left(1 + \frac{\alpha_\varepsilon(x_j)}{2}\frac{h_j}{\varepsilon}\right)^{-1} \geqslant \exp(-(\theta/2)x_i/\varepsilon), \quad 1 \leqslant i \leqslant N. \tag{3.2.18}$$

When h_i is such that $h_{i+1} = h_i = h$ and $h/\varepsilon \leqslant CN^{-1}\ln N$ then for sufficiently large N we have

$$\frac{1}{2}\alpha_\varepsilon(x_i)\alpha_\varepsilon(x_{i+1}) + \varepsilon D^+\alpha_\varepsilon(x_i) \geqslant \frac{1}{2}\alpha_\varepsilon(x_i)^2 + \varepsilon\alpha_\varepsilon'(x_{i+1}) \geqslant \frac{\theta^2}{2}. \tag{3.2.19}$$

When $\sigma < 1/2$, for $i \geqslant N/2$ we have

$$|\varphi_\varepsilon(x_i)| \leqslant |\varphi_\varepsilon(0)|e^{-(\theta/2)x_{\frac{N}{2}}/\varepsilon} \leqslant |\varphi_\varepsilon(0)|N^{-1} \ \text{ and } \ \alpha_\varepsilon(x_i) \geqslant \theta(1 - e^{-2\theta x_{\frac{N}{2}}/\varepsilon}) \geqslant \theta/2. \tag{3.2.20}$$

Consider the mesh functions

$$\Psi^{N\pm}(x_i) = |w_\varepsilon(0)|\hat{W}^N(x_i) + \frac{2}{\theta}|\varphi_\varepsilon(0)|\max_{\Omega_\varepsilon^N}\{|D^+V_\varepsilon^N(x_i)|\}N^{-1}(1-x_i) \pm W_\varepsilon^N(x_i)$$

which are nonnegative at $x_i = 0, 1$. Using (3.2.18)-(3.2.20) and Lemma 3.2.2, for meshpoints $x_i \in [x_1, x_{K-1}]$, where $K = N$ if $\sigma = 1/2$ and $K = N/2$ if $\sigma < 1/2$, we have $h_{i+1} = h_i = h$ and $h/\varepsilon \leqslant CN^{-1} \ln N$. Thus for sufficiently large N we have

$$\begin{aligned}
&{\mathcal{L}_\varepsilon}^N \Psi^{N\pm}(x_i) \\
&\leqslant -\frac{|w_\varepsilon(0)|}{2\varepsilon}\left(\frac{\alpha_\varepsilon(x_i)\alpha_\varepsilon(x_{i+1})}{2} + \varepsilon D^+\alpha_\varepsilon(x_i)\right)\hat{W}^N(x_{i+1}) + |\varphi_\varepsilon(0)| \max_{\Omega_\varepsilon^N}\{|D^+ V_\varepsilon^N(x_i)|\} e^{-(\theta/2)x_i/\varepsilon} \\
&\leqslant -\frac{1}{\varepsilon}\left(\frac{|w_\varepsilon(0)|}{8}\theta^2 - \varepsilon|\varphi_\varepsilon(0)| \max_{\Omega_\varepsilon^N}\{|D^+ V_\varepsilon^N(x_i)|\}\right) e^{-(\theta/2)x_i/\varepsilon} \leqslant 0.
\end{aligned}$$

For all other meshpoints i.e. $x_i \in [x_K, x_{N-1}]$, when $K = N/2$, we have

$$\begin{aligned}
&{\mathcal{L}_\varepsilon}^N \Psi^{N\pm}(x_i) \\
&\leqslant -\frac{2}{\theta}|\varphi_\varepsilon(0)| \max_{\Omega_\varepsilon^N}\{|D^+ V_\varepsilon^N(x_i)|\} N^{-1}\alpha_\varepsilon(x_{\frac{N}{2}}) + |\varphi_\varepsilon(0)| \max_{\Omega_\varepsilon^N}\{|D^+ V_\varepsilon^N(x_i)|\} e^{-(\theta/2)x_{\frac{N}{2}}/\varepsilon} \leqslant 0.
\end{aligned}$$

Using Theorem 3.2.2 we have $|W_\varepsilon^N(x_i)| \leqslant C\hat{W}^N(x_i) + CN^{-1}$.

We finish the proof by establishing an upper bound on $\hat{W}$. Note the Rectangle Rule for Numerical Integration: Partition the interval $[a, b]$ into N^* subintervals with width $h^* = 1/N^*$, where $t_j = a + j h^*$. Then

$$\int_a^b f(s)\, ds = h^* \sum_{j=1}^{N^*} f(t_j) + O((b-a)h^{*2}\|f''\|). \tag{3.2.21}$$

Using this rectangle rule with $\hat{W}^N(x_i)$ for $x_i \leqslant \sigma$ when $\sigma < \frac{1}{2}$ or for $x_i \leqslant x_N$ when $\sigma = \frac{1}{2}$ we have

$$\frac{\theta}{2\varepsilon}\sum_{j=1}^{i} e^{-rx_j/\varepsilon} h \leqslant \frac{\theta}{2\varepsilon}\int_0^{x_i} e^{-rs/\varepsilon}\, ds + C\frac{h^2}{\varepsilon^2} \leqslant C + CN^{-2}(\ln(N))^2.$$

Hence using ((2.2.19), pg. 19) and (3.2.1b), for the same values of x_i, we have

$$\hat{W}^N(x_i) \leqslant \prod_{j=1}^{i} \exp\left(-\frac{\alpha_\varepsilon(x_j)^2}{8}\left(\frac{h}{\varepsilon}\right)^2\right)\exp\left(-\frac{\alpha_\varepsilon(x_j)}{2}\frac{h}{\varepsilon}\right) \tag{3.2.22a}$$

$$\leqslant \exp(C(N^{-1}\ln(N))^2 N)\exp(-(\theta/2)x_i/\varepsilon)\exp\left(\frac{\theta}{2\varepsilon}\sum_{j=1}^{i} e^{-rx_j/\varepsilon} h\right) \leqslant Ce^{-(\theta/2)x_i/\varepsilon}. \tag{3.2.22b}$$

Finally, since $\hat{W}^N$ is monotone decreasing, then using (3.2.8) with (3.2.22), we have $\hat{W}^N(x_i) \leqslant CN^{-1}$ for $i \geqslant \frac{N}{2}$ when $\sigma < \frac{1}{2}$. □

A bound on the error $Y_\varepsilon^N - y_\varepsilon$ is given in the following lemma.

Lemma 3.2.4. *If y_ε is the solution of ($\mathscr{D}_\varepsilon$) and ${\overline{Y}_\varepsilon}^N$ is the linear interpolation of Y_ε^N, the solution of ($\mathscr{D}_\varepsilon^N$), then*

$$\|{\overline{Y}_\varepsilon}^N - y_\varepsilon\|_{[0,1]} \leqslant CN^{-1}\ln N.$$

Proof. First, if $\sigma < 1/2$ then for $i \geqslant N/2$, using Lemmas 3.2.1-3.2.3 and (3.2.8), we have

$$|(Y_\varepsilon^N - y_\varepsilon)(x_i)| \leqslant |W_\varepsilon^N(x_{N/2})| + |w_\varepsilon(\sigma)| + |(V_\varepsilon^N - v_\varepsilon)(x_i)| \leqslant CN^{-1}.$$

We now need to examine the error over all meshpoints $x_i \in [0, x_K]$ where $K = N$ if $\sigma = 1/2$ and $K = N/2$ if $\sigma < 1/2$. The error $E^N(x_i) := (Y_\varepsilon^N - y_\varepsilon)(x_i)$ is defined as a solution of the following

$$\mathcal{L}_\varepsilon{}^N E^N(x_i) = (\mathcal{L}_\varepsilon - \mathcal{L}_\varepsilon{}^N) y_\varepsilon, \quad x_i \in (0, x_K), \quad E^N(0) = 0, \quad |E^N(x_K)| \leqslant CN^{-1}. \tag{3.2.23}$$

For $x_i \in (0, x_K)$ we have $h_{i+1} = h_i = h$ and $h/\varepsilon \leqslant CN^{-1} \ln N$. Using (3.2.1), (3.2.3) and Lemma 3.2.1, observe that for any $s \in [x_{i-1}, x_{i+1}] \subset [0, x_K)$ we have a bound on $|\varepsilon w_\varepsilon''(s) - \varepsilon w_\varepsilon''(x_i)|$ as follows

$$\left[\|b'\| \|w_\varepsilon\|_{[x_{i-1}, x_i]} + \left(\|b\| + \int_{\xi=0}^{x_{i+1}} \left| a_\varepsilon'(\xi) \right| \, d\xi \right) \|w_\varepsilon'\|_{[x_{i-1}, x_i]} + \|a_\varepsilon\| \|w_\varepsilon''\|_{[x_{i-1}, x_i]} \right. \tag{3.2.24a}$$

$$\left. + \|\varphi_\varepsilon\| \|v_\varepsilon''\| + \left(\|a_0'\| + \int_{\xi=0}^{x_{i+1}} \left| a_\varepsilon'(\xi) \right| d\xi \right) \|v_\varepsilon'\| \right] |s - x_i| \leqslant Ch(1 + \varepsilon^{-2} e^{-(\theta/2)x_{i-1}/\varepsilon}). \tag{3.2.24b}$$

Thus using Lemma 3.2.1 with standard local truncation error estimates and using (3.2.24) with (3.2.1c) and (3.2.15) we have

$$|(\mathcal{L}_\varepsilon - \mathcal{L}_\varepsilon{}^N) y_\varepsilon(x_i)| \leqslant Ch(1 + \varepsilon^{-2} e^{-(\theta/2)x_{i-1}/\varepsilon}). \tag{3.2.25}$$

Using (3.2.18) and (3.2.19), consider the mesh functions

$$\Psi^{N\pm}(x_i) = Ch\varepsilon^{-1} \hat{W}^N(x_i) + Ch(1 - x_i) \pm E^N(x_i)$$

which are nonnegative at $x_i = x_0, x_K$. Using the bound in (3.2.25) we have

$$\mathcal{L}_\varepsilon{}^N \Psi^{N\pm}(x_i) \leqslant -C' h\varepsilon^{-2} e^{-(\theta/2)x_i/\varepsilon} - Ch\alpha_\varepsilon(x_i) + Ch + Ch\varepsilon^{-2} e^{-(\theta/2)x_i/\varepsilon}.$$

Note that for $k^* = (4\varepsilon/\theta)\ln(1/\varepsilon)$ we have the inequalities

$$1 + \varepsilon^{-2} e^{-(\theta/2)x/\varepsilon} \leqslant 2\varepsilon^{-2} e^{-(\theta/2)x/\varepsilon}, \quad x \leqslant k^*, \tag{3.2.26a}$$

$$1 + \varepsilon^{-2} e^{-(\theta/2)x/\varepsilon} \leqslant 2, \quad x > k^*, \qquad \alpha_\varepsilon(x_i) \geqslant \theta/2, \quad x_i \geqslant k^* - h. \tag{3.2.26b}$$

Either there exists an integer $T \leqslant K - 1$ that is the largest integer s.t. $x_T \leqslant k^*$ ($\sharp$) or $k^* > x_{K-1}$ ($\flat$). Using (3.2.26), on meshpoints $x_i \in [x_1, x_{K-1}]$ in case ($\flat$) or on meshpoints $x_i \in [x_1, x_T]$ in case ($\sharp$), we have the bound

$$\mathcal{L}_\varepsilon{}^N \Psi^{N\pm}(x_i) \leqslant -(C' - C) h\varepsilon^{-2} e^{-(\theta/2)x_i/\varepsilon} \leqslant 0.$$

In case ($\sharp$), if $T < K - 1$ then on meshpoints $x_i \in [x_{T+1}, x_{K-1}]$ we have

$$\mathcal{L}_\varepsilon{}^N \Psi^{N\pm}(x_i) \leqslant -C_2 h\alpha_\varepsilon(k^* - h) + Ch \leqslant 0.$$

Complete the proof using Theorem 3.2.2. The global bound follows as in [22, pg. 381]. □

3.3: NONLINEAR PROBLEM

3.3.1 Continuous Problem

Consider the following problem class on the unit interval $\Omega = (0,1)$. Find y_ε such that

$$\begin{gathered}(\varepsilon y_\varepsilon'' + (F(y_\varepsilon))' - b y_\varepsilon)(x) = q(x), \qquad x \in \Omega, \qquad y_\varepsilon(0) = 0, \quad y_\varepsilon(1) = B > 0, \\ b, q \in C^2[0,1], \quad b(x) \geqslant 0, \quad x \in \overline{\Omega}, \qquad F \in C^3[0, 2(B + \sqrt{\|q\|})].\end{gathered} \tag{$\mathscr{F}_\varepsilon$}$$

We consider this problem for F and B satisfying

$$B^2 - 2(B\|b\| + \max_{x\in\Omega}\{0, q(x)\}) > \gamma^2, \quad \gamma > 0. \tag{3.3.1a}$$

$$F'(s) =: f(s) \geqslant s, \quad s \in [0, 2(B + \sqrt{\|q\|})]. \tag{3.3.1b}$$

Note that a Burger's type equation of the form $(\tilde{\varepsilon} y'' + \alpha y y' - \tilde{b} y)(x) = \tilde{q}(x)$, for any $\alpha > 0$, is contained in the problem class ($\mathscr{F}_\varepsilon$)-(3.3.1), which can be seen be dividing all terms by α.

Consider the class of general quasilinear problems of the form

$$\varepsilon z_\varepsilon''(t) = H(t, z_\varepsilon, z_\varepsilon') = c(t, z_\varepsilon) z_\varepsilon'(t) + d(t, z_\varepsilon), \quad t \in J = (j_1, j_2), \tag{3.3.2a}$$

$$z(j_1) = b_1, \quad z(j_2) = b_2, \tag{3.3.2b}$$

where $c, d \in C[J \times \mathbb{R}, \mathbb{R}]$. For this problem, we define lower and upper solutions and the Nagumo condition as follows.

Definition 3.3.1. *A function $\underline{z} \in C^1(J)$ is a lower solution of (3.3.2) if $\varepsilon \underline{z}''(t) \geqslant H(t, \underline{z}, \underline{z}')$ on (j_1, j_2) and $\underline{z}(j_i) \leqslant b_i$, $i = 1, 2$. An upper solution $\overline{z} \in C^1(J)$ is defined analogously, with both inequalities reversed. Let $p, q \in C[J, \mathbb{R}]$ with $p(t) \leqslant q(t)$ on J. Suppose that for s satisfying $p(t) \leqslant s(t) \leqslant q(t)$, $t \in J$ and $s' \in \mathbb{R}$ we have*

$$|H(t, s, s')| \leqslant h(|s'|) \tag{3.3.3}$$

where $h \in C[[0, \infty], (0, \infty)]$. If

$$\int_\lambda^\infty \frac{\xi}{h(\xi)} d\xi > \max_{t\in J} q(t) - \min_{t\in J} p(t), \tag{3.3.4}$$

where $\lambda(j_2 - j_1) = \max\{|p(j_1) - q(j_2)|, |p(j_2) - q(j_1)|\}$, then we say that H satisfies Nagumo's condition on J relative to p, q.

Note from (3.3.2), for any bounded s, p and q s.t $p(t) \leqslant s(t) \leqslant q(t)$ on J, we have

$$|H(t, s, s')| \leqslant \max_{p(t)\leqslant s(t)\leqslant q(t)} |c(t, s)||s'(t)| + \max_{p(t)\leqslant s(t)\leqslant q(t)} |d(t, s)|.$$

Thus if $\underline{z}$ and $\overline{z}$ are any bounded lower and upper solutions of (3.3.2) with $\underline{z}(t) \leqslant \overline{z}(t)$ on J then by taking $h(\xi) := C(1 + \xi)$ in (3.3.3) where C depends on c, d, $\underline{z}$ and $\overline{z}$, we can easily show that F satisfies Nagumo's condition on J relative to $\underline{z}, \overline{z}$.

Lemma 3.3.1. *[5, §1.5, Th^m 1.5.1] Let $\underline{z},\overline{z}\in C^1[J,\mathbb{R}]$ be, respectively, lower and upper solutions of (3.3.2) on J such that $\underline{z}(t)\leqslant\overline{z}(t)$ on J. Suppose further that $H(t,z_\varepsilon,z'_\varepsilon)$ satisfies Nagumo's condition on J relative to the pair $\underline{z}$, $\overline{z}$. Then, for any $\underline{z}(j_1)\leqslant b_1\leqslant\overline{z}(j_1)$, $\underline{z}(j_2)\leqslant b_2\leqslant\overline{z}(j_2)$, the problem (3.3.2) has a solution $z_\varepsilon\in C^2[J,\mathbb{R}]$ with $\underline{z}(t)\leqslant z_\varepsilon(t)\leqslant\overline{z}(t)$.*

Remark: For any problem from the class (3.3.2), it suffices to construct a lower and upper solution of the problem to show existence of a bounded solution.

Lemma 3.3.2. *Assuming (3.3.1), there exists a unique solution $y_\varepsilon\in C^2[0,1]$ of the problem ($\mathscr{F}_\varepsilon$) satisfying*

$$\alpha_\varepsilon(x):=\gamma(1-e^{-(\gamma/2)x/\varepsilon})\leqslant y_\varepsilon(x)\leqslant B+\sqrt{\|q\|}(2-x),\quad x\in\overline{\Omega}. \tag{3.3.5}$$

Proof. Consider the function $\overline{y}(x)=B+\sqrt{\|q\|}(2-x)$. Using (3.3.1b), we have

$$\varepsilon\overline{y}''+f(\overline{y})\overline{y}'-b\overline{y}-q=-\sqrt{\|q\|}f(\overline{y})-b\overline{y}+q\leqslant-\|q\|+\|q\|=0.$$

Thus, $\overline{y}$ is an upper solution of ($\mathscr{F}_\varepsilon$). Consider the singularly perturbed Riccati problem: Find $\underline{y}:[0,1]\to\mathbb{R}$ such that

$$\varepsilon\underline{y}'+\tfrac{1}{2}(\underline{y}^2-g^2)=0,\quad \underline{y}(0)=0, \tag{3.3.6a}$$

$$g(x):=\sqrt{B^2-2(B\|b\|+\max_{x\in\Omega}\{0,q(x)\})(1-x)}. \tag{3.3.6b}$$

Note that $g'(x)\geqslant 0$ and using (3.3.1a) we have $g(x)\geqslant g(0)>\gamma>0$. This is the problem studied in [22], with the result that $B\geqslant\underline{y}(x)\geqslant\alpha_\varepsilon(x)$ where α_ε is as defined in (3.3.5). Using (3.3.6a) we have $\varepsilon\underline{y}''+\underline{y}\,\underline{y}'=g\,g'=B\|b\|+\max_{x\in\Omega}\{0,q(x)\}$. Thus we can show that $\underline{y}$ is a lower solution of ($\mathscr{F}_\varepsilon$) and the bound in (3.3.5) follows. Hence from Lemma 3.3.1, ($\mathscr{F}_\varepsilon$) has a solution $y_\varepsilon\in C^2[0,1]$ satisfying $\underline{y}\leqslant y_\varepsilon\leqslant\overline{y}$.

Suppose y_1 and y_2 are two solutions of ($\mathscr{F}_\varepsilon$). Then $\underline{y}\leqslant y_1$, $y_2\leqslant\overline{y}$ and $\Delta y:=y_1-y_2$ satisfies

$$\varepsilon(\Delta y)''+f(y_1)(\Delta y)'+\Big(y_2'\textstyle\int_0^1 f'(y_2+t(\Delta y))\,dt-b\Big)(\Delta y)=0,\quad(\Delta y)(0)=(\Delta y)(1)=0. \tag{3.3.7}$$

Clearly 0 is both a lower and an upper solution of (3.3.7). Thus using Lemma 3.3.1, the solution of ($\mathscr{F}_\varepsilon$) is unique. □

Comparing the bound in (3.3.5) with the condition (3.2.1b) in the linear problem, motivates us to follow the analysis used in the linear problem for this nonlinear problem.

We decompose the solution y_ε into the sum of a regular component and a layer component. The regular component is defined as the solution of

$$(\varepsilon v_\varepsilon''+(F(v_\varepsilon))'-bv_\varepsilon)(x)=q(x),\quad x\in\Omega,\quad v_\varepsilon(0)=(v_0+\varepsilon v_1)(0),\quad v_\varepsilon(1)=B, \tag{3.3.8a}$$

where $v_\varepsilon = v_0 + \varepsilon v_1 + \varepsilon^2 v_2$ and v_0, v_1, v_2 satisfy the nonlinear problems

$$((F(v_0))' - b v_0)(x) = q(x), \quad x \in [0,1), \quad v_0(1) = B, \tag{3.3.8b}$$

$$(f(v_0)v_1' + (v_0'\mathcal{T}_1 - b)v_1)(x) = -v_0''(x), \quad x \in (0,1), \quad v_1(1) = 0; \quad v_1(0) := \lim_{t \downarrow 0} v_1(t), \tag{3.3.8c}$$

$$\begin{gathered}(\varepsilon v_2'' + f(v_\varepsilon)v_2' + (v_0' + \varepsilon v_1')(\mathcal{T}_1 + \mathcal{T}_2 v_1 + \varepsilon \mathcal{T}_2 v_2)v_2 - b v_2)(x) = -(\mathcal{T}_1 v_1 v_1' + v_1'')(x), \\ x \in (0,1), \quad v_2(0) = v_2(1) = 0.\end{gathered} \tag{3.3.8d}$$

$$\mathcal{T}_1 := \int_0^1 f'(v_0 + \varepsilon v_1 t)\, dt, \qquad \mathcal{T}_2 := \int_0^1 t \int_0^1 f''(v_0 + \varepsilon v_1 t + \varepsilon^2 v_2 s)\, ds\, dt. \tag{3.3.8e}$$

Note that the equations in (3.3.8) were derived using ((2.2.2), pg 16). The layer component is defined as the solution of the problem

$$\begin{gathered}(\varepsilon w_\varepsilon'' + f(y_\varepsilon)w_\varepsilon' + \left(v_\varepsilon' \int_0^1 f'(v_\varepsilon + t w_\varepsilon)\, dt - b\right) w_\varepsilon)(x) = 0, \\ x \in \Omega, \quad w_\varepsilon(0) = -v_\varepsilon(0), \quad w_\varepsilon(1) = 0.\end{gathered} \tag{3.3.9}$$

Bounds on both components and their derivatives are given in the following lemma.

Lemma 3.3.3. *Assuming (3.3.1) and the conditions on the problem data in ($\mathcal{F}_\varepsilon$), for $k = 0,1,2,3$, the solutions v_ε and w_ε of (3.3.8) and (3.3.9) respectively, uniquely exist and satisfy the bounds*

$$\|v_\varepsilon^{(k)}\| \leqslant C(1 + \varepsilon^{2-k}) \quad \textit{and} \quad |w_\varepsilon^{(k)}(x)| \leqslant C\varepsilon^{-k} e^{-(\gamma/2)x/\varepsilon}, \quad x \in \Omega.$$

Proof. Using a suitable transform, we can easily extend the definition of upper and lower solutions of initial value problems (see §2.2.1.2, pg. 15) to the case of terminal value problems. Using (3.3.1b) and (3.3.6b), we can show that $\overline{v}(x) = B + \sqrt{\|q\|}(2-x)$ and $\underline{v}(x) = g(x)$ are upper and lower solutions of (3.3.8b). Thus (3.3.8b) has a solution v_0 with

$$\gamma < g(0) \leqslant v_0 \leqslant C. \tag{3.3.10}$$

Since $b, q \in C^2[0,1]$ and $f \in C^2[0, 2(B + \sqrt{\|q\|})]$, the bounds $\|v_0^{(k)}\| \leqslant C$, $k = 1,2,3$, follow from (3.3.8b).

For (3.3.8c), in the same manner as (3.3.8b), we can show using the upper and lower solutions, $\overline{v}$ and -$\overline{v}$ respectively, that $\|v_1^{(k)}\| \leqslant C$, $k = 0,1,2$, where

$$\overline{v} := \frac{\|v_0''\|}{\|v_0'\|\|f'\| + \|b\| + 1} \left(\exp\left(\frac{1}{\gamma}(\|v_0'\|\|f'\| + \|b\| + 1)(1-x) \right) - 1 \right).$$

Before examining (3.3.8d), we can bound v_ε. Note that using (3.3.1a) and (3.3.10), for sufficiently small ε, we have

$$v_\varepsilon(0) = (v_0 + \varepsilon v_1)(0) \geqslant g(0) - C\varepsilon \geqslant \gamma. \tag{3.3.11}$$

Again, consider the problem (3.3.6), but with $\underline{y}(0) = \gamma$. Since $g(x) > \gamma$, it is easily checked that γ is a lower solution of (3.3.6). Thus, in the same manner as in Lemma 3.3.2, we can show that

there is a unique solution of (3.3.8a) satisfying

$$\gamma \leqslant \underline{y} \leqslant v_\varepsilon \leqslant B + 2\sqrt{\|q\|}. \tag{3.3.12}$$

For (3.3.8d), using $f(v_\varepsilon) \geqslant v_\varepsilon \geqslant \gamma$, we can show for sufficiently small ε that $\overline{v}$ s.t.

$$\overline{v} := C_3 \left(\exp\left(\frac{4}{\gamma} \left((\|v_0'\| + \varepsilon \|v_1'\|)(\|f'\| + \|v_1\|\|f''\|) + \|b\| + 1 \right)(1-x) \right) - 1 \right)$$

$$C_3 := \frac{3(\|v_1''\| + \|v_1\|\|v_1'\|\|f'\|)}{(\|v_0'\| + \varepsilon\|v_1'\|)(\|f'\| + \|v_1\|\|f''\|) + \|b\| + 1}$$

and $-\overline{v}$ are upper and lower solutions respectivley. Hence $\|v_2\| \leqslant C$. We bound the derivatives of v_2 in the same manner as in Lemma 3.2.1. Using the mean value theorem and (3.3.8d), there exists a point $z \in (0, \varepsilon)$ such that $\varepsilon |v_2'(z)| \leqslant \|v_2\|$. Integrating (3.3.8d) over $[0, \eta]$ for any $0 < \eta \leqslant 1$, we have

$$\varepsilon |v_2'(\eta) - v_2'(0)| \leqslant C \max\{\|f\|, \|f'\|, \|f''\|, \|v_0'\|, \|v_1\|, \|v_1'\|, \|v_1''\|, \|v_2\|, \|b\|\}.$$

Thus letting $\eta = z$, we find the bound $|\varepsilon v_2'(0)| \leqslant C$, then letting $\eta = x \in (0,1)$ we obtain the bound $|\varepsilon v_2'(x)| \leqslant C$. Retrieve the bound $\varepsilon \|v_2''\| \leqslant C/\varepsilon$ using (3.3.8d). Use $v_\varepsilon = v_0 + \varepsilon v_1 + \varepsilon^2 v_2$ to bound v_ε' and v_ε'' and complete the proof for the regular component by establishing the required bound on v_ε''' using (3.3.8a).

To prove the bound on the layer component, consider the function

$$\underline{w}(x) = w_\varepsilon(0) \exp\left(-\frac{1}{2\varepsilon} \int_{t=0}^{x} \alpha_\varepsilon(t)\, dt \right),$$

where α_ε is as defined in (3.3.5). Note that $w_\varepsilon(0) = -v_\varepsilon(0) \leqslant -\gamma$ thus $\underline{w}(x) < 0$. We can show that

$$\varepsilon \alpha_\varepsilon'(x) + \frac{1}{2}\alpha_\varepsilon^2(x) \geqslant \frac{3\gamma^2}{8}.$$

Moreover, we have

$$\left| v_\varepsilon' \int_0^1 f'(v_\varepsilon + t\,\underline{w})\, dt - b \right| \leqslant \|v_\varepsilon'\|\|f'\| + \|b\| \leqslant C.$$

Thus using $f(y_\varepsilon) \geqslant y_\varepsilon \geqslant \alpha_\varepsilon$ and (3.3.9), for sufficiently small ε, we have

$$\varepsilon \underline{w}'' + f(y_\varepsilon)\underline{w}' + \left(v_\varepsilon' \int_0^1 f'(v_\varepsilon + t\,\underline{w})\, dt - b \right) \underline{w} \geqslant \tfrac{1}{2\varepsilon}((\alpha_\varepsilon^2/2 + \varepsilon\alpha_\varepsilon') - C\varepsilon)(-\underline{w}) \geqslant 0.$$

Hence $\underline{w}$ is a lower solution of (3.3.9) and since 0 is an upper solution, using (3.3.5), we have

$$|w_\varepsilon(x)| \leqslant |w_\varepsilon(0)| \exp\left(-\frac{1}{2\varepsilon} \int_{t=0}^{x} \alpha_\varepsilon(t)\, dt \right) \leqslant C|w_\varepsilon(0)| e^{-(\gamma/2)x/\varepsilon}, \quad x \in \overline{\Omega}. \tag{3.3.13}$$

Bounds on the derivatives of w_ε may be established in the same manner as with the layer component in Lemma 3.2.1. □

3.3.2 The Discrete Problem and Error Analysis

We consider the following nonlinear finite difference scheme. Find Y_ε^N such that

$$(\varepsilon D^+D^- Y_\varepsilon^N + D^+F(Y_\varepsilon^N) - bY_\varepsilon^N)(x_i) = q(x_i), \quad x_i \in \Omega_\varepsilon^N, \quad Y_\varepsilon^N(0) = 0, \quad Y_\varepsilon^N(1) = B, \qquad (\mathscr{F}_\varepsilon^N)$$

where, assuming (3.3.1a), Ω_ε^N is the piecewise-uniform fitted mesh described in the same manner as (3.2.8) but with the transition point

$$\sigma := \min\left\{\frac{1}{2}, \frac{2\varepsilon}{\gamma}\ln N\right\}. \tag{3.3.14}$$

Note that in the discrete nonlinear problem $(\mathscr{F}_\varepsilon^N)$, we use a different approximation to the second derivative term to what we used in the discrete linear problem $(\mathscr{D}_\varepsilon^N)$. This is related to the fact that the continuous problem $(\mathscr{F}_\varepsilon)$ may be written in the form $(\varepsilon y' + F(y))' - by = q$.

Note also, that using (2.2.2), we can express $D^+F(Y_\varepsilon^N(x_i))$ as

$$D^+F(Y_\varepsilon^N(x_i)) = \left(\int_0^1 f(tY_\varepsilon^N(x_{i+1}) + (1-t)Y_\varepsilon^N(x_i))\,dt\right) D^+Y_\varepsilon^N(x_i). \tag{3.3.15}$$

We will suggest a method for solving the nonlinear scheme ($(\mathscr{F}_\varepsilon^N)$, (3.3.14)) in §3.4 later, however we mention that the expression above suggests a choice for linearising the scheme.

Consider a discrete nonlinear problem of the form

$$\mathcal{N}^N Z^N(\lambda_i) := \varepsilon D^+[D^- Z^N + J(\lambda_i, Z^N(\lambda_i))](\lambda_i) = K(\lambda_i, Z^N), \tag{3.3.16a}$$

$$\lambda_i \in \Lambda^N, \quad Z^N(0) = b_0, \quad Z^N(1) = b_1, \tag{3.3.16b}$$

where $J \in C^{0,1}[S,R]$, $J_y(x,y) \geqslant 0$ for $(x,y) \in S \times R$; $K \in C^{0,0}[\mathbb{R},\mathbb{R}]$; Λ^N is an arbitrary mesh and $S, R \subseteq \mathbb{R}$. For this problem, we define discrete lower and upper solutions as follows.

Definition 3.3.2. *A mesh function $\underline{Z}^N$ on Λ^N is a discrete lower solution of (3.3.16) if $\mathcal{N}^N\underline{Z}^N(\lambda_i) \geqslant K(\lambda_i, \underline{Z}^N(\lambda_i))$ on Λ^N and $\underline{Z}^N(i) \leqslant b_i$, $i = 0,1$. A discrete upper solution $\overline{Z}^N$ on Λ^N is defined analogously, with both inequalities reversed.*

We now show that existence of upper and lower solutions implies existence of a solution to (3.3.16). The proof of [11, Th$^{\text{m}}$ 5.2] is easily tailored to prove the next lemma.

Lemma 3.3.4. *Let $\underline{Z}^N$ and $\overline{Z}^N$ on Λ^N be discrete lower and upper solutions of (3.3.16) respectively such that $\underline{Z}^N(\lambda_i) \leqslant \overline{Z}^N(\lambda_i)$ for $\lambda_i \in \Lambda^N$ and $\underline{Z}^N$, $\overline{Z}^N \in R$. Then (3.3.16) has a solution Z with $\underline{Z}^N \leqslant Z^N \leqslant \overline{Z}^N$ on Λ^N.*

Proof. Let $L_1^N, L_2^N \in R$ be two discrete lower solutions of (3.3.16). Define the mesh function L_3^N on all $\lambda_i \in \Lambda^N$ by $L_3^N(\lambda_i) := \max\{L_1^N(\lambda_i), L_2^N(\lambda_i)\}$. At any mesh point λ_i where $L_3^N(\lambda_i) = L_1^N(\lambda_i)$, we have

$$D^+[J(\lambda_i, L_3(\lambda_i)] - D^+[J(\lambda_i, L_1(\lambda_i)] = D^+[(L_3 - L_1)(\lambda_i) \int_0^1 J_y(\lambda_i, (L_1 + t(L_3 - L_1))(\lambda_i))\, dt]$$

$$= \lambda_{i+1}^{-1}[(L_3 - L_1)(\lambda_{i+1}) \int_0^1 J_y(\lambda_{i+1}, (L_1 + t(L_3 - L_1))(\lambda_{i+1}))\, dt - 0] \geqslant 0$$

Likewise for any mesh point λ_i where $L_3^N(\lambda_i) = L_2^N(\lambda_i)$. Thus it is easily shown that L_3^N is a discrete lower solution on Λ^N and the remainder of the proof follows that in [11, Th$^{\underline{\text{m}}}$ 5.2]. □

Remark: The discrete nonlinear problems we will see below are contained within the problem class (3.3.16) with $S = \Omega$ and $R = [0, 2(B + \sqrt{\|q\|})]$. Hence, to bound a solution to a discrete problem below, it suffices to construct discrete lower and upper solutions $\underline{Z}^N(x_i)$ and $\overline{Z}^N(x_i)$ that satisfy $0 \leqslant \underline{Z}^N(x_i), \overline{Z}^N(x_i) \leqslant 2(B + \sqrt{\|q\|})$.

Lemma 3.3.5. *Assuming (3.3.1), if Y_ε^N is the solution to ($\mathscr{T}_\varepsilon^N$) then*

$$A_\varepsilon^N(x_i) := \gamma \left(1 - \prod_{j=1}^{i} \left(1 + \frac{\gamma}{2} \frac{h_j}{\varepsilon}\right)^{-1}\right) \leqslant Y_\varepsilon^N(x_i) \leqslant B + \sqrt{\|q\|}(2 - x_i), \qquad x_i \in \overline{\Omega}_\varepsilon^N. \tag{3.3.17}$$

Proof. Consider the mesh function $\overline{Y}^N(x_i) = B + \sqrt{\|q\|}(2 - x_i)$, $x_i \in \overline{\Omega}_\varepsilon^N$. Using (3.3.1b) and (3.3.15), we have

$$\begin{aligned}
&(\varepsilon D^+ D^- \overline{Y}^N + D^+ F(\overline{Y}^N) - b\overline{Y} - q)(x_i) \\
\leqslant &- \left(\int_0^1 f(t\overline{Y}^N(x_{i+1}) + (1-t)\overline{Y}^N(x_i))\, dt\right) \sqrt{\|q\|} + \|q\| \\
\leqslant &- \frac{1}{2}\left(\overline{Y}^N(x_{i+1}) + \overline{Y}^N(x_i)\right) \sqrt{\|q\|} + \|q\| \leqslant -\|q\| + \|q\| = 0.
\end{aligned}$$

Thus $\overline{Y}^N$ is a discrete upper solution of ($\mathscr{T}_\varepsilon^N$).

Consider the discrete Riccati problem

$$\varepsilon D^- \underline{Y}^N(x_i) + \tfrac{1}{2}(\underline{Y}^N(x_i)^2 - g(x_i)^2) = 0, \qquad x_i \in \Omega_\varepsilon^N, \qquad \underline{Y}(0) = 0, \tag{3.3.18}$$

where g is as defined in (3.3.6b). From the results in [22], we have $A_\varepsilon^N \leqslant \underline{Y}^N \leqslant B$, where A_ε^N is as defined in (3.3.5). Note that we use the fact that the mesh (3.3.14) is identical to that used in [22]. Thus we can use the results in [22] directly. If the meshes were not identical, we would possibly have to perform a more fuller discrete analysis on (3.3.18) to establish bounds on the solution. Using (3.3.18) we have

$$\varepsilon D^+ D^- \underline{Y}^N(x_i) + \tfrac{1}{2} D^+ \underline{Y}^N(x_i)^2 = \tfrac{1}{2} D^+ g(x_i)^2 = B\|b\| + \max_{x \in \Omega}\{0, q(x)\}. \tag{3.3.19}$$

Since $g' \geqslant 0$, we can easily check that g is a discrete upper solution (see Th$^{\underline{m}}$ 2.2.4, pg. 18) for (3.3.18). Thus $D^+\underline{Y}^N(x_i) \geqslant 0$. Hence, using (3.3.1b) and (3.3.15), we have

$$\begin{aligned} D^+F(\underline{Y}^N(x_i)) &= \left(\int_0^1 f(t\,\underline{Y}(x_{i+1})+(1-t)\underline{Y}^N(x_i))\,dt\right) D^+\underline{Y}(x_i) \\ &\geqslant \tfrac{1}{2}\left(\underline{Y}^N(x_{i+1})+\underline{Y}^N(x_i)\right) D^+\underline{Y}^N(x_i) = \tfrac{1}{2}D^+[\underline{Y}^N(x_i)^2] \end{aligned}$$

We can then use this to show that $\underline{Y}^N$ is a discrete lower solution for ($\mathscr{F}_\varepsilon^N$). □

As in the continuous case, we decompose the discrete solution into the sum of a discrete regular component, V_ε^N, and a discrete layer component, W_ε^N. The discrete regular component is defined as the solution of the problem

$$(\varepsilon D^+D^-V_\varepsilon^N + D^+F(V_\varepsilon^N) - bV_\varepsilon^N)(x_i) = q(x_i), \quad x_i \in \Omega_\varepsilon^N, \quad V_\varepsilon^N(0) = v_\varepsilon(0), \quad V_\varepsilon^N(1) = B. \tag{3.3.20}$$

The discrete layer component is defined as the solution of

$$\left(\varepsilon D^+D^-W_\varepsilon^N + D^+\left[\left(\int_0^1 f(tY_\varepsilon^N+(1-t)V_\varepsilon^N)\,dt\right)W_\varepsilon^N\right] - bW_\varepsilon^N\right)(x_i) = 0, \tag{3.3.21a}$$

$$x_i \in \Omega_\varepsilon^N, \quad W_\varepsilon^N(0) = w_\varepsilon(0) = -v_\varepsilon(0), \quad W_\varepsilon^N(1) = w_\varepsilon(1) = 0. \tag{3.3.21b}$$

Lemma 3.3.6. *Assuming (3.3.1), if V_ε^N is the solution of (3.3.20) and W_ε^N is the solution of (3.3.21) then for sufficiently small ε, we have*

$$\gamma \leqslant V_\varepsilon^N(x_i) \leqslant B + \sqrt{\|q\|}(2-x_i), \quad x_i \in \Omega^N. \tag{3.3.22a}$$

$$|W_\varepsilon^N(x_i)| \leqslant \begin{cases} Ce^{-(\gamma/2)x_i/\varepsilon} + CN^{-1}, & 0 \leqslant i \leqslant N\,(\sigma = \frac{1}{2}), \quad 0 \leqslant i \leqslant \frac{N}{2},\ (\text{if } \sigma < \frac{1}{2}) \\ CN^{-1}, & \frac{N}{2} \leqslant i \leqslant N,\ (\text{if } \sigma < \frac{1}{2}). \end{cases} \tag{3.3.22b}$$

Proof. The bound in (3.3.22a) can be proved by repeating the proof of Lemma 3.3.5 with $\underline{Y}(0) = \gamma \leqslant v_\varepsilon(0)$, in (3.3.18), for sufficiently small ε and using (3.3.11).

Clearly 0 is a discrete upper solution of (3.3.21). Consider the mesh function $\underline{W}^N$ satisfying

$$\left(\varepsilon D^+D^-\underline{W}^N + D^+\left[\left(\int_0^1 f(tY_\varepsilon^N+(1-t)V_\varepsilon^N)\,dt\right)\underline{W}^N\right]\right)(x_i) = 0, \quad \underline{W}^N(0) = w_\varepsilon(0), \quad \underline{W}^N(1) = 0.$$

This means $\underline{W}^N$ satisfies

$$\varepsilon D^-(\underline{W}^N(x_i) - \underline{W}^N(1)) + \left(\int_0^1 f(tY_\varepsilon^N+(1-t)V_\varepsilon^N)\,dt\right)\underline{W}^N(x_i) = 0, \quad \underline{W}^N(0) = w_\varepsilon(0). \tag{3.3.23}$$

Using (3.3.1b) with the bounds in Lemma 3.3.5 and (3.3.22a) we have

$$\int_0^1 f(tY_\varepsilon^N+(1-t)V_\varepsilon^N)\,dt \geqslant \int_0^1 tY_\varepsilon^N+(1-t)V_\varepsilon^N\,dt = \tfrac{1}{2}(Y_\varepsilon^N+V_\varepsilon^N) \geqslant \gamma/2.$$

Hence, we can show that

$$\underline{\underline{W}}^N(x_i) := w_\varepsilon(0)\prod_{j=1}^{i}\left(1+\frac{\gamma}{2}\frac{h_j}{\varepsilon}\right)^{-1}, \quad \underline{\underline{W}}^N(x_0) := w_\varepsilon(0),$$

and 0 are respectively, discrete lower and upper solutions of (3.3.23), which can then be shown to be, in turn, a discrete lower solution of (3.3.21). The bounds in (3.3.22b) can be established in the same manner as in Lemma 3.2.3. □

We present bounds on the error $V_\varepsilon^N - v_\varepsilon$ in the following lemma.

Lemma 3.3.7. *Assuming (3.3.1a), if v_ε is the solution of (3.3.8) and V_ε^N is the solution of (3.3.20) then*

$$|(V_\varepsilon^N - v_\varepsilon)(x_i)| \leqslant CN^{-1}, \quad x_i \in \overline{\Omega}_\varepsilon^N.$$

Proof. The error $E^N(x_i) := V_\varepsilon^N - v_\varepsilon$ is defined as the solution of

$$\left(\varepsilon D^+D^-E^N + D^+\left[\left(\int_0^1 f(tV_\varepsilon^N + (1-t)v_\varepsilon)\,dt\right)E^N\right] - bE^N\right)(x_i) = \tau^N(x_i), \ , \tag{3.3.24a}$$

$$\tau^N := \varepsilon(\tfrac{d^2}{dx^2} - D^+D^-)v_\varepsilon + (\tfrac{d}{dx} - D^+)F(v_\varepsilon), \quad x_i \in \Omega_\varepsilon^N, \quad E^N(0) = E^N(1) = 0, \tag{3.3.24b}$$

Using the notation $h_i = x_i - x_{i-1}$, and recalling $F \in C^3[0, 2(B + \sqrt{\|q\|})]$ by standard local truncation error estimates and Lemma 3.3.3 we have

$$\begin{aligned}
\tau^N(x_i) &= (\varepsilon(\tfrac{d^2}{dx^2} - D^+D^-)v_\varepsilon + (\tfrac{d}{dx} - D^+)F(v_\varepsilon))(x_i) \\
&= (\varepsilon(\tfrac{d}{dx} - D^+)v_\varepsilon' + D^+(\tfrac{d}{dx} - D^-)v_\varepsilon + (\tfrac{d}{dx} - D^+)F(v_\varepsilon))(x_i) \\
&\leqslant C\varepsilon h_{i+1}\|v_\varepsilon'''\| + \varepsilon D^+(v_\varepsilon' - D^-v_\varepsilon)(x_i) + Ch_{i+1}\max\{\|F''\|, \|F'\|, \|v_\varepsilon'\|, \|v_\varepsilon''\|\} \\
&\leqslant CN^{-1} + \varepsilon D^+(v_\varepsilon' - D^-v_\varepsilon)(x_i) := CN^{-1} + \varepsilon D^+\tau_1^N(x_i).
\end{aligned}$$

Consider the mesh function $\overline{E}^N$ satisfying $\overline{E}^N(0) = \overline{E}^N(1) = 0$ and

$$\left(\varepsilon D^+D^-\overline{E}^N + D^+\left[\left(\int_0^1 f(tV_\varepsilon^N + (1-t)v_\varepsilon)\,dt\right)\overline{E}^N\right]\right)(x_i) = -CN^{-1} + \varepsilon D^+\tau_1^N(x_i).$$

This means $\overline{E}^N$ satisfies $\overline{E}^N(0) = 0$ and

$$\varepsilon D^-(\overline{E}^N(x_i) - \overline{E}^N(1)) + \left(\int_0^1 f(tV_\varepsilon^N + (1-t)v_\varepsilon)\,dt\right)\overline{E}^N(x_i) = CN^{-1}(1-x_i) + \varepsilon(\tau_1^N(x_i) - \tau_1^N(1)). \tag{3.3.25}$$

Using Lemma 3.3.3 and (3.3.22a) we have $(V_\varepsilon^N + v_\varepsilon)/2 \geqslant \gamma$ and $|\tau_1^N| \leqslant CN^{-1}$. Then it is easily checked that the quantities $-\varepsilon\frac{2}{\gamma}CN^{-1}$ and $\frac{2}{\gamma}CN^{-1}$ are respectively, discrete lower and upper solutions of (3.3.25), which can then be shown to be, in turn, a discrete upper solution of (3.3.24). We construct a discrete lower solution in an analogous manner to complete the proof. □

Lemma 3.3.8. *Assuming (3.3.1), if y_ε is the solution of ($\mathscr{F}_\varepsilon$) and $\overline{Y}_\varepsilon{}^N$ is the linear interpolation of Y_ε^N, the solution of ($\mathscr{F}_\varepsilon^N$), then*

$$\|\overline{Y}_\varepsilon^N - y_\varepsilon\|_{[0,1]} \leqslant CN^{-1}\ln N.$$

Proof. First, if $\sigma < 1/2$ then for $i \geqslant N/2$, using Lemmas 3.3.3, 3.3.6 and 3.3.7, we have

$$|(Y_\varepsilon^N - y_\varepsilon)(x_i)| \leqslant |W_\varepsilon^N(x_{N/2})| + |w_\varepsilon(\sigma)| + |(V_\varepsilon^N - v_\varepsilon)(x_i)| \leqslant CN^{-1}.$$

We now need to examine the error over all meshpoints $x_i \in [0, x_K]$, where $K = N$ if $\sigma = 1/2$ and $K = N/2$ if $\sigma < 1/2$. The error $E^N(x_i) := Y_\varepsilon^N - y_\varepsilon$ is defined as a solution of

$$\left(\varepsilon D^+D^-E^N + D^+\left[\left(\int_0^1 f(tY_\varepsilon^N + (1-t)y_\varepsilon)\,dt\right)E^N\right] - bE^N\right)(x_i) = \tau^N(x_i), \quad x_i \in \Omega_\varepsilon^N \tag{3.3.26a}$$

$$\tau^N := \varepsilon\left(\tfrac{d^2}{dx^2} - D^+D^-\right)y_\varepsilon + \left(\tfrac{d}{dx} - D^+\right)F(y_\varepsilon), \quad E^N(0) = 0, \quad |E^N(x_k)| \leqslant CN^{-1}. \tag{3.3.26b}$$

For $x_i \in (0, x_K)$ we have $h_{i+1} = h_i = h$ and $h/\varepsilon \leqslant CN^{-1}\ln N$. Using Lemma 3.3.3 we have

$$\begin{aligned}\left(\tfrac{d}{dx} - D^+\right)F(y_\varepsilon(x_i)) &= \frac{1}{h_{i+1}}\int_{x_i}^{x_{i+1}} F(y_\varepsilon(x_i)) - F(y_\varepsilon(t))\,dt \\ &\leqslant C\|f\|h \max_{t\in[x_i,x_{i+1}]}|y_\varepsilon'(t)| \leqslant Ch(1+\varepsilon^{-1}e^{-(\gamma/2)x_i/\varepsilon})\end{aligned}$$

For any $s \in [x_{i-1}, x_{i+1}]$, using $(\mathscr{F}_\varepsilon)$ and Lemma 3.3.3, we have

$$\varepsilon|y_\varepsilon''(s) - y_\varepsilon''(t)| \leqslant [\|q'\| + \|b'\|\|y_\varepsilon\| + \|b\|\max_s|y_\varepsilon'(s)| + \|f\|\max_s|y_\varepsilon''(s)| + \|f'\|\max_s y_\varepsilon'(s)^2]|s - x_i|$$

$$\leqslant Ch(1+\varepsilon^{-1}e^{-(\gamma/2)x_{i-1}/\varepsilon} + \varepsilon^{-2}e^{-(\gamma/2)x_{i-1}/\varepsilon} + \varepsilon^{-2}e^{-(\gamma/2)x_{i-1}/\varepsilon}) \leqslant Ch(1+\varepsilon^{-2}e^{-(\gamma/2)x_{i-1}/\varepsilon}).$$

Hence using ((2.2.19), pg. 19), (3.2.15) and $e^{-(\gamma/2)h/\varepsilon} \leqslant C$ we have

$$\begin{aligned}|\tau^N(x_i)| &\leqslant Ch(1+\varepsilon^{-2}e^{-(\gamma/2)x_i/\varepsilon}) \leqslant Ch\left(1+\varepsilon^{-2}\left(1+\frac{\gamma}{2}\frac{h}{\varepsilon}\right)^{-i}\right) \\ &= Ch - Ch\frac{2}{\gamma}\varepsilon^{-1}D^+\left[\left(1+\frac{\gamma}{2}\frac{h}{\varepsilon}\right)^{-(i-1)}\right] =: Ch - Ch\varepsilon^{-1}D^+T^N(x_i).\end{aligned}$$

Consider the mesh function $\overline{E}^N$ satisfying $\overline{E}^N(0) = 0$, $\overline{E}^N(1) = CN^{-1}$ and

$$\left(\varepsilon D^+D^-\overline{E}^N + D^+\left[\left(\int_0^1 f(tY_\varepsilon^N + (1-t)y_\varepsilon)\,dt\right)\overline{E}^N\right]\right)(x_i) = -Ch + Ch\varepsilon^{-1}D^+T^N(x_i).$$

This means $\overline{E}^N$ satisfies $\overline{E}^N(0) = 0$ and

$$\varepsilon D^-(\overline{E}^N(x_i) - \overline{E}^N(x_K)) + \left(\int_0^1 f(tY_\varepsilon^N + (1-t)y_\varepsilon)\,dt\right)\overline{E}^N(x_i) \tag{3.3.27a}$$

$$= Ch(x_k - x_i) + Ch\varepsilon^{-1}(T^N(x_i) - T^N(x_K)) + \left(\int_0^1 f(tY_\varepsilon^N + (1-t)y_\varepsilon)\,dt\right)\overline{E}^N(x_K). \tag{3.3.27b}$$

We now construct a discrete upper solution of (3.3.27), but establish a few inequalities before doing so. Since $h/\varepsilon \leqslant CN^{-1}\ln N$, we have, for sufficiently large N,

$$\frac{1}{2}A_\varepsilon^N(x_i)A_\varepsilon^N(x_{i-1}) + \varepsilon D^-A_\varepsilon^N(x_i) \geqslant \frac{1}{4}A_\varepsilon^N(x_i)^2 + \varepsilon D^-A_\varepsilon^N(x_i) \geqslant \frac{\gamma^2}{4}. \tag{3.3.28a}$$

Using ((2.2.19), pg. 19), define and bound the mesh function $\hat{Y}^N$ as follows

$$\hat{Y}^N(x_i) := \prod_{j=1}^{i}\left(1+\frac{A_\varepsilon^N(x_j)}{2}\frac{h}{\varepsilon}\right)^{-1} \geqslant e^{-(\gamma/2)x_i/\varepsilon}. \tag{3.3.28b}$$

For sufficiently small ε and sufficiently large N, the integer k in the interval $(2\varepsilon\ln(\frac{4}{\gamma h}), 2\varepsilon\ln(\frac{4}{\gamma h})+1)$ satisfies $k<K$. Using (3.3.28b) and ((2.2.19), pg. 19), it follows

$$\hat{Y}^N(x_k) \geqslant e^{-(\gamma/2)(h/\varepsilon)k} \geqslant \frac{1}{4}e^{-(\gamma/2)h/\varepsilon} \geqslant \frac{1}{8}, \tag{3.3.28c}$$

$$A_\varepsilon^N(x_k) \geqslant \gamma\left(1-\left(1+\frac{\gamma}{2}\frac{h}{\varepsilon}\right)^{-2\varepsilon/(\gamma h)\ln 4}\right) \geqslant \frac{\gamma}{2}. \tag{3.3.28d}$$

Using (3.3.1b) with Lemmas 3.3.5 and 3.3.5 and ((2.2.19), pg. 19), we have

$$\begin{aligned}&\int_0^1 f(t\,Y_\varepsilon^N+(1-t)y_\varepsilon)\,dt \geqslant \int_0^1 t\,Y_\varepsilon^N+(1-t)y_\varepsilon\,dt\\ =&\tfrac{1}{2}(Y_\varepsilon^N+y_\varepsilon) \geqslant \tfrac{1}{2}(A_\varepsilon^N+\alpha_\varepsilon) \geqslant \tfrac{1}{2}(A_\varepsilon^N+A_\varepsilon^N)=A_\varepsilon^N.\end{aligned}$$

Consider the mesh function $\hat{E}^N := Ch\varepsilon^{-1}(\kappa_1 A_\varepsilon^N \hat{Y}^N+\kappa_2)$ where we choose the $\kappa_i's$ later. Using ((2.2.19), pg. 19) and (3.3.28), we have

$$\begin{aligned}&\varepsilon D^-\hat{E}^N(x_i)+A_\varepsilon^N\hat{E}^N(x_i)-Ch\varepsilon^{-1}-\varepsilon D^-\hat{E}^N(x_K)-C\hat{E}^N(x_k)\\ \geqslant&\left(\kappa_1\frac{\gamma^2}{4}e^{-(\gamma/2)x_i/\varepsilon}+\kappa_2 A_\varepsilon^N(x_i)-1\right)Ch\varepsilon^{-1} \geqslant 0,\end{aligned}$$

if $\kappa_1 \geqslant 64/\gamma^2$ and $\kappa_2 \geqslant 4/\gamma$. Using (3.3.5) and (3.3.5) with ((2.2.19), pg. 19), we have $\frac{1}{2}(Y_\varepsilon^N+y_\varepsilon) \geqslant A_\varepsilon^N$. Thus we can show that 0 and $\hat{E}$ are respectively, discrete lower and upper solutions of (3.3.27), which can then be shown to be, in turn, a discrete upper solution of (3.3.26). We construct a discrete lower solution in an analogous manner to complete the proof. The global bound follows as in [22, pg. 381]. □

Remark: The analysis throughout §3.3 can be easily extended to the following problem class on the unit interval $\Omega=(0,1)$. Find y_ε such that

$$(\varepsilon y_\varepsilon''+(F(y_\varepsilon))')(x)=G(x,y_\varepsilon(x)), \qquad x\in\Omega, \qquad y_\varepsilon(0)=0, \quad y_\varepsilon(1)=B>0,$$

where G satisfies $|G(x,y)|\leqslant C$, $0\leqslant x\leqslant 1$, $y\in\mathbb{R}$; and

$$\left|\frac{\partial^{i+j}G}{\partial x^i\partial y^j}(x,y)\right|\leqslant C, \quad 1\leqslant i+j\leqslant 2; \quad G_y(x,y)\geqslant 0, \quad F'(y)=f(y)\geqslant \alpha y, \quad \alpha>0$$

$$\text{for all} \quad 0\leqslant x\leqslant 1,\ |y|\leqslant 2(B+\frac{1}{\alpha}\sqrt{\|G\|}).$$

Define the parameter ζ as

$$G_y(x,y)\leqslant\zeta, \quad (x,y)\in[0,1]\times[0,B+\frac{2}{\alpha}\sqrt{\|G\|}].$$

The condition (3.3.1a) can now be replaced by

$$B^2-\frac{2}{\alpha}(B\zeta+\max_{x\in\Omega}\{0,G(x,0)\}) \geqslant \gamma_*^2>0. \tag{3.3.29}$$

Under these assumptions, Lemmas 3.3.1 - 3.3.8 all hold with the updated γ_* defined in (3.3.29).

3.4: NUMERICAL EXAMPLES

We can solve for the numerical scheme (($\mathscr{D}_\varepsilon^N$), (3.2.8)) exactly. For the nonlinear problem ($\mathscr{F}_\varepsilon$), in [1], Osher presents a difference scheme with which to approximate the solution of the nonlinear problem

$$\varepsilon y'' - (\tilde{G}(y))' - b(x,y) = 0, \quad x \in (0,1), \quad y(0) = y_0, \quad y(1) = y_1,$$
$$b_y(x,y) \geqslant \beta > 0, \quad \tilde{G} \in C^1(\mathbb{R}), \quad b \in C^1(\mathbb{R}^2).$$

The scheme can be written as follows; find a mesh function Y^N that satisfies

$$\mathcal{N}(Y^N(x_i)) := \frac{2h_i}{(h_{i+1}+h_i)} D^-[\varepsilon D^+ Y^N(x_i) - g(Y^N(x_{i+1}), Y^N(x_i))] - b(x_i, Y^N(x_i)) = 0, \quad (3.4.1a)$$

$$x_i \in \Omega^N, \quad Y^N(0) = A, \quad Y^N(1) = B, \quad \text{on the grid} \quad \Omega^N = \{x_i\}_{i=1}^N, \quad h_i = x_i - x_{i-1}, \quad (3.4.1b)$$

where $g(u,v) \in C^1(\mathbb{R}^2)$ satisfies certain monotonicity conditions. The operator D^- applied to g is defined as

$$D^- g(Y^N(x_{i+1}), Y^N(x_i)) = \quad (3.4.1c)$$
$$D^- \left[\int_0^{Y^N(x_i)} \mathcal{B}(\tilde{G}'(s) \geqslant 0)\tilde{G}'(s)\, ds\right] + (h_{i+1}/h_i) D^+ \left[\int_0^{Y^N(x_i)} \mathcal{B}(\tilde{G}'(s) < 0)\tilde{G}'(s)\, ds\right], \quad (3.4.1d)$$

where $\mathcal{B}$ is a Boolean function such that $\mathcal{B}(I) = 1$ or 0 if the Boolean I is true or false respectively. Osher establishes stablility for implicit and explicit schemes associated with (3.4.1) of the form

$$\text{Implicit:} \quad \mathcal{N}(Y^N(x_i, t_j)) = D_t^- Y^N(x_i, t_j),$$
$$\text{Explicit:} \quad \mathcal{N}(Y^N(x_i, t_j)) = D_t^+ Y^N(x_i, t_j),$$
$$j = 1,2,3,\ldots \quad k = t_j - t_{j-1}, \quad Y^N(x_i, 0) = U^N(x_i), \quad x_i \in \Omega,$$

where U^N is the initial condition and where the CFL condition (Courant-Friedrichs-Lewy condition) is assumed for the explicit scheme, which can be summarised by the following bound

$$\frac{\varepsilon k}{2 \min {h_i}^2} \leqslant C.$$

Note that the CFL condition is a condition required for the convergence of explicit difference schemes. On the Shishkin mesh (3.3.14), the required CFL condition is overly restrictive because we would require

$$\frac{k}{C\varepsilon N^{-2} \ln^2(N)} \leqslant C.$$

To solve the implicit scheme we are required to linearise the nonlinear difference operator $\mathcal{N}$. Osher suggests Newton's method, but owing to the requirement of a sufficiently close initial condition, we linearise the scheme (($\mathscr{F}_\varepsilon^N$), (3.3.14)) based on the expression (3.3.15). To approximate the solution of ($\mathscr{F}_\varepsilon$), we use the following Numerical Scheme

Numerical Scheme 3.1. *Find $Y_\varepsilon^N(x_i,t_j)$ such that*

$$(\varepsilon D_x^+ D_x^- Y_\varepsilon^N + \tilde{F} D_x^+ Y_\varepsilon^N - b Y_\varepsilon^N)(x_i,t_j) = (q + D_t^- Y_\varepsilon^N)(x_i,t_j),$$
$$\tilde{F}(x_i,t_{j-1}) := \left(\int_0^1 f(t\, Y_\varepsilon^N(x_{i+1},t_{j-1}) + (1-t) Y_\varepsilon^N(x_i,t_{j-1}))\, dt\right)$$
$$x_i \in \Omega_\varepsilon^N, \quad t_0 = 0, \quad k_j := t_j - t_{j-1}, \quad j = 1,2,3,\ldots$$
$$Y_\varepsilon^N(x_i,0) = \textit{some positive initial condition}, \quad x_i \in \Omega_\varepsilon^N,$$
$$Y_\varepsilon^N(0,t_j) = 0, \quad Y_\varepsilon^N(1,t_j) = B, \quad t_j \geqslant 0,$$

where $b(x_i,t_j) = b(x_i)$ and $q(x_i,t_j) = q(x_i)$ where b and q are as in ($\mathscr{F}_\varepsilon$) and Ω_ε^N is the mesh described in (3.3.14).

The number of iterations that we compute could be decided by the traditional method where by we compute $Y_\varepsilon^N(x_i,t_1)$, $Y_\varepsilon^N(x_i,t_2)$, $Y_\varepsilon^N(x_i,t_3)$, ... until the first time an integer J is observed satisfying

$$\max_{x_i \in \overline{\Omega}_\varepsilon^N} |Y_\varepsilon^N(x_i,t_J) - Y_\varepsilon^N(x_i,t_{J-1})| \leqslant tol, \tag{3.4.2}$$

where tol is some prescribed tolerance. We would then take $Y_\varepsilon^N(x_i,t_J)$ as the approximation to the solution of ($\mathscr{F}_\varepsilon$). However, we will choose to implement a time step manipulation routine as outlined in [7, pg. 196] which is inspired by the wish for the Numerical Scheme 3.1 to reach a steady state. The routine is outlined as follows.

Algorithm 3.1.

#1: Suppose the initial time step is $k_1 = k^*$. At time t_{j_1}, compute $Y_\varepsilon^N(x_i,t_{j_1+1})$, $Y_\varepsilon^N(x_i,t_{j_1+2})$, $Y_\varepsilon^N(x_i,t_{j_1+3})$, ... using the time step $k_j = k_{j_1}$. At each iteration, calculate

$$d(j) = \max_{x_i \in \overline{\Omega}_\varepsilon^N} |D_t^- Y_\varepsilon^N(x_i,t_j)| = \frac{1}{k_j} \max_{x_i \in \overline{\Omega}_\varepsilon^N} |Y_\varepsilon^N(x_i,t_j) - Y_\varepsilon^N(x_i,t_{j-1})|.$$

#2: Continue computing the iterates until one of the following occurs:

a) There is a first instance where an integer $J \leqslant 90$ is observed such that

$$d(J) \leqslant tol. \tag{3.4.3}$$

In this case, take $Y_\varepsilon^N(x_i,t_J)$ as the approximation to the solution of ($\mathscr{F}_\varepsilon$).

b) There is a first instance where an integer $J_{temp} < 90$ is observed such that

$$d(J_{temp}) > d(J_{temp} - 1).$$

In such a case, we recompute $Y_\varepsilon^N(x_i,t_j)$ for $j = J_{temp}$ repeatedly, using the time step $k_{J_{temp}}^n = 2^{-n} k_{J_{temp}}$ on the n-th re-computation, until the first re-computation such that

$$d(J_{temp}) \leqslant d(J_{temp} - 1),$$

say after the r-th re-computation. Record $Y_\varepsilon^N(x_i,t_j) = Y_\varepsilon^N(x_i,t_{J_{temp}})$ for $j = J_{temp}$ and return to step #1 with $t_{j_1} = t_{J_{temp}}$ and $k_{j_1} = k^r_{J_{temp}}$.

c) *You have computed $Y_\varepsilon^N(x_i,t_{90})$. In such a case, discard all the computed iterates and return to step #1 with $t_{j_1} = t_1$ and redefine $k_1 = \frac{1}{2}k^*$.*

In the next two examples, we compute numerical approximations U_ε^N of $(\mathscr{D}_\varepsilon)$ and $(\mathscr{F}_\varepsilon)$ using the Numerical Scheme $((\mathscr{D}_\varepsilon^N)$, (3.2.8)) and the Numerical Scheme 3.1 with Algorithm 3.1 respectively. We will present tables displaying the computed rates of convergence R_ε^N and R^N defined by

$$D_\varepsilon^N := \max_{x_i\in\overline{\Omega}_\varepsilon^N} |(U_\varepsilon^N - \overline{U}_\varepsilon^{2N})(x_i)|, \quad D^N := \max_\varepsilon D_\varepsilon^N, \tag{3.4.4a}$$

$$R_\varepsilon^N := \log_2 \frac{D_\varepsilon^N}{D_\varepsilon^{2N}} \quad \text{and} \quad R^N := \log_2 \frac{D^N}{D^{2N}}. \tag{3.4.4b}$$

where $\overline{U}_\varepsilon^{2N}$ is the interpolation of U_ε^{2N}, the numerical solution using $2N$ mesh intervals.

Experimentally, we found that Algorithm 3.1's success and execution time is sensitive to the given initial guess, much more so than when using the traditional method (3.4.2). To construct Table 3.2, we use the following initial conditions to compute the numerical approximation U_ε^N:

$$\text{if} \quad \varepsilon = 1, \quad \text{then use } g \text{ as defined in (3.3.6b) as the initial condition;} \tag{3.4.5a}$$

$$\text{if} \quad \varepsilon \leqslant \tfrac{1}{2}, \quad \text{then use } U_{2\varepsilon}^N \text{ as the initial condition.} \tag{3.4.5b}$$

We use a tolerance of 10^{-10}.

Example 3.1 (**Linear Case**)
In this example we consider a linear problem from the class $(\mathscr{D}_\varepsilon)$ with

$$a_\varepsilon(x) = 2\tanh(4x/\varepsilon), \quad b(x) = 1-\cos(3x), \quad q(x) = \tfrac{1}{2} - x \quad \text{and} \quad A = B = 1. \tag{3.4.6}$$

It can be easily shown that $2\tanh(\frac{4}{\varepsilon}x) \geqslant 2(1-e^{-4x/\varepsilon})$. Thus, in (3.2.8), we take $\sigma = \min\{\frac{1}{2}, \varepsilon \ln N\}$. Table 3.1 displays the computed rates of convergence R_ε^N and the uniform rates of convergence R^N. The computed rates are in line with the theoretical rates of convergence established in Lemma 3.2.4.

	$\mathbf{R}_{\varepsilon}^{\mathbf{N}}$					
ε	**N=32**	**N=64**	**N=128**	**N=256**	**N=512**	**N=1024**
$\mathbf{2^0}$	0.97	0.98	0.99	1.00	1.00	1.00
$\mathbf{2^{-1}}$	0.94	0.97	0.98	0.99	1.00	1.00
$\mathbf{2^{-2}}$	0.89	0.94	0.97	0.99	0.99	1.00
$\mathbf{2^{-3}}$	0.50	0.89	0.94	0.97	0.98	0.99
$\mathbf{2^{-4}}$	0.69	0.70	0.77	0.80	0.84	0.80
$\mathbf{2^{-5}}$	0.68	0.71	0.77	0.80	0.84	0.86
$\mathbf{2^{-6}}$	0.68	0.71	0.77	0.80	0.84	0.86
$\mathbf{2^{-7}}$	0.68	0.72	0.77	0.80	0.84	0.85
$\mathbf{2^{-8}}$	0.68	0.72	0.77	0.80	0.84	0.85
.	.	.	.	.	.	.
.	.	.	.	.	.	.
$\mathbf{2^{-20}}$	0.68	0.72	0.77	0.80	0.84	0.85
$\mathbf{R^N}$	0.68	0.72	0.77	0.80	0.84	0.85

Table 3.1: Computed rates of convergence R_{ε}^{N} and R^{N} (as defined in (3.4.4)), measured from the numerical solutions of ($\mathscr{D}_{\varepsilon}$) with the problem data (3.4.6), solved exactly using the numerical method (($\mathscr{D}_{\varepsilon}^{N}$), (3.2.8)).

Example 3.2 (**Nonlinear Case**)

In this example we consider a nonlinear problem from the class ($\mathscr{F}_{\varepsilon}$). We consider this problem with

$$F(y)=y^2-\tfrac{1}{10}\cos(5y^2),\ \ b(x)=\tfrac{1}{4}(1+\sin(x)),\ \ q(x)=\tfrac{1}{2}\cos(3x),\ \ A=0,\ \ B=2.1,\ \ \gamma=1. \quad (3.4.7)$$

For such an F, we have

$$F'(y)=f(y)=2y+y\sin(5y^2)\geqslant y,$$

and we can easily compute the term $\tilde{F}$ in the Numerical Scheme 3.1. We generate numerical approximations using the Numerical Scheme 3.1 with the time step Algorithm 3.1 using a tolerance of 10^{-8}. Table 3.2 displays the computed rates of convergence R_{ε}^{N} and the uniform rates of convergence R^{N}. The computed rates are again in line with the theoretical rates of convergence given in Lemma 3.3.8.

	$\mathbf{R}_{\varepsilon}^{\mathbf{N}}$					
ε \ **N**	**64**	**128**	**256**	**512**	**1024**	**2048**
$\mathbf{2^{-0}}$	0.98	0.99	0.99	1.00	1.00	1.00
$\mathbf{2^{-1}}$	0.97	0.99	0.99	1.00	1.00	1.00
$\mathbf{2^{-2}}$	0.96	0.98	0.99	0.99	1.00	1.00
$\mathbf{2^{-3}}$	0.95	0.96	0.98	0.99	0.99	1.00
$\mathbf{2^{-4}}$	1.02	0.94	0.96	0.98	0.99	1.00
$\mathbf{2^{-5}}$	0.79	0.73	0.74	0.80	0.77	0.84
$\mathbf{2^{-6}}$	0.78	0.79	0.70	0.79	0.83	0.85
$\mathbf{2^{-7}}$	0.77	0.72	0.75	0.80	0.83	1.94
$\mathbf{2^{-8}}$	0.77	0.72	0.75	0.80	0.83	0.85
$\mathbf{2^{-9}}$	0.77	0.72	0.75	0.80	0.83	0.85
$\mathbf{2^{-10}}$	0.76	0.72	0.75	0.80	0.83	0.85
.	.	.	.	.	.	.
.	.	.	.	.	.	.
$\mathbf{2^{-20}}$	0.76	0.72	0.75	0.80	0.83	0.85
$\mathbf{R^N}$	**1.01**	**0.72**	**0.75**	**0.80**	**0.79**	**0.84**

Table 3.2: Computed rates of convergence R_{ε}^{N} and R^{N} (as defined in (3.4.4)), measured from the numerical solutions of ($\mathscr{F}_{\varepsilon}$) with the problem data (3.4.7), approximated using the Numerical Scheme 3.1 (with Algorithm 3.1 and (3.4.5)).

CHAPTER: 4

NONLINEAR INTERIOR LAYER PROBLEM

4.1: INTRODUCTION

In this chapter, we examine nonlinear singularly perturbed problems of the form

$$(\varepsilon u'' - u u' - b u)(x) = 0, \quad b(x) \geqslant 0, \quad x \in (0,1), \quad u(0) > 0 > u(1). \tag{4.1.1}$$

We will show that solutions to (4.1.1) can exhibit an interior layer centred around a unique point $d_\varepsilon \in (0,1)$. However, the exact location of this point d_ε is not explicitly determined and we construct a finite difference scheme based on an approximate location of the point given in [12].

In [31], Shishkin examines a problem class containing (4.1.1). A numerical scheme is constructed that uses a classical approach when $\varepsilon \geqslant CN^{-2/5}$. When $\varepsilon \leqslant CN^{-2/5}$, Shishkin derives an approximation d^* to d_ε and considers left and right boundary turning point problems on $(0, d^*)$ and $(d^*, 1)$ respectively to approximate the global solution u of (4.1.1). Numerical approximations to the solutions of these left and right problems are generated and used to construct a global approximation U^N for (4.1.1). The error bounds presented in the paper can be described as follows:

$$\|U^N - u\| \leqslant CN^{-1/5}, \quad \text{in a neighbourhood outside } d^*, \tag{4.1.2a}$$

$$\|U^N - \tilde{u}\| \leqslant CN^{-1/5}, \quad \text{in a neighbourhood around } d^*, \tag{4.1.2b}$$

where $\tilde{u}(t) = u(t + (d_\varepsilon - d^*))$ is a transformation of u. However, since d_ε remains unknown, this is a theoretical transformation. In [32], Shishkin uses the same basis to examine the time dependent problem corresponding to (4.1.1). However, the algorithm is considerably more intricate mainly due to the fact that the location of the internal layer needs to be accurately determined at all time levels. In Chapter 6, we experiment with this algorithm and describe the algorithm in [31] for the steady state problem (4.1.1). Below we confine our discussion to the

steady-state problem (4.1.1).

In §4.4, we present numerical results for a monotone scheme on a piecewise-uniform Shishkin mesh which suggest that this method is essentially first order convergent when applied to (4.1.1). However we do not provide any numerical analysis for this scheme in this chapter.

4.2: Continuous Problem

Consider the following problem class: Find y_ε such that

$$\begin{aligned}(\varepsilon y_\varepsilon'' - (F(y_\varepsilon))' - b y_\varepsilon)(x) = q(x), \quad x \in \Omega := (0,1), \quad y_\varepsilon(0) = A > 0, \quad y_\varepsilon(1) = B < 0,\\ b, q \in C^2[0,1], \quad b(x) \geqslant 0, \quad x \in \overline{\Omega}, \quad F \in C^3[-2(|B| + \sqrt{\|q\|}),\ 2(A + \sqrt{\|q\|})].\end{aligned} \tag{$\mathcal{G}_\varepsilon$}$$

We consider this problem for the boundary conditions A, B and the function F satisfying

$$A^2 - 2(A\|b\| + \max_{x\in[0,1]}\{0, q(x)\}) > \gamma_L^2, \quad \gamma_L > 0, \tag{4.2.1a}$$

$$|B|^2 - 2(|B|\|b\| + |\min_{x\in[0,1]}\{0, q(x)\}|) > \gamma_R^2, \quad \gamma_R > 0, \tag{4.2.1b}$$

$$F'(s) =: f(s), \quad f(s) > 0,\ s > 0, \quad f(0) = 0, \quad f(s) < 0,\ s < 0, \tag{4.2.1c}$$

$$|f(s)| \geqslant |s|, \quad \forall\ s \in [-2(|B| + \sqrt{\|q\|}),\ 2(A + \sqrt{\|q\|})]. \tag{4.2.1d}$$

We place an additional restriction on f below in (4.2.6) so that the solution to ($\mathcal{G}_\varepsilon$) exhibits an interior layer. Since the problem ($\mathcal{G}_\varepsilon$) is contained within the problem class ((3.3.2), pg. 70), the definition's of upper and lower solutions and Nagumo's condition hold as in (Def$^{n}_{=}$ 3.3.1, pg. 70). Hence it suffices to construct upper and lower solutions to establish the existence of a solution to ($\mathcal{G}_\varepsilon$) (see Lemma 3.3.1, pg. 71).

Lemma 4.2.1. *Assuming (4.2.1), there exists a unique solution $y_\varepsilon \in C^2[0,1]$ of the problem ($\mathcal{G}_\varepsilon$) satisfying*

$$B - 2\sqrt{\|q\|} \leqslant y_\varepsilon(x) \leqslant A + 2\sqrt{\|q\|}, \quad x \in \overline{\Omega}. \tag{4.2.2}$$

Proof. Consider the function $\underline{y}(x) = B - \sqrt{\|q\|}(2 - x)$. Clearly $\underline{y} < 0$ and $\underline{y}' \geqslant 0$. Using (4.2.1), we have

$$\varepsilon \underline{y}'' - f(\underline{y})\underline{y}' - b\underline{y} - q \geqslant -\underline{y}\,\underline{y}' - \|q\| \geqslant (|B| + \sqrt{\|q\|})\sqrt{\|q\|} - \|q\| \geqslant 0.$$

Thus, $\underline{y}$ is a lower solution of ($\mathcal{G}_\varepsilon$). We can similarly establish that the function $\overline{y}(x) = A + \sqrt{\|q\|}(1+x)$ is an upper solution of ($\mathcal{G}_\varepsilon$). Establish uniqueness in the same manner as in Lemma 3.3.2 to complete the proof. □

From ($\mathcal{G}_\varepsilon$), the left and right reduced solutions, r_L and r_R respectively, satisfy

$$(F(r_{L\backslash R}))'(x) + b\, r_{L\backslash R}(x) = -q(x), \quad r_L(0) = A, \quad r_R(1) = B. \tag{4.2.3}$$

The following Lemma establishes that both reduced solutions are bounded away from zero.

Lemma 4.2.2. *Assuming (4.2.1), the reduced solutions of* ($\mathscr{G}_\varepsilon$) *defined by* (4.2.3) *uniquely exist and satisfy*

$$0<\gamma_L<r_L(x)\leqslant A+2\sqrt{\|q\|},\qquad 0>-\gamma_R>r_R(x)\geqslant B-2\sqrt{\|q\|},\qquad x\in\overline{\Omega}. \tag{4.2.4}$$

Proof. Recall the definition of upper and lower solutions for initial value problems in (§2.2.1.2, pg. 15). Note, that using a suitable transform, we can easily extend the definition to the case of terminal value problems. We can easily establish that $\overline{r}(x)=A+\sqrt{\|q\|}(1+x)$ is an upper solution for ((4.2.3); r_L). Consider the function

$$\underline{r}(x)=\sqrt{A^2-2(A\|b\|+\max\{0,q(x)\})x},$$

which, by noting (4.2.1), is strictly positive. We find that

$$\underline{r}\,\underline{r}'=-(A\|b\|+\max\{0,q(x)\})<0.$$

Thus we can show that

$$f(\underline{r})\underline{r}'+b\underline{r}+q\leqslant\underline{r}\,\underline{r}'+\|b\|A+\max\{0,q(x)\}\leqslant 0.$$

Hence, from (4.2.1), we have $r_L>\gamma_L>0$. In the same manner, we can show that the functions

$$\underline{r}(x)=B-\sqrt{\|q\|}(2-x)\quad\text{and}\quad\overline{r}(x)=\sqrt{|B|^2-2(|B|\|b\|+|\min\{0,q(x)\}|)(1-x)}$$

are lower and upper solutions of ((4.2.3); r_R) respectively. We can establish uniqueness in the usual manner. □

From the analysis in [12], Howes presents sufficient conditions for the occurrence of an interior layer in the solution of ($\mathscr{G}_\varepsilon$) are: if

$$r_L(x)>0,\quad\text{for}\quad x\in[0,x_L],\quad 0<x_L<1, \tag{4.2.5a}$$

$$r_R(x)<0,\quad\text{for}\quad x\in[x_R,1],\quad 0<x_R<1, \tag{4.2.5b}$$

$$x_R<x_L,\quad\text{and}\quad J(x):=\int_{r_R(x)}^{r_L(x)}f(s)\,ds\ \text{has a zero at}\ x^*\in[x_R,x_L], \tag{4.2.5c}$$

then an ε-width interior layer occurs around the point x^*. In our case, from (4.2.4), we have $x_L\equiv 1$ and $x_R\equiv 0$. At this point, we place an additional restriction on f as follows; for f in (($\mathscr{G}_\varepsilon$), (4.2.1)), assume there exists x^* satisfying

$$\exists\ x^*\in(0,1)\quad\text{such that}\quad\int_{r_R(x^*)}^{r_L(x^*)}f(s)\,ds=0. \tag{4.2.6}$$

Note that we refer to x^* as Howes' point.

4.2.1 Split the problem into left and right problems

From Lemma 4.2.1, we have $y_\varepsilon \in C^2[0,1]$, hence there is a smallest point $d_\varepsilon \in (0,1)$ s.t.

$$y_\varepsilon(d_\varepsilon) = 0. \tag{4.2.7}$$

We split the problem $(\mathscr{G}_\varepsilon)$ into left and right problems defined either side of d_ε as follows

$$y_\varepsilon(x) = y_L(x), \;\; x \leqslant d_\varepsilon; \qquad y_\varepsilon(x) = y_R(x), \;\; x \geqslant d_\varepsilon;$$

$$(\varepsilon y_L'' - f(y_L)y_L' - by_L)(x) = q(x), \quad x \in (0, d_\varepsilon), \quad y_L(0) = A, \quad y_L(d_\varepsilon) = 0, \tag{$\mathscr{G}_L$}$$

$$(\varepsilon y_R'' - f(y_R)y_R' - by_R)(x) = q(x), \quad x \in (d_\varepsilon, 1), \quad y_R(d_\varepsilon) = 0, \quad y_R(1) = B. \tag{$\mathscr{G}_R$}$$

These are boundary value problems from the problem class $(\mathscr{F}_\varepsilon)$ examined in §3.3.1, Chapter 3, pg. 70. Using those results under the assumptions (4.2.1), we can find that the solutions to $(\mathscr{G}_L)$ and $(\mathscr{G}_R)$, y_L and y_R respectively, uniquely exist and satisfy

$$0 \leqslant \gamma_L(1 - e^{-(\gamma_L/2)(d_\varepsilon - x)/\varepsilon}) \leqslant y_L(x) \leqslant A + 2\sqrt{\|q\|}, \quad x \in [0, d_\varepsilon], \tag{4.2.8a}$$

$$B - 2\sqrt{\|q\|} \leqslant y_R(x) \leqslant -\gamma_R(1 - e^{-(\gamma_R/2)(x - d_\varepsilon)/\varepsilon}) \leqslant 0, \quad x \in [d_\varepsilon, 1]. \tag{4.2.8b}$$

Hence

$$y_\varepsilon(x) \equiv y_L(x), \quad x \in [0, d_\varepsilon] \quad \text{and} \quad y_\varepsilon(x) \equiv y_R(x), \quad x \in [d_\varepsilon, 1].$$

Note the implication that d_ε is the only zero of y_ε in $[0,1]$. We decompose each $y_{L\backslash R}$ into a regular component $v_{L\backslash R}$ and a layer component $w_{L\backslash R}$. The regular components satisfy

$$(\varepsilon v_{L\backslash R}'' - f(v_{L\backslash R})v_{L\backslash R}' - bv_{L\backslash R})(x) = q(x), \quad x \in (0, d_\varepsilon)\backslash(d_\varepsilon, 1), \tag{4.2.9a}$$

$$v_L(0) = A, \quad v_L(d_\varepsilon) = v_L^*, \quad v_R(d_\varepsilon) = v_R^*, \quad v_R(1) = B, \tag{4.2.9b}$$

where v_L^* and v_R^* are chose appropriately so that we may bound the derivatives of $v_{L\backslash R}$ uniformly. The layer components are defined as the solutions of the problems

$$(\varepsilon w_{L\backslash R}'' - f(y_{L\backslash R})w_{L\backslash R}' + \left(v_{L\backslash R}' \textstyle\int_0^1 f'(v_{L\backslash R} + t\, w_{L\backslash R})\, dt - b\right) w_{L\backslash R})(x) = 0 \;, \tag{4.2.10a}$$

$$x \in (0, d_\varepsilon)\backslash(d_\varepsilon, 1), \tag{4.2.10b}$$

$$w_L(0) = 0, \quad w_L(d_\varepsilon) = -v_L(d_\varepsilon), \quad w_R(d_\varepsilon) = -v_R(d_\varepsilon), \quad , w_R(1) = 0. \tag{4.2.10c}$$

Lemma 4.2.3. *Assuming (4.2.1), for $k = 0,1,2,3$ the solutions v_L, w_L, v_R and w_R of (4.2.9)-(4.2.10), uniquely exist and satisfy the bounds*

$$\|v_L^{(k)}\| \leqslant C(1 + \varepsilon^{2-k}), \quad |w_L^{(k)}(x)| \leqslant C\varepsilon^{-k} e^{-(\gamma_L/2)(d_\varepsilon - x)/\varepsilon}, \quad x \in (0, d_\varepsilon),$$
$$\|v_R^{(k)}\| \leqslant C(1 + \varepsilon^{2-k}), \quad |w_R^{(k)}(x)| \leqslant C\varepsilon^{-k} e^{-(\gamma_R/2)(x - d_\varepsilon)/\varepsilon}, \quad x \in (d_\varepsilon, 1).$$

Proof. Using (4.2.1), we can proof this Lemma in the same manner as Lemma 3.3.3 in Chapter 3, pg. 72. □

Note that the location of the point d_ε has not been determined.

4.2.2 Alternative Problem

We now consider an alternative problem to simulate an interior layer at a known point p^*, close to d_ε; Find z_ε such that

$$z_\varepsilon(x) := z_L(x), \quad x \leqslant p^*; \qquad z_\varepsilon(x) := z_R(x), \quad x \geqslant p^*;$$

$$(\varepsilon z_L'' - f(z_L)z_L' - bz_L)(x) = 0, \quad x \in (0, p^*), \quad z_L(0) = A, \quad z_L(p^*) = 0, \tag{$\mathscr{H}_L$}$$

$$(\varepsilon z_R'' - f(z_R)z_R' - bz_R)(x) = 0, \quad x \in (p^*, 1), \quad z_R(p^*) = 0,\ z_R(1) = B. \tag{$\mathscr{H}_R$}$$

The problems ($\mathscr{H}_L$) and ($\mathscr{H}_R$) are analogues of ($\mathscr{G}_L$) and ($\mathscr{G}_R$). We decompose z_L into a regular component v_L and a layer component ω_L and similarly $z_R = v_R + \omega_R$. Bounds on these components and their derivatives are given in the following lemma.

Lemma 4.2.4. *Assuming (4.2.1), for $k = 1, 2, 3$, if $z_L = v_L + \omega_L$ and $z_R = v_R + \omega_R$ are the decompositions into a regular and layer component of z_L and z_R respectively then for sufficiently small ε, we have*

$$0 \leqslant \gamma_L(1 - e^{-(\gamma_L/2)(p^* - x)/\varepsilon}) \leqslant z_L(x) \leqslant A + 2\sqrt{\|q\|}, \quad x \in [0, p^*],$$

$$B - 2\sqrt{\|q\|} \leqslant z_R(x) \leqslant -\gamma_R(1 - e^{-(\gamma_R/2)(x - p^*)/\varepsilon}) \leqslant 0, \quad x \in [p^*, 1].$$

$$v_L(x) \geqslant \gamma_L > 0 \quad x \in [0, p^*] \quad \textit{and} \quad v_R(x) \leqslant -\gamma_R < 0 \quad x \in [p^*, 1],$$

$$\|v_L^{(k)}\| \leqslant C(1 + \varepsilon^{2-k}) \quad \textit{and} \quad |\omega_L^{(k)}(x)| \leqslant C\varepsilon^{-k} e^{-(\gamma_L/2)(p^* - x)/\varepsilon}, \quad x \in (0, p^*),$$

$$\|v_R^{(k)}\| \leqslant C(1 + \varepsilon^{2-k}) \quad \textit{and} \quad |\omega_R^{(k)}(x)| \leqslant C\varepsilon^{-k} e^{-(\gamma_R/2)(x - p^*)/\varepsilon}, \quad x \in (p^*, 1).$$

Proof. The first two bounds can be established in the same manner as in Lemma 3.3.2 and the remaining bounds in the same manner as in Lemma 3.3.3. □

We now present a bound on the difference between y_ε and z_ε under the assumption

$$|d_\varepsilon - p^*| \leqslant C\varepsilon. \tag{4.2.11}$$

Lemma 4.2.5. *Assuming (4.2.11), if y_ε is the solution of ($\mathscr{G}_\varepsilon$) and z_ε is the solution of ($\mathscr{H}_L$)-($\mathscr{H}_R$) then*

$$|(y_\varepsilon - z_\varepsilon)(x)| \leqslant \frac{C}{\varepsilon}|d_\varepsilon - p^*|, \quad x \in \overline{\Omega}.$$

Proof. Without loss of generality, assume that $d_\varepsilon \leqslant p^*$. We will examine the difference $\chi_\varepsilon := z_\varepsilon - y_\varepsilon$ over the intervals $[0, d_\varepsilon]$, $[d_\varepsilon, p^*]$ and $[p^*, 1]$ separately. On each interval, using ($\mathscr{G}_\varepsilon$) and ($\mathscr{H}_L$)-($\mathscr{H}_R$), we can show that χ_ε satisfies

$$(\varepsilon\chi_\varepsilon' - \left(\int_0^1 f(tz_\varepsilon + (1-t)y_\varepsilon)\, dt\right)\chi_\varepsilon)'(x) - b\chi_\varepsilon(x) = 0. \tag{4.2.12}$$

Considering χ_ε over $[0,d_\varepsilon]$ we have $\chi_\varepsilon(0)=0$ and using Lemma 4.2.4 and (4.2.11), we have $\chi_\varepsilon(d_\varepsilon)=z_L(d_\varepsilon)-0>0$ and

$$\chi_\varepsilon(d_\varepsilon)=z_L(d_\varepsilon)=z_L(d_\varepsilon)-z_L(p^*)=\int_{p^*}^{d_\varepsilon} z_L'(t)\,dt\leqslant(p^*-d_\varepsilon)\max_{x\in[d_\varepsilon,p^*]}|z_L'(t)|$$
$$\leqslant C(1+\varepsilon^{-1})(p^*-d_\varepsilon)\max_{x\in[d_\varepsilon,p^*]}|e^{-(\gamma_L/2)(p^*-x)/\varepsilon}|\leqslant C(p^*-d_\varepsilon)\varepsilon^{-1}.$$

Clearly $\underline{\chi}=0$ is a lower solution for (4.2.12) over $(0,d_\varepsilon)$. Consider the function $\overline{\chi}$ that satisfies

$$(\varepsilon\overline{\chi}'-\left(\int_0^1 f(tz_\varepsilon+(1-t)y_\varepsilon)\,dt\right)\overline{\chi})'(x)=0,\quad \overline{\chi}(0)=0,\quad \overline{\chi}(d_\varepsilon)=C\varepsilon^{-1}(p^*-d_\varepsilon).\tag{4.2.13}$$

That means $\overline{\chi}$ satisfies

$$\varepsilon(\overline{\chi}'(x)-\overline{\chi}'(0))-\left(\int_0^1 f(tz_\varepsilon+(1-t)y_\varepsilon)\,dt\right)\overline{\chi}(x)=0,\quad \overline{\chi}(d_\varepsilon)=C\varepsilon^{-1}(p^*-d_\varepsilon).\tag{4.2.14}$$

Using upper and lower solutions with (4.2.14), we can show that $0\leqslant\overline{\chi}\leqslant C\varepsilon^{-1}(p^*-d_\varepsilon)$ and hence we can use (4.2.13) to show that $\overline{\chi}$ is an upper solution of (4.2.12). Hence $0\leqslant\chi_\varepsilon(x)\leqslant C\varepsilon^{-1}(p^*-d_\varepsilon)$ for $x\in[0,d_\varepsilon]$. We can bound $\chi_\varepsilon(p^*)$, and hence χ_ε, equivalently on $[d_\varepsilon,p^*]$ and $[p^*,d_\varepsilon]$ to complete the proof. Note that the case where $d_\varepsilon>p^*$ mirrors the above. □

4.3: The Discrete Problem and Error Analysis

To numerically approximate the solution of $(\mathscr{G}_\varepsilon)$ we consider the following discretisation of $(\mathscr{H}_L)$, $(\mathscr{H}_R)$: Find Z_ε^N such that

$$Z_\varepsilon^N(x_i) := Z_L^N(x_i),\ i \le \tfrac{N}{2}; \qquad Z_\varepsilon^N(x_i) := Z_R^N(x_i),\ i > \tfrac{N}{2};$$

$$D^+[\varepsilon D^- Z_L^N - F(Z_L^N)] - bZ_L^N(x_i) = 0, \quad 0 < x_i < x_{\frac{N}{2}}, \quad Z_L^N(0) = A, \quad Z_L^N(p^*) = 0, \qquad (\mathscr{H}_L^N)$$

$$D^-[\varepsilon D^+ Z_R^N - F(Z_R^N)] - bZ_R^N(x_i) = 0, \quad x_{\frac{N}{2}} < x_i < 1, \quad Z_R^N(p^*) = 0, \quad Z_R^N(1) = B. \qquad (\mathscr{H}_R^N)$$

on a piecewise-uniform mesh Ω_ε^N. Motivated by Lemma 4.2.4, the mesh Ω_ε^N is defined as

$$x_i \in \Omega_\varepsilon^N : x_i = \left\{ \begin{array}{cc} \frac{4(p^*-\sigma_0)}{N} i, & 0 \leqslant i \leqslant \frac{N}{4}, \\ p^* - \sigma_0 + \frac{4\sigma_0}{N}(i - \frac{N}{4}), & \frac{N}{4} < i \leqslant \frac{N}{2}, \\ p^* + \frac{4\sigma_1}{N}(i - \frac{N}{2}), & \frac{N}{2} < i \leqslant \frac{3N}{4}, \\ p^* + \sigma_1 + \frac{4(1-p^*-\sigma_1)}{N}(i - \frac{3N}{4}), & \frac{3N}{4} < i \leqslant N, \end{array} \right\} \tag{4.3.1a}$$

$$\sigma_j := \min\left\{ \frac{p^* + (1-2p^*)j}{2}, \frac{2\varepsilon}{\gamma_j} \ln N \right\}, \quad \gamma_0 = \gamma_L, \quad \gamma_1 = \gamma_R, \quad j = 0, 1. \tag{4.3.1b}$$

Again, the problems $(\mathscr{H}_L)$, $(\mathscr{H}_R)$ and $(\mathscr{H}_L^N)$, $(\mathscr{H}_R^N)$ are from the class of problems studied in §3.3.2 of Chapter 3 and the next Lemma follows.

Lemma 4.3.1. *Assuming (4.2.4), if z_ε is the solution of $(\mathscr{H}_L)$, $(\mathscr{H}_R)$ and Z_ε^N is the solution of $(\mathscr{H}_L^N)$, $(\mathscr{H}_R^N)$ then*

$$|(Z_\varepsilon^N - z_\varepsilon)(x_i)| \leqslant CN^{-1} \ln N, \quad x_i \in \Omega_\varepsilon^N.$$

Finally, we can establish a bound on $y_\varepsilon - Z_\varepsilon^N$ in the following Lemma.

Lemma 4.3.2. *Assuming (4.2.4), if y_ε is the solution of $(\mathscr{G}_\varepsilon)$ and Z_ε^N is the solution of $(\mathscr{H}_L^N)$, $(\mathscr{H}_R^N)$ then*

$$|(y_\varepsilon - Z_\varepsilon^N)(x_i)| \leqslant \frac{C}{\varepsilon} |d_\varepsilon - p^*| + CN^{-1} \ln N, \quad x_i \in \Omega_\varepsilon^N.$$

Proof. Combine lemmas 4.2.5 and 4.3.1. □

Observe that if the point p^* was within $O(\varepsilon)$ of the point d_ε, then Lemma 4.3.2 would not suffice to guarantee convergence.

4.4: Numerical Example

The numerical algorithm described in §4.3 solves two boundary turning point problems joined together at p^*. The algorithm involves a nonlinear finite difference operator and a Shishkin mesh centred about an unspecified point p^*. In this final section, we present an algorithm which linearises this discrete problem using a continuation method and $q := x^*$ with x^* as in (4.2.6). At each new time level in the continuation method, we do not determine where the discrete approximation $\bar{Y}(x_i, t_k) = 0$. Hence, we employ a scheme, motivated by the discussion in §3.4, pg. 80.

In this example we consider a problem from the class $(\mathscr{G}_\varepsilon)$ as follows

$$(\varepsilon u'' - u u' - b u)(x) = 0, \;\; x \in (0,1), \quad u(0) = A = 2.1, \;\; u(1) = B = -2.15, \quad b(x) \equiv 1/4. \tag{4.4.1a}$$

We choose $\gamma_{L\backslash R}$ in (4.2.1) with the values

$$\gamma_L = 1.8, \quad \gamma_R = 1.75. \tag{4.4.1b}$$

In such a case, we find that the reduced solutions defined in (4.2.3) can be solved exactly as

$$r_L(x) = A - bx > 0, \quad r_R(x) = B + b(1-x) < 0. \tag{4.4.1c}$$

Hence, we can solve the integral in (4.2.6) exactly as

$$\int_{r_R(x^*)}^{r_L(x^*)} f(s)\, ds = \frac{1}{2}(r_L + r_R)(r_L - r_R)(x^*) = 0 \Leftrightarrow r_L(x^*) = r_R(x^*) \Leftrightarrow x^* = \frac{1}{2b}(A + B + b) = 0.4. \tag{4.4.1d}$$

We numerical approximate the solution of (4.4.1) with the following numerical scheme.

Numerical Scheme 4.1. *Find $Y_\varepsilon^N(x_i, t_j)$ such that*

$$(\varepsilon D_x^- D_x^+ Y_\varepsilon^N - \frac{\alpha}{2} Y_\varepsilon^{N,-} D_x^- Y_\varepsilon^N - b\, Y_\varepsilon^N)(x_i, t_j) = D_t^- Y_\varepsilon^N(x_i, t_j), \quad \textit{if} \quad Y_\varepsilon^N(x_i, t_{j-1}) \geqslant 0$$

$$(\varepsilon D_x^+ D_x^- Y_\varepsilon^N - \frac{\alpha}{2} Y_\varepsilon^{N,+} D_x^+ Y_\varepsilon^N - b\, Y_\varepsilon^N)(x_i, t_j) = D_t^- Y_\varepsilon^N(x_i, t_j), \quad \textit{if} \quad Y_\varepsilon^N(x_i, t_{j-1}) \geqslant 0$$

$$Y_\varepsilon^{N,-}(x_i, t_j) = (Y_\varepsilon^N(x_i, t_{j-1}) + Y_\varepsilon^N(x_{i-1}, t_{j-1})), \quad Y_\varepsilon^{N,+}(x_i, t_j) = (Y_\varepsilon^N(x_{i+1}, t_{j-1}) + Y_\varepsilon^N(x_i, t_{j-1})),$$

$$x_i \in \Omega_\varepsilon^N, \quad Y_\varepsilon^N(0, t_j) = A, \quad Y_\varepsilon^N(1, t_j) = B,$$

where Ω_ε^N is the mesh described in (4.3.1) with $p^* = x^*$ (as in 4.4.1d) and $\alpha = 1$.

Note that Ω_ε^N remains fixed with $p^* := x_*$ at all time levels.

As per the discussion in §3.4, we wish to use the time step manipulation routine described in Algorithm 3.1 with the Numerical Scheme 4.1. However, experimentally, we found that this Algorithm's success and execution time is somewhat more sensitive to the given initial guess in the

Numerical Scheme 4.1 that to the initial guess in the Numerical Scheme 3.1. So much so that we found that the routine of generating initial conditions described in (3.4.5) was unsuccessful (that is, we observed Algorithm 3.1 performing an inordinate number of re-computations). To construct Table 4.1, we generate initial conditions as follows:

To generate $Y^N_{\varepsilon,pow}$, the final time iterate of using the Numerical Scheme 4.1 with the Algorithm 3.1 with a prescribed tolerance $tol = 10^{-pow}$, $pow \geqslant 1$, we follow the steps

$$\text{Compute } Y^N_{\varepsilon,pow_j}, \text{ for } pow_j = 0, 1, \dots pow, \text{ where;} \tag{4.4.2a}$$

$$\text{if} \quad pow_j = 1, \quad \text{then use} \tag{4.4.2b}$$

$$g(x_i) := \left\{ \; r_L(x_i) \text{ if } x_i < x^*, \qquad 0 \text{ if } x_i = x^*, \qquad r_R(x_i) \text{ if } x_i > x^* \; \right\} \tag{4.4.2c}$$

$$\text{as the initial condition where } r_L \text{ and } r_R \text{ are as defined in (4.2.4);} \tag{4.4.2d}$$

$$\text{if} \quad 2 \leqslant pow_j \leqslant pow, \quad \text{then use } Y^N_{\varepsilon,pow_j-1} \text{ as the initial condition.} \tag{4.4.2e}$$

We compute numerical approximations U^N_ε using the Numerical Scheme 4.1 using Algorithm 3.1 and (4.4.2) with a tolerance of 10^{-5}. Table 4.1 displays the computed rates of convergence R^N_ε and the uniform rates of convergence R^N defined in 3.4.4. The computed rates are tending to first order for sufficiently small ε.

	$\mathbf{R}_{\varepsilon}^{\mathbf{N}}$						
ε \ **N**	**N=32**	**N=64**	**N=128**	**N=256**	**N=512**	**N=1024**	**N=2048**
$\mathbf{2^{-0}}$	0.43	1.12	1.11	0.91	1.07	0.99	0.99
$\mathbf{2^{-1}}$	-0.79	1.49	0.76	0.78	1.16	0.97	0.98
$\mathbf{2^{-2}}$	2.20	0.34	1.52	1.45	1.28	0.95	0.94
$\mathbf{2^{-3}}$	1.29	1.12	-0.59	0.04	1.06	-0.92	0.18
$\mathbf{2^{-4}}$	0.34	0.95	1.07	1.46	0.97	0.96	0.62
$\mathbf{2^{-5}}$	0.58	0.70	0.76	0.81	1.00	1.29	0.15
$\mathbf{2^{-6}}$	0.58	0.70	0.77	0.80	0.51	1.85	0.71
$\mathbf{2^{-7}}$	0.58	0.70	0.76	0.60	0.92	1.80	0.26
$\mathbf{2^{-8}}$	0.58	0.70	0.76	0.60	0.86	1.62	0.94
$\mathbf{2^{-9}}$	0.58	0.70	0.76	0.60	0.82	1.65	0.94
$\mathbf{2^{-10}}$	0.58	0.70	0.76	0.59	0.82	1.66	0.94
$\mathbf{2^{-11}}$	0.58	0.70	0.76	0.59	0.80	1.67	0.94
.	.	.	.	.	.	.	.
.	.	.	.	.	.	.	.
$\mathbf{2^{-20}}$	0.58	0.70	0.76	0.59	0.80	1.67	0.94
$\mathbf{R^N}$	**0.34**	**0.95**	**0.77**	**0.21**	**1.06**	**-0.92**	**0.18**

Table 4.1: Computed rates of convergence R_{ε}^{N} and R^{N} (as defined in (3.4.4)), measured from the numerical solutions of the Numerical Scheme 4.1 using Algorithm 3.1 and (4.4.2) with the problem data (4.4.1).

CHAPTER: 5

LINEAR INTERIOR LAYER PROBLEM

5.1: INTRODUCTION

Interior layers exhibiting a hyperbolic tangent profile can arise in solutions of singularly perturbed quasilinear problems of the form

$$(\varepsilon u'' - u\,u' - b\,u)(x) = q(x), \quad x \in (0,1), \quad b(x) \geq 0, \quad u(0) > 0, \quad u(1) < 0. \tag{5.1.1}$$

Asymptotic expansions can be used to locate the interior point d_ε, where $u(d_\varepsilon) = 0$, to within an $O(\varepsilon)$ neighbourhood of some known point x^*. That is, $d_\varepsilon \in (x^* - C\varepsilon, x^* + C\varepsilon)$ (see Howes [12]). Note that Howes deals with nonlinear problems like (5.1.1) in non-conservative form. Any future extension of our analysis for the linear problem studied here to the quasilinear problem (5.1.1) could rely on [12, Th$\overset{\text{m}}{=}$ 5.5] to locate the $O(\varepsilon)$ layer region. This is the motivation for studying the problem class ($\mathscr{I}_\varepsilon$) where the differential equation is in non-conservative form.

In this chapter, we examine numerical methods for a class of linear problems associated with the above nonlinear problem. For example, problems of the form

$$\varepsilon y''(x) - 2\tanh\left(\frac{d-x}{2\varepsilon}\right) y'(x) - y(x) = q(x), \quad x \in (0,1), \quad y(0) > 0 > y(1), \quad d \in (0,1), \tag{5.1.2}$$

will be studied. For such a problem, an interior layer forms around the interior point d. A parameter-uniform numerical method, based on an upwind finite difference operator and a piecewise-uniform Shishkin mesh, will be constructed and analysed for these type of problems. We will also consider the effect of centring the piecewise-uniform mesh at some point $d^N \in (d - C\varepsilon \ln N, d + C\varepsilon \ln N)$. The resulting numerical analysis may prove useful in any future examination of the nonlinear problem (5.1.1), where the point p is only known to lie within some interval $(d^* - C\varepsilon, d^* + C\varepsilon)$.

Singularly perturbed turning point problems of the form

$$-\varepsilon y''(x) - a(x)y'(x) + b(x)y(x) = q(x), \quad x \in (0,1), \quad a(d) = 0, \quad d \in (0,1), \quad b > 0,$$

have been studied by several authors (Farrell [6], Berger et al.[4]). In this case, where the convective coefficient a is independent of ε, the nature of any interior layer is different to the problem being considered here. The quantity $b(d)/a'(d)$ determines the existence and character of an interior layer in the vicinity of the point d. Also, the restriction $|a'(x)| \geqslant \frac{1}{2}|a'(d)|$, $x \in (0,1)$ is placed on this problem, whereas in (5.1.2), the convective coefficient $\tilde{a} := 2\tanh(\frac{d-x}{2\varepsilon})$ only satisfies $|\tilde{a}'(x)| \geqslant \frac{1}{2}|\tilde{a}'(d)|$ on an $O(\varepsilon)$-neighbourhood around $x = d$.

Exponential interior layers can be generated by considering linear problems with discontinuous coefficients of the form

$$\varepsilon y''(x) - a(x)y'(x) - b(x)y(x) = q(x), \quad x \in (0,d)\cup(d,1)$$
$$a(x) \geq \alpha > 0,\ x < d, \quad a(x) \leq -\alpha < 0,\ x > d, \quad a(d^+) \neq a(d^-).$$

Interior layers of exponential type form in the vicinity of the point of discontinuity in the coefficient a (Farrell et al. [8]). The numerical analysis associated with such problems relies heavily on the fact that the coefficient a is strictly bounded away from zero in the interval $(0,d)\cup(d,1)$. In §5.4, the interior layer in the solution of a problem with a discontinuous convection coefficient is shown to be different to the interior layer generated from the problem class $(\mathscr{I}_\varepsilon)$ examined below.

In §5.2 we state the class of problems examined in this chapter and derive a priori bounds on the derivatives of the solutions. In §5.3, we construct and analyse a set of numerical methods for this class of problems. The numerical methods consist of an upwind finite difference operator on piecewise uniform meshes, which are fine in the vicinity of the interior layer. In the final section, some numerical results are presented to illustrate the theoretical error bounds.

5.2: Continuous Problem

Consider the following problem class on $\Omega = (0,1)$. Find $y_\varepsilon \in C^2(\Omega)$ such that

$$\begin{aligned} &\mathcal{L}_\varepsilon y_\varepsilon(x) := (\varepsilon y_\varepsilon'' - a_\varepsilon y_\varepsilon' - b y_\varepsilon)(x) = q(x), \quad x \in \Omega, \quad y_\varepsilon(0) = y_0 > 0,\ y_\varepsilon(1) = y_1 < 0, \\ &a_\varepsilon, b, q \in C^2((0,1)\setminus\{d\}) \cap C^0[0,1], \quad b(x) \geqslant 0,\ x \in \overline{\Omega}, \\ &a_\varepsilon(x) > 0 \text{ for } x \in [0,d), \quad a_\varepsilon(d) = 0, \quad a_\varepsilon(x) < 0 \text{ for } x \in (d,1]. \end{aligned} \tag{$\mathscr{I}_\varepsilon$}$$

We will show that the solution to $(\mathscr{I}_\varepsilon)$ exhibits an interior layer in a neighbourhood of the point d. Additional restrictions on the function a_ε are listed in (5.2.1) below.

Assumptions on the coefficient a_ε in ($\mathscr{I}_\varepsilon$)

Denote $\Omega^- := (0,d)$, $\Omega^+ := (d,1)$ and $\overline{\Omega}^\pm$ as the closures of $\Omega^\pm$. Define the limiting functions a_0^- and a_0^+ as

$$a_0^-(x) := \lim_{\varepsilon\to 0} a_\varepsilon(x),\ x\in[0,d), \quad a_0^+(x) := \lim_{\varepsilon\to 0} a_\varepsilon(x),\ x\in(d,1], \quad a_0^\pm(d) := \lim_{x\to d^\pm} a_0^\pm(x). \tag{5.2.1a}$$

Assume the following conditions on a_ε;

$$|a_\varepsilon(x)| > |\alpha_\varepsilon(x)|, \quad x\neq d, \quad \alpha_\varepsilon(x) := \theta\tanh(r(d-x)/\varepsilon), \quad \theta > 2r > 0, \quad x\in\overline{\Omega}, \tag{5.2.1b}$$

$$\int_0^x \left|a_\varepsilon'(t)\right| dt \leqslant C, \quad x\in\overline{\Omega}, \tag{5.2.1c}$$

$$\varphi_\varepsilon^\pm(x) := (a_0^\pm - a_\varepsilon)(x) \quad \text{satisfies} \quad |\varphi_\varepsilon^\pm(x)| \leqslant |\varphi_\varepsilon^\pm(d)| e^{\pm\frac{\theta}{2\varepsilon}(d-x)}, \quad x\in\overline{\Omega}^\pm. \tag{5.2.1d}$$

Note that (5.2.1b) implies $a_0^-(x)\geqslant\theta$, $x\in\overline{\Omega}^-$ and $a_0^+(x)\leqslant-\theta$, $x\in\overline{\Omega}^+$.

The differential operator $\mathcal{L}_\varepsilon$ defined in problem ($\mathscr{I}_\varepsilon$) satisfies the following minimum principle.

Theorem 5.2.1. *Let $\mathcal{L}_\varepsilon$ be the differential operator defined in ($\mathscr{I}_\varepsilon$) and $z\in C^2(\Omega)\cap C^0(\overline{\Omega})$. If $\min\{z(0),z(1)\}\geqslant 0$ and $\mathcal{L}_\varepsilon z(x)\leqslant 0$ for $x\in\Omega$, then $z(x)\geqslant 0$ for all $x\in\overline{\Omega}$.*

Proof. The proof is by contradiction. Assume that there exist a point $p\in\overline{\Omega}$ such that $z(p)<0$. It follows from the hypotheses that $p\notin\{0,1\}$. Define the auxiliary function $u = z\exp(\frac{1}{2\varepsilon}\int_x^d \alpha_\varepsilon(t)dt)$ and note that $u(p)<0$. Choose $s\in\Omega$ such that $u(s)=\min u(x)<0$. Therefore, from the definition of s, we have $u'(s)=0$ and $u''(s)\geqslant 0$. But then, using $\alpha_\varepsilon^2 > 2\varepsilon\alpha_\varepsilon'$ and noting $\varepsilon\alpha_\varepsilon'(d) = -r\theta < 0$, we have the following contradiction:

$$\mathcal{L}_\varepsilon z(s) = [\varepsilon u'' + \frac{1}{4\varepsilon}(\alpha_\varepsilon(2a_\varepsilon-\alpha_\varepsilon) - 2\varepsilon\alpha_\varepsilon' + 4\varepsilon b)(-u)](s)\exp\left(-\frac{1}{2\varepsilon}\int_x^d \alpha_\varepsilon(t)dt\right) > 0.$$

□

Theorem 5.2.2. *Assuming (5.2.1), there exists a unique solution, y_ε, of ($\mathscr{I}_\varepsilon$) such that*

$$|y_\varepsilon^{(k)}(x)| \leqslant C\varepsilon^{-k}, \quad k=0,1,2, \quad x\in\overline{\Omega}.$$

Proof. Define the two barrier functions

$$\psi^\pm(x) := \frac{\|q\|}{2\theta r}[(x-d)\alpha_\varepsilon(x)+\theta] + \max\{|y_0|,|y_1|\} \pm y_\varepsilon(x),$$

which are nonnegative at $x=0,1$. From (5.2.1) we have

$$\varepsilon\alpha_\varepsilon'' - a_\varepsilon\alpha_\varepsilon' \begin{cases} \geqslant \\ \leqslant \end{cases} \varepsilon\alpha_\varepsilon'' - \alpha_\varepsilon\alpha_\varepsilon' = (\frac{2r}{\theta}-1)\alpha_\varepsilon\alpha_\varepsilon' \begin{cases} \geqslant 0, & x\leqslant d, \\ \leqslant 0, & x\geqslant d, \end{cases}, \tag{5.2.2a}$$

$$2\varepsilon\alpha_\varepsilon' - a_\varepsilon\alpha_\varepsilon \leqslant 2\varepsilon\alpha_\varepsilon' - \alpha_\varepsilon^2 = (\frac{2r}{\theta}-1)\alpha_\varepsilon^2 - 2\theta r \leqslant -2\theta r, \quad x\in\overline{\Omega}. \tag{5.2.2b}$$

Using the definition of the problem ($\mathscr{I}_\varepsilon$) and the inequalities (5.2.2), we can deduce that

$$\mathcal{L}_\varepsilon \psi^\pm \leqslant \frac{\|q\|}{2\theta r}[(x-d)(\varepsilon\alpha_\varepsilon'' - a_\varepsilon\alpha_\varepsilon') + (2\varepsilon\alpha_\varepsilon' - a_\varepsilon\alpha_\varepsilon)] + \|q\| \leqslant 0.$$

Thus a solution to ($\mathscr{I}_\varepsilon$) exists and is unique.

Using (5.2.1c), the derivatives of y_ε can be bounded in the same manner as in [7, Lemma 3.2].

□

We split the problem ($\mathscr{I}_\varepsilon$) into left and right problems around $x = d$ as follows. Define the left and right problems by

$$y_\varepsilon(x) = y_L(x),\ x \leqslant d; \qquad y_\varepsilon(x) = y_R(x),\ x \geqslant d;$$

$$\mathcal{L}_\varepsilon y_L(x) = q(x), \quad x \in \Omega^-, \quad y_L(0) = y_0, \quad y_L(d) = y_\varepsilon(d), \tag{$\mathscr{I}_L$}$$

$$\mathcal{L}_\varepsilon y_R(x) = q(x), \quad x \in \Omega^+ \quad y_R(d) = y_\varepsilon(d), \quad y_R(1) = y_1. \tag{$\mathscr{I}_R$}$$

From §3.2.1 in Chapter 3, we have the existence of a unique y_L and y_R s.t. $\|y_{L\backslash R}^{(k)}\| \leqslant C\varepsilon^{-k}$, $k = 0,1,2$. We decompose each $y_{L\backslash R}$ into the sum of a regular component, $v_{L\backslash R}$, and a layer component, $w_{L\backslash R}$. If a_ε satisfied the bound $a_\varepsilon \geqslant C > 0$ for all $x \in (0,d)$, then, as in [8], we would simply define the left regular component as the solution of $\mathcal{L}_\varepsilon v_L = q$ with suitable boundary conditions and the left layer component as the solution of $\mathcal{L}_\varepsilon w_L = 0$, $w_L(0) = 0$, $w_L(1) = (y_\varepsilon - v_L)(d)$. Since a_ε does not satisfy such a lower bound, we study the problem

$$\mathcal{L}^- v_L(x) := (\varepsilon v_L'' + a_0^- v_L' - b v_L)(x) = q(x),\ x \in \Omega^-,\ v_L(0) = y_0,\ v_L(d) = (v_0 + \varepsilon v_1)(d), \tag{5.2.3a}$$

where $v_L = v_0 + \varepsilon v_1 + \varepsilon^2 v_2$ and the subcomponents v_0, v_1, v_2 satisfy

$$(a_0^- v_0' + b v_0)(x) = -q(x), \quad x \in (0,d], \quad v_0(0) = y_0, \tag{5.2.3b}$$

$$(a_0^- v_1' + b v_1)(x) = v_0''(x), \quad x \in (0,d), \quad v_1(0) = 0; \qquad v_1(d) := \lim_{t \uparrow d} v_1(t), \tag{5.2.3c}$$

$$\mathcal{L}^- v_2(x) = -v_1''(x), \quad x \in \Omega^-, \quad v_2(0) = v_2(d) = 0. \tag{5.2.3d}$$

Note that in problem (5.2.3a), the coefficient a_ε, of the first derivative term, has been replaced by the strictly positive a_0^- defined in (5.2.1). We incorporate the error $(\mathcal{L}_\varepsilon - \mathcal{L}^-)v_L$ into the layer component w_L, which is, noting (5.2.1d), defined as the solution of

$$\mathcal{L}_\varepsilon w_L(x) = \varphi_\varepsilon^- v_L'(x), \quad x \in \Omega^-, \quad w_L(0) = 0, \quad w_L(d) = (y_\varepsilon - v_L)(d). \tag{5.2.3e}$$

Similarly v_R and w_R satisfy

$$\mathcal{L}^+ v_R(x) := (\varepsilon v_R'' + a_0^+ v_R' - b v_R)(x) = q(x), \quad x \in \Omega^+, \quad v_R(d) = v^*, \quad v_R(1) = y_1, \tag{5.2.4a}$$

$$\mathcal{L}_\varepsilon w_R(x) = \varphi_\varepsilon^+ v_R'(x), \quad x \in \Omega^+, \quad w_R(d) = (y_\varepsilon - v_R)(d), \quad w_R(1) = 0, \tag{5.2.4b}$$

where v^* is chosen in an analogous fashion to $v_L(d)$ so that we may bound the derivatives of v_R uniformly. The following Lemma establishes bounds on the regular and layer components.

Lemma 5.2.1. *If v_L and w_L are the solutions of (5.2.3) and v_R and w_R are the solutions of (5.2.4) and θ is given in (5.2.1b) then for $k=0,1,2$, we have the following bounds:*

$$|v_L^{(k)}(x)| \leqslant C(1+\varepsilon^{2-k}) \quad \textit{and} \quad |w_L^{(k)}(x)| \leqslant C\varepsilon^{-k} e^{-(\theta/2)(d-x)/\varepsilon}, \quad x \in \Omega^-,$$
$$|v_R^{(k)}(x)| \leqslant C(1+\varepsilon^{2-k}) \quad \textit{and} \quad |w_R^{(k)}(x)| \leqslant C\varepsilon^{-k} e^{-(\theta/2)(x-d)/\varepsilon}, \quad x \in \Omega^+.$$

Proof. The proof is analogous to the proof of Lemma 3.2.1. For this proof, we establish a required inequality in the following. Note that

$$\int_x^d \alpha_\varepsilon(t)\, dt = \frac{\varepsilon\theta}{r} \ln(\cosh(\tfrac{r}{\varepsilon}(d-x))),$$

thus we can use (5.2.1) and the inequality $\cosh t \geqslant \frac{1}{2}e^t$, $t>0$, to show that

$$e^{-(\theta/2)(d-x)/\varepsilon} \leqslant \exp\left(-\frac{1}{2\varepsilon}\int_x^d \alpha_\varepsilon(t)dt\right) \leqslant 2^{\theta/2r} e^{-(\theta/2)(d-x)/\varepsilon}. \tag{5.2.5}$$

□

5.3: The Discrete Problem and Error Analysis

Given the bounds in Lemma 5.2.1 on the solution y_ε of ($\mathscr{I}_\varepsilon$), (5.2.1)), it is natural to refine the mesh in the vicinity of the point d. We examine such a mesh below. In addition, we consider the effect of centring the mesh at some other point d^N near the point d.

Consider the following finite difference method. Find Y_ε^N such that

$$\mathcal{L}_\varepsilon{}^N Y_\varepsilon^N(x_i) := (\varepsilon\delta^2 - a_\varepsilon D - b)Y_\varepsilon^N(x_i) = q(x_i), \quad x_i \in \Omega_\varepsilon^N, \quad Y_\varepsilon^N(0)=y_0, \quad Y_\varepsilon^N(1)=y_1,$$
$$D := \begin{cases} D^- & \text{if } a_\varepsilon(x_i) \geqslant 0 \\ D^+ & \text{if } a_\varepsilon(x_i) < 0 \end{cases}, \quad \delta^2 Z^N(x_i) := \tfrac{D^+(Z^N(x_i)-Z^N(x_{i-1}))}{(h_{i+1}+h_i)/2}, \quad h_i := x_i - x_{i-1}, \tag{$\mathscr{I}_\varepsilon^N$}$$

where $D^\pm$ are the standard forward and backward finite difference operators. We define the piecewise uniform mesh, Ω_ε^N, with a refined mesh centred at d^N by

$$|d^N - d| < p\sigma, \ \ p \leqslant \tfrac{1}{2}, \quad \mu := \tfrac{1}{2}\min\{d^N, 1-d^N\}, \quad \sigma := \min\{\mu, \tfrac{\varepsilon}{r}\ln N\}, \tag{5.3.1a}$$

$$H_0 := \tfrac{4}{N}(d^N - \sigma), \qquad h := \tfrac{4}{N}\sigma, \qquad H_1 := \tfrac{4}{N}(1-d^N-\sigma), \tag{5.3.1b}$$

$$\overline{\Omega}_\varepsilon^N := \left\{ x_i \;\middle|\; \begin{array}{ll} x_i = H_0 i, & 0 \leqslant i \leqslant \frac{N}{4}, \\ x_i = x_{\frac{N}{4}} + h(i-\frac{N}{4}), & \frac{N}{4} < i \leqslant \frac{3N}{4}, \\ x_i = x_{\frac{3N}{4}} + H_1(i-\frac{3N}{4}), & \frac{3N}{4} < i \leqslant N. \end{array} \right\}, \quad \Omega_\varepsilon^N := \overline{\Omega}_\varepsilon^N \setminus \{x_0, x_N\}. \tag{5.3.1c}$$

Note, if $d^N = d$ then set $p = 0$. If $d^N \neq d$, then the mesh is not aligned to the point d.

To ease notation, we may write any mesh function $Z^N(x_i)$ as Z_i^N.

To prove the existence of a discrete solution to $(\mathscr{I}_\varepsilon^N)$, we construct discrete analogues of the barrier functions used in Theorem 5.2.2. However, in place of α_ε in these barrier functions, we will construct and use a discrete analogue A_ε^N.

We identify the nearest mesh point to the left of d in this non-aligned mesh as x_Q. That is

$$x_Q := \max\{x_i |\, x_i \leqslant d\}. \tag{5.3.2}$$

Note from (5.3.1), that x_Q is a mesh point within in the refined mesh. Define the following mesh functions

$$S^N(x_i) := (1+\rho)^{Q-i} - (1-\rho)^{Q-i}, \quad C^N(x_i) := (1+\rho)^{Q-i} + (1-\rho)^{Q-i}, \tag{5.3.3a}$$

$$T^N(x_i) := \frac{S^N(x_i)}{C^N(x_i)}, \qquad \rho = rh\varepsilon^{-1}, \qquad 0 \leqslant i \leqslant N. \tag{5.3.3b}$$

The mesh functions S^N, C^N and T^N can be thought of as discrete analogues of the continuous functions $2\sinh$, $2\cosh$ and $\tanh$ centred at x_Q respectfully. Note that from (5.3.1), we have $\rho \leqslant CN^{-1}\ln N \to 0$ as $N \to \infty$, $\forall\ \varepsilon$. Some properties of these mesh functions are given in the following Lemma.

Lemma 5.3.1. *For sufficiently large N, the mesh functions S^N and C^N defined in (5.3.3) satisfy:*

$$S^N(x_{i-1}) > S^N(x_i),\ \forall i; \qquad S^N(x_i) > 0,\ i < Q; \qquad S^N(x_Q) = 0; \qquad S^N(x_i) < 0,\ i > Q; \tag{5.3.4a}$$

$$C^N(x_{i-1}) > C^N(x_i),\ i < Q; \quad C^N(x_{i-1}) < C^N(x_i),\ i > Q; \quad C^N(x_i) \geqslant C^N(x_Q) = 2,\ \forall i; \tag{5.3.4b}$$

$$\left.\begin{array}{ll} i \leqslant Q-2, & \frac{C^N(x_i)}{1+\rho} \\ Q-1 \leqslant i, & C^N(x_i) \end{array}\right\} \leqslant C^N(x_{i+1}) \leqslant \left\{\begin{array}{ll} C^N(x_i), & i < Q \\ \frac{C^N(x_i)}{1-\rho}, & Q \leqslant i \end{array}\right. ; \tag{5.3.4c}$$

$$\left.\begin{array}{ll} i \leqslant Q, & C^N(x_i) \\ Q < i, & (1-\rho)C^N(x_i) \end{array}\right\} \leqslant C^N(x_{i-1}) \leqslant \left\{\begin{array}{ll} (1+\rho)C^N(x_i), & i < Q \\ C^N(x_i), & Q \leqslant i \end{array}\right. ; \tag{5.3.4d}$$

$$T^N(x_i) > 0,\ i < Q; \qquad T^N(x_Q) = 0; \qquad T^N(x_i) < 0,\ i > Q; \tag{5.3.4e}$$

$$|T^N(x_i)| < 1, \qquad |T^N(x_i) - \tanh\left(\frac{r}{\varepsilon}(Q-i)h\right)| \leqslant CN\rho^2,\ \forall i; \tag{5.3.4f}$$

$$\min\left\{T^N(x_{\frac{N}{4}}),\ |T^N(x_{\frac{3N}{4}})|\right\} \geqslant 1 - C\rho > \tfrac{1}{2}. \tag{5.3.4g}$$

Proof. Clearly $C_i^N \geqslant 2$, $\forall\ i$ and $S_i^N \geqslant 0$, $i \leqslant Q$, $S_i^N \leqslant 0$, $i \geqslant Q$. Use $S_i^N - S_{i-1}^N = -\rho C_i^N$ and $C_i^N - C_{i-1}^N = -\rho S_i^N$ to establish the bounds in (5.3.4a) and (5.3.4b). For (5.3.4c), we can show $C_{i-1}^N = C_i^N + \rho S_i^N$. We can use

$$C_i^N < S_i^N < C_i^N \tag{5.3.5}$$

to show that $(1-\rho)C_i^N < C_{i-1}^N < (1+\rho)C_i^N$. Combine these with (5.3.4b) to establish (5.3.4c). For (5.3.4d), we can show that $C_{i+1}^N = \frac{1}{1-\rho^2}(C_i^N - \rho S_i^N)$. Thus from (5.3.5), we have $C_{i+1}^N < \frac{1+\rho}{1-\rho^2}C_i^N = \frac{1}{1-\rho}C_i^N$. Similarly $C_{i+1}^N > \frac{1}{1+\rho}C_i^N$. Combine these with (5.3.4b) to establish (5.3.4d). The expressions in (5.3.4e) follow from (5.3.4a) and (5.3.4b). The bound in (5.3.4f) follows from (5.3.5). Using ((2.2.19), pg. 19) we can show that for any sufficiently small $\overline{\rho} > 0$ and $0 \leqslant j \leqslant N$, we have

$$(1 - CN\overline{\rho}^2)\sinh\overline{\rho}j - CN\overline{\rho}^2 \leqslant \tfrac{1}{2}[(1+\overline{\rho})^j - (1-\overline{\rho})^j] \leqslant (1+CN\overline{\rho}^2)\sinh\overline{\rho}j + CN\overline{\rho}^2, \tag{5.3.6a}$$

$$(1 - CN\overline{\rho}^2)\cosh\overline{\rho}j \leqslant \tfrac{1}{2}[(1+\overline{\rho})^i + (1-\overline{\rho})^i] \leqslant \cosh\overline{\rho}j. \tag{5.3.6b}$$

With a change of variables, we can prove the bound in (5.3.4g) using (2.2.19), (5.3.6) with (5.3.3) for sufficiently large N. Note that using (5.3.1) and (5.3.2), for sufficiently large N we have

$$x_Q - x_{\frac{N}{4}} \geqslant (1-p)\sigma \quad \Rightarrow \quad Q - \tfrac{N}{4} \geqslant \tfrac{(1-p)N}{4}, \tag{5.3.7a}$$

$$x_{\frac{3N}{4}} - x_Q \geqslant (1-p)\sigma \quad \Rightarrow \quad \tfrac{3N}{4} - Q \geqslant \tfrac{(1-p)N}{4}. \tag{5.3.7b}$$

For $i = \frac{N}{4}$ and for sufficiently large N, using (5.3.7), we can write $C_i^N \leqslant (1+C\rho)(1+\rho)^{Q-\frac{N}{4}}$ and $S_i^N \geqslant (1-C\rho)(1+\rho)^{Q-\frac{N}{4}}$. Hence $S_i^N/C_i^N \geqslant 1 - C\rho > \frac{1}{2}$. We can write a similar statement for $i = \frac{3N}{4}$. □

Define the difference operators

$$D_h^- Z(x_i) := \tfrac{1}{h}(Z(x_i) - Z(x_{i-1})), \quad D_h^+ := D_h^- Z(x_{i+1}), \quad \delta_h^2 := \tfrac{1}{h}[(D_h^+ - D_h^-)Z(x_i)]. \tag{5.3.8}$$

Observe that in the fine mesh; $D_h^- = D^-$ and in the coarse mesh; $D_h^- \neq D^-$. The purpose of defining such operators is for convenience. We present identities and inequalities that result when these operators are applied to the mesh function T^N in the following Lemma.

Lemma 5.3.2. *Assuming (5.2.1), then for sufficiently large N, the operators in (5.3.8) and the mesh function T^N defined in (5.3.3) satisfy:*

$$D_h^- T^N(x_i) < 0, \quad 0 < i \leqslant N, \quad D_h^+ T^N(x_i) < 0, \quad 0 \leqslant i < N, \tag{5.3.9a}$$

$$\frac{1+\rho}{1-\rho} D_h^- T^N(x_i) \leqslant D_h^+ T^N(x_i) \leqslant D_h^- T^N(x_i), \quad 0 < i < Q, \tag{5.3.9b}$$

$$D_h^+ T^N(x_Q) = D_h^- T^N(x_Q), \tag{5.3.9c}$$

$$\frac{1+\rho}{1-\rho} D_h^+ T^N(x_i) \leqslant D_h^- T^N(x_i) \leqslant D_h^+ T^N(x_i), \quad Q < i < N, \tag{5.3.9d}$$

$$|T^N(x_i) - T^N(x_{\frac{N}{4}})| \leqslant C\rho, \quad i < \tfrac{N}{4}, \quad |T^N(x_i) - T^N(x_{\frac{3N}{4}})| \leqslant C\rho, \quad i > \tfrac{3N}{4}, \tag{5.3.9e}$$

$$\max\{\varepsilon |D_h^+ T^N(x_{\frac{N}{4}})|,\ \varepsilon |D_h^- T^N(x_{\frac{3N}{4}})|\} \leqslant 5r\theta N^{-2(1-p)}, \quad \textit{when} \quad \sigma = \tfrac{\varepsilon}{r} \ln N, \tag{5.3.9f}$$

$$\varepsilon \delta_h^2 T - \theta T D_h^- T \geqslant 0, \ 0 < i < Q, \qquad \varepsilon \delta_h^2 T - \theta T D_h^+ T \leqslant 0, \ Q < i < N, \tag{5.3.9g}$$

$$T^N(x_i) T^N(x_{i-1}) - \tfrac{\varepsilon}{\theta}(D_h^- + D_h^+) T^N(x_i) \geqslant 2r, \qquad 0 < i \leqslant Q, \tag{5.3.9h}$$

$$T^N(x_{i+1}) T^N(x_i) - \tfrac{\varepsilon}{\theta}(D_h^- + D_h^+) T^N(x_i) \geqslant 2r, \qquad Q < i < N. \tag{5.3.9i}$$

Proof. Using (5.3.3) with (5.3.8), we can show that

$$D_h^- T^N(x_i) = \frac{r}{\varepsilon}(T_i^N T_{i-1}^N - 1) = \frac{-4r/\varepsilon(1-\rho^2)^{Q-i}}{C_i^N C_{i-1}^N}, \qquad \delta_h^2 T^N(x_i) = \frac{r}{\varepsilon} T_i^N (D^+ + D^-) T_i^N. \tag{5.3.10}$$

Use Lemma 5.3.1 and (5.3.10) to establish (5.3.9a), (5.3.9c) and (5.3.9e). For (5.3.9b), using Lemma 5.3.1 we have

$$C_{i+1}^N C_i^N \geqslant \frac{1}{(1+\rho)^2} C_i^N C_{i-1}^N.$$

Thus

$$D_h^+ T^N(x_i) = \frac{-4r/\varepsilon(1-\rho^2)^{Q-(i+1)}}{C_{i+1}^N C_i^N} \geqslant \frac{(1+\rho)^2}{1-\rho^2} \frac{-4r/\varepsilon(1-\rho^2)^{Q-i}}{C_i^N C_{i-1}^N} = \frac{1+\rho}{1-\rho} D_h^- T^N(x_i).$$

Also, from Lemma 5.3.1 and (5.3.10) we have $\delta_h^2 T^N(x_i) \leqslant 0$, $i \leqslant Q$. Thus using (5.3.8), we have

$$D_h^+ T^N(x_i) \leqslant D_h^- T^N(x_i), \quad i \leqslant Q.$$

Verify (5.3.9d) in the same manner. For (5.3.9f), when $i = \frac{N}{4}$ then using Lemma 5.3.1 and (5.3.3) we have

$$C_{i+1}^N C_i^N \geqslant {C_{i+1}^N}^2 = [(1+\rho)^{Q-(i+1)} + (1-\rho)^{Q-(i+1)}]^2 \geqslant (1+\rho)^{2(Q-(i+1))}. \tag{5.3.11}$$

Using (5.3.7), (5.3.11), ((2.2.19), pg. 19) and assuming $\sigma = \frac{\varepsilon}{r} \ln N$, we have

$$D_h^+ T^N(x_i) = \frac{-4r\varepsilon^{-1}(1-\rho^2)^{Q-(i+1)}}{C_{i+1}^N C_i^N} \geqslant -4r\varepsilon^{-1} \frac{(1+\rho)^{Q-(i+1)}(1-\rho)^{Q-(i+1)}}{(1+\rho)^{2(Q-(i+1))}}$$

$$= -\frac{1+\rho}{1-\rho} 4r\varepsilon^{-1} \left(\frac{1-\rho}{1+\rho}\right)^{Q-\frac{N}{4}} \geqslant -5r\varepsilon^{-1} e^{-2\rho(Q-\frac{N}{4})} = -5r\varepsilon^{-1} N^{-2(1-p)}.$$

Use (5.3.9a) to bound $D_h^+ T^N(x_i)$ from above. Bound $D^- T^N(x_{\frac{3N}{4}})$ in the same manner. For the first inequality in (5.3.9g), using (5.2.1), (5.3.10) and (5.3.9b) with Lemma 5.3.1 and (5.3.9a) for $i < Q$, we have

$$\varepsilon\delta_h^2 T_i^N - \theta T_i^N D_h^- T_i^N = T_i^N(r(D^+ + D^-)A_i^N - \theta D_h^- T_i^N) \geqslant T_i^N\left(\frac{2r}{(1-\rho)} - \theta\right) D_h^- T_i^N \geqslant 0.$$

The second inequality in (5.3.9g) is established in the same manner. For (5.3.9h) on $0 < i \leqslant Q$, using (5.2.1), Lemma 5.3.1, (5.3.9a) and (5.3.10) we have

$$T_i^N T_{i-1}^N - \frac{\varepsilon}{\theta}(D_h^- + D_h^+)T_i^N \geqslant T_i^N T_{i-1}^N - \frac{2\varepsilon}{\theta} D_h^- T_i^N = \frac{2r}{\theta} + \left(1 - \frac{2r}{\theta}\right) T_i^N T_{i-1}^N \geqslant \frac{2r}{\theta}.$$

The bound (5.3.9i) is established in the same manner. □

We now define the discrete function A_ε^N which will replace α_ε in discrete analogues of the barrier functions in Theorem 5.2.2. We distinguish between the cases $\sigma < \mu$ ($\sigma \equiv C\varepsilon \ln N$) and $\sigma = \mu$ ($\sigma \equiv C$). When $\sigma < \mu$, we define A_ε^N as follows

$$A_\varepsilon^N(x_i) := \begin{cases} A_\varepsilon^N(x_{\frac{N}{4}}) + (x_{\frac{N}{4}} - x_i)\frac{5r}{2\mu} N^{-(1-2p)}, & 0 \leqslant i < \frac{N}{4}, \\ \theta T^N(x_i), & \frac{N}{4} \leqslant i \leqslant \frac{3N}{4}, \\ A_\varepsilon^N(x_{\frac{3N}{4}}) - (x_i - x_{\frac{3N}{4}})\frac{5r}{2\mu} N^{-(1-2p)}, & \frac{3N}{4} < i \leqslant N. \end{cases} \tag{5.3.12a}$$

When $\sigma = \mu$, we consider the case $\mu = \frac{1}{2}(1 - d^N)$ (where $H_0 \geqslant h = H_1$) and define A_ε^N as follows

$$A_\varepsilon^N(x_i) := \begin{cases} A_\varepsilon^N(x_{\frac{N}{4}}) + \frac{H_0}{h}\theta(T(x_i) - T(x_{\frac{N}{4}})), & 0 \leqslant i < \frac{N}{4}, \\ \theta T^N(x_i), & \frac{N}{4} \leqslant i \leqslant N. \end{cases} \tag{5.3.12b}$$

When $\mu = \frac{d^N}{2}$ (where $H_0 = h \leqslant H_1$) we can define A_ε^N in the same manner. We prove convergence of A_ε^N to α_ε in the following Lemma.

Lemma 5.3.3. *For sufficiently large N, the value p defined in (5.3.1), the function α_ε defined in (5.2.1) and the mesh function A_ε^N defined in (5.3.12) satisfy:*

$$|(\alpha_\varepsilon - A_\varepsilon^N)(x_i)| \leqslant CN^{-1}(\ln N)^2 + CN^{-(1-2p)}.$$

Proof. First, using (5.3.1), (5.3.2) and the identity

$$\tanh(X+Y) = \frac{\tanh(X) + \tanh(Y)}{1 + \tanh(X)\tanh(Y)}$$

we have

$$\begin{aligned} \tanh(r(x_Q - x_i)/\varepsilon) &= \tanh[r(d - x_i)/\varepsilon + r(x_Q - d)/\varepsilon] \\ &= \frac{\tanh(r(d-x_i)/\varepsilon) + \tanh(r(x_Q - d)/\varepsilon)}{1 + \tanh(r(d-x_i)/\varepsilon)\tanh(r(x_Q - d)/\varepsilon)} \\ &\leqslant \frac{\tanh(r(d-x_i)/\varepsilon) + \rho}{1-\rho} \leqslant \tanh(r(d-x_i)/\varepsilon) + C\rho. \end{aligned}$$

Construct a corresponding lower bound to give

$$|\tanh(r(d-x_i)/\varepsilon)-\tanh(r(x_Q-x_i)/\varepsilon)|\leqslant C\rho\leqslant CN^{-1}\ln N,\quad \forall i. \tag{5.3.13}$$

Consider values for $i\in S$ where

$$S:=\left\{\begin{array}{ll}\left[\frac{N}{4},\frac{3N}{4}\right], & \text{if}\quad \sigma<\mu,\\ \left[\frac{N}{4},N\right], & \text{if}\quad \sigma=\frac{1}{2}(1-d^N),\\ \left[0,\frac{3N}{4}\right], & \text{if}\quad \sigma=\frac{d^N}{2}\end{array}\right\}\cap\mathbb{Z}.$$

Using (5.3.1), we have

$$x_Q-x_i=x_{\frac{N}{4}}+h(Q-\tfrac{3N}{4})-x_{\frac{N}{4}}-h(i-\tfrac{3N}{4})=(Q-i)h.$$

Now using Lemma 5.3.2 we have $|A_\varepsilon^N(x_i)-\theta\tanh(\frac{r}{\varepsilon}(x_Q-d))|\leqslant CN\rho^2$. For all other $i\notin S$, using Lemma 5.3.2 and (5.3.12) we have

$$\begin{aligned}
&|A_i^N-\theta\tanh(r(x_Q-x_i)/\varepsilon)|\leqslant\theta|T^N_{\frac{N}{4},\frac{3N}{4}}+CN^{-(1-2p)}+C|T_i^N-T^N_{\frac{N}{4},\frac{3N}{4}}|-\theta\tanh(r(x_Q-x_i)/\varepsilon)|\\
&\leqslant C|T^N_{\frac{N}{4},\frac{3N}{4}}-1|+CN^{-(1-2p)}+C\rho+C|1-\theta\tanh(r(x_Q-x_i)/\varepsilon)|\\
&\leqslant C\rho+CN^{-(1-2p)}+C\rho+C|1-\theta\tanh(r(x_Q-x_{\frac{N}{4},\frac{3N}{4}})/\varepsilon)|\\
&\leqslant C\rho+CN^{-(1-2p)}+C|1-\theta\tanh(r(Q-(\tfrac{N}{4},\tfrac{3N}{4}))h/\varepsilon)|\\
&\leqslant C\rho+CN^{-(1-2p)}+C|1-T^N_{\frac{N}{4},\frac{3N}{4}}|+C|T^N_{\frac{N}{4},\frac{3N}{4}}-\theta\tanh(r(Q-(\tfrac{N}{4},\tfrac{3N}{4}))h/\varepsilon)|\\
&\leqslant C\rho+CN^{-(1-2p)}+C\rho+CN\rho^2.
\end{aligned}$$

Thus, $\forall\ i$, we have

$$|A_\varepsilon^N(x_i)-\theta\tanh\left(\frac{r}{\varepsilon}(x_Q-x_i)\right)|\leqslant C\rho+CN^{-(1-2p)}+CN\rho^2\leqslant CN^{-(1-2p)}+CN^{-1}(\ln N)^2. \tag{5.3.14}$$

Combine (5.3.13) and (5.3.14) to complete the proof. □

By the assumption (5.2.1b), and assuming N is sufficiently large, we have

$$|a_\varepsilon(x_i)|\geqslant|A_\varepsilon^N(x_i)|,\quad x_i\in\overline{\Omega}_\varepsilon^N.$$

The finite difference operator ${\mathcal{L}_\varepsilon}^N$ satisfies the following discrete minimum principle, the proof of which is standard.

Theorem 5.3.1. *Let ${\mathcal{L}_\varepsilon}^N$ be the difference operator defined in ($\mathcal{I}_\varepsilon^N$) and Z be a mesh function on $\overline{\Omega}_\varepsilon^N$. If $\min\{Z(x_0),Z(x_N)\}\geqslant 0$ and ${\mathcal{L}_\varepsilon}^N Z(x_i)\leqslant 0$ for $x_i\in\Omega_\varepsilon^N$, then $Z(x_i)\geqslant 0$ for all $x_i\in\overline{\Omega}_\varepsilon^N$.*

Theorem 5.3.2. *There exists a unique solution, Y_ε^N, of ($\mathcal{I}_\varepsilon^N$) such that*

$$|Y_\varepsilon^N(x_i)|\leqslant C,\quad x_i\in\overline{\Omega}_\varepsilon^N.$$

Proof. We first establish the following list of inequalities;

$$\varepsilon\delta^2 A_\varepsilon^N(x_i) - A_\varepsilon^N(x_i) D^- A_\varepsilon^N(x_i) \geqslant 0, \qquad 0 < i < Q, \tag{5.3.15a}$$

$$\varepsilon\delta^2 A_\varepsilon^N(x_i) - A_\varepsilon^N(x_i) D^+ A_\varepsilon^N(x_i) \leqslant 0, \qquad Q < i < N, \tag{5.3.15b}$$

$$A_\varepsilon^N(x_i) A_\varepsilon^N(x_{i-1}) - \frac{2\varepsilon}{h_{i+1}+h_i}(h_i D^- + h_{i+1} D^+) A_\varepsilon^N(x_i) \geqslant \theta r, \quad 0 < i \leqslant Q, \tag{5.3.15c}$$

$$A_\varepsilon^N(x_{i+1}) A_\varepsilon^N(x_i) - \frac{2\varepsilon}{h_{i+1}+h_i}(h_i D^- + h_{i+1} D^+) A_\varepsilon^N(x_i) \geqslant \theta r, \quad Q < i < N, \tag{5.3.15d}$$

which are discrete counterparts to the inequalities (5.2.2). Recall from the assumption (5.2.1) that $\theta > 2r$. We first consider the case where $\sigma < \mu$. Using (5.3.12a) we can show that

$$D^- A_\varepsilon^N(x_i) = -\frac{5r}{2\mu} N^{-(1-2p)},\ 0 < i \leqslant \tfrac{N}{4},\ \tfrac{3N}{4} < i \leqslant N;\ \ D^- A_\varepsilon^N(x_i) = \theta D_h^- T_i^N,\ \tfrac{N}{4} < i \leqslant \tfrac{3N}{4}; \tag{5.3.16a}$$

$$\delta^2 A_\varepsilon^N(x_i) = \begin{cases} 0, & \max\{i, N-i\} < \frac{N}{4}, \\ \frac{2(D^+ - D^-)(A_i^N)}{h + H_{0,1}}, & i = \frac{N}{4}, \frac{3N}{4}, \\ \theta \delta_h^2 T_i^N, & \frac{3N}{4} < i < N. \end{cases} \tag{5.3.16b}$$

For (5.3.15a), the result is trivial for $0 < i < \frac{N}{4}$. For $i = \frac{N}{4}$, using Lemma 5.3.2 and (5.3.16), for sufficiently large N, we have

$$\begin{aligned} (\varepsilon\delta^2 - A_i^N D^-) A_i^N &= (\frac{N\varepsilon}{2d^N} + A_i^N)(-D^- A_i^N) + \frac{N}{2d^N}\varepsilon D^+ A_i^N \\ &\geqslant \frac{5r\theta}{4\mu} N^{-(1-2p)} - \frac{N}{2d^N}(5r\theta N^{-2(1-p)}) \geqslant 0. \end{aligned}$$

For $\frac{N}{4} < i < Q$, use (5.3.9g). Bound (5.3.15b) in the same manner. For (5.3.15c), for $0 < i \leqslant \frac{N}{4}$, using (5.3.9), for sufficiently large N, we have

$$A_i^N A_{i-1}^N - \frac{\varepsilon}{h_{i+1}+h_i}(h_i D^- + h_{i+1} D^+) A_i^N \geqslant A_i^N A_{i-1}^N \geqslant {A_{\frac{N}{4}}^N}^2 \geqslant (1 - C\rho)^2 \theta^2 \geqslant \tfrac{1}{2}\theta^2 > \theta r.$$

For $\frac{N}{4} < i \leqslant Q$, use (5.3.9g). The bound (5.3.15d) is established in the same manner.

Next, consider the case where $\sigma = \mu = \frac{1}{2}(1 - d^N)$. Using (5.3.12b) we can show that

$$D^- A_\varepsilon^N(x_i) = \theta D_h^- T(x_i), \quad 0 < i \leqslant N,$$

$$\delta^2 A_\varepsilon^N(x_i) = \frac{h}{H_0}\theta\delta_h^2 T_i^N,\ i < \tfrac{N}{4};\ \ \delta^2 A_\varepsilon^N(x_i) = \frac{2h}{H_0 + h}\theta\delta_h^2 T_i^N,\ i = \tfrac{N}{4};\ \ \delta^2 A_\varepsilon^N(x_i) = \theta\delta_h^2 T_i^N,\ i > \tfrac{N}{4}.$$

Using Lemma 5.3.2 and $H_0 \geqslant h = H_1$, we can prove (5.3.15a)-(5.3.15d), in the same manner as the case $\sigma < \mu$. The case $\sigma = \mu = \frac{d^N}{2}$ follows suit.

Define the discrete barrier functions

$$\psi^\pm(x_i) := \frac{\|q\|}{\theta r}[(x_i - x_Q) A_\varepsilon^N(x_i) + \max_{x_i \in \overline{\Omega}_\varepsilon^N}\{(x_i - x_Q) A_\varepsilon^N(x_i)\}] + \max\{|A|, |B|\} \pm Y_\varepsilon^N(x_i), \tag{5.3.18}$$

which are nonnegative at $x=0,1$. Using (5.3.12a) and Lemma 5.3.2 we have

$$D^{\pm}[(x_i-x_Q)A_\varepsilon^N(x_i)] = (x_i-x_Q)D^{\pm}A_\varepsilon^N(x_i) + A_\varepsilon^N(x_{i\pm1}) \begin{cases} \geqslant 0, & i \leqslant Q, \\ \leqslant 0, & i \geqslant Q. \end{cases}$$

Using this and the bounds in (5.3.15), we can show that $\mathcal{L}_\varepsilon{}^N \psi^{\pm}(x_i) \leqslant 0$ for $x_i \in \Omega_\varepsilon^N$. Thus using Theorem 5.3.1, we have $|Y_\varepsilon^N| \leqslant C$ on $\overline{\Omega}_\varepsilon^N$. Existence and uniqueness follow from (5.3.18). □

Akin to the continuous problem ($\mathscr{I}_\varepsilon$), we split the discrete problem ($\mathscr{I}_\varepsilon^N$) into left and right discrete problems centred around $x=x_Q$ (5.3.2) as follows. Define the discrete left and right problems by

$$Y_\varepsilon^N(x_i) = \left\{ Y_L^N(x_i),\ x_i \leqslant x_Q, \qquad Y_R^N(x_i),\ x_i \geqslant x_Q, \right\}$$

$$\mathcal{L}_\varepsilon{}^N Y_L^N(x_i) = q(x_i), \quad x_i \in \Omega_\varepsilon^N \cap (0,x_Q), \quad Y_L^N(0)=y_0, \quad Y_L^N(x_Q) = Y_\varepsilon^N(x_Q), \tag{$\mathscr{I}_L^N$}$$

$$\mathcal{L}_\varepsilon{}^N Y_R^N(x_i) = q(x_i), \quad x_i \in \Omega_\varepsilon^N \cap (x_Q,1), \quad Y_R^N(x_Q) = Y_\varepsilon^N(x_Q), \quad Y_R^N(1)=y_1. \tag{$\mathscr{I}_R^N$}$$

We decompose each $Y_{L\backslash R}^N$ into the sum of a regular component, $V_{L\backslash R}^N$, and a layer component, $W_{L\backslash R}^N$. We define V_L^N as the solution of

$$\begin{aligned} \mathcal{L}^{-,N} V_L^N(x_i) := (\varepsilon\delta^2 + a_0^- D^- - b)V_L^N(x_i) = q(x_i), \quad x_i \in \Omega_\varepsilon^N \cap (0,x_Q), \\ V_L^N(0)=y_0, \quad V_L^N(x_Q) = (V_0^N + \varepsilon V_1^N)(x_Q), \end{aligned} \tag{5.3.19a}$$

where $V_L^N = V_0^N + \varepsilon V_1^N + \varepsilon^2 V_2^N$ and V_0^N, V_1^N, V_2^N satisfy

$$(a_0^- D^- + b)V_0^N(x_i) = -q(x_i), \quad x_i \in \Omega_\varepsilon^N \cap (0,x_Q], \quad V_0^N(0)=y_0, \tag{5.3.19b}$$

$$(a_0^- D^- + b)V_1^N(x_i) = \delta^2 V_0^N(x_i),\ x_i \in \Omega_\varepsilon^N \cap (0,x_Q),\ V_1^N(0)=0; \quad V_1^N(x_Q) := V_1^N(x_{Q-1}), \tag{5.3.19c}$$

$$\mathcal{L}^{-,N} V_2^N(x_i) = -\delta^2 V_1^N(x_i), \quad x_i \in \Omega_\varepsilon^N \cap (0,x_Q), \quad V_2^N(0) = V_2^N(x_Q) = 0. \tag{5.3.19d}$$

We incorporate the error $(\mathcal{L}_\varepsilon{}^N - \mathcal{L}^{-,N})V_L^N$ into the discrete layer component, W_L^N, which is, noting (5.2.1d), defined as the solution of the following discrete problem

$$\mathcal{L}_\varepsilon{}^N W_L^N(x_i) = \varphi_\varepsilon^- D^- V_L^N(x_i),\ x_i \in \Omega_\varepsilon^N \cap \Omega^-,\ W_L^N(0)=0,\ W_L^N(x_Q) = (Y_L^N - V_L^N)(x_Q). \tag{5.3.19e}$$

Similarly V_R^N and W_R^N satisfy

$$\mathcal{L}^{+,N} V_R^N(x_i) := (\varepsilon\delta^2 + a_0^+ D^+ - b)V_R^N(x_i) = q(x_i), \quad x_i \in \Omega_\varepsilon^N \cap (x_Q,1), \tag{5.3.20a}$$

$$V_R^N(x_Q) = V^*, \quad V_R^N(1) = y_1, \tag{5.3.20b}$$

$$\mathcal{L}_\varepsilon{}^N W_R^N(x_i) = \varphi_\varepsilon^+ D^+ V_R^N(x_i), \quad x_i \in \Omega_\varepsilon^N \cap (x_Q,1), \tag{5.3.20c}$$

$$W_R^N(x_Q) = (Y_R^N - V_R^N)(x_Q), \quad W_R^N(1) = 0. \tag{5.3.20d}$$

where V^* is defined analogously to $V_L^N(x_Q)$ in (5.3.19). We now determine bounds on $V_{L\backslash R}^N$, $W_{L\backslash R}^N$, $D^{\pm}V_{L\backslash R}^N$ and on the error $|V_{L\backslash R}^N - v_{L\backslash R}|$. But first we present a mesh function that we will

use in the barrier functions for the layer component, along with some of its properties, in the following Lemma.

Lemma 5.3.4. *For sufficiently large N, the mesh function $\hat{W}^N$ defined below satisfies*

$$\hat{W}^N(x_i) := \prod_{j=i+1}^{Q} \left(1 + \frac{\alpha_\varepsilon(x_j)}{2}\frac{h_j}{\varepsilon}\right)^{-1}, \quad 0 \leqslant i < Q, \quad \hat{W}^N(x_Q) := 1,$$

$$\hat{W}^N(x_i) \geqslant (1 - C\rho)e^{-(\theta/2)(d-x_i)/\varepsilon}, \quad 0 \leqslant i \leqslant Q,$$

$$\hat{W}^N(x_i) \leqslant Ce^{-(\theta/2)(d-x_i)/\varepsilon}, \quad \tfrac{N}{4} \leqslant i \leqslant Q\,(\sigma < \mu), \quad 0 \leqslant i \leqslant Q\,(\sigma = \mu),$$

$$|\hat{W}^N(x_i)| \leqslant CN^{-(1-p)}, \quad i \leqslant \tfrac{N}{4}\,(\sigma < \mu).$$

Proof. We can easily bound $\hat{W}^N$ from below using (5.2.1), (5.3.1), ((2.2.19), pg. 19) and (5.3.7) as follows

$$\begin{aligned}
\hat{W}^N(x_i) &\geqslant \prod_{j=i+1}^{Q} \exp\left(-\frac{\alpha_\varepsilon(x_j)}{2\varepsilon}h_j\right) = \exp\left(-\frac{1}{2\varepsilon}\sum_{j=i+1}^{Q}\alpha_\varepsilon(x_j)h_j\right) \geqslant \exp\left(-\frac{\theta}{2\varepsilon}\sum_{j=i+1}^{Q}h_j\right) \\
&= \exp\left(-\frac{\theta}{2\varepsilon}(x_Q - x_i)\right) = \exp\left(-\frac{\theta}{2\varepsilon}(x_Q - d)\right)\exp\left(-\frac{\theta}{2\varepsilon}(d - x_i)\right) \\
&\geqslant (1 - C\rho)\exp\left(-\frac{\theta}{2\varepsilon}(d - x_i)\right).
\end{aligned}$$

Using (5.3.7) with the rectangle rule (3.2.21) on $\frac{N}{4} \leqslant i \leqslant Q$ when $(\sigma < \mu)$ or on $0 \leqslant i \leqslant Q$ when $(\sigma = \mu)$, we have

$$\frac{1}{2\varepsilon}\sum_{j=i+1}^{Q}\alpha_\varepsilon(x_j)h_j \geqslant \frac{1}{2\varepsilon}\int_{x_i}^{x_Q}\alpha_\varepsilon(t)\,dt - C(h/\varepsilon)^2 \geqslant \frac{1}{2\varepsilon}\int_{x_i}^{x_Q}\alpha_\varepsilon(t)\,dt - CN^{-2}(\ln N)^2. \tag{5.3.22}$$

Using ((2.2.19), pg. 19) with (5.2.1), (5.2.5), (5.3.1), (5.3.7) and (5.3.22), for sufficiently large N, we have

$$\begin{aligned}
\hat{W}^N(x_i) &\leqslant \prod_{j=i+1}^{Q}\exp\left(-\frac{\alpha_\varepsilon(x_j)}{2\varepsilon}h_j\right)\exp\left(\frac{1}{2}\left(\frac{\alpha_\varepsilon(x_j)}{2\varepsilon}h_j\right)^2\right) \\
&\leqslant \exp\left(CN(N^{-1}\ln N)^2\right)\exp\left(-\frac{1}{2\varepsilon}\sum_{j=i+1}^{Q}\alpha_\varepsilon(x_j)h_j\right) \\
&\leqslant C\exp\left(-\frac{1}{2\varepsilon}\int_{x_i}^{x_Q}\alpha_\varepsilon(t)\,dt\right) \leqslant C\exp\left(-\frac{1}{2\varepsilon}\int_{x_i}^{d}\alpha_\varepsilon(t)\,dt\right) \leqslant C\exp\left(-\frac{\theta}{2\varepsilon}(d - x_i)\right).
\end{aligned}$$

Finally, we have

$$\hat{W}^N(x_i) - \hat{W}^N(x_{i-1}) = \frac{\alpha_\varepsilon(x_i)h_i}{2\varepsilon}\hat{W}^N(x_i) > 0.$$

Thus for $i \leqslant \frac{N}{4}$ when $(\sigma < \mu)$, using (5.2.1) and (5.3.7) we have

$$\hat{W}^N(x_i) \leqslant \hat{W}^N(x_{\frac{N}{4}}) \leqslant Ce^{-(\theta/2)(d-x_{N/4})/\varepsilon} \leqslant CN^{-(1-p)}.$$

□

Lemma 5.3.5. *If v_L, w_L are the solutions of (5.2.3), v_R, w_R are the solutions of (5.2.4), V_L^N, W_L^N are the solutions of (5.3.19) and V_R^N, W_R^N are the solutions of (5.3.20) then we have the bounds*

$$|D^- V_L^N(x_i)| \leqslant C, \;\; x_i \in \Omega_\varepsilon^N \cap (0, x_Q]; \quad |(V_L^N - v_L)(x_i)| \leqslant CN^{-1} x_i, \;\; x_i \in \overline{\Omega}_\varepsilon^N \cap [0, x_Q],$$

$$|D^+ V_R^N(x_i)| \leqslant C, \;\; x_i \in \Omega_\varepsilon^N \cap [x_Q, 1); \quad |(V_R^N - v_R)(x_i)| \leqslant CN^{-1}(1 - x_i), \;\; x_i \in \overline{\Omega}_\varepsilon^N \cap [x_Q, 1],$$

$$|W_L^N(x_i)| \leqslant \begin{cases} Ce^{-(\theta/2)(d-x_i)/\varepsilon} + CN^{-(1-p)}, & \frac{N}{4} \leqslant i \leqslant Q \;\; (\text{if } \sigma < \mu), \quad 0 \leqslant i \leqslant Q \;\; (\text{if } \sigma = \mu), \\ CN^{-(1-p)}, & 0 \leqslant i \leqslant \frac{N}{4} \;\; (\text{if } \sigma < \mu), \end{cases}$$

$$|W_R^N(x_i)| \leqslant \begin{cases} Ce^{-(\theta/2)(x_i-d)/\varepsilon} + CN^{-(1-p)}, & Q \leqslant i \leqslant \frac{3N}{4} \;\; (\text{if } \sigma < \mu), \quad Q \leqslant i \leqslant N \;\; (\text{if } \sigma = \mu), \\ CN^{-(1-p)}, & \frac{3N}{4} \leqslant i \leqslant N \;\; (\text{if } \sigma < \mu). \end{cases}$$

Proof. The bounds on the components $v_{L\backslash R}$ and $V_{L\backslash R}$ can be proved analogously to Lemma 3.2.2.

To bound the layer component W_L^N, we first establish a few inequalities. Using $\frac{1}{2}e^t \leqslant \cosh t \leqslant e^t$, $t > 0$ and using (5.2.1), (5.3.7) and Lemma 5.3.2, bound φ_ε^- and a_ε for sufficiently large N as follows

$$\hat{W}^N(x_{i-1}) \geqslant \exp\left(-\frac{\theta}{2\varepsilon}(d - x_i + h)\right) \geqslant \frac{1}{2} e^{-(\theta/2)(d-x_i)/\varepsilon},$$

$$\frac{N}{4} < i < Q \;\; (\text{if } \sigma < \mu), \;\; 0 < i < Q \;\; (\text{if } \sigma = \mu),$$

$$a_\varepsilon(x_i) \geqslant \frac{\theta}{2}, \quad 0 \leqslant i \leqslant \tfrac{N}{4}, \;\; (\text{if } \sigma < \mu) \qquad |\varphi_\varepsilon^-(x_i)| \leqslant N^{-(1-p)}, \quad 0 \leqslant i \leqslant \tfrac{N}{4} \;\; (\text{if } \sigma < \mu).$$

By constructing suitable barrier functions, we complete the proof in an analogous manner as Lemma 3.2.3. □

A bound on the error $Y_\varepsilon^N - y_\varepsilon$ is given in the following lemma.

Theorem 5.3.3. *If y_ε is the solution of $(\mathscr{I}_\varepsilon, (5.2.1))$ and Y_ε^N is the solution of $(\mathscr{I}_\varepsilon^N, (5.3.1))$, then*

$$\|\overline{Y}_\varepsilon^N - y_\varepsilon\|_{[0,1]} \leqslant CN^{-1}(\ln N)^2 + CN^{-(1-p)},$$

where $|d^N - d| < p\sigma$ and $p \leqslant \frac{1}{2}$ is defined in (5.3.1) and $\overline{Y}_\varepsilon^N$ is the linear interpolation of Y_ε^N.

Proof. First, if $\sigma < \mu$ then for $i \leqslant \frac{N}{4}$, using Lemma 5.2.1, Lemma 5.3.5 and (5.3.1), (5.3.7) we have

$$|(Y_\varepsilon^N - y_\varepsilon)(x_i)| \leqslant |W_L^N(x_i)| + |w_L(x_i)| + |(V_L^N - v_L)(x_i)| \leqslant CN^{-(1-p)}.$$

Similarly, for $i \geqslant \frac{3N}{4}$, we have $|(Y_\varepsilon^N - y_\varepsilon)(x_i)| \leqslant CN^{-(1-p)}$.

We now need to examine the error over all mesh points $x_i \in [x_L, x_R]$ where $x_L = 0$ if $\sigma = \mu$

or $x_L = x_{\frac{N}{4}}$ if $\sigma < \mu$ and $x_R = 1$ if $\sigma = \mu$ or $x_R = x_{\frac{3N}{4}}$ if $\sigma < \mu$. Note the implication that for any $x_i \in (x_L, x_R)$, we have $h_i/\varepsilon \leqslant CN^{-1}\ln N$. The error $E^N(x_i) := (Y_\varepsilon^N - y_\varepsilon)(x_i)$ is defined as a solution of the following

$$\mathcal{L}_\varepsilon{}^N E^N(x_i) = (\mathcal{L}_\varepsilon - \mathcal{L}_\varepsilon{}^N) y_\varepsilon, \quad x_i \in \Omega_\varepsilon^N \cap (x_L, x_R), \quad |E(x_{L\backslash R})| \leqslant CN^{-(1-p)}.$$

For any $s \in [x_{i-1}, x_{i+1}] \subset [x_L, x_R] \cap \overline{\Omega}_\varepsilon^N$, using $(\mathscr{I}_\varepsilon)$, (5.2.1) and Theorem 5.2.2, we can bound $\varepsilon|y_\varepsilon''(s) - y_\varepsilon''(x_i)|$ as follows

$$\varepsilon|y_\varepsilon''(s) - y_\varepsilon''(x_i)| \leqslant (\|a_\varepsilon\|\|y_\varepsilon''\| + (\|b\| + \int_0^{x_{i+1}} \left|a_\varepsilon'(\xi)\right| \, d\xi)\|y_\varepsilon'\| + \|b'\|\|y_\varepsilon\| + \|f'\|)|s - x_i| \leqslant C\frac{h_i}{\varepsilon^2}. \tag{5.3.24}$$

Thus using (5.3.24) with (3.2.15) we have

$$|(\mathcal{L}_\varepsilon - \mathcal{L}_\varepsilon{}^N) y_\varepsilon(x_i)| \leqslant Ch_i\varepsilon^{-2} \leqslant C\varepsilon^{-1}N^{-1}\ln N, \quad x_i \in \Omega_\varepsilon^N \cap (x_L, x_R).$$

Hence, using the barrier functions in (5.3.18) we can show that

$$|E(x_i)| \leqslant C\varepsilon^{-1}N^{-1}\ln N[(x_i - x_Q)A_\varepsilon^N(x_i) + \max_{x_i \in \overline{\Omega}_\varepsilon^N \cap [x_L, x_R]} \{(x_i - x_Q)A_\varepsilon^N(x_i)\}] + CN^{-(1-p)}$$

$$\leqslant \begin{cases} \frac{C\sigma}{\varepsilon}N^{-1}\ln N + CN^{-(1-p)} \leqslant CN^{-1}(\ln N)^2 + CN^{-(1-p)}, & \sigma < \mu, \\ \frac{C}{\varepsilon}N^{-1}\ln N + CN^{-(1-p)} \leqslant CN^{-1}(\ln N)^2 + CN^{-(1-p)}, & \sigma = \mu. \end{cases}$$

The global bound follows as in [22, pg. 381]. □

5.4: Numerical Examples

Example 5.1

In this example, we consider the problem class $(\mathscr{I}_\varepsilon)$ with

$$a_\varepsilon(x) = (2.25 + x^2)\tanh(\tfrac{1.1}{\varepsilon}(0.6 - x)), \quad b(x) = e^{-5x}, \tag{5.4.1a}$$

$$q(x) = \cos(3x), \quad A = 2, \quad B = -3, \quad d = 0.6. \tag{5.4.1b}$$

We choose $r = 1$ and $\theta = 2.1$. We consider various values for the parameter p in (5.3.1a).

$$\begin{gathered} \text{To generate a value of } d^N \text{ associated with some } p, \text{ we start with} \\ \text{a scale factor of } \kappa = 0.99 \text{ and reduce by } 0.01 \text{ until} \\ d^N = d \pm \kappa p \min\{\tfrac{1}{2}\min(d, 1-d), \tfrac{\varepsilon}{r}\ln N\} \text{ satisfies } |d - d^N| < p\sigma. \end{gathered} \tag{5.4.2}$$

We solve the scheme $((\mathscr{I}_\varepsilon^N)$, (5.3.1)) exactly to generate numerical approximations U_ε^N. We consider $p = 0$, $p = 0.5$ and $p = 1$ and using (5.4.2) we centre the mesh at $d^N = d$, $d^N \approx d - 0.5\sigma$ and $d^N \approx d - \sigma$ (test case). Figure 5.1 contains plots of Numerical Solutions, for these three cases, of $(\mathscr{I}_\varepsilon^N)$ for this example. Note, the fine mesh locations are superimposed onto the graph.

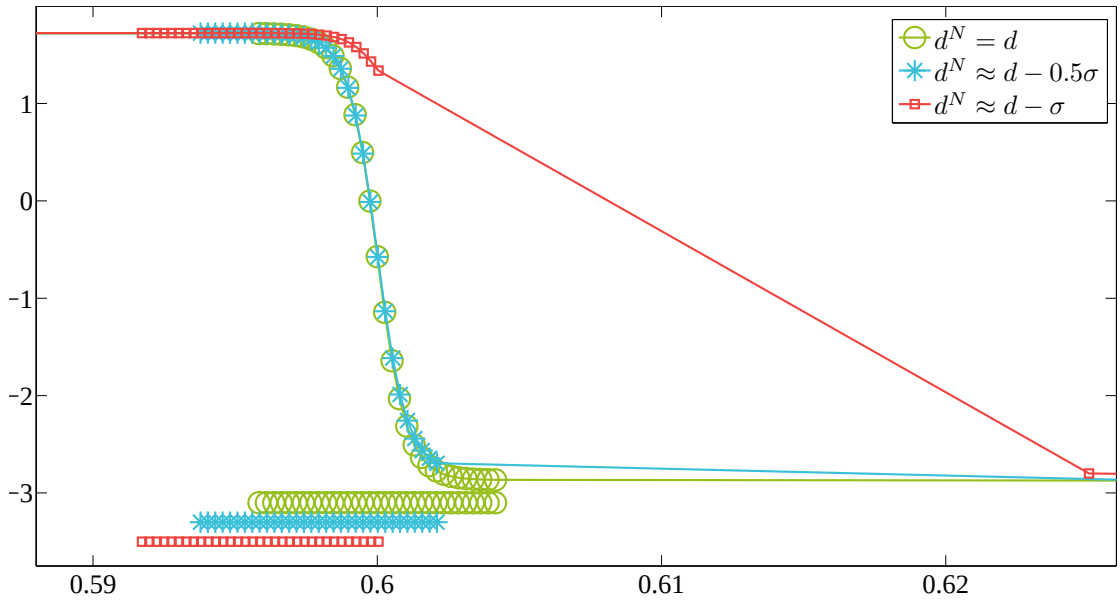

Figure 5.1: Plot of the numerical solutions of $(\mathscr{I}_\varepsilon)$ with the problem data (5.4.1), solved exactly using the numerical method ($(\mathscr{I}_\varepsilon^N)$, (5.3.1), (5.4.2)), over $x_i \in [0.588, 0.626]$ for $d^N = d$, $d^N \approx d - 0.5\sigma$ and $d^N \approx d - \sigma$ where $\varepsilon = 10^{-3}$ and $N = 64$ including superimpositions of fine mesh locations.

We compute the approximate errors

$$\tilde{E}_\varepsilon^N = \max_{\Omega_\varepsilon^N \cup \Omega_\varepsilon^{8192}} |\overline{U}_\varepsilon^N - \overline{U}_\varepsilon^{8192}| \tag{5.4.3}$$

where $\overline{U}_\varepsilon^N$ is the interpolation of U_ε^N, the numerical solution of $(\mathscr{I}_\varepsilon^N)$ using N mesh intervals, onto the mesh $\Omega_\varepsilon^N \cup \Omega_\varepsilon^{8192}$. Table 5.1 displays the approximate errors $\tilde{E}_\varepsilon^N$ and the uniform errors $\tilde{E}^N = \max_\varepsilon E_\varepsilon^N$, using (5.4.3) . Shifting the mesh off-centre within the limit of $p \leqslant \frac{1}{2}$ has little to no effect on the differences. We further test for an effect of the value of p by producing the computed rates of convergence R_ε^N and the uniform rates of convergence R^N (as defined in ((3.4.4), pg. 82)), presented in Table 5.1. The $N^{-(1-p)}$ factor established in Theorem 5.3.3 is not evident for $p \leqslant \frac{1}{2}$. However, for $p = 1$ we see a collapse in the computed rates of convergence.

	$\mathbf{d^N = d}$					$\mathbf{d^N \approx d + 0.5\sigma}$					$\mathbf{d^N \approx d + \sigma}$				
ε \ N	**32**	**64**	**128**	**256**	**512**	**32**	**64**	**128**	**256**	**512**	**32**	**64**	**128**	**256**	**512**
	$\tilde{\mathbf{E}}_\varepsilon^{\mathbf{N}}$														
$\mathbf{2^{-0}}$	0.004	0.002	0.001	0	0	0.005	0.002	0.001	0	0	0.006	0.003	0.001	0.001	0
$\mathbf{2^{-2}}$	0.085	0.044	0.022	0.011	0.005	0.15	0.076	0.038	0.019	0.009	0.181	0.092	0.046	0.023	0.011
$\mathbf{2^{-4}}$	0.218	0.116	0.059	0.03	0.014	0.245	0.133	0.07	0.036	0.018	0.95	0.421	0.21	0.104	0.051
$\mathbf{2^{-6}}$	0.241	0.147	0.087	0.05	0.027	0.29	0.157	0.086	0.049	0.027	2.603	1.805	0.992	0.441	0.211
$\mathbf{2^{-8}}$	0.243	0.147	0.087	0.05	0.027	0.311	0.167	0.09	0.049	0.027	3.711	3.274	2.628	1.808	0.983
$\mathbf{2^{-10}}$	0.244	0.147	0.087	0.05	0.027	0.317	0.171	0.092	0.049	0.027	4.136	3.953	3.648	3.172	2.492
$\mathbf{2^{-12}}$	0.244	0.147	0.087	0.05	0.027	0.318	0.172	0.092	0.05	0.027	4.269	4.176	4.029	3.765	3.407
$\mathbf{2^{-14}}$	0.244	0.147	0.087	0.05	0.027	0.319	0.172	0.093	0.05	0.027	4.306	4.252	4.154	3.981	3.686
$\mathbf{2^{-16}}$	0.244	0.147	0.087	0.05	0.027	0.319	0.172	0.093	0.05	0.027	4.326	4.275	4.181	4.073	3.904
$\mathbf{2^{-18}}$	0.244	0.147	0.087	0.05	0.027	0.319	0.172	0.093	0.05	0.027	4.328	4.292	4.232	4.135	3.969
$\mathbf{2^{-20}}$	0.244	0.147	0.087	0.05	0.027	0.319	0.172	0.093	0.05	0.027	4.34	4.307	4.248	4.151	3.986
$\mathbf{E^N}$	**0.244**	**0.147**	**0.088**	**0.05**	**0.028**	**0.319**	**0.172**	**0.093**	**0.05**	**0.027**	**4.34**	**4.307**	**4.248**	**4.151**	**3.986**
	$\mathbf{R}_\varepsilon^{\mathbf{N}}$														
$\mathbf{2^{-0}}$	0.99	0.99	0.99	1	1	1.06	1.01	1	1	1	1.11	1.01	1	1	1
$\mathbf{2^{-2}}$	0.84	0.92	0.96	0.98	0.99	0.84	0.91	0.96	0.98	0.99	0.84	0.91	0.95	0.98	0.99
$\mathbf{2^{-4}}$	0.72	0.85	0.92	0.96	0.98	0.71	0.82	0.89	0.94	0.97	0.85	0.85	0.89	0.94	0.97
$\mathbf{2^{-6}}$	0.36	0.57	0.61	0.75	0.8	0.84	0.85	0.69	0.73	0.79	-0.24	0.36	0.94	0.89	0.91
$\mathbf{2^{-8}}$	0.4	0.58	0.61	0.75	0.8	0.85	0.88	0.78	0.77	0.78	-0.74	-0.54	-0.22	0.35	0.9
$\mathbf{2^{-10}}$	0.41	0.58	0.61	0.75	0.8	0.85	0.88	0.79	0.81	0.78	-0.85	-0.74	-0.66	-0.52	-0.21
$\mathbf{2^{-12}}$	0.41	0.58	0.61	0.75	0.8	0.85	0.88	0.79	0.82	0.78	-0.8	-0.64	-0.65	-0.67	-0.64
$\mathbf{2^{-14}}$	0.41	0.58	0.61	0.75	0.8	0.84	0.88	0.79	0.82	0.78	-0.46	-0.43	-0.42	-0.49	-0.59
$\mathbf{2^{-16}}$	0.41	0.58	0.61	0.75	0.8	0.84	0.88	0.79	0.82	0.78	-0.17	-0.32	-0.23	-0.24	-0.33
$\mathbf{2^{-18}}$	0.41	0.58	0.61	0.75	0.8	0.84	0.88	0.79	0.82	0.78	-0.09	-0.28	-0.16	-0.12	-0.13
$\mathbf{2^{-20}}$	0.41	0.58	0.61	0.75	0.8	0.84	0.88	0.79	0.82	0.78	-0.07	-0.27	-0.14	-0.08	-0.06
$\mathbf{R^N}$	**0.72**	**0.62**	**0.61**	**0.63**	**0.87**	**0.84**	**0.88**	**0.76**	**0.82**	**0.79**	**-0.11**	**-0.05**	**-0.02**	**0**	**0**

Table 5.1: Approximate errors $\tilde{E}_\varepsilon^N$ (as defined in (5.4.3)) and computed rates of convergence R_ε^N and R^N (as defined in ((3.4.4), pg. 82)), measured from the numerical solutions of ($\mathscr{I}_\varepsilon$) with the problem data (5.4.1), solved exactly using the numerical method (($\mathscr{I}_\varepsilon^N$), (5.3.1), (5.4.2)) for $d^N = d$, $d^N \approx d - 0.5\sigma$ and $d^N \approx d - \sigma$.

Example 5.2

In [8], the following problem class was studied: Find $z \in C^1(0,1)$ such that

$$(\varepsilon z'' - \tilde{a} z')(x) = q(x), \quad x \in (0,1) \setminus d, \quad z(0) = z_0,\ z(1) = z(1), \tag{5.4.4a}$$

$$\tilde{a}(x) > \tilde{\alpha} > 0,\ x < \tilde{d}, \quad \tilde{a}(x) < -\tilde{\alpha},\ x > \tilde{d}. \tag{5.4.4b}$$

The convection coefficient $\tilde{a}$ has a discontinuity at $x = \tilde{d}$. Note that we have transformed the problem in [8] with $x = 1 - \hat{x}$. The Scheme analysed in [8] with which to numerically solve (5.4.4) can be written as follows

Numerical Scheme 5.1 ([8]). *Find a mesh function Z^N such that*

$$(\varepsilon\delta^2 Z^N + \tilde{a}\tilde{D}Z^N)(x_i) = \tilde{q}(x_i), \quad x_i \in \Omega^N \setminus \{x_{\frac{N}{2}}\}, \quad Z^N(0) = z_0, \quad Z^N(1) = z_1, \tag{5.4.5}$$

$$D^- Z^N(x_{\frac{N}{2}}) = D^+ Z^N(x_{\frac{N}{2}}), \tag{5.4.6}$$

$$\tilde{D} := \begin{cases} D^- & \text{if } i < \frac{N}{2} \\ D^+ & \text{if } i > \frac{N}{2} \end{cases} \tag{5.4.7}$$

where Ω^N is described as

$$x_i \in \Omega_\varepsilon^N : x_i = \left\{ \begin{array}{cc} \frac{4(d-\sigma_0)}{N} i, & 0 \leqslant i \leqslant \frac{N}{4}, \\ d - \sigma_0 + \frac{4\sigma_0}{N}(i - \frac{N}{4}), & \frac{N}{4} < i \leqslant \frac{N}{2}, \\ d + \frac{4\sigma_1}{N}(i - \frac{N}{2}), & \frac{N}{2} < i \leqslant \frac{3N}{4}, \\ d + \sigma_1 + \frac{4(1-d-\sigma_1)}{N}(i - \frac{3N}{4}), & \frac{3N}{4} < i \leqslant N, \end{array} \right\} \tag{5.4.8a}$$

$$\sigma_j := \min\left\{ \frac{d + (1-2d)j}{2}, \frac{\varepsilon}{\tilde{\alpha}} \ln N \right\}, \quad j = 0, 1. \tag{5.4.8b}$$

We compare numerical solutions (Z_ε^N), generated from the Numerical Scheme 5.1, with numerical solutions (U_ε^N), generated from the Numerical Scheme ($(\mathscr{I}_\varepsilon^N)$, (5.3.1)) when we choose a_ε s.t. $a_\varepsilon \to \tilde{a}$ as $\varepsilon \to 0$. We consider $(\mathscr{I}_\varepsilon)$ and (5.4.4) with

$$d = \tilde{d} = 0.6, \quad a_\varepsilon(x) = 2.25 \tanh((0.6 - x)/\varepsilon), \tag{5.4.9a}$$

$$\tilde{a}(x) = 2.25, \quad x < d, \quad \tilde{a}(x) = -2.25, \quad x > d, \tag{5.4.9b}$$

$$b(x) = 0, \quad q(x) = \tilde{q}(x) = \cos(3x), \quad A = z_0 = 2, \quad B = z_1 = -3. \tag{5.4.9c}$$

We choose $r = 1$ and $\theta = 2.1$.

We solve both problems numerically for various values of ε and N. In Table 5.2, we present the maximum pointwise differences defined by

$$\tilde{E}_\varepsilon^N := \max_{x_i \in \Omega_\varepsilon^N} |\overline{Z}_\varepsilon^N - U_\varepsilon^N|, \tag{5.4.10}$$

where $\overline{Z}_\varepsilon^N$ is the interpolant of Z_ε^N.

	$\tilde{E}_\varepsilon^N$						
ε \ N	**N=32**	**N=64**	**N=128**	**N=256**	**N=512**	**N=1024**	**N=2048**
10^{-1}	0.3573	0.3894	0.4259	0.4457	0.4534	0.4557	0.456
10^{-2}	0.3518	0.4	0.4288	0.4389	0.4423	0.4442	0.445
10^{-3}	0.338	0.3881	0.4212	0.4342	0.4395	0.4424	0.4437
10^{-4}	0.3364	0.3866	0.4199	0.4332	0.4387	0.4418	0.4433
10^{-5}	0.3363	0.3864	0.4198	0.4331	0.4386	0.4417	0.4432
10^{-6}	0.3363	0.3864	0.4198	0.4331	0.4386	0.4417	0.4432

Table 5.2: Maximum pointwise differences $\tilde{E}_\varepsilon^N$ (as defined in (5.4.10)), between the Numerical Solutions of ($\mathscr{I}_\varepsilon$), with convection coefficient a_ε), approximated by solving the Numerical Scheme ($\mathscr{I}_\varepsilon^N$), (5.3.1)) exactly and the Numerical Solutions of ((5.4.4), with convection coefficient $\tilde{a}$), approximated by solving the Numerical Scheme 5.1 exactly, all with the problem data (5.4.9), where $\lim_{\varepsilon\downarrow 0} a_\varepsilon = \tilde{a}$.

Remark: In the nonlinear problem (1) the convection coefficient u of u' is C^1. In an attempt to mimic the analysis of the linear problem in studying the nonlinear problem (1), it is felt that analysing the linear problem with a continuous convection coefficient rather than the discontinuous coefficient is more appropriate. Table 5.2 indicates that even though $a_\varepsilon(x) \to \tilde{a}(x)$ for small ε, the solutions to ($\mathscr{I}_\varepsilon$) and (5.4.4) are distinct and the character of the interior layer is different in both solutions.

Example 5.3 (**Equivalent time-dependent problem associated with** ($\mathscr{I}_\varepsilon$))
In this example, we consider the following finite difference scheme:

Numerical Scheme 5.2. *Find Y_ε^N such that*

$$\mathcal{L}_\varepsilon^{N,M} Y_\varepsilon^N(x_i,t_j) := (\varepsilon\delta^2 - a_\varepsilon D_x - b - D_t^-) Y_\varepsilon^N(x_i,t_j) = q(x_i,t_j),$$

$$x_i \in \Omega^N, \quad t_j \in \Gamma^M = \{t_j = Tj/M,\ 0 \leqslant j \leqslant M\},$$

$$Y_\varepsilon^N(0,t_j) = A, \quad Y_\varepsilon^N(1,t_j) = B, \quad t_j > 0, \quad Y_\varepsilon^N(x_i,0) = g(x_i), \quad x_i \in \overline{\Omega}^N$$

$$D_x := \{D_x^-, \quad a_\varepsilon(x_i,t_j) \geqslant 0, \qquad D_x^+, \quad a_\varepsilon(x_i,t_j) < 0\},$$

where Ω^N is as defined in (5.3.1) and a_ε, b and q as in ($\mathscr{I}_\varepsilon$).

This scheme is the scheme ($\mathscr{I}_\varepsilon^N$, (5.3.1)) with the addition of time dependence. We consider

the Numerical Scheme 5.2 with

$$a_\varepsilon(x,t)=(2.25+x^2)\tanh(\tfrac{1.1}{\varepsilon}(0.6-x)),\quad b(x,t)=e^{-5x}, \tag{5.4.11a}$$

$$q(x,t)=\cos(3x),\quad A=2,\quad B=-3,\quad d=0.6,\quad g(x)=Bx+A(1-x). \tag{5.4.11b}$$

We choose $2<\theta<2.25$ and $r=1$. We let $p=0$ and center the mesh at d and we also consider $p=0.5$ and centre the mesh at $d^N\approx d+0.5\sigma$ ($|d^N-d|<0.5\sigma$). Note that, apart from zero order, we do not set any compatibility conditions here. Table 5.3 shows the computed rates of convergence R_ε^N and R^N defined by

$$E_\varepsilon^N(x_i,t_j)=|(Y_\varepsilon^{N,N}-\overline{Y}_\varepsilon^{2N,2N})(x_i,t_j)|,\quad D_\varepsilon^N:=\max_{(x_i,t_j)\in\overline{\Omega}^N\times\Gamma^N}E^N(x_i,t_j), \tag{5.4.12a}$$

$$D^N:=\max_\varepsilon D_\varepsilon^N,\quad R_\varepsilon^N:=\log_2\frac{D_\varepsilon^N}{D_\varepsilon^{2N}}\quad\text{and}\quad R^N:=\log_2\frac{D^N}{D^{2N}}, \tag{5.4.12b}$$

where $\overline{Y}_\varepsilon^{2N,2N}$ is the bilinear interpolation of $Y_\varepsilon^{2N,2N}$, a numerical solution of the Numerical Scheme 5.2 using $2N$ mesh intervals in both space and time.

	$\mathbf{R_\varepsilon^N}$											
	p = 0						**p = 0.5**					
N / ε	**N=8**	**N=16**	**N=32**	**N=64**	**N=128**	**N=256**	**N=8**	**N=16**	**N=32**	**N=64**	**N=128**	**N=256**
$\mathbf{2^{-0}}$	0.48	0.71	0.71	0.82	0.90	0.95	0.68	0.72	0.72	0.82	0.90	0.95
$\mathbf{2^{-1}}$	0.49	0.75	0.85	0.91	0.95	0.97	0.88	0.74	0.85	0.92	0.96	0.98
$\mathbf{2^{-2}}$	0.53	0.72	0.83	0.92	0.96	0.98	0.36	0.67	0.82	0.91	0.95	0.98
$\mathbf{2^{-3}}$	0.41	0.64	0.79	0.88	0.93	0.97	0.07	0.45	0.65	0.84	0.90	0.95
$\mathbf{2^{-4}}$	0.48	0.32	0.68	0.81	0.89	0.94	0.09	0.44	0.64	0.77	0.86	0.92
$\mathbf{2^{-5}}$	0.45	0.42	0.56	0.65	0.72	0.74	-0.06	0.52	0.70	0.69	0.76	0.89
$\mathbf{2^{-6}}$	0.42	0.40	0.53	0.60	0.68	0.78	-0.14	0.47	0.67	0.72	0.74	0.80
$\mathbf{2^{-7}}$	0.41	0.39	0.50	0.56	0.64	0.72	-0.19	0.44	0.66	0.69	0.71	0.75
$\mathbf{2^{-8}}$	0.41	0.39	0.49	0.54	0.60	0.63	-0.21	0.42	0.65	0.67	0.69	0.71
$\mathbf{2^{-9}}$	0.41	0.38	0.49	0.52	0.56	0.59	-0.22	0.42	0.64	0.66	0.67	0.67
$\mathbf{2^{-10}}$	0.42	0.38	0.48	0.52	0.54	0.56	-0.22	0.41	0.64	0.65	0.65	0.63
$\mathbf{2^{-11}}$	0.42	0.38	0.48	0.51	0.53	0.55	-0.22	0.41	0.64	0.65	0.65	0.61
$\mathbf{2^{-12}}$	0.42	0.38	0.48	0.51	0.52	0.54	-0.22	0.41	0.63	0.65	0.64	0.60
.	.	.	.	.	.	.	.	.	.	.	.	.
.	.	.	.	.	.	.	.	.	.	.	.	.
.	.	.	.	.	.	.	.	.	.	.	.	.
$\mathbf{2^{-20}}$	0.42	0.38	0.48	0.51	0.52	0.53	-0.23	0.41	0.63	0.65	0.64	0.59
$\mathbf{R^N}$	**0.42**	**0.38**	**0.48**	**0.51**	**0.52**	**0.53**	**-0.23**	**0.41**	**0.63**	**0.65**	**0.64**	**0.59**

Table 5.3: Computed rates of convergence R_ε^N and R^N (as defined in (5.4.12)), measured from the numerical solutions of the numerical method 5.2, with the problem data, including q, as in (5.4.11).

We repeat this example except we chose q so that compatibility conditions at the corners are

satisfied i.e. $(\varepsilon g_{xx} - a_\varepsilon g_x - bg - g_t)(c,0) = q(c)$, for $c = 0, 1$. An example of such a q is

$$q(x) = (5a_\varepsilon(0) - 2b(0))\cos\tfrac{\pi}{2}x + (5a_\varepsilon(1) + 3b(1))\sin\tfrac{\pi}{2}x. \tag{5.4.13}$$

	$\mathbf{R_\varepsilon^N}$											
	p = 0						**p = 0.5**					
N / ε	**N=8**	**N=16**	**N=32**	**N=64**	**N=128**	**N=256**	**N=8**	**N=16**	**N=32**	**N=64**	**N=128**	**N=256**
$\mathbf{2^{-0}}$	0.57	0.74	0.85	0.92	0.96	0.98	0.53	0.73	0.84	0.92	0.96	0.98
$\mathbf{2^{-1}}$	0.53	0.73	0.88	0.94	0.97	0.98	0.43	0.71	0.86	0.93	0.97	0.98
$\mathbf{2^{-2}}$	0.39	0.66	0.83	0.91	0.95	0.98	0.47	0.55	0.78	0.89	0.94	0.97
$\mathbf{2^{-3}}$	1.06	0.57	0.77	0.87	0.93	0.96	1.06	0.36	0.63	0.78	0.89	0.94
$\mathbf{2^{-4}}$	1.06	0.58	0.66	0.82	0.90	0.95	1.03	0.49	0.61	0.76	0.87	0.93
$\mathbf{2^{-5}}$	0.73	0.92	0.77	0.66	0.71	0.74	0.63	0.78	0.63	0.66	0.77	0.91
$\mathbf{2^{-6}}$	0.65	0.85	0.94	0.65	0.71	0.82	0.48	0.82	0.63	0.75	0.78	0.84
$\mathbf{2^{-7}}$	0.61	0.82	0.95	0.71	0.70	0.81	0.46	0.83	0.64	0.76	0.78	0.84
$\mathbf{2^{-8}}$	0.59	0.81	0.94	0.75	0.69	0.80	0.45	0.82	0.67	0.76	0.78	0.84
$\mathbf{2^{-9}}$	0.58	0.80	0.93	0.77	0.69	0.79	0.44	0.81	0.68	0.76	0.78	0.83
$\mathbf{2^{-10}}$	0.57	0.80	0.93	0.78	0.69	0.79	0.44	0.80	0.69	0.75	0.78	0.83
.	.	.	.	.	.	.	.	.	.	.	.	.
.	.	.	.	.	.	.	.	.	.	.	.	.
.	.	.	.	.	.	.	.	.	.	.	.	.
$\mathbf{2^{-20}}$	0.57	0.80	0.92	0.79	0.68	0.78	0.43	0.80	0.69	0.75	0.78	0.83
$\mathbf{R^N}$	**0.57**	**0.80**	**0.92**	**0.79**	**0.68**	**0.78**	**0.43**	**0.80**	**0.69**	**0.75**	**0.78**	**0.83**

Table 5.4: Computed rates of convergence R_ε^N and R^N (as defined in (5.4.12)), measured from the numerical solutions of the numerical method 5.2, with the problem data (5.4.11) except with q as in (5.4.13).

Furthermore, Figures 5.2-5.5 display contour plots of the computed error, $|(Y_\varepsilon^{1024,1024} - \overline{Y}_\varepsilon^{2048,2048})(x_i,t_j)|$, for $\varepsilon = 2^{-15}$, but with computing the scheme 5.2 with either q defined in ($\mathscr{I}_\varepsilon$) or in (5.4.13). Note that the graphs in Figures 5.3 and 5.5 are the same graphs that are shown in Figures 5.2 and 5.4 only on a finer interval on the x-axis.

Observe the significant influence of the compatability condition (5.4.13) on the distribution of the error. When there is only minimal compatibility imposed, the errors are largest along the characteristics emanating from the corners. When additional compatibility is imposed, the largest error is at the interior layer.

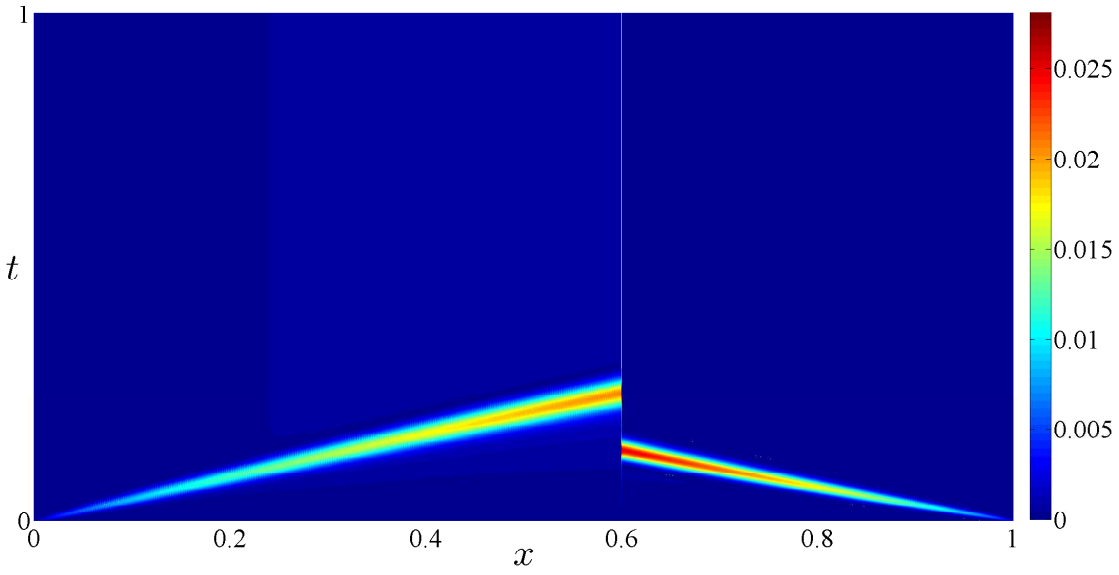

Figure 5.2: Contour plot of the computed error $E_\varepsilon^{1024}(x_i,t_j)$ (as defined in (5.4.12)) over $(x_i,t_j)\in[0,1]\times[0,1]$, computed using the numerical method 5.2, with the problem data, including q, as in (5.4.11), with $d=0.6$ and $\varepsilon=2^{-15}$.

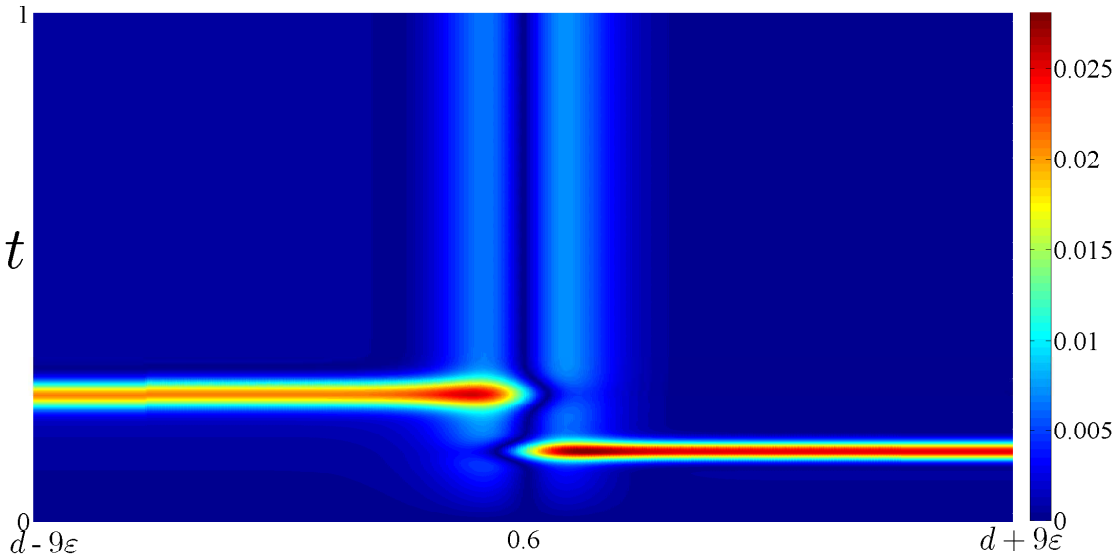

Figure 5.3: Contour plot of the computed error $E_\varepsilon^{1024}(x_i,t_j)$ (as defined in (5.4.12)) over $(x_i,t_j)\in[d-9\varepsilon,d+9\varepsilon]\times[0,1]$, computed using the numerical method 5.2, with the problem data, including q, as in (5.4.11), with $d=0.6$ and $\varepsilon=2^{-15}$.

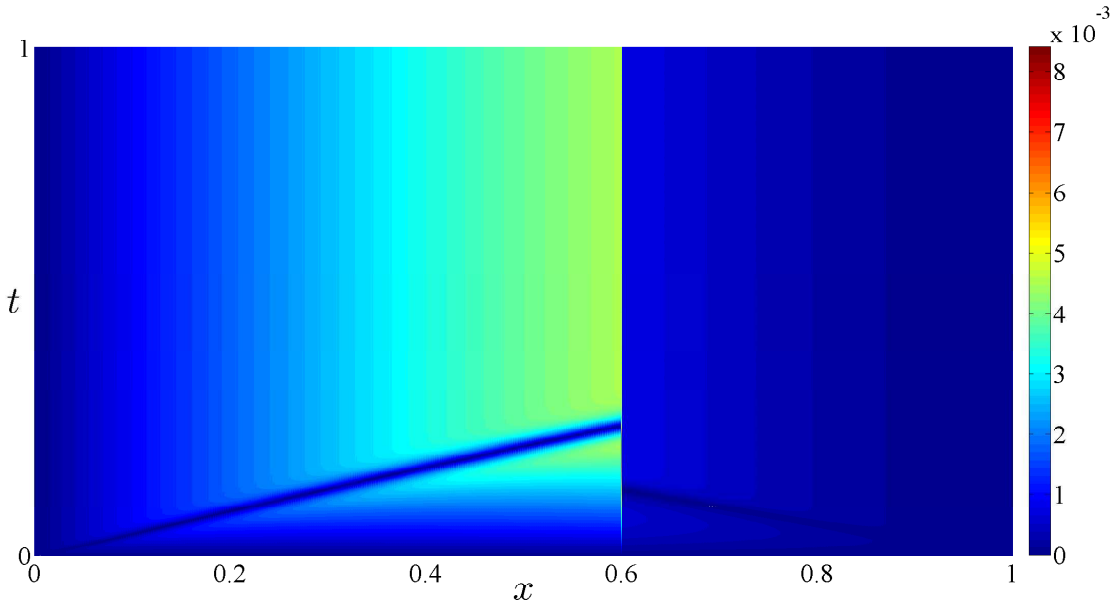

Figure 5.4: Contour plot of the computed error $E_\varepsilon^{1024}(x_i,t_j)$ (as defined in (5.4.12)) over $(x_i,t_j)\in[0,1]\times[0,1]$, computed using the numerical method 5.2, with the problem data (5.4.11), except with q as in (5.4.13), with $d=0.6$ and $\varepsilon=2^{-15}$.

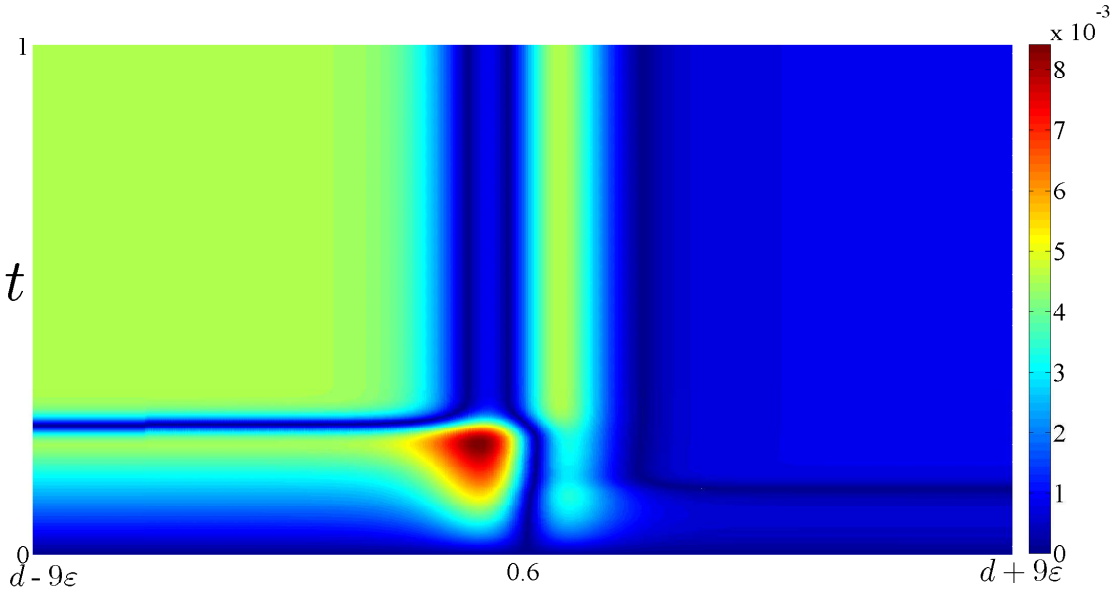

Figure 5.5: Contour plot of the computed error $E_\varepsilon^{1024}(x_i,t_j)$ (as defined in (5.4.12)) over $(x_i,t_j)\in[d-9\varepsilon,d+9\varepsilon]\times[0,1]$, computed using the numerical method 5.2, with the problem data (5.4.11), except with q as in (5.4.13), with $d=0.6$ and $\varepsilon=2^{-15}$.

CHAPTER: 6

SHISHKIN ALGORITHM

6.1: INTRODUCTION

In [32] Shishkin presented a computational algorithm that is parameter-uniform for a class of time-dependent quasilinear singularly perturbed differential equations, whose solutions contain an internal shock layer. The algorithm is intricate, mainly due to the fact that the location of the internal layer is tracked at all time levels and the path of the inflexion point is approximated by a sufficiently smooth curve in time. No numerical experiments were presented in [1] to illustrate the details of the algorithm in practice.

The established error bounds in [32] cannot immediately be described as parameter-uniform. The error bounds can be described in the same manner as (4.1.2, §4.1) whereby a uniform convergence rate is established in an area away from the smooth curve and a uniform convergence rate is also established in an area around the smooth curve, but which is reliant on an insufficiently known transformation. We describe this error bound below before presenting some numerical experiments.

6.2: OUTLINE OF THE SHISHKIN ALGORITHM

We describe the algorithm applied to a sub-class of the problem class considered in [32]. We make minor modifications below for practical purposes to ease implementation. In the case of a notable modification, a remark is included to inform the reader. Consider the following problem class on the domain $G = \Omega \times (0,T]$, $\Omega = (0,1)$, $\Gamma = (0,T)$; Find y_ε such that

$$\begin{aligned} \left(\varepsilon \tfrac{\partial^2}{\partial x^2} - 2y_\varepsilon \tfrac{\partial}{\partial x} - b - \tfrac{\partial}{\partial t}\right) y_\varepsilon(x,t) = q(x,t), \quad (x,t) \in G, \\ y_\varepsilon(0,t) = A > 0, \quad y_\varepsilon(1,t) = B < 0, \quad t \in [0,T], \\ y_\varepsilon(x,0) = u_\varepsilon(x;d), \quad x \in \Omega, \quad b(x,t) \geqslant 0, \quad (x,t) \in \overline{G}, \end{aligned} \tag{$\mathscr{J}_\varepsilon$}$$

where $u_\varepsilon(0;d)=A$, $u_\varepsilon(d;d)=0$ and $u_\varepsilon(1;d)=B$ for some $d\in(0,1)$. On either side of d, the initial condition can be decomposed into a regular component v and a layer component w. On the interval $[0,d]$, $u_\varepsilon=v_L+w_L$ and on $[d,1]$, $u_\varepsilon=v_R+w_R$ where v_L, v_R and a sufficient number of their derivatives are bounded independently of ε. Also it is assumed

$$|w^{(k)}_{L(R)}(x)|\leqslant C\varepsilon^{-k}e^{-C\frac{|d-x|}{\varepsilon}},\quad 1\leqslant k\leqslant 5,\quad x\in[0,d]\,([d,1]).$$

For a sample initial condition, we take $u_\varepsilon=u_L$, $x\leqslant d$ and $u_\varepsilon=u_R$, $x>d$ where u_L and u_R are the solutions of the linear singularly perturbed b.v.p.'s:

$$\left(\varepsilon\frac{d^2}{dx^2}-a_L\frac{d}{dx}-b_L\right)u_L(x)=q_L(x),\quad x\in(0,d),\quad u_L(0)=A,\quad u_L(d)=0, \tag{6.2.1a}$$

$$\left(\varepsilon\frac{d^2}{dx^2}+a_R\frac{d}{dx}-b_R\right)u_R(x)=q_R(x),\quad x\in(d,1),\quad u_R(d)=0,\quad u_R(1)=B, \tag{6.2.1b}$$

$$a_L(x)\geqslant\alpha_L>0,\ x\in[0,d],\quad a_R(x)\leqslant-\alpha_R<0,\ x\in[d,1]. \tag{6.2.1c}$$

Note that we consider left and right problems to ensure $u_\varepsilon(d)=0$. Denote N and M as the space and time discretisation parameters respectively. For convenience, we define the following Shishkin meshes

$$\bar\Omega_L^{N,d,\theta}=\left\{x_i\;\middle|\;\begin{array}{ll}x_i=\frac{2(d-\sigma_d)}{N}i, & 0\leqslant i\leqslant\frac{N}{2},\\ x_i=d-\sigma_d+\frac{2\sigma_d}{N}(i-\frac{N}{2}), & \frac{N}{2}<i\leqslant N,\end{array}\right\}, \tag{6.2.2a}$$

$$\bar\Omega_R^{N,d,\theta}=\left\{x_i\;\middle|\;\begin{array}{ll}x_i=d+\frac{2\sigma_{1-d}}{N}i, & 0\leqslant i\leqslant\frac{N}{2},\\ x_i=d+\sigma_{1-d}+\frac{2(1-d-\sigma_{1-d})}{N}(i-\frac{N}{2}), & \frac{N}{2}<i\leqslant N,\end{array}\right\}, \tag{6.2.2b}$$

$$\sigma_\mu=\min\left\{\frac{\mu}{2},\theta\varepsilon\log N\right\},\quad \Omega^{N,d,\theta}_{L\backslash R}=\bar\Omega^{N,d,\theta}_{L\backslash R}\setminus\{x_0,x_N\}. \tag{6.2.2c}$$

We define the numerical approximation $U^N_\varepsilon(x;d)$, of the initial condition u_ε, as the solution of the following discretisation of (6.2.1):

$$U^N_\varepsilon(x_i;d)=U^N_L(x_i),\ x_i\in\bar\Omega_L^{\frac{N}{2},d,\alpha_L},\quad U^N_\varepsilon(x_i;d)=U^N_R(x_i),\ x_i\in\bar\Omega_R^{\frac{N}{2},d,\alpha_R}, \tag{6.2.3a}$$

$$(\varepsilon\delta^2-a_LD^--b_L)U^N_L(x_i)=q_L(x_i),\quad x_i\in\Omega_L^{\frac{N}{2},d,\frac{1}{\alpha_L}},\quad U^N_L(0)=A,\ U^N_L(d)=0, \tag{6.2.3b}$$

$$(\varepsilon\delta^2+a_RD^+-b_R)U^N_R(x_i)=q_R(x_i),\quad x_i\in\Omega_R^{\frac{N}{2},d,\frac{1}{\alpha_R}},\quad U^N_R(d)=0,\ U^N_R(1)=B. \tag{6.2.3c}$$

If $\varepsilon>(N^{-2/5}+M^{-2/5})$ then we discretise the parabolic problem ($\mathscr{J}_\varepsilon$) on a uniform grid as follows: Find Y^N_ε such that

$$\begin{aligned}&(\varepsilon D_x^-D_x^+Y^N_\varepsilon-D_x^-(Y^N_\varepsilon)^2-bY^N_\varepsilon-D_t^-Y^N_\varepsilon)(x_i,t_j)=q(x_i,t_j),\quad (x_i,t_j)\in G^{N,M},\\ &Y^N_\varepsilon(0,t_j)=A,\ Y^N_\varepsilon(1,t_j)=B,\ t_j\in\overline\Gamma^M,\quad Y^N_\varepsilon(x_i,0)=\bar U_\varepsilon(x_i;d),\ x_i\in\Omega^N,\end{aligned} \tag{$\mathscr{J}^N_\varepsilon$}$$

where $\overline\Omega^N=\overline\Omega\cap\{x_i|x_i=\frac{i}{N},\ i=0,\ldots,N\}$, $\Omega^N=\Omega\cap\overline\Omega^N$, $\overline\Gamma^M=\overline\Gamma\cap\{t_j|t_j=\frac{j}{M},\ j=0,\ldots,M\}$, $\Gamma^M=\Gamma\cap\overline\Gamma^M$, $\overline G^{N,M}=\overline\Omega^N\times\overline\Gamma^M$, $G^{N,M}=G\cap\overline G^{N,M}$ and $\bar U_\varepsilon$ is the linear interpolant of $\{U^N_L,U^N_R\}$

(6.2.3) onto Ω.

If $\varepsilon \leqslant (N^{-2/5} + M^{-2/5})$ then we follow the algorithm outlined below. There exists a function $s(t)$ for which $y_\varepsilon(s(t),t) = 0$, $(s(t),t) \in \overline{G}$. A transition layer appears in the vicinity of $s(t)$ for all $t \in [0,T]$. Consider the following reduced left and right boundary initial value problems:

$$\left(-2y_L\frac{\partial}{\partial x} - b - \frac{\partial}{\partial t}\right) y_L(x,t) = q(x,t), \quad (x,t) \in ((0,d]\times(0,T]) \cap G, \tag{6.2.4a}$$

$$y_L(0,t) = A, \quad t \in [0,T], \qquad y_L(x,0) = v_L(x), \quad x \in (0,d] \cap \Omega, \tag{6.2.4b}$$

$$\left(-2y_R\frac{\partial}{\partial x} - b - \frac{\partial}{\partial t}\right) y_R(x,t) = q(x,t), \quad (x,t) \in ([d,1)\times(0,T]) \cap G, \tag{6.2.4c}$$

$$y_R(x,0) = v_R(x), \quad x \in [d,1) \cap \Omega, \qquad y_R(1,t) = B, \quad t \in [0,T]. \tag{6.2.4d}$$

Define

$$y(\eta,t) = \begin{cases} y_L(x,t) & \eta < d, \\ (y_L + y_R)(d,t) & \eta = d, \\ y_R(x,t) & \eta > d. \end{cases}$$

The leading term of the asymptotic expansion of $s(t)$ in ε is the solution, s_0, of the nonlinear initial value problem

$$s_0'(t) = y(s_0(t),t), \quad t \in (0,T], \quad s_0(0) = d. \tag{6.2.5}$$

We wish to discretise (6.2.4)-(6.2.5), but first we construct a global approximation V_L^N to v_L by interpolation and extrapolation as follows:

$$V_L^N(\eta) = \begin{cases} \bar{U}_L^N(\eta), & 0 \leqslant \eta \leqslant x_{\frac{N}{4}}, \\ p_L(\eta) = \alpha\eta^2 + \beta\eta + \gamma, & x_{\frac{N}{4}} < \eta \leqslant d, \end{cases}, \quad x_{\frac{N}{4}} \in \bar{\Omega}_L^{\frac{N}{2},d,\frac{1}{\alpha_L}},$$

where $\bar{U}_L$ is the linear interpolant of U_L^N and α, β and γ are chosen so that $p_L(x_{\frac{N}{4}}) = U_L^N(x_{\frac{N}{4}})$, $D^- p_L(x_{\frac{N}{4}}) = D^- U_L^N(x_{\frac{N}{4}})$ and $\delta^2 p_L(x_{\frac{N}{4}-1}) = \delta^2 U_L^N(x_{\frac{N}{4}-1})$. We construct V_R^N in an analogous manner.

Discretising (6.2.4), we solve the following reduced left and right discrete boundary initial value problems:

$$(-2Y_L^N D_x^- - D_t^- - b)Y_L^N(x_i,t_j) = q(x_i,t_j), \quad (x_i,t_j) \in ((0,d]\times(0,T]) \cap G^{N,M},$$
$$Y_L^N(0,t_j) = A, \quad t_j \in \overline{\Gamma}^M, \quad Y_L^N(x_i,0) = V_L^N(x_i), \quad x_i \in (0,d] \cap \Omega^N,$$

$$(-2Y_R^N D_x^+ - D_t^- - b)Y_R^N(x_i,t_j) = q(x_i,t_j), \quad (x_i,t_j) \in ([d,1)\times(0,T]) \cap G^{N,M},$$
$$Y_R^N(x_i,0) = V_R^N(x_i), \quad x_i \in [d,1) \cap \Omega^N, \quad Y_R^N(1,t_j) = B, \quad t_j \in \overline{\Gamma}^M.$$

Define

$$Y^N(\eta,t_j)=\begin{cases} Y_L^N(x_i,t_j) & \eta\in[x_i,x_{i+1})\subset\overline{\Omega}^N,\ \eta<d,\ t_j\in\overline{\Gamma}^M \\ (Y_L^N+Y_R^N)(d,t_j) & \eta=d,\ \text{only if } d\in\overline{\Omega}^N,\ t_j\in\overline{\Gamma}^M, \\ Y_R^N(x_i,t_j) & \eta\in[x_i,x_{i+1})\subset\Omega^N,\ \eta>d,\ t_j\in\overline{\Gamma}^M \end{cases}$$

and discretise (6.2.5) and solve for $S^{M/2}$, the discrete approximation to s_0, using $M/2$ uniform mesh intervals with the following Runge Kutta scheme

$$\hbar=2\frac{T}{M},\ S^{M/2}(\tau_0)=d,\quad S^{M/2}(\tau_j)=S^{M/2}(t_{2(j-1)})+\frac{\hbar}{6}(k_1+2k_2+2k_3+k_4), \tag{6.2.6a}$$

$$k_1=Y^N(S^{M/2}(t_{2(j-1)}),t_{2(j-1)}),\quad k_2=Y^N(S^{M/2}(t_{2(j-1)})+\tfrac{k_1}{2},t_{2j-1}), \tag{6.2.6b}$$

$$k_3=Y^N(S^{M/2}(t_{2(j-1)})+\tfrac{k_2}{2},t_{2j-1}),\quad k_4=Y^N(S^{M/2}(t_{2(j-1)})+k_3,t_{2j}). \tag{6.2.6c}$$

$$j=1,\dots,M/2,\quad \tau_j\in\overline{\Gamma}^{\frac{M}{2}},\quad t_l\in\overline{\Gamma}^M,\quad l=0,\dots,M. \tag{6.2.6d}$$

Note *The algorithm in [32] states that a backward Eular scheme can be used to discretise (6.2.5), however for higher accuracy, we choose to use a Runge Kutta (RK) scheme. Note also, that we approximate $S^{M/2}$ on $M/2+1$ mesh points since the RK scheme requires evaluation of Y^N on the mid-points of the uniform mesh used in the RK scheme, which is possible because Y^N is evaluated on a uniform mesh in time with $M+1$ mesh-points, all either overlapping of lying half way between the RK mesh-points. An alternative method is to use $M+1$ mesh points with the RK scheme to solve for S^M and use interpolation to approximate Y^N at the midpoints, however we did not desire any extra error, however small.*

Note *Later, for practical purposes, we need to define $S^{M/2}$ beyond T. We extend Y^N to $\bar{Y}^N$ s.t*

$$\bar{Y}^N(\eta,t_j)=Y^N(\eta,t_j),\quad t_j\leqslant T,\quad t_j\in\overline{\Gamma}^M\qquad \textit{and}\qquad \bar{Y}^N(\eta,t)=Y(\eta,T),\quad t>T,$$

which is suitable assuming Y_L^N and Y_R^N have reached steady-state by time T. We can then continue to solve iteratively for $S^{M/2}$ beyond T as far as required on the extended mesh

$$\bar{\Gamma}^+=\overline{\Gamma}^{\frac{M}{2}}\cup\{\tau_{i+\frac{M}{2}}=\hbar i|i=1,2,3,\dots\}.$$

The algorithm now performs a "smoothing" routine on $S^{M/2}$ to retrieve a continuous function $s^*(t)$. Construct the piecewise constant function $\bar{s}$ as follows

$$\bar{s}(\eta)=\begin{cases} d, & \eta\leqslant 0 \\ S^{M/2}(\tau_j), & \eta\in(\tau_{j-1},\tau_j]\subset\bar{\Gamma}^+. \end{cases} \tag{6.2.7}$$

The algorithm requires the construction of a "piecewise-quadratic, nonnegative, compactly supported function", ω, with support on the set $[-L,L]$, $L=\frac{1}{\sqrt{M}}$, with $\omega\in C^1(-L,L)$ and

$\int_{-L}^{L} \omega(\chi)\, d\chi = 1$ where M is the time discretisation parameter. An example of such a function is

$$\omega(\chi) = \begin{cases} \frac{2}{L^3}(\chi + L)^2, & \chi \in [-L, -\frac{L}{2}), \\ -\frac{2}{L^3}\chi^2 + \frac{1}{L}, & \chi \in [-\frac{L}{2}, \frac{L}{2}), \\ \frac{2}{L^3}(\chi - L)^2, & \chi \in [\frac{L}{2}, L]. \end{cases}$$

The function s^* is then constructed as follows

$$s^*(t) = \int_{t-L}^{t+L} \bar{s}(\eta)\omega(\eta - t)\, d\eta. \tag{6.2.8}$$

Note that $s^*(0) \neq d$. The integral in $s^*(t)$ and in it's derivative $s^{*\prime}(t)$ can be solved exactly by integrating over seperate intervals according to (6.2.7).

Note *The reason why we extend the definition of $S^{M/2}$ is so that $s^*(T)$ and $s^{*\prime}(T)$ are well defined.*

Applying the transform

$$\xi(x,t) = \tfrac{1}{2}(1 + \mu(x,t)(x - s^*(t))), \quad \mu(x,t) := \begin{cases} \frac{1}{s^*(t)}, & \text{for } x \leqslant s^*(t), \\ \frac{1}{1-s^*(t)}, & \text{for } x > s^*(t), \end{cases} \tag{6.2.9}$$

to the domains G and Ω, the problem ($\mathscr{J}_\varepsilon$) is transformed to the following problem ($\tilde{\mathscr{J}}_\varepsilon$):

$$\left(\frac{1}{\kappa_1^2}\left[\varepsilon\frac{\partial^2}{\partial\xi^2} + \kappa_1(\kappa_2 s^{*\prime}(t) - 2\tilde{y}_\varepsilon^{\pm})\frac{\partial}{\partial\xi}\right] - \tilde{b} - \frac{\partial}{\partial t}\right)\tilde{y}_\varepsilon^{\pm}(\xi,t) = \tilde{q}(\xi,t),$$

$$(\xi,t) \in \tilde{G}^{\pm}, \quad \kappa_1 = \kappa(s^*(t)), \quad \kappa_2 = \kappa(\xi), \quad \kappa(\lambda) = \begin{cases} 2\lambda, & \xi < \frac{1}{2}, \\ 2(1-\lambda), & \xi > \frac{1}{2}, \end{cases}, \tag{$\tilde{\mathscr{J}}_\varepsilon$}$$

$$\tilde{G}^+ = ((0, \tfrac{1}{2}) \times [0,T]) \cap \tilde{G}, \quad \tilde{G}^- = ((\tfrac{1}{2}, 1) \times [0,T]) \cap \tilde{G},$$

$$\tilde{y}_\varepsilon^-(0,t) = A, \quad \tilde{y}_\varepsilon^-(\tfrac{1}{2},t) = 0, \quad \tilde{y}_\varepsilon^+(\tfrac{1}{2},t) = 0, \quad \tilde{y}_\varepsilon^+(1,t) = B, \ t \in [0,T],$$

where $\tilde{G}$ is the transformed domain $\xi(G)$ and $\tilde{g}(\xi,t) = g(x^{-1}(\xi,t),t)$ where g is any of the functions b, q or u_ε.

Note *The transformation proposed in [32] is $\xi(x,t) = \frac{1}{2}(1 + x - s^*(t))$ i.e. with $\mu(x,t) = 1$ which maps $s^*(t) \mapsto \frac{1}{2}$ for all t. However, this transformation does not result in a rectangular domain when applied to $\bar{G}$ which would be ideal to solve the corresponding discrete problem, hence we modify the original prescribed transformation.*

We discretise $(\tilde{\mathscr{J}}_\varepsilon)$ as follows:

$$\left(\tfrac{1}{\kappa_1^2}\left[\varepsilon D_\xi^{S_1} D_\xi^{-S_1}\tilde{Y}_\varepsilon^{\pm,N} + \kappa_1\left(\kappa_2 s^{*\prime}(t_j) D_\xi^{S_2}\tilde{Y}_\varepsilon^{\pm,N} - D_\xi^{S_1}(\tilde{Y}_\varepsilon^{\pm,N})^2\right)\right] - \tilde{b} - D_t^-\tilde{Y}_\varepsilon^{\pm,N}\right)(\xi_i,t_j)$$

$$= \tilde{q}(\xi_i,t_j), \quad (\xi_i,t_j)\in\tilde{G}^{\frac{N}{2},M\pm}, \quad D_\xi^{S_1} = \begin{cases} D_\xi^-, & \xi_i \leqslant \frac{1}{2}, \\ D_\xi^+, & \xi_i > \frac{1}{2}, \end{cases}, \; D_\xi^{S_2} = D_\xi^{\operatorname{sgn}(\kappa_1\kappa_2 s^{*\prime}(t_j))},$$

$$\tilde{G}^{\frac{N}{2},M+} = \tilde{G}^+ \cap (\Omega_L^{\frac{N}{2},\frac{1}{2},\theta}\times\overline{\Gamma}^M), \; \tilde{G}^{\frac{N}{2},M-} = \tilde{G}^- \cap (\Omega_R^{\frac{N}{2},\frac{1}{2},\theta}\times\overline{\Gamma}^M), \qquad (\tilde{\mathscr{J}}_\varepsilon{}^N)$$

$$\theta > \tfrac{1}{5}\|y_L - y_R\|, \quad \kappa_1 = \kappa(s^*(t_j)), \quad \kappa_2 = \kappa(\xi_i),$$

$$\tilde{Y}_\varepsilon^{-,N}(0,t_j) = A, \quad \tilde{Y}_\varepsilon^{\pm,N}(\tfrac{1}{2},t_j) = 0, \quad \tilde{Y}_\varepsilon^{+,N}(1,t_j) = B, \;\; t_j\in\overline{\Gamma}^M,$$

$$\tilde{Y}_\varepsilon^{\pm,N}(\xi_i,0) = U^{*,N}(\xi_i) = \bar{U}_\varepsilon^N(\xi_i;s^*(0)), \qquad \xi_i\in\Omega_{L\backslash R}^{\frac{N}{2},\frac{1}{2},\theta}.$$

In [32], $U^{*,N}$ is not necessarily the discrete initial condition U_ε^N under the transform ξ but is prescribed as any function "somehow constructed" such that $|(U^* - \tilde{u}_\varepsilon)(\xi_i)| \leqslant C(N^{-1}+M^{-1})$. We propose to take

$$U^{*,N}(\xi_i) = \bar{U}_\varepsilon^N(\xi_i;s^*(0)) \tag{6.2.10}$$

where $\bar{U}_\varepsilon^N(\xi_i;s^*(0))$ is the interpolant of $U_\varepsilon^N(\xi_i;s^*(0))$ onto $[0,1]$ where $U_\varepsilon^N(\xi_i;s^*(0))$ is the solution of (6.2.3) centred at $s^*(0)$. Note that $\xi(s^*(0),t) = \frac{1}{2}$ and so $\tilde{Y}_\varepsilon^{\pm,N}(\frac{1}{2},t_j) = 0$ for all $t_j\in\overline{\Gamma}^M$. From the definition of s^* in (6.2.8), $s^*(0)\to d$ as $M\to\infty$ since $L\to 0$ and hence ω tends to the δ-function as $M\to\infty$. In this experiment, we do not establish the rate, in terms of N and M, at which $U_\varepsilon^N(\xi_i;s^*(0))$ converges to $u_\varepsilon(x;d)$.

Note *If $\tilde{x}_i\in\Omega$ is such that $\tilde{x}_i = \xi^{-1}(\xi_i)$ and Z^N is the inverse transform of $\tilde{Y}_\varepsilon^{\pm,N}$, that is $Z^N(\tilde{x}_i,t_j) = \tilde{Y}_\varepsilon^{\pm,N}(\xi^{-1}(\xi_i),t_j)$, then the error bounds presented in [32] for $\varepsilon\leqslant(N^{-2/5}+M^{-2/5})$ can be described as follows. For all $\tilde{x}_i\in\Omega$ such that $|\tilde{x}_i - s^*(t)|\geqslant C>0$, the following pointwise error bound holds:*

$$|(y_\varepsilon - Z^N)(\tilde{x}_i,t_j)| \leqslant C(N^{-1/5}(\ln N)^{1/2} + M^{-1/5}(\ln M)^{1/2}). \tag{6.2.11}$$

For all $\tilde{x}_i\in\Omega$ such that $|\tilde{x}_i - s^*(t)|\leqslant C$, the following error bound holds:

$$|y_\varepsilon(\tilde{x}_i + (s(t)-s^*(t)),t_j) - Z^N(\tilde{x}_i,t_j)| \leqslant C(N^{-1/5}(\ln N)^{1/2} + M^{-1/5}(\ln M)^{1/2}). \tag{6.2.12}$$

The error bound in (6.2.12) can be interpreted as meaning that if the solution y_ε is transformed using the map $y_\varepsilon(x)\mapsto y_\varepsilon((x+(s-s^*)(t))$ then Z^N is a uniform approximation for the solution y_ε under this transform. However, since s and hence $s-s^*$ is not sufficiently approximated, we would view this numerical method as theoretical rather than practical for sufficiently small values of ε.

Note *In [31], Shishkin examines a class of problems containing the steady state problem corresponding to $(\mathscr{J}_\varepsilon)$: Find u_ε such that*

$$\begin{aligned} (\varepsilon u_\varepsilon'' - 2u_\varepsilon u_\varepsilon' - b)(x) &= q(x), \quad x\in(0,1), \\ u_\varepsilon(0) = A > 0, \quad u_\varepsilon(1) &= B < 0, \quad b(x)\geqslant\beta>0. \end{aligned} \tag{$\mathscr{K}_\varepsilon$}$$

The algorithm details mirror those outlined above for $(\mathscr{J}_\varepsilon)$ and we will only briefly explain the algorithm in [31] below. If $\varepsilon > N^{-2/5}$ then discretise $(\mathscr{K}_\varepsilon)$ on a uniform mesh. If $\varepsilon \leqslant N^{-2/5}$ then approximate $s \in (0,1)$ such that $u_\varepsilon(s) = 0$ as follows. Consider the following reduced initial and terminal value problems:

$$(-2u'_{L\backslash R}u_{L\backslash R} - b\,u_{L\backslash R})(x) = q(x), \quad x \in (0,1]\backslash[0,1), \tag{6.2.13a}$$

$$u_L(0) = A, \quad u_R(1) = B. \tag{6.2.13b}$$

An approximation for s is taken as s_0, the solution of $(u_L + u_R)(s_0) = 0$. Note that this means s_0 is identical to Howes' point in this case. Continue and complete the algorithm using s_0 in the same manner as $s^*(t)$ is used to complete the algorithm outlined in the above section. Analogous bounds as (6.2.11) (for mesh points away from s_0) and (6.2.12) (for mesh points near s_0) are presented. Hence, we would view the algorithm as more theoretical rather than practical.

6.3: Numerical Example

Example 6.1

In this example we solve $((\mathscr{J}_\varepsilon^N)$, (6.2.3)) and $((\tilde{\mathscr{J}}_\varepsilon^N)$, (6.2.3)) with

$$a_L, a_R \equiv 2, \;\; b_L(x) = b_R(x) = 1 + \cos(3x), \;\; q_L(x) = q_R(x) = \sin(3x), \;\; b \equiv 1, \tag{6.3.1a}$$

$$f(x,t) = \cos(4x), \;\; A = 2, \;\; B = 3, \;\; d = 0.4 \text{ and } T = 1. \tag{6.3.1b}$$

We choose $\theta = \frac{1}{2}|A - B|$ in $(\tilde{\mathscr{J}}_\varepsilon^N)$. A graph of a numerical solution of $(\tilde{\mathscr{J}}_\varepsilon^N)$ with the transform ξ reversed is displayed in Figure 6.1. In Figure 6.2, we see a plot of $S^{M/2}$ and s^*. We solve for $Y_\varepsilon^{N,M}$ where

$$Y_\varepsilon^{N,M}(x_i) = \begin{cases} Y_\varepsilon^N(x_i), & x_i \in \overline{\Omega}^N, \quad \varepsilon > (N^{-2/5} + M^{-2/5}), \\ \tilde{Y}_\varepsilon^{-,N}(x_i), & x_i \leqslant \frac{1}{2}, \quad \varepsilon \leqslant (N^{-2/5} + M^{-2/5}), \\ \tilde{Y}_\varepsilon^{+,N}(x_i), & x_i > \frac{1}{2}, \quad \varepsilon \leqslant (N^{-2/5} + M^{-2/5}), \end{cases}$$

where Y_ε^N is the solution of $(\mathscr{J}_\varepsilon^N)$ and $\tilde{Y}_\varepsilon^{\pm,N}(x_i)$ are the numerical solutions of $(\tilde{\mathscr{J}}_\varepsilon^N)$, all using N and M mesh intervals in space and time respectively. Note, we linearise the nonlinear term $D_\xi^-(\tilde{Y}_\varepsilon^{+,N})^2(\xi_i, t_j)$ in $(\tilde{\mathscr{J}}_\varepsilon^N)$ by replacing it with

$$(\tilde{Y}_\varepsilon^{+,N}(\xi_i, t_{j-1}) + \tilde{Y}_\varepsilon^{+,N}(\xi_{i-1}, t_{j-1}))D_\xi^- \tilde{Y}_\varepsilon^{+,N}(\xi_i, t_j).$$

We linearise $D_\xi^+(\tilde{Y}_\varepsilon^{-,N})^2(\xi_i, t_j)$ analogously. We compute differences D_ε^N and rates R_ε^N for various values of N and ε presented in Table 6.1 where

$$D_\varepsilon^N := \max_{(x_i,t_j) \in \overline{\tilde{G}}^{\frac{N}{2},N-} \cup \overline{\tilde{G}}^{\frac{N}{2},N+}} |(Y_\varepsilon^{N,N} - \bar{Y}_\varepsilon^{2N,N})(x_i)|, \quad D^N := \max_\varepsilon D_\varepsilon^N, \tag{6.3.2a}$$

$$R_\varepsilon^N := \log_2 \frac{D_\varepsilon^N}{D_\varepsilon^{2N}} \quad \text{and} \quad R^N := \log_2 \frac{D^N}{D^{2N}}, \tag{6.3.2b}$$

where $\bar{Y}_\varepsilon^{2N,N}$ is the interpolation of $Y_\varepsilon^{2N,N}$ onto the grid $\overline{\tilde{G}}^{\frac{N}{2},N-} \cup \overline{\tilde{G}}^{\frac{N}{2},N+}$.

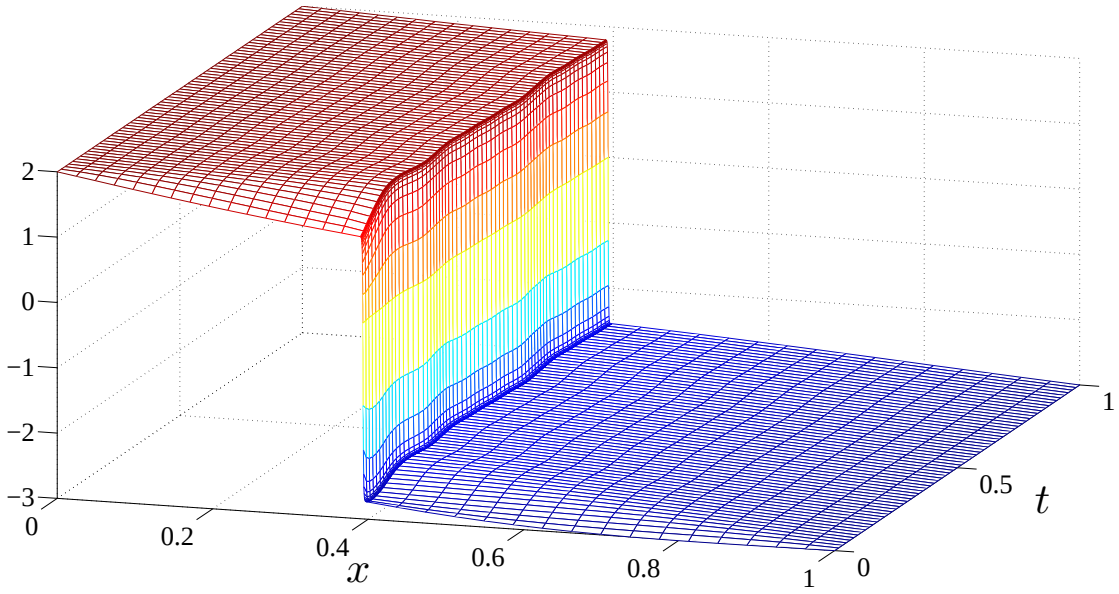

Figure 6.1: Plot of the numerical solution of ($\mathscr{J}_\varepsilon$), (6.2.1)), with the problem data as in (6.3.1), computed using the numerical method (($\tilde{\mathscr{J}}_\varepsilon{}^N$), (6.2.2)), under the reverse of transform ξ (defined in (6.2.9)), for $\varepsilon = 2^{-10}$ and $N = M = 64$.

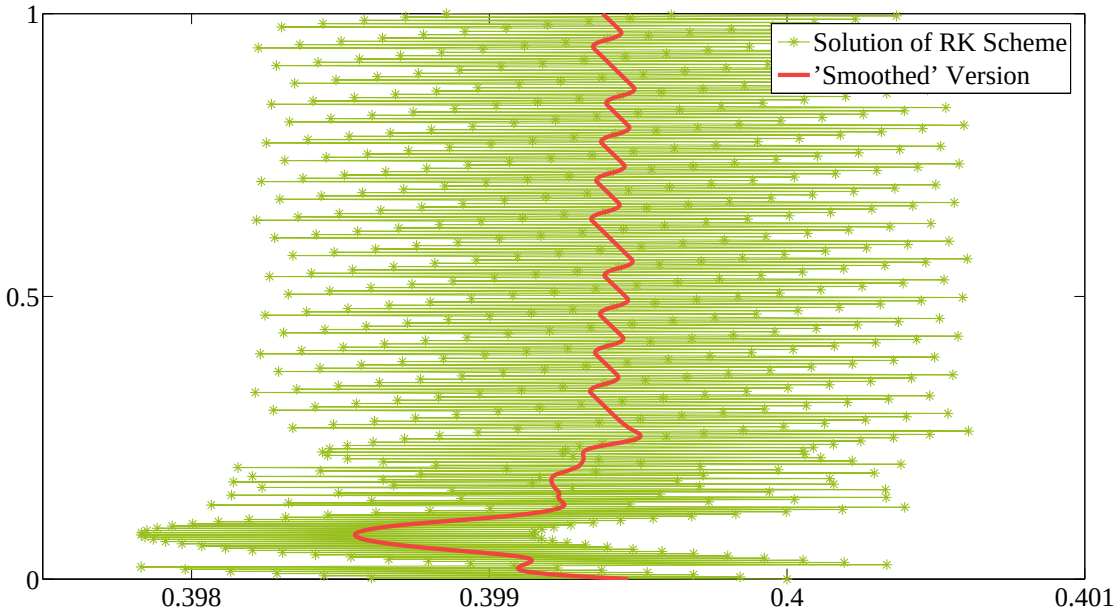

Figure 6.2: Plot of t versus $S^{M/2}$ where $S^{M/2}$ is the solution of the Runge-Kutta scheme (6.2.6) with the problem data (6.3.1) and a plot of t versus $s^*(t)$ (where $s^*(t)$ is the associated "smoothed" continuous function defined in (6.2.8)) for $M = 1024$ over $t \in [0, T]$

	R_ε^N						
ε	**N=32**	**N=64**	**N=128**	**N=256**	**N=512**	**N=1024**	**N=2048**
$\mathbf{2^{-0}}$	1.03	1.01	1.01	1.00	1.00	1.00	1.00
$\mathbf{2^{-1}}$	1.01	1.01	1.01	1.01	1.00	1.00	1.00
$\mathbf{2^{-2}}$	1.01	1.02	1.03	1.02	1.01	1.01	1.00
$\mathbf{2^{-5}}$	0.31	0.90	0.74	0.91	0.97	0.33	1.10
$\mathbf{2^{-6}}$	0.32	0.45	0.38	0.37	0.77	0.56	1.00
$\mathbf{2^{-7}}$	0.35	0.46	0.38	0.58	0.64	0.41	0.85
$\mathbf{2^{-8}}$	0.37	0.47	0.38	0.58	0.64	0.41	0.85
$\mathbf{2^{-9}}$	0.38	0.47	0.38	0.58	0.64	0.40	0.84
$\mathbf{2^{-10}}$	0.39	0.47	0.38	0.57	0.64	0.40	0.84
$\mathbf{2^{-11}}$	0.39	0.47	0.38	0.57	0.64	0.40	0.84
$\mathbf{2^{-12}}$	0.39	0.47	0.38	0.57	0.64	0.40	0.84
$\mathbf{2^{-13}}$	0.39	0.47	0.38	0.57	0.64	0.40	0.84
$\mathbf{2^{-14}}$	0.40	0.47	0.38	0.57	0.64	0.40	0.84
$\mathbf{2^{-15}}$	0.40	0.47	0.38	0.57	0.64	0.40	0.84
$\mathbf{2^{-16}}$	0.41	0.47	0.38	0.57	0.64	0.40	0.84
$\mathbf{2^{-17}}$	0.43	0.47	0.38	0.57	0.64	0.40	0.84
$\mathbf{2^{-18}}$	1.19	0.47	0.38	0.57	0.64	0.40	0.84
$\mathbf{2^{-19}}$	3.43	0.47	0.38	0.57	0.64	0.40	0.84
$\mathbf{2^{-20}}$	3.43	0.47	0.38	0.57	0.64	0.40	0.84
$\mathbf{R^N}$	**2.88**	**0.90**	**0.50**	**0.39**	**0.77**	**0.45**	**0.84**

Table 6.1: Computed rates of convergence R_ε^N and R^N (as defined in (6.3.2)), measured from the numerical solutions of (($\mathscr{J}_\varepsilon$),(6.2.1)) and (($\tilde{\mathscr{J}}_\varepsilon$),(6.2.1)), with the problem data as in (6.3.1), approximated using the numerical methods (($\mathscr{J}_\varepsilon^N$), (6.2.3), (6.2.2)) and (($\tilde{\mathscr{J}}_\varepsilon{}^N$), (6.2.3), (6.2.10), (6.2.2)) respectively, for sample values of N and ε.

Note that in Table 6.1, the rows for $\varepsilon = 2^{-3}, 2^{-4}$ have been excluded, because over this parameter range of $(\varepsilon,\ N)$, two separate numerical algorithms are implemented either side of the constraint $\varepsilon = N^{-0.4}$. It is difficult to interpret the significance of the two mesh differences D_ε^N, when two distinct algorithms are being utilized in the computation of D_ε^N.

The computed rates of uniform convergence R^N oscillate in Table 6.1, but overall they indicate a uniform rate of convergence of 0.4 or greater for this particular test example.

Example 6.2

In this example, we compare numerical approximations generated from the Numerical Methods 4.1 and (($\tilde{\mathscr{J}}_\varepsilon{}^N$), (6.2.3), (6.2.10), (6.2.2)). We consider the two schemes for the problem data

$$\varepsilon = 2^{-10}, \quad \alpha = 2, \quad a_L = a_R \equiv 1, \quad b = b_L = b_R \equiv 1, \tag{6.3.3a}$$

$$q = q_L = q_R \equiv 0, \quad A = 1.5, \quad B = -1.4, \quad x^* = 0.6. \tag{6.3.3b}$$

Note, from (3.3.29), we choose γ_L and γ_R in (4.3.1) as

$$\gamma_L = \gamma_L^* = 0.85\ (< \sqrt{A^2 - \tfrac{2}{\alpha}A\|b\|} = 0.866), \quad \gamma_R = \gamma_R^* = 0.74\ (< \sqrt{A^2 - \tfrac{2}{\alpha}A\|b\|} = 0.748). \tag{6.3.3c}$$

For this value of ε, we consider the approximations Y^N generated from the Numerical Method 4.1 for $N = 32, 64, 128, 256, 512, 1024$. For each of these values of N, we generate approximations U^N using the method (($\tilde{\mathscr{J}_\varepsilon}^N$), (6.2.3), (6.2.10), (6.2.2)) for times $T = 1, 2, 3, \ldots, 20$ using N space mesh intervals and $M = NT$ time mesh intervals. For the latter approximations, we only consider the value of the approximations at the final time T. Figures 6.3-6.5 display all these approximations for each value of N. Note that all approximations, for all N and T, are plotted over the interval $[0.585, 0.64]$. From the graphs, we can see that the approximations obtained from the Shishkin algorithm (outlined in this chapter above) do not reach a steady state, at least for $T = 20$. Ideally, to compare the algorithms, we would choose a final time and take the value of the approximation using the Shishkin algorithm at that time and compare to an approximation generated using the Numerical Method 4.1, over a range of ε and N. However, the final time value we choose remains an open question. Table 6.2 displays the maximum pointwise differences defined as

$$\max_{\tau_i \in \Omega_S \cup \Omega_O} |(\overline{Y}^N - \overline{U}_T^N)(\tau_i)| \tag{6.3.4}$$

where Ω_S is the mesh used in the scheme (($\tilde{\mathscr{J}_\varepsilon}^N$), (6.2.3), (6.2.10), (6.2.2)), Ω_O is the mesh used in the numerical scheme 4.1, $\overline{Y}^N$ is the linear interpolant of Y^N and $\overline{U}_T^N$ is the linear interpolant of U^N at the final time $T = 5$.

ε \ N	**N=32**	**N=64**	**N=128**	**N=256**	**N=512**	**N=1024**
$\mathbf{2^{-8}}$	0.6573	0.4758	0.2858	0.1640	0.0907	0.0482
$\mathbf{2^{-10}}$	0.7208	0.4610	0.2702	0.1499	0.0762	0.0342
$\mathbf{2^{-12}}$	0.7121	0.4508	0.2591	0.1400	0.0670	0.0265
$\mathbf{2^{-14}}$	0.6758	0.4081	0.2211	0.1034	0.0378	0.0295

Table 6.2: Computed global maximum point wise errors (as defined in (6.3.4)) calculated from the numerical approximations generated by the Numerical Schemes 4.1 and (($\tilde{\mathscr{J}_\varepsilon}^N$), (6.2.3), (6.2.10), (6.2.2)) at the final time value $T = 5$ using $M = NT$ time mesh intervals, where all approximations are computed using the problem data (6.3.3) and $N = 32, 64, \ldots$ space mesh intervals.

In conclusion, it remains unknown as to when the Shishkin algorithm reaches a steady state. However, in these numerical experiments, approximations obtained from the Numerical Scheme 4.1 based on centring a Shishkin mesh at Howes' point 4.2.6 appear to converge to approximations obtained from the algorithm outlined in this chapter. Hence, before we can make a more solid claim, more experimentation is needed.

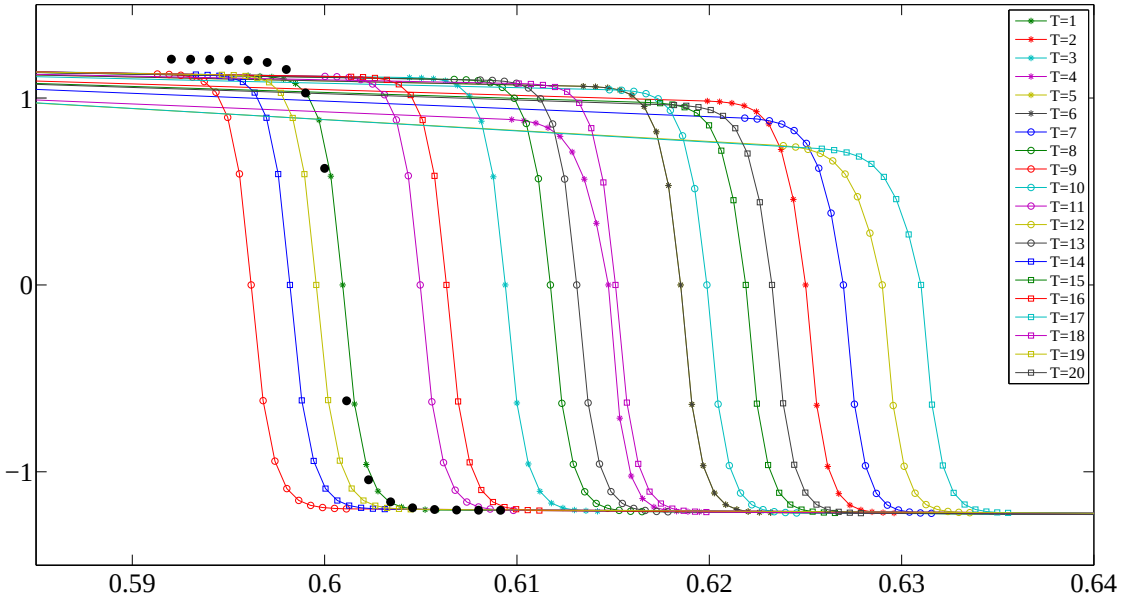

(a) $N = 32$

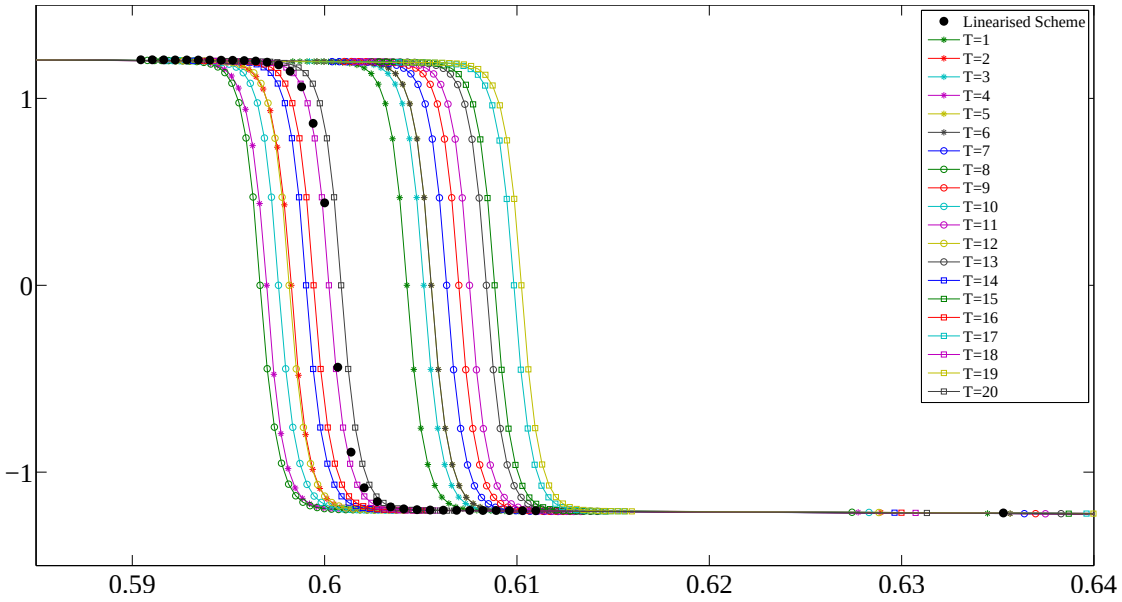

(b) $N = 64$

Figure 6.3: Black-dot plots of the numerical approximations generated by the Numerical Scheme 4.1 and coloured plots of the numerical approximations generated by $((\tilde{\mathscr{J}}_\varepsilon{}^N)$, (6.2.3), (6.2.10), (6.2.2)) at the final time values $T = 1,2,3,\ldots,20$ using $M = NT$ time mesh intervals, where all approximations are computed using the problem data (6.3.3) and (a) $N = 32$ and (b) $N = 64$ space mesh intervals.

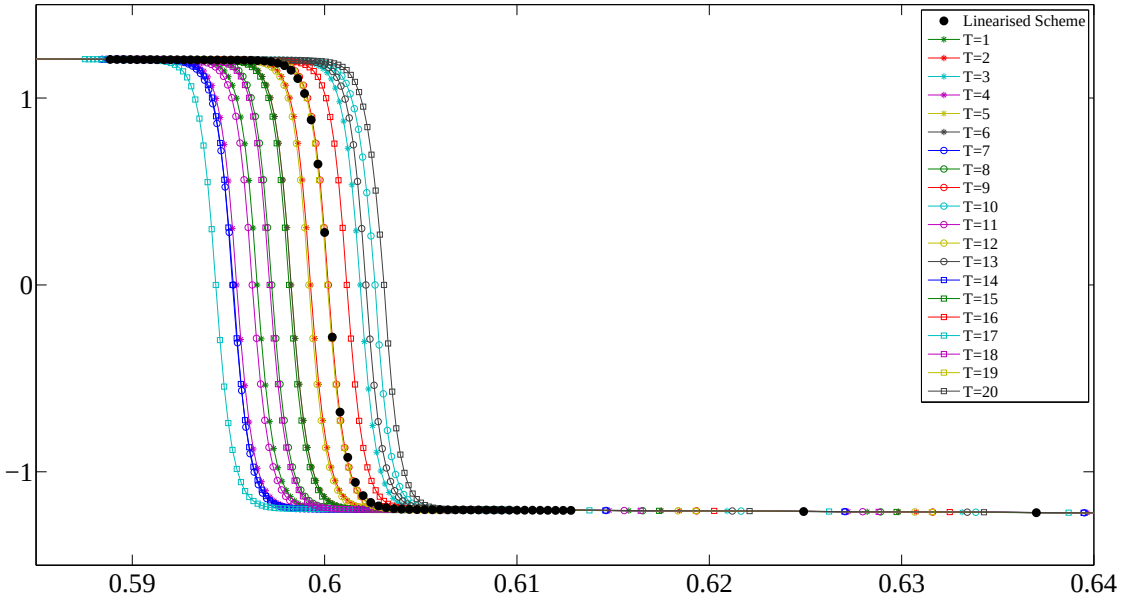

(a) $N = 128$

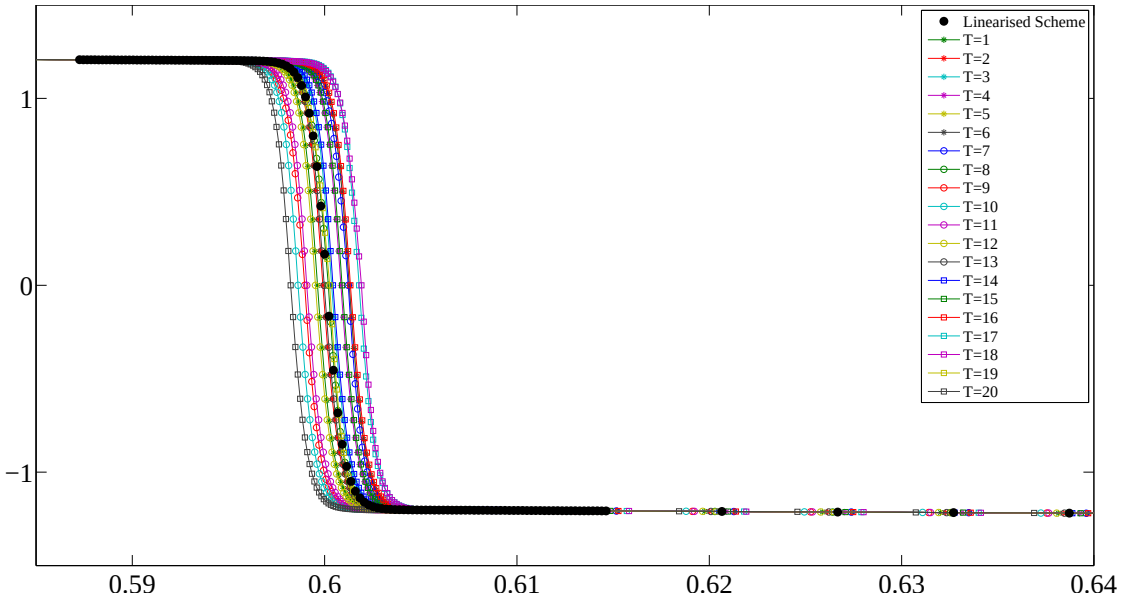

(b) $N = 256$

Figure 6.4: Black-dot plots of the numerical approximations generated by the Numerical Scheme 4.1 and coloured plots of the numerical approximations generated by $((\tilde{\mathscr{J}}_\varepsilon{}^N)$, (6.2.3), (6.2.10), (6.2.2)) at the final time values $T = 1,2,3,\ldots,20$ using $M = NT$ time mesh intervals, where all approximations are computed using the problem data (6.3.3) and (c) $N = 128$ and (d) $N = 256$ space mesh intervals.

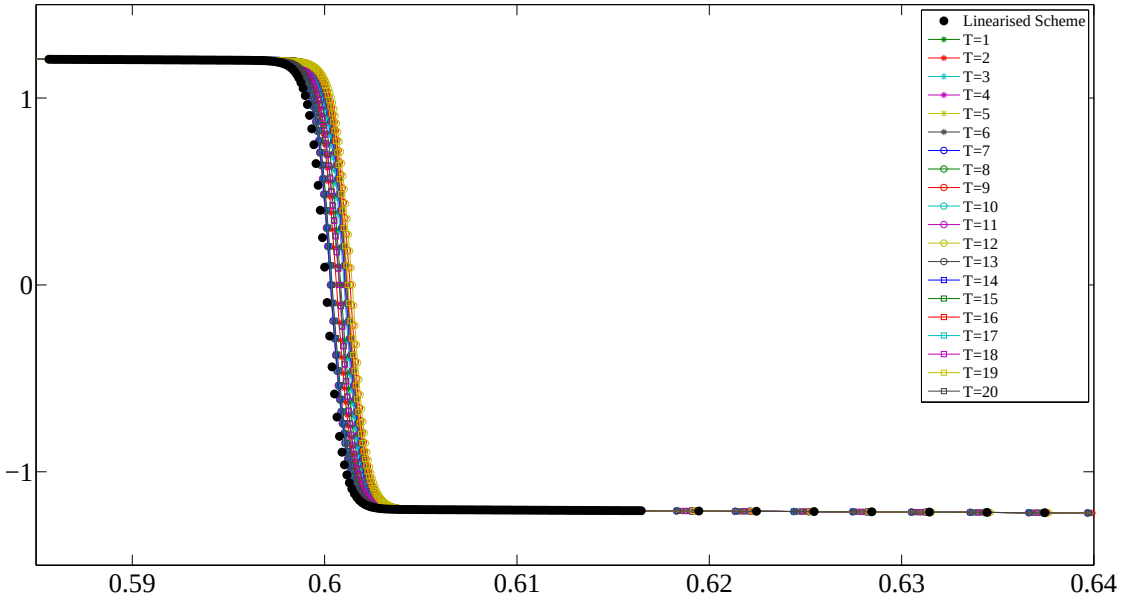

(a) $N = 512$

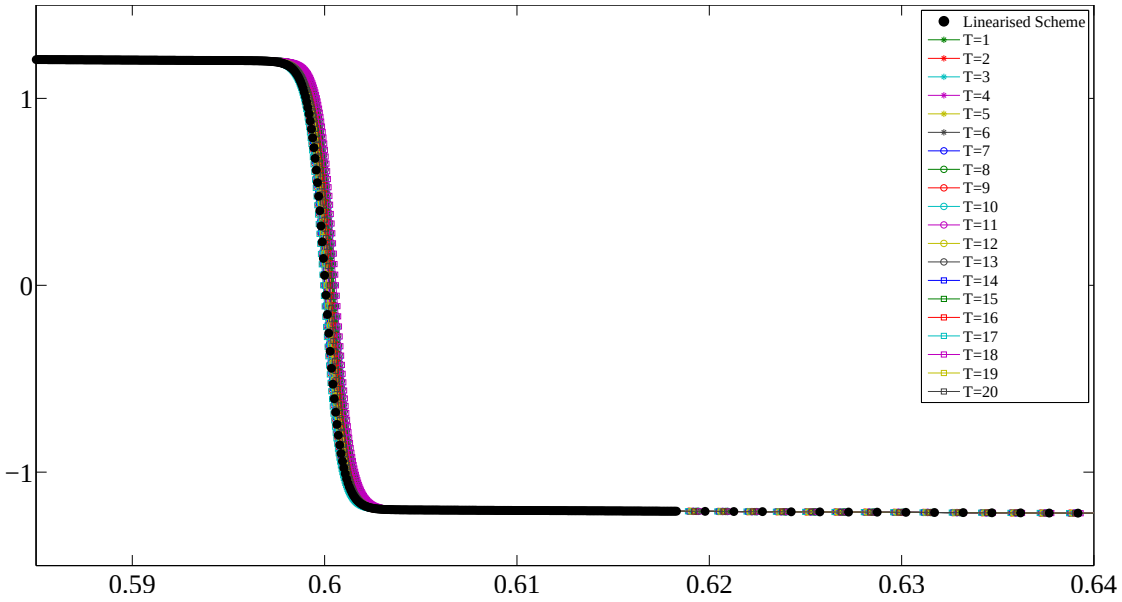

(b) $N = 1024$

Figure 6.5: Black-dot plots of the numerical approximations generated by the Numerical Scheme 4.1 and coloured plots of the numerical approximations generated by $((\tilde{\mathscr{J}}_\varepsilon{}^N)$, (6.2.3), (6.2.10), (6.2.2)) at the final time values $T = 1,2,3,\ldots,20$ using $M = NT$ time mesh intervals, where all approximations are computed using the problem data (6.3.3) and (c) $N = 512$ and (d) $N = 1024$ space mesh intervals.

CONCLUSIONS

In Chapter 2, we examined nonlinear initial value problems. Under certain restrictions on the nonlinearity, a wide range of nonlinear problem classes can be examined. These restrictions assist in the analysis where by the problems can, in a sense, be linearised. When these restrictions are removed, then it appears that such wide classes of problems cannot be analysed as easily and we consider these problem classes on a case-by-case basis.

The issue of whether it is possible to establish parameter uniform convergence for initial value problems where the initial condition is arbitrary close to an unstable reduced solution remains unresolved.

Furthermore, our approximations to functions y that satisfy a fundamental character such that $\varepsilon y' + y^n = 0$, $y(0) > 0$, produce convergence rates that deteriorate with n, as confirmed experimentally. Clearly, increasing n does 'increase' the non-linearity of the problem. However, it hardly adds to any exoticism of the problem that it should cause such a considerable slump in convergence rates. We are left to ask if there is a remedy to this undesirable anomaly?

In Chapter 3, we examine linear and nonlinear boundary turning point problems. Analysis of the linear problem aides in the analysis of the nonlinear problem more subtly than transparently whereby it acquaints us with using a bound of the convection co-efficient of the form $C(1 - e^{-Cx/\varepsilon})$.

The original analysis for the nonlinear problem, as published in [24], was for the Burgers' problem $\varepsilon y'' + yy' - by = q$. The analysis was subsequently updated, to examine the more general problem $\varepsilon y'' + f(y)y' - by = q$, $f(s) \geqslant s$, using the same routine as for the Burgers' problem. This inspires the idea, that even though our mantra regarding nonlinear problems is to study them case-by-case, it may help to 'strip' a nonlinear problem down to its related fundamental problem to assist in the analysis.

Furthermore in Chapter 3, we see another difficulty when analysing linear over nonlinear prob-

lems as alluded to in the introduction - the effect of the boundary conditions. The analysis in Chapter 3 immediately covers a problem such as $\varepsilon y'' + \sqrt{y}y' - y = 0$, $y(0) = 0$, $y(1) = B_1 = 0.5$ because $\sqrt{s} \geqslant s$ on $[0, 2B_1](\equiv [0,1])$. However, the analysis does not cover the problem $\varepsilon y'' + \sqrt{y}y' - y = 0$, $y(0) = 0$, $y(1) = B_2 = 0.51$ since $\sqrt{s} \not\geqslant s$ for all $s \in [0, 2B_2]$ where the only difference is that the boundary condition has been slightly changed.

In Chapter 4, we consider approximating the solution to a Burgers'-type problem using two boundary turning point problems. It appears that we would need to be 'super-close' (within $O(\varepsilon^2)$) to the unknown root for such a method to be effective. Until such an approximation is found, this method is viewed as highly impractical. We are convinced that successfully analysing and constructing a parameter-uniform numerical method for Burgers equation with an interior layer, crucially depends on knowledge of the location of the zero of the solution.

In chapter 5, we consider a linear interior layer problem. A finite difference scheme is applied to the problem on the global domain. We consider 'off-centring' the Shishkin mesh from its ideal location. A limit on the distance of the new centring point from the ideal centring point is $C\varepsilon$. Supposing this method could be replicated for a nonlinear difference scheme considered on its global domain, then it would be a considerably more practical method than that examined in Chapter 4 as we would only need to be within $O(\varepsilon)$ of the unknown root for the method to be effective.

Hence, the next step in this research is to mimic the numerical analysis performed in Chapter 5 for the nonlinear Burgers' equation problem. That is, consider centring the mesh at some other point p, and identify in the analysis how close p needs to be to the root in order to preserve parameter-uniform convergence. The construction of a parameter-uniform numerical method to solve the steady-state Burgers' problem with an interior layer remains an open question.

BIBLIOGRAPHY

[1] L. Abrahamsson and S. Osher. Monotone difference schemes for singular perturbation problems. *SIAM Journal on Numerical Analysis*, 19(5):979–992, 1982.

[2] A.S. Bakhvalov. On the optimization of methods for solving boundary value problems with boundary layers. *Zh. Vychisl. Mat. i Mat. Fis.*, 9:841–859, 1969.

[3] M. Bardi, A. Cesaroni, and L. Manca. Convergence by viscosity methods in multiscale financial models with stochastic volatility. *SIAM Journal of Financial Mathematics*, 1:230–265, 2010.

[4] A.E. Berger, H. Han, and R.B. Kellogg. A priori estimates and analysis of a numerical method for a turning point problem. *Mathematics of Computation*, 42(166):465–492, 1984.

[5] S.R. Bernfield and V. Lakshmikantham. *An Introduction to Nonlinear Boundary Value Problems*. Academic Press, New York, 1974.

[6] P.A. Farrell. Sufficient conditions for the uniform convergence of a difference scheme for a singularly perturbed turning point problem. *SIAM Journal on Numerical Analysis*, 25(3):618–643, 1988.

[7] P.A. Farrell, A.F. Hegarty, J.J.H. Miller, E. O'Riordan, and G.I. Shishkin. *Robust Computational Techniques for Boundary Layers*. Chapman and Hall/CRC, Boca Raton, FL, 2000.

[8] P.A. Farrell, A.F. Hegarty, J.J.H. Miller, E. O'Riordan, and G.I. Shishkin. Global maximum norm parameter-uniform numerical method for a singularly perturbed convection-diffusion problem with discontinuous convection coefficient. *Mathematical and Computer Modelling*, 40:1375–1392, 2004.

[9] P.A. Farrell, J.J.H. Miller, E. O'Riordan, and G.I. Shishkin. On the non-existence of ϵ–uniform finite difference methods on uniform meshes for semilinear two-point boundary value problems. *Mathematics of Computation*, 67(222):603–617, 1998.

[10] P.A. Farrell, E. O'Riordan, J.J.H. Miller, and G.I. Shishkin. Parameter-uniform fitted mesh method for quasilinear differential equations with boundary layers. *Computational Methods in Applied Mathematics*, 1(2):154–172, 2001.

[11] P.A. Farrell, E. O'Riordan, and G.I. Shishkin. A class of singularly perturbed semilinear differential equations with interior layers. *Mathematics of Computation*, 74(252):1759–1776, 2005.

[12] F.A. Howes. Boundary-interior layer interactions in nonlinear singular perturbation theory. *Memoirs of the American Mathematical Society*, 15(203), 1978.

[13] R.E. O'Malley, Jr. *Singular Perturbation Methods for Ordinary Differential Equations*. Springer Verlag, New York, 1991.

[14] L.V. Kalachev, T.C. Kelly, M.J. O'Callaghan, A.V. Pokrovskii, and A.V. Pokrovskiy. Analysis of threshold-type behaviour in mathematical models of the intrusion of a novel macroparasite in a host colony. *Mathematical Medicine and Biology*, 28(4):287–333, 2011.

[15] N. Kopteva and M. Stynes. Stabalised approximation of interior-layer solutions of a singularly perturbed semilinear reaction-diffusion problem. *Numerische Mathematik*, 119(4):787–810, 2011.

[16] G.S. Ladde, V. Lakshmikantham, and A.S. Vatsala. *Monotone Iterative Techniques for Nonlinear Differential Equations*. Pitman Publishing, London, 1985.

[17] T. Linß. Robustness of an upwind finite difference scheme for semilinear convection-diffusion problems with boundary turning points. *Journal of Computational Mathematics*, 21(4):401–410, 2003.

[18] T. Linß, H.-G. Roos, and R. Vulanović. Uniform pointwise convergence on Shishkin-type meshes for quasilinear convection-diffusion problems. *SIAM Journal on Numerical Analysis*, 38(3):897–912, 2000.

[19] J. Lorenz. Analysis of difference shemes for a stationary shock problem. *SIAM Journal on Numerical Analysis*, 21(6):1038–1053, 1984.

[20] J.J.H. Miller, E. O'Riordan, and G.I. Shishkin. *Fitted Numerical Methods for Singular Perturbation Problems*. World Scientific, Singapore, 1996.

[21] K.W. Morton. *Numerical Solution of Convection-Diffusion Problems*. Chapman and Hall, London, 1996.

[22] M.J. O'Reilly and E. O'Riordan. A Shishkin mesh for a singularly perturbed Riccati equation. *Journal of Computational and Applied Mathematics*, 181(2):372–387, 2005.

[23] E. O'Riordan and J. Quinn. Numerical method for a nonlinear singularly perturbed interior layer problem. In *BAIL 2010 - Boundary and Interior Layers*, volume 81 of *Lecture Notes in Computational Science and Engineering*, pages 187–195, Berlin/Heidelberg, 2011. Springer. C. Clavero, J. L. Gracia and F. J. Lisbona (editors).

[24] E. O'Riordan and J. Quinn. Parameter-uniform numerical methods for some linear and nonlinear singularly perturbed convection diffusion boundary turning point problems. *BIT Numerical Mathematics*, 51(2):317–337, 2011.

[25] E. O'Riordan and J. Quinn. Parameter-uniform numerical methods for some singularly perturbed nonlinear initial value problems. *Numerical Algorithms*, 2012.
doi: http://dx.doi.org/10.1007/s11075-012-9552-3.

[26] E. O'Riordan and J. Quinn. A singularly perturbed convection diffusion turning point problem with an interior layer. *Computational Methods in Applied Mathematics*, 12(2):206–220, 2012.

[27] S. Osher. Nonlinear singular perturbation problems and one sided difference schemes. *SIAM Journal on Numerical Analysis*, 18(1):129–144, 1981.

[28] E. L. Reiss. A new asymptotic method for jump phenomena. *SIAM Journal on Applied Mathematics*, 39(3):440–455, 1980.

[29] H.-G. Roos, M. Stynes, and L. Tobiska. *Robust Numerical Methods for Singularly Perturbed Differential Equations*, volume 24 of *Springer Series in Computational Mathematics*. Springer, Berlin, second edition, 2008.

[30] G.I. Shishkin. A difference scheme for a singularly perturbed equation of parabolic type with a discontinous initial condition. *Soviet Math. Dokl.*, 37(3):792–796, 1988.

[31] G.I. Shishkin. Grid approximation of a singularly perturbed quasilinear equation in the presence of a transition layer. *Russian Acad. Sci. Dokl. Math.*, 47(1):83–88, 1993.

[32] G.I. Shishkin. Difference approximation of the Dirichlet problem for a singularly perturbed quasilinear parabolic equation in the presence of a transition layer. *Russian Acad. Sci. Dokl. Math.*, 48(2):346–352, 1994.

[33] R. Vulanović. Continuous and numerical analysis of a boundary shock problem. *Bulletin of the Australian Mathematical Society*, 41:75–86, 1990.

[34] R. Vulanović. Boundary shock problems and singularly perturbed Riccati equations. In *BAIL 2008 - Boundary and Interior Layers*, volume 69 of *Lecture Notes in Computational Science and Engineering*, pages 277–285, Berlin/Heidelberg, 2008. Springer. A.F. Hegarty, N. Kopteva, E. O'Riordan and M. Stynes (editors).

[35] R. Vulanović. A uniform numerical method for a boundary-shock problem. *International Journal of Numerical Analysis & Modeling*, 7(3):567–579, 2010.

[36] A.I. Zadorin and V.N. Ignat'ev. A difference scheme for a nonlinear singularly perturbed equation of second order. *Zhurnal Vychislitel'noi Matematiki i Matematicheskoi Fiziki*, 30:1425–1430, 1990.